

AN ABSTRACT OF THE THESIS OF

Wanjia Zhang for the degree of Doctor of Philosophy in Chemistry  
Presented on January 10, 1991.

TITLE: A Mechanistic Study of the Distribution of Amphiphilic  
Organic Compounds between Water and Organic Sorbents

Redacted for Privacy

Abstract approved: \_\_\_\_\_

 John C. Westall

This study was conducted to elucidate some factors that control the distribution of amphiphilic organic compounds (ionic and nonionic) between water and organic solvents and sorbents. Specifically, two types of systems were studied: (i) the speciation of LiCl, KCl, NaCl, HCl, MgCl<sub>2</sub>, and CaCl<sub>2</sub> in the two-phase system water | water saturated 1-octanol; (ii) the distribution of anionic surfactants (alkylbenzenesulfonates) and nonionic surfactants (monoalkyl ether of polyethyleneglycols) between water and environmental sorbent materials (soils, sediments, and aquifer materials). The motivation for this research is the need to understand the factors that control the sorption of these amphiphilic organic compounds in the environment.

A technique was developed to determine the conductivity and permittivity (dielectric constant) of high-impedance electrolyte solutions. The technique is based on the use of a computer

controlled lock-in amplifier to analyze the frequency-dependent impedance of a liquid sample. The resistances of the samples were determined up to  $10\text{ M}\Omega$  with precision better than 3%, and the capacitances in the range 90 - 900 pF, with a precision better than 0.2%.

Speciation of LiCl, NaCl, KCl, HCl,  $\text{MgCl}_2$  and  $\text{CaCl}_2$  between octanol and water was studied by conductometry. The distribution of the MX salts was explained by the species  $\text{M}^+$ ,  $\text{X}^-$ , and MX in the octanol phase. For HCl, the conductivity study suggested the presence of triple ions such as  $\text{H}_2\text{Cl}^+$  or  $\text{HCl}_2^-$  in the octanol. The distribution of the  $\text{MX}_2$  salts was explained by the presence of  $\text{MX}^+$ ,  $\text{X}^-$ , and  $\text{MX}_2$  in the octanol.

Adsorption of linear alkylbenzenesulfonates (LAS) on natural sorbents was interpreted by both hydrophobic and electrostatic interactions. Addition of  $\text{Ca}^{2+}$  significantly increased the adsorption of the anionic surfactant LAS. This phenomenon suggests the formation of LAS- $\text{Ca}^+$  complex either on the surface or in the solution. Addition of  $\text{Ca}^{2+}$  had no effect on the adsorption of monoalkyl ethers of polyethylene glycol (AE). Nonlinear adsorption isotherms, which were observed for both LAS and AE, were attributed to surface heterogeneity. The concentration distribution ratio of LAS correlated with the fraction of organic carbon of sorbent, but that of AE does not. Hemimicelle formation was observed in the adsorption of LAS. The pH, ionic strength of solution, and chain length of LAS affected this formation. The electrophoretic mobilities of sorbent particles reflected the amount of LAS adsorbed.

A Mechanistic Study  
of the Distribution of Amphiphilic Organic Compounds  
between Water and Organic Sorbents

by  
Wanjia Zhang

A THESIS  
submitted to  
Oregon State University

in partial fulfillment of  
the requirement for the  
degree of  
Doctor of Philosophy

Completed January 10, 1991

Commencement June 1991

APPROVED:

Redacted for Privacy

\_\_\_\_\_  
Professor of Chemistry in charge of major

Redacted for Privacy

\_\_\_\_\_  
Chairman of Department of Chemistry

Redacted for Privacy

\_\_\_\_\_  
Dean of Graduate School

Date thesis is presented January 10, 1991

Typed by Wanjia Zhang for Wanjia Zhang

## DEDICATIONS

To my husband, Yuqi Zhao:

- We have walked together through beautiful roads and rough roads, steep mountains and sunny beaches. Your love, care, and understanding have been with me every day on the long way to achieve my goal.

To my daughter, Jennie, and my son, Andrew:

- "Mommy is going to become a doctor."

"Am I sick, mommy?"

Yes, they are lovely. Whenever I went back home from school, their lovely smiles always cheered me up and gave me more energy during the last six years.

To my mother-in-law, Guizhen Ma:

- Her kindness and love means a lot in this thesis. She helped me to take care of my children and family at the time when I needed her the most.

To my father, Derui Zhang and mother, Yikuan Cai:

- I still remember what they told me six years ago when I was on my way to the U.S., "Wanjia, go there and get it, we know you can do it!"

## ACKNOWLEDGMENT

To my major professor, Dr. John C. Westall for his guidances, advice, and discussion.

To my colleagues, Dudley Jayasinghe, Bruce Brownawell, C. Annette Johnson, Hua Chen, Fred Rea, Julia Hatfield, Armando Herbelin, and John Jones for their respect, suggestions and discussion.

To my committee members, especially to Dr. James D. Ingle for his kindness, understanding and advice.

To Department of Chemistry, Oregon State University, for allowing me to do the research with the department facilities and for the financial support during my first and last years as teaching assistant.

To the Soap and Detergent Association and the Ecological Research Division, Office of Health and Environmental Research (OHER), U.S. Department of Energy (DOE) under Contract DE-AC06-76RLO 1830 as part of OHER's Subsurface Science Program for their support on this research.

## TABLE OF CONTENTS

CHAPTER 1. INTRODUCTION.....	1
Distribution of inorganic salts between octanol and water..	2
Adsorption of surfactants on environmental materials.....	3
REFERENCES.....	6
CHAPTER 2. DEVELOPMENT OF TECHNIQUES FOR DETERMINATION OF CONDUCTIVITY AND RELATIVE PERMITTIVITY OF NONAQUEOUS SOLUTIONS.	8
INTRODUCTION.....	9
THEORY.....	13
Equivalent circuit of a conductance cell.....	13
Simplification of the equivalent circuit.....	15
Techniques for determination of Rcell and Ccell.....	18
Measurement circuit.....	18
Method for data analysis.....	21
Determination of Rcell and Ccell'.....	22
Cable capacitance, C2.....	24
Stray capacitance.....	25
EXPERIMENTS.....	27
Materials and equipment.....	27
Sample preparations.....	28
Measurement procedures.....	29
RESULTS AND DISCUSSION.....	30
Verification of methods.....	30
Determination of the effective cable capacitance.....	30
Determination of Cstray.....	30
Frequency dependence of Zcell, Xcell, and Rcell for a test cell.....	32
Determination of Rcell of KCl in water-saturated octanol...	32
Frequency dependence of Rcell.....	32
Bright Pt. vs. black Pt electrodes.....	39
Determination of permittivity of alcohol/water mixtures....	42
Apparent frequency dependence of the capacitance Ccell'.	42
Calibration curve of Ccell' vs. $\epsilon$ .....	46
Permittivities of pentanol-water and octanol-water mixtures.....	46
CONCLUSIONS.....	52
REFERENCES.....	53
CHAPTER 3. THE DISTRIBUTION OF LiCl, NaCl, KCl, HCl, MgCl <sub>2</sub> AND CaCl <sub>2</sub> BETWEEN OCTANOL AND WATER.....	56
INTRODUCTION.....	57

THEORY.....	59
Distributions.....	61
Numerical method for multicomponent equilibria.....	61
Activity and concentration of salts in water and octanol	63
EXPERIMENTS.....	70
Materials.....	70
Conductivity of octanol saturated with aqueous salt solutions.....	70
RESULTS.....	72
The distribution of LiCl, NaCl, KCl.....	72
The distribution of HCl.....	78
The distribution of MgCl <sub>2</sub> and CaCl <sub>2</sub> .....	80
DISCUSSION.....	83
Ion-pair formation.....	83
Limiting equivalent conductivity.....	86
SUMMARY.....	88
REFERENCES.....	89
CHAPTER 4. METHODS FOR THE STUDY OF ADSORPTION OF SURFACTANTS ON ENVIRONMENTAL SORBENTS.....	91
INTRODUCTION.....	92
Properties of surfactants.....	92
Adsorption of surfactants on pristine surfaces.....	93
Adsorption of surfactants on heterogeneous materials.....	95
EXPERIMENTAL METHODS.....	99
Materials and equipment.....	99
Clay mineral analysis.....	102
Pretreatment of sorbents.....	106
Determination of distribution ratio $D_c$ .....	110
Alternative procedure for analyzing LAS adsorbed on sorbent.....	114
The method for determination of pH.....	115
Determination of adsorption of surfactants on different materials.....	116
VERIFICATION OF METHODS.....	117
Quality control.....	117
Calibrations.....	117
Precision.....	117
Material recovery.....	125
Control of pH.....	129
Comparison of methods.....	129
Adsorption of C-12 LAS and C-12 TMAC on different materials.....	129

Methods for washing sorbent .....	133
Methods for determination of C-12 LAS adsorbed on sorbent.....	136
SUMMARY.....	138
REFERENCES.....	139
CHAPTER 5. ADSORPTION OF ALKYL ETHERS OF POLY(ETHYLENE GLYCOL) ON ENVIRONMENTAL SORBENTS.....	142
INTRODUCTION.....	143
EXPERIMENTS.....	145
Materials and equipment.....	145
Determination of distribution ratio $D_c$ .....	145
RESULTS AND DISCUSSION.....	148
Adsorption of $A_{13}E_6$ on different soil sorbents.....	148
The effect of added $Ca^{2+}$ on adsorption of $A_{13}E_m$ .....	153
The effect of salt concentration on adsorption of $A_{13}E_m$ .....	154
SUMMARY.....	156
REFERENCES.....	157
CHAPTER 6. ADSORPTION OF LINEAR ALKYL BENZENESULFONATES ON ENVIRONMENTAL MATERIALS.....	158
INTRODUCTION.....	159
THEORY.....	162
Partition constant $K_p$ and distribution ratio $D_c$ .....	162
Adsorption of nonpolar hydrophobic compounds.....	162
Adsorption of hydrophobic ionic compounds.....	163
Isotherms.....	164
EXPERIMENTAL METHODS.....	167
Materials and equipment.....	167
Determination of distribution ratios.....	168
RESULTS.....	170
Adsorption of C-12 LAS on different soil sorbents.....	170
Effect of $Ca^{2+}$ on the adsorption of LAS.....	170
Isotherms of C-12 LAS on EPA-12 at different sorbent concentrations.....	176
DISCUSSION.....	179
Adsorption energy of LAS.....	179
Hydrophobic interactions.....	179
Specific interactions with surface functional groups....	181

Electrostatic interactions.....	182
Contribution of LAS to total surface charge.....	183
Nonlinearity of isotherms.....	184
Adsorption of C-12 LAS on different soil sorbents.....	186
Effect of the ratio of solids to liquid in the slurry...	188
SUMMARY.....	190
REFERENCES.....	191
CHAPTER 7. ADSORPTION OF LINEAR ALKYL BENZENESULFONATES (LAS) AT THE PARTICLE-WATER INTERFACE: A STUDY OF ISOTHERMS AND ELECTROPHORETIC MOBILITIES.....	
	193
INTRODUCTION.....	194
THEORY.....	196
Electrical double layer, electrophoretic mobility, and zeta potential.....	196
The mechanisms of adsorption and S-type isotherm.....	200
Methods for calculation of aggregation number, $n_H$ .....	205
EXPERIMENTS.....	210
Materials.....	210
Adsorption isotherms.....	210
Electrophoretic mobilities.....	213
Control of pH.....	218
RESULTS.....	222
Effect of chain length on adsorption of LAS.....	222
Effect of chain length on mobility of sorbent particles....	222
Effect of pH on adsorption of C-12 LAS.....	227
Effect of salt concentration on adsorption of C-12 LAS.....	228
DISCUSSION.....	234
S-type isotherms on pristine and environmental sorbents....	234
Adsorption of LAS: sorbate-sorbent interactions.....	235
Negatively charged LAS being adsorbed on negatively charged surface.....	235
Quantification of electrostatic energy in Region I.....	236
Nonlinearity of isotherms.....	242
Adsorption of LAS: sorbate-sorbate interactions.....	243
Hemimicelle formation.....	243
$C_{HM}(w)$ and $\Gamma_{HM}$ .....	243
Aggregation number of hemimicelle, $n_H$ .....	249
SUMMARY.....	252
REFERENCES.....	254

CHAPTER 8. CONCLUSIONS.....	256
BIBLIOGRAPHY.....	260
APPENDIX I. A BASIC LAUGUAGE PROGRAM FOR EXPERIMENTAL CONTROL, DATA COLLECTION, AND DATA ANALYSIS BY PC - LOCK-IN AMPLIFIER SYSTEM.....	269
APPENDIX II. X-RAY IDENTIFICATION OF CLAY MINERALS IN ENVIRONMENTAL MATERIALS.....	278
Standard D spacing of common clays for X-ray identification....	279
Results of clay mineral analysis for environmental materials...	280
REFERENCES.....	289

## LIST OF FIGURES

<u>Figure</u>	<u>Page</u>
CHAPTER 2	
2.1.	The equivalent circuit of a conductance cell. 14
2.2a.	Schematic diagram of equivalent circuit with stray capacitance and cable capacitance. 19
2.2b.	Schematic diagram of equivalent circuit for calculation 20
2.3.	The frequency-dependence of the value of $R_{cell}$ calculated for two values of $C_{in}'$ . 31
2.4.	The frequency-dependence of $R_{cell}$ , $X_{Ccell}'$ , and $Z_{cell}$ for test cell ( $R_{cell} = 5.0 \text{ M}\Omega$ ). 34
2.5.	The frequency-dependence of $R_{cell}$ for samples of octanol saturated with KCl aqueous solutions. 37
2.6.	The frequency-dependence of $R_{cell}$ , $X_{Ccell}'$ , and $Z_{cell}$ for octanol saturated with 0.01 M aqueous KCl solutions. 38
2.7.	Time-dependence of resistivity, $R_{cell}/(l/A)$ : a comparison of bright platinum electrodes with platinum black electrodes for octanol saturated with 0.01 M KCl aqueous solution. 40
2.8.	Time-dependence test of resistivity, $R_{cell}/(l/A)$ , determined by platinum black electrodes with octanol saturated with KCl aqueous solutions. 41
2.9.	The frequency-dependence of $C_{cell}'$ for some organic solvents. 43
2.10.	The frequency-dependence of $C_{cell}'$ for mixed solvents. 44
2.11.	The frequency-dependence of $R_{cell}$ , $X_{cell}'$ , and $Z_{cell}$ for octanol saturated with water. 45
2.12.	Calibration curve for determination of relative permittivity. 47
2.13.	Relative permittivity as a function of mole fraction of alcohol for 1-pentanol - water and 1-octanol - water mixtures. 50

<u>Figure</u>	<u>Page</u>
CHAPTER 3	
3.1. The molal mean activity coefficients, $\gamma_{ms}^m$ , as a function of the molal concentration for binary electrolytes in water.	68
3.2. The specific conductivity of octanol that has been equilibrated with an aqueous salt solution of LiCl, NaCl, or KCl with the indicated mean molar activity.	74
3.3. The specific conductivity of octanol that has been equilibrated with a HCl solution of the indicated mean molar activity.	79
3.4. The specific conductivity of octanol that has been equilibrated with an aqueous salt solution of $MgCl_2$ or $CaCl_2$ with the indicated mean molar activity.	81
CHAPTER 4	
4.1a. Clay mineral analysis procedures: the preparation of sample suspensions.	104
4.1b. Clay mineral analysis procedures: the treatment of sample slides for X-ray diffraction analysis.	105
4.2a. The flow chart for the procedures of washing sorbents: an individual tube washing method.	108
4.2b. The flow chart for the procedures of washing sorbents: a large volume washing method.	109
4.3a. The flow chart of the procedures for batch adsorption experiments: by a combustion method.	111
4.3b. The flow chart of the procedures for batch adsorption experiments: by an extraction method.	112
4.4a. Calibration curve for the determination of LAS in the aqueous phase.	119
4.4b. Calibration curve for the determination of LAS in the sorbent phase by combustion method.	120
4.4c. Calibration curves for the determination of C-12 LAS in the aqueous and the sorbent phase by extraction method.	121
4.5a. Control charts for calibration of C-12 LAS in aqueous phase.	122

<u>Figure</u>	<u>Page</u>
4.5b. Control charts for calibration of C-12 LAS in the sorbent phase.	123
4.5c. Control charts for combustion recovery of C-12 LAS in the sorbent phase.	
4.6a. Control charts for material recoveries of C-12 TMAC and $A_{13}E_m$ .	127
4.6b. Control charts for material recoveries of LAS.	128
4.7a. A control chart for calibration of pH: the slope k.	130
4.7b. A control chart for calibration of pH: the intercept $E^{\circ'}$ .	131
4.8. Test of washing times: $A_{260}$ vs. $C_s(w)$ .	134
4.9. Comparison small vs. large volume washing methods.	135
4.10. Comparison of combustion vs. extraction and concentration difference methods for analysis of C-12 LAS adsorbed on soil sorbent EPA-12.	137
CHAPTER 5	
5.1. Adsorption isotherms of $A_{13}E_6$ on different sorbents.	149
5.2. Effect of added $Ca^{2+}$ on adsorption of $A_{13}E_m$ .	152
5.3. Effect of added $NaN_3$ on adsorption of $A_{13}E_m$ .	155
Chapter 6	
6.1a. Adsorption isotherms of C-12 LAS on different sorbents at higher concentrations of C-12 LAS.	172
6.1b. Adsorption isotherms of C-12 LAS on different sorbents at lower concentrations of C-12 LAS.	173
6.2. Effect of added $Ca^{2+}$ on adsorption of LAS.	174
6.3. Adsorption isotherms of C-12 LAS on sorbent EPA-12 at different ratios of sorbent to solution.	177
CHAPTER 7	
7.1. The electrical double layer at solid/liquid interface.	197
7.2. Adsorption density of dodecyl sulfonate ions on alumina and the zeta potential of alumina as a function of the concentration of sodium dodecyl sulfonate.	201

<u>Figure</u>	<u>Page</u>
7.3a. Schematic description of S-type isotherm by patchwise adsorption model.	203
7.3b. Configuration of adsorbed anionic surfactant molecules.	204
7.4. A flow chart of the procedures for determination of zeta potentials.	214
7.5a. Precision of $\mu$ measurements.	219
7.5b. Precision of $\zeta$ measurements.	220
7.6. Effect of chain length on adsorption of LAS on EPA-12.	224
7.7a. Electrophoretic mobility of the sorbent EPA-12 particles as a function of aqueous concentration of C-10, C-12, and C-14 LAS.	225
7.7b. Electrophoretic mobility of the sorbent EPA-12 particles as a function of surface concentration of C-10, C-12, and C-14 LAS.	226
7.8a. Control of pH for adsorption isotherm of C-12 LAS on soil EPA-12 at pH $4.94 \pm 0.04$ .	229
7.8b. Control of pH for adsorption isotherm of C-12 LAS on soil EPA-12 at pH $7.31 \pm 0.03$ .	230
7.8c. Control of pH for adsorption isotherm of C-12 LAS on soil EPA-12 at pH $8.89 \pm 0.14$ .	231
7.9. Adsorption isotherms of C-12 LAS on soil EPA-12 at different pH: 4.94, 7.31, and 8.89.	232
7.10. Adsorption isotherms of C-12 LAS on soil EPA-12 in 0.01 M $\text{NaN}_3$ and 0.001 M $\text{NaN}_3$ .	233
7.11a. A comparison of $\Delta \log K$ vs. $\Delta \log D_c$ for C-10 LAS.	240
7.11b. A comparison of $\Delta \log K$ vs. $\Delta \log D_c$ for C-12 LAS.	241
7.12a. Effect of chain length on hemimicelle formation.	244
7.12b. Effect of pH on hemimicelle formation.	245
7.12c. Effect of salt concentration on hemimicelle formation.	246

## LIST OF TABLES

<u>Table</u>	<u>Page</u>
CHAPTER 2	
2.1. Studies of conductivities of nonaqueous electrolyte solutions.	10
2.2. Values of $R_{cell}$ and $C_{cell}'$ for the test cells.	33
2.3. Values of $R_{cell}$ and $C_{cell}'$ for the samples of octanol saturated with KCl aqueous solutions.	36
2.4. Relative permittivity and capacitance at 25 °C for some organic solvents and alcohol/water mixture.	48
CHAPTER 3	
3.1. Distribution reactions of inorganic salts between octanol and water, and ion-pair formation reactions of inorganic salts in octanol.	60
3.2a. Mathematical formulation of the Donnan equilibrium model for distribution of LiCl, NaCl, and KCl between octanol and water. The numbers in the table are the stoichiometric coefficients of the components in species, that is, the $a(i, j)$ in Equation 3.1 - 3.3.	64
3.2b. Mathematical formulation of the Donnan equilibrium model for distribution of $MgCl_2$ and $CaCl_2$ between octanol and water. The numbers in the table are the stoichiometric coefficients of the components in species, that is, the $a(i, j)$ in Equation 3.1 - 3.3.	65
3.2c. Mathematical formulation of the Donnan equilibrium model for distribution of HCl between octanol and water. The numbers in the table are the stoichiometric coefficients of the components in species, that is, the $a(i, j)$ in Equation 3.1 - 3.3.	66
3.3. The equilibrium constants for distribution and ion-pair formation reactions.	73
3.4. Conductivity of electrolytes in octanol saturated with water at 25 °C.	77
3.5. The limiting equivalent conductivities of the inorganic salts in water and alcohols at 25 °C.	87

<u>Table</u>		<u>Page</u>
CHAPTER 4		
4.1.	Studies of adsorption of surfactants on prinstine sorbents.	94
4.2.	Studies of adsorption of surfactants on natural materials	96
4.3.	Overview of the methods and tests on adsorption of surfactants.	100
4.4.	Surfactants and characteristics.	101
4.5.	Properties of environmental sorbents.	103
4.6.	Verification of analytical methods for batch adsorption experiments: the calibrations.	118
4.7.	Verification of analytical methods for batch adsorption experiments: the material recoveries.	126
4.8.	Adsorption of surfactants on experimental materials	132
CHAPTER 5		
5.1.	Adsorption isotherms of $A_{13}E_6$ on different soil sorbents ( $C_s(w) = 0.024 \text{ g/mL}$ ) in $0.01 \text{ M NaN}_3$ . Values of parameters are determined from Freundlich model.	150
CHAPTER 6		
6.1.	Electrostatic model for adsorption	166
6.2.	Adsorption isotherms of LAS C-12 LAS on different soil sorbents ( $0.024 \text{ g/mL}$ ) in $0.01 \text{ M NaN}_3$ . Values of parameters from Freundlich and electrostatic models.	171
6.3.	Effect of $H^+$ and $Ca^{2+}$ on $D_c$ of LAS homologs on EPA-12 in $0.01 \text{ M NaN}_3$ . Parameter for Equation: $\log D_c = a \log [i] + b \text{ n-CH}_2^- + c$	175
6.4.	Adsorption Isotherms of C-12 LAS on EPA-12 in $0.01 \text{ M NaN}_3$ with different solid concentrations. Values of parameters from Freundlich Model.	178

TablePage

## CHAPTER 7

7.1.	The effect of chain length, pH, and ionic strength on the parameters $K_p$ and $n$ of the Freundlich isotherm in Region I and the aggregation number $n_H$ in Region II for adsorption of LAS on soil EPA-12.	223
7.2.	Parameters of Figure 7.12 a, b	239
7.3.	The aggregation number, $n_H$ , of ionic surfactants on pristine surfaces.	251

<u>Table</u>	<u>Page</u>
APPENDIX II	
II.1a. Results of x-ray identification for clay minerals in soil EPA-1.	282
II.1b. Results of x-ray identification for clay minerals in soil EPA-12.	283
II.1c. Results of x-ray identification for clay minerals in soil EPA-13.	284
II.1d. Results of x-ray identification for clay minerals in soil EPA-16.	285
II.1e. Results of x-ray identification for clay minerals in soil EPA-25.	286
II.1f. Results of x-ray identification for clay minerals in Lula Aquifer.	287
II.2. Clay mineral compositions in the environmental sorbents.	288

# LIST OF SYMBOLS

Symbol	Definition	Units
A	A matrix	-
A <sub>260</sub>	UV absorbance at wavelength of 260 nm	
a <sub>M</sub>	molar activity of cation	mol L <sup>-1</sup>
a <sub>ms</sub>	molar mean salt activity	mol L <sup>-1</sup>
a <sub>ms</sub> <sup>m</sup>	molal mean salt activity	mol kg <sup>-1</sup>
a <sub>X</sub>	molar activity of anion	mol L <sup>-1</sup>
C	interfacial capacitance	F m <sup>-2</sup>
C <sub>1</sub>	capacitance of cable #1	pF
C <sub>2</sub>	capacitance of cable #2	pF
C <sub>cable</sub>	cable capacitance	pF
C <sub>cell</sub>	cell capacitance	pF
C <sub>cell</sub> '	effective cell capacitance	pF
C <sub>edl</sub>	electrical double layer capacitance	pF
C <sub>i</sub>	concentration for species i	mol L <sup>-1</sup>
C <sub>i</sub> (s)	concentration of component i in sorbent	mol g <sup>-1</sup>
C <sub>i</sub> (w)	concentration of component i in water	mol L <sup>-1</sup>
C <sub>in</sub>	equipment input capacitance	pF
C <sub>in</sub> '	effective input capacitance	pF
CMC	critical micelle concentration	mol L <sup>-1</sup>
C <sub>0</sub> (w)	initial aqueous concentration	mol L <sup>-1</sup>
C <sub>stray</sub>	stray capacitance	pF
C <sub>s</sub> (w)	concentration of sediment in solution	g mL <sup>-1</sup>

Symbol	Definition	Units
$D_c$	concentration distribution ratio	$\text{mL g}^{-1}$
$E$	measured cell potential	mV
$E^{\circ'}$	thermodynamic constant specific to a given potentiometric cell	mV
$F$	Faraday constant	$\text{C mol}^{-1}$
$f$	frequency	Hz
$f_{oc}$	fraction of organic carbon in sediment or soil	-
$i_{A-B}$	complex current at A-B of the circuit	A
$i_B$	complex current at B of the circuit	A
$k$	slope in Nernst equation	
$K$	adsorption constant	$\text{m}^3 \text{ kg}^{-1}$
$K_i$	distribution equilibrium constant for species i	
$K_{ow}$	distribution constant between octanol and water	-
$K_p$	distribution constant between two phases	-
$1/A$	cell constant	$\text{cm}^{-1}$
$m$	molal concentration	$\text{mol kg}^{-1}$
$M$	molar mass of the salt	$\text{kg mol}^{-1}$
$n$	constant of Freundlich isotherm equation	-
$n$	number of methylene units in alkyl chain	-
$R$	ideal gas constant	$\text{J mol}^{-1} \text{ K}^{-1}$
$R_{cell}$	resistance of solution	$\text{M}\Omega$
$R_{in}$	equipment input resistance	$\text{M}\Omega$
$R_m$	measuring resistor	$\text{M}\Omega$

Symbol	Definition	Units
$s$	specific surface area	$\text{m}^2 \text{ kg}^{-1}$
$s$	the Onsager slope	
$T$	total concentration of a particular component	$\text{mol L}^{-1}$
$T$	temperature	K
$V_A$	complex voltage at point A of the circuit	mV
$V_B$	complex voltage at point B of the circuit	mV
$V_{A-B}$	complex voltage at A-B of the circuit	mV
$X_c$	capacitive reactance	$\text{M}\Omega$
$X_{\text{cell}}$	cell capacitive reactance	$\text{M}\Omega$
$X_{\text{H}_2\text{O}}$	mole fraction of water	-
$X_j$	free concentration of component j	$\text{mol L}^{-1}$
$X_{\Psi}$	Nernst item in Donnan equilibrium model	
$Y$	concentration difference	$\text{mol L}^{-1}$
$Z_{\text{cell}}$	impedance of cell	$\text{M}\Omega$
$Z_i$	charge on ion i	
$Z_{\text{in}}$	input impedance of input circuit	$\text{M}\Omega$
$Z_r$	Faradaic impedance	$\text{M}\Omega$
$\pi$	3.14159	
$\epsilon_0$	permittivity of free space	-
$\epsilon$	dielectric constant	-

Symbol	Definition	Units
$\Phi_D$	phase ratio in Donnan equilibrium model	-
$\kappa$	specific conductivity of salt	$\text{nS cm}^{-1}$
$\kappa^\circ$	specific conductivity of blank	$\text{nS cm}^{-1}$
$\lambda$	equivalent conductivity for ion i	$\text{cm}^2 \text{ S mol}^{-1}$
$\lambda^\circ$	equivalent conductivity for ion i extrapolated to infinite dilution	$\text{cm}^2 \text{ S mol}^{-1}$
$\Lambda$	equivalent conductivity of solution	$\text{cm}^2 \text{ S mol}^{-1}$
$\Lambda^\circ$	equivalent conductivity of solution extrapolated to infinite dilution	$\text{cm}^2 \text{ S mol}^{-1}$
$\nu$	stoichiometric coefficient	-
$\rho$	density of solution	$\text{kg dm}^{-3}$
$\rho^\circ$	density of solvent	$\text{kg dm}^{-3}$
$\gamma_{\text{ms}}^{\text{m}}$	molal mean salt activity coefficient	-
$\mu$	electrophoretic mobility of colloid particle	$\mu\text{m sec}^{-1} \text{ cm V}^{-1}$
$\eta$	viscosity of solvent	$\text{g cm}^{-1} \text{ sec}^{-1}$
$\zeta$	zeta potential of colloid	mV
$\sigma$	surface charge	$\text{C m}^{-2}$
$\Psi$	surface potential	V

A MECHANISTIC STUDY  
OF THE DISTRIBUTION OF AMPHIPHILIC ORGANIC COMPOUNDS  
BETWEEN WATER AND ORGANIC SORBENTS

CHAPTER 1

INTRODUCTION

This study was conducted to elucidate some of the factors that control the distribution of amphiphilic organic compounds (ionic and nonionic) between water and organic solvents and sorbents. Specifically, two types of systems were studied:

- (i) the speciation of LiCl, KCl, NaCl, HCl, MgCl<sub>2</sub>, and CaCl<sub>2</sub> in the two-phase system water | water-saturated octanol;
- (ii) the distribution of anionic surfactants (alkylbenzene-sulfonates) and neutral surfactants (monoalkyl ether of polyethylene glycols) between water and natural materials (soils, sediments, and aquifer materials).

The motivation for this research is the need to understand the factors that control the sorption of these amphiphilic organic compounds in the environment. Sorption affects not only the transport of the compounds in the aqueous environment, but also chemical and biological

transformations of the compounds and their biological availability. Thus an understanding of sorption is a prerequisite to research on fate and effects of these compounds. How the study of the two systems described above relates to the adsorption of amphiphilic organic compounds in the environment is discussed briefly below.

Distribution of inorganic salts between octanol and water. The two-phase octanol-water system has been used extensively in environmental and medicinal chemistry as a reference system for the distribution of nonpolar organic compounds between aqueous and nonaqueous phases (Leo and Hansch, 1971; Lyman et al., 1982). Correlations have been made between octanol-water partition constants and properties such as solubility, chromatographic retention, soil-water or sediment-water distribution ratios, and bioavailability or bioconcentration factors (e.g., Karickhoff et al., 1979; Veith et al., 1980; Hansch and Dunn, 1972; Schellenberg et al., 1984).

Whereas the octanol-water reference system is most readily applicable for the distribution of nonpolar organic compounds, its applicability for ionogenic and ionic organic compounds is being investigated (Schellenberg et al., 1984; Westall et al., 1985; Johnson and Westall, 1990). The goal of this approach is to describe the energy of adsorption of amphiphilic organic compounds in terms of three components: hydrophobic, electrostatic, and specific chemical interactions. The octanol-water system is a logical candidate as a reference system for hydrophobic interactions, due to the widespread use of that system as a reference for distribution of nonpolar organic compounds.

However, the transfer of an organic ion from water to octanol requires the transfer of a counter-ion; thus the observed distribution ratio becomes dependent on the nature and concentration of counter-ions in the water. In most simple distribution experiments, the counter-ions are those of a simple inorganic salt or buffer. However, even for these ions, a systematic investigation of the distribution between octanol and water still has not been made.

As an initial step towards understanding the behavior of organic ions in the octanol-water system, this study was undertaken to elucidate the distribution and speciation of simple salts ( $\text{LiCl}$ ,  $\text{NaCl}$ ,  $\text{KCl}$ ,  $\text{HCl}$ ,  $\text{MgCl}_2$  and  $\text{CaCl}_2$ ) between water and water-saturated octanol.

The method used for elucidation of speciation is conductometry. In Chapter 2 a method for determination of the conductivity and relative permittivity of water-saturated octanol is described; the conductivity data are used to elucidate speciation, and the permittivity data are used to estimate activity coefficients and ion-pair formation constants. The results of the speciation study are described in Chapter 3.

#### Adsorption of surfactants on environmental materials.

Surfactants are used in large quantities in industrial and consumer products and enter the environment through a variety of routes. Even though many of these compounds are reasonably degradable and not particularly toxic, the magnitude of the quantities in use requires that possible effects of these compounds in the environment be investigated thoroughly.

Several aspects of the environmental behavior of these compounds have been studied, including transport and fate (Thurman et al., 1986; Games 1983; Urano and Saito, 1984; Holysh et al., 1986; Sedlak and Booman, 1986), kinetics of degradation (Sales et al., 1987; Larson 1983; Robeck et al., 1963; Scheunert et al., 1987), and toxicity to organisms (Lewis and Wee, 1983).

Surfactants used in this research are homologs of alkylbenzene sulfonates (LAS) and homologs of monoalkyl ethers of polyethylene glycol (AE). A cationic surfactant, dodecyltrimethylammonium chloride (C-12 TMAC) was also briefly investigated in this study.

The distribution of the surfactants between aqueous solutions and environmental sorbents (e.g., soils, sediments, and aquifer materials) was studied primarily through equilibration of the surfactant between the sorbent and the solution in batch slurries, followed by phase separation and analysis. Experimental methods are described in detail in Chapter 4.

The adsorption of LAS and AE were studied as a function of homolog,  $\text{Ca}^{2+}$  concentration in solution, sorbent type, and sorbent concentration. The isotherms for adsorption of LAS were described empirically by the Freundlich isotherm and mechanistically with an electrostatic model. The adsorption of AE was described by a Freundlich isotherm. The isotherms of these surfactants were generally determined with low surfactant concentration in solution (less than 650 nM) and low surface surfactant concentration (less than 300 nmol/g). The experimental results for AE are described in Chapter 5 and those for LAS in Chapter 6.

The electrophoretic mobilities of the sorbent particles have also been determined as a function of LAS concentration. Hemimicelle formation has been observed from both the mobility experiments and the corresponding adsorption isotherms. The effects of the alkyl chain length of the LAS, the  $H^+$  concentration, and the ionic strength on LAS concentration at the onset of hemimicelle formation has been observed. The results of the electrophoretic mobility study are presented in Chapter 7.

A summary of results is presented in Chapter 8. The reader of this thesis should be aware that the chapters of the thesis are written in "proto-manuscript" form to facilitate submission of the chapters for publication; thus there is unavoidably some duplication of material from chapter to chapter.

## REFERENCES

- Games, L. M. "Practical Applications and Comparisons of Environmental Exposure Assessment Models" in Aquatic Toxicology and Hazard Assessment: Sixth Symposium, ASTM STP 802; Bishop, W. E., Cardwell, R. D., and Heidolph, B. B., Eds.; American Society for Testing and Materials, Philadelphia, 1983, 282-299.
- Hansch, C.; Dunn, W. J. III. J. Pharm. Sci. 1972, 61, 1-7.
- Holysh, M.; Paterson, S.; Mackay, D.; Bandurraga, M. M. Chemosphere 1986, 15, 3-20.
- Johnson, C. A.; Westall, J. C. Environ. Sci. Technol. 1990, 24, 1869-1875.
- Karickhoff S. W.; Brown, D. S.; Scott, T. A. Water Res. 1979, 13, 241-248.
- Larson, R. J. Residue Reviews 1983, 85, 159-171.
- Leo, A.; Hansch, C. J. Org. Chem. 1971, 36, 1539-1544.
- Lewis, M. A.; Wee, V. T. Environ. Tox. Chem. 1983, 2, 105-118.
- Lyman, W. J.; Reehl, W. F.; Rosenblatt, D. H. Handbook of Chemical Property Estimation Methods; McGraw-Hill: New York, 1982.
- Pilarczyk, M. and Klinszporn, L. Electrochimica Acta 1986, 31, 185-192.
- Robeck, G. G.; Cohen, J. M.; Sayers, W. T.; Woodward, R. L. Journal WPCF. 1963, 35, 1225-1236.
- Sales, D.; Quiroga, J. M.; Gomez-Parra, A. Environ. Sci. Technol. 1987, 39, 385-392.
- Schellenberg K.; Leuenberger, C.; Schwarzenbach R. P. Environ. Sci. Technol. 1984, 18, 652-657.
- Scheunert, I.; Vockel, D.; Schmitzer, J. Chemosphere 1987, 16, 1031-1041.
- Sedlak, R. I.; Booman, K. A. SDA Annual Convention 1986.
- Thurman, E. M.; Barber, L. B. Jr.; LeBlanc, D. Journal of Contaminant Hydrology 1986, 1, 143-161.
- Urano, K. and Saito, M. Chemosphere 1984, 13, 285-292.

Veith S. D.; Macek, D. J.; Petrocelli, S. R.; Carroll, J. Aquatic Toxicology, Eaton J. G., Passish P. R., Hendricks A. C., Eds; ASTM STP 707, 1980.

Westall, J. C.; Johnson, C. A.; Zhang, W. Environ. Sci. Technol. 1990, 24, 1803-1810.

## CHAPTER 2

### DEVELOPMENT OF TECHNIQUES FOR DETERMINATION OF CONDUCTIVITY AND RELATIVE PERMITTIVITY OF NONAQUEOUS SOLUTIONS

## INTRODUCTION

The conductivity of electrolyte solutions is of interest to those who study the behavior of organic and inorganic ions in solutions. Conductivity has been used in the study of ion association (Fuoss, 1978; Doe et al., 1984; Pilarczyk and Klinszporn, 1986; Hafez et al., 1987; Westall et al., 1990), ion complexation (Tanaka and Harada, 1976), and micellization of ionic surfactants (van Os et al., 1987; Okubo, 1988). A reliable determination of conductivity of electrolyte solutions requires the understanding of both physical and chemical processes which occur in the conductance cell and the understanding of factors which are within the measurement circuit.

Comprehensive reviews on the techniques of conductance determination have been made by Evans and Matesich (1973), Kratochvil and Yeager (1972), and Braunstein and Robbins (1971). Some recent studies of the conductivity of nonaqueous electrolyte solutions are summarized in Table 2.1.

The classical means used to determine the conductivity of electrolyte solutions is the AC Wheatstone bridge. This technique has been applied to determine the conductivity of both aqueous and nonaqueous solutions (Huang and Gilkerson, 1983; Mornica et al., 1984; Hafez et al., 1987). In the classical AC Wheatstone bridge, the frequency is fixed or adjusted manually. Other conductometers are equipped with circuitry to adjust the frequency automatically to optimize the ratio of signal to capacitive interference (Doe et al., 1984; Fang and Venable, 1987).

Table 2.1. Studies of conductivities of nonaqueous electrolyte solutions<sup>a</sup>.

Solvent	Equipment apparatus	$l/A$ $\text{cm}^{-1}$	Measurement Frequency kHz	$R^b$ $\text{k}\Omega$	Year	References Investigator
<u>Alcohols</u>						
MeOH	bridge	2.2	10		1965	Kay, et al.
EtOH, PrOH	bridge	0.8			1968	Evans and Gardam
BuOH, PhOH	bridge				1969	Evans and Gardam
iPrOH	bridge				1970	Matesich, et al.
iBuOH, iPhOH	bridge		2 and 5		1975	Broadwater, et al.
OcOH	bridge				1975	Highsmith
MeOH	bridge	0.08487	3		1979	Ono, et al.
OcOH					1982	Beronius, et al.
iPrOH	bridge	0.46694	2, 5, 10		1983	Wellington, Evans
iPrOH	bridge	0.28386	0.5, 1, 2		1983	Huang, Gilkerson
MeOH	conductometer				1984	Doe, et al.
<u>Alcohol/water mixtures</u>						
MeOH/Water	bridge	0.7422			1956	Shedlovsky, Kay
EtOH/Water	bridge		0.5-5		1965	Haves and Kay
EtOH/Water	bridge	0.43184	5 and 10		1967	Spivey, et al.
		6.4832				
PrOH/Water	bridge				1967	Goffredi, et al.
tBuOH/Water	bridge				1970	Broadwater, Kay
MeOH/Water	bridge		1		1978	Tissier, et al.
MeOH/Water	bridge				1985	Papadopoulos
<u>Other solvents</u>						
AN, DMF, PC and DMSO	amplifier and bridge		0.7-5		1976	Tanaka, Harada
AN	bridge	1.06565	2.5, 10	0.6-25.1	1984	Mornica, et al.
		0.04550				
THF	bridge	0.1	3	0.128-4.21	1985	Salomon, Plichta
DMF	bridge	0.30037	3	0.070-15	1986	Pilarczyk, et al.
DMF	bridge	0.03565	3	0.197-0.98	1987	Hafez, et al.
	conductometer		0.070, 1		1987	Fang, Venable

<sup>a</sup>. The symbol  $l/A$  represents cell constant of conductance cell in unit of  $\text{cm}^{-1}$ .

<sup>b</sup>. The symbol  $R$  represents measured resistance.

An alternative to the bridge-based methods is direct measurement of the real and imaginary components of an applied signal with a lock-in amplifier (DeSieno et al., 1971; Tanaka and Harada, 1976). This method, which has been used in this study, is particularly suited to the determination of the conductivities of high-impedance nonaqueous solutions.

In this technique, a conductivity cell, which is filled with a nonaqueous solution, is connected in series with a precision low-inductance metal-film resistor. The complex voltages across the cell and the resistor are measured by a lock-in amplifier. The resistance and capacitance of the cell are determined by analysis of an equivalent circuit, which includes the impedance of the cell, the impedance of the input circuit of the AC voltmeter, and the stray capacitances.

The measurements are performed over the AC frequency range of 5 Hz to 5 kHz. It has been verified that the effects of stray capacitances are accounted for satisfactorily through this approach. A computer is used to control the frequency and to collect and analyze the data. The typical magnitude of resistance measured for the samples is on the order of 1 to 10 M $\Omega$ .

A related technique has been developed to determine the relative permittivity (the dielectric constant) of solvents or solvent mixtures. The technique is similar to the one used for the determination of conductivity, except that the quantity of interest is capacitance, not resistance. In order to examine the effect of frequency on the measured capacitances, the determination is performed over the AC frequency range of 5 Hz to 100 kHz. The

frequency-independent capacitance of the 1-octanol - water and 1-pentanol - water mixtures were found at the range of frequency higher than a few kilohertz. The magnitude of capacitance of the samples are in the range of 90 to 900 pF.

The development of the methods for determination of conductivity and permittivity are described in detail in this chapter. Two applications of these techniques will be discussed: (i) determination of permittivities of alcohol-water mixtures (this chapter) and (ii) determination of conductivity of inorganic electrolytes in water saturated octanol (Chapter 3).

## THEORY

To determine accurately the conductivity and relative permittivity of high-impedance nonaqueous solutions, it is important to understand what physical and chemical processes occur within a conductance cell during the measurement and what factors in the external circuit may affect the determinations. The foci of this section will be (i) the equivalent circuit of a conductance cell; (ii) the measurement circuit; and (iii) the method for data analysis.

### Equivalent circuit of a conductance cell

Several processes can take place within a conductance cell during the measurement of conductivity (Braunstein and Robbins, 1971). To simplify the problem, a conductance cell can be represented as an electric equivalent circuit with simple electronic components, as shown in Figure 2.1a. Each component in the circuit represents an electrochemical process. The circuit in Figure 2.1a consists of four components:

(i) resistance of the cell,  $R_{\text{cell}}$ , which is related to the migration of ions in the electric field of the cell. From the  $R_{\text{cell}}$  the solution conductivity can be obtained:

$$\kappa = (1/R_{\text{cell}}) (1/A) \quad (2.1)$$

where  $\kappa$  is the specific conductivity in  $\text{S cm}^{-1}$ ,  $1/A$  is cell constant in  $\text{cm}^{-1}$ , and  $R_{\text{cell}}$  is in ohm ( $\Omega$ ).

### Equivalent Circuit of a Conductance Cell

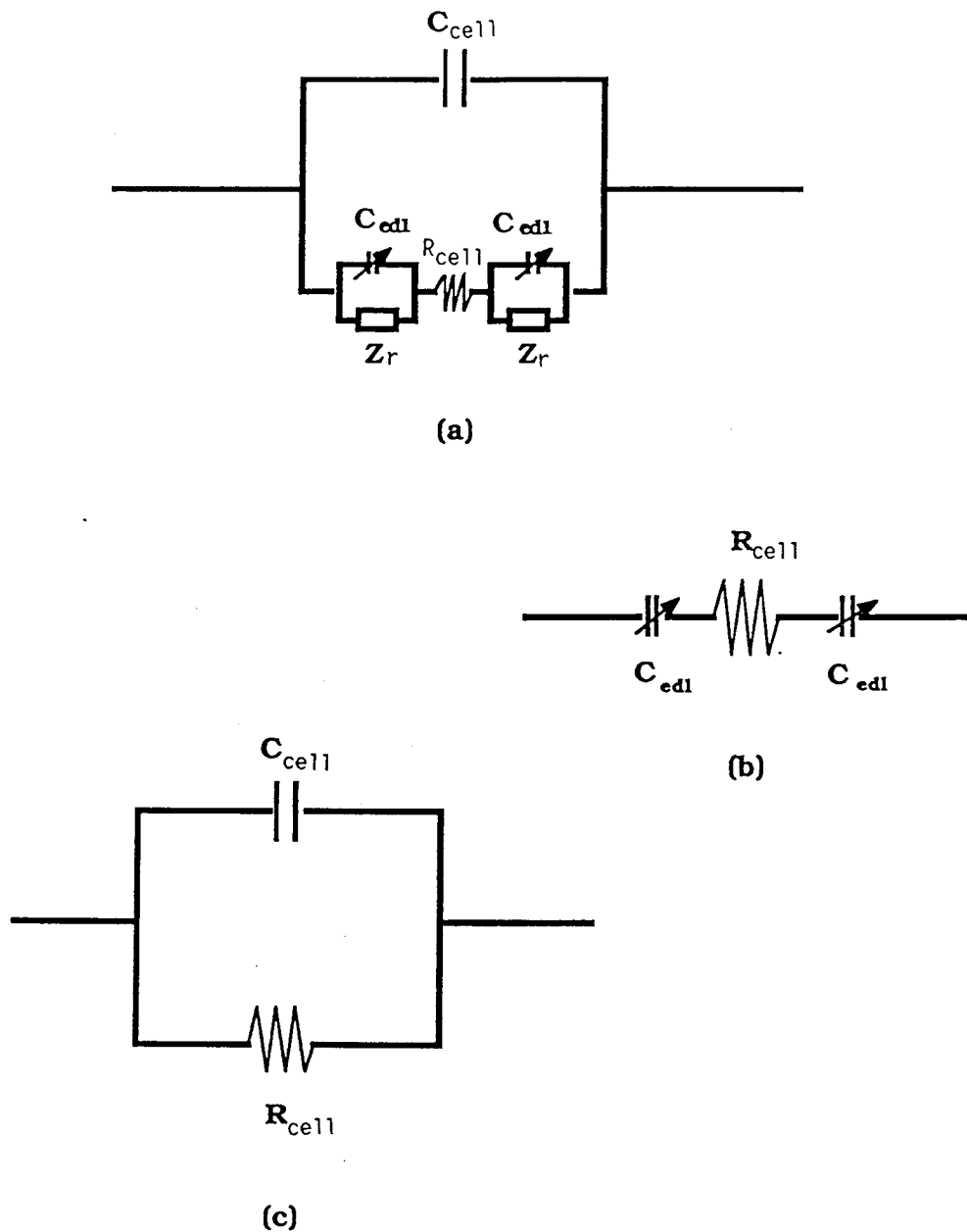


Figure 2.1. The equivalent circuit of a conductance cell: (a) combination of a resistance with a series capacitance and a parallel capacitance; (b) a series RC combination; (c) a parallel RC combination.

(ii) electrical-double-layer capacitance,  $C_{edl}$ , which represents the capacitance at the electrode surfaces due to electrical double layer phenomena. As shown in Figure 2.1a, the  $C_{edl}$  is in series with the  $R_{cell}$ . The typical value of  $C_{edl}$  is on an order of  $0.01 - 0.1 \text{ F m}^{-2}$  (Robinson and Stokes, 1968; and Kissinger and Heinemann, 1984).

(iii) the capacitance of the cell,  $C_{cell}$ , which is related to the permittivity of the solution and the dimensions of the cell:

$$C_{cell} = ( \epsilon_0 A/l ) \epsilon \quad (2.2)$$

where  $\epsilon_0$  is the permittivity of free space,  $\epsilon$  is the relative permittivity (the dielectric constant) of the medium, and  $A/l$  is the reciprocal of the cell constant. The typical value of  $C_{cell}$  is on the order of  $10 - 100 \text{ pF cm}^{-2}$  (Kissinger and Heinemann, 1984).

(iv) Faradaic impedance,  $Z_r$ , which is related to electron transfer between the electrode and species in solution. In this study the applied voltages are not large enough to cause electrolysis of the solvent, and there are no other electroactive species in solution. Thus the value of  $Z_r$  is very large and practically irrelevant for the conditions of this study; charge transfer at the electrode surface takes place through  $C_{edl}$ .

Simplification of the equivalent circuit. In this study, two parameters are of interest: the ohmic resistance of the cell,  $R_{cell}$ , for the determination of conductivity, and the capacitance of the cell,  $C_{cell}$ , for the determination of permittivity. The key to the determination of the value of one circuit element (e.g.,  $R_{cell}$  or

$C_{cell}$ ) while reducing interference from the others is the control of the frequency of the applied signal.

As we already know, capacitive reactance  $X_C$  is a frequency-dependent quantity, expressed as:

$$X_C = 1 / ( 2\pi f C ) \quad (2.3)$$

where  $f$  is frequency in Hertz (Hz),  $C$  is capacitance in farads (F), and  $X_C$  is the capacitive reactance in ohm ( $\Omega$ ). Therefore, for a given capacitance, the change in frequency will change the magnitude of the capacitive reactance and its contribution to the total impedance ( $Z$ ) in the circuit.

Thus the equivalent circuit shown in Figure 2.1a can be simplified into two extreme cases (assuming that the Faradaic impedance  $Z_F$  is not significant): (i) at low-frequencies, a series RC combination as shown in Figure 2.1b, and (ii) at high frequencies, a parallel RC combination shown in Figure 2.1c.

The equivalent circuit with a series RC combination, as shown in Figure 2.1b, is generally considered to be the case for determination of conductivity of aqueous electrolyte solutions and nonaqueous solutions with higher electrolyte concentrations. In these cases, the magnitude of  $R_{cell}$  is relatively small, e.g., on the order of  $10^2$  -  $10^4 \Omega$  for aqueous electrolyte solutions (Braunstein and Robbins, 1971), and the magnitude of the capacitive reactance  $X_C$  from the  $C_{ed}$  is on the same order as the magnitude of  $R_{cell}$ , especially, over low frequency range. Therefore, the contribution to the total impedance from the  $C_{ed}$  is significant, whereas the contribution

from the  $C_{cell}$  can be considered to be negligible since the  $X_C$  from the  $C_{cell}$  is much larger than the  $R_{cell}$ . In order to reduce the magnitude of  $X_{Ced}$  relative to  $R_{cell}$ , the measurement of conductivity is typically carried out at the frequency level of 1-10 kHz.

For determination of the conductivity of high impedance nonaqueous solutions, however, the magnitude of  $R_{cell}$  is relatively large, e.g., on the order of  $10^6 - 10^7 \Omega$  for the samples of 1-octanol saturated with KCl aqueous solutions. In this case, the effect from the  $C_{ed}$  is insignificant, whereas the magnitude of  $X_C$  from the  $C_{cell}$  can be on the same order as the  $R_{cell}$  especially over high frequency range. In this situation, the equivalent circuit of a conductance cell can be simplified as a parallel RC combination, as shown in Figure 2.1c. The contribution of  $X_C$  from  $C_{cell}$  to the total impedance can be reduced by determining the conductivity over low-frequency range.

For determination of the relative permittivity, the capacitance of the cell,  $C_{cell}$ , is the key parameter. The magnitude of  $X_C$  from  $C_{cell}$  is usually much larger than the magnitude of  $R_{cell}$ , as described in previous section. In this case, large portion of current will pass through the  $R_{cell}$  instead of  $C_{cell}$ . In order to decrease the magnitude of  $X_C$  from  $C_{cell}$ , the measurement of capacitance is generally performed over high frequency range.

In this study, the parallel RC combination, as shown in Figure 2.1c, is chosen as the equivalent circuit.

## Techniques for determination of $R_{\text{cell}}$ and $C_{\text{cell}}$

Measurement circuit. In the previous section, the electrochemical processes and the equivalent circuit of a conductance cell have been discussed. The focus of this section is the external measurement circuit. The equivalent circuit used in this study for determination of conductivity and permittivity is shown in Figure 2.2a. The circuit consists of several elements.

A sine wave ( $V_{\text{in}}$ ) of known amplitude, frequency, and phase is generated by the lock-in amplifier. The sine wave is applied across a series combination of the conductance cell, which is represented as the parallel  $R_{\text{cell}}$  and  $C_{\text{cell}}$  (from Figure 2.1c) and a low-inductance current-measuring resistor,  $R_m$ . The amplitude and phase of the sine wave is measured at Point B with the two-phase lock-in amplifier.

The cell can be either a real conductance cell or a test cell, for example, a low-inductance resistor. In parallel with the conductance cell is a stray capacitance,  $C_{\text{stray}}$ . Other capacitances are  $C_1$  and  $C_2$ , the cable capacitances.

Across the input of the lock-in amplifier is an input impedance, which is represented as the parallel RC combination,  $R_{\text{in}}$  and  $C_{\text{in}}$ , in accordance with the circuit diagram of the instrument. The reason why the input impedance of the lock-in amplifier is included in the equivalent circuit is because the resistances of the nonaqueous solutions used in this study are so high (e.g. in an order of 1 - 10 M $\Omega$ ) that the presence of  $R_{\text{in}}$  and  $C_{\text{in}}$  may affect the determination of either  $R_{\text{cell}}$  or  $C_{\text{cell}}$ .

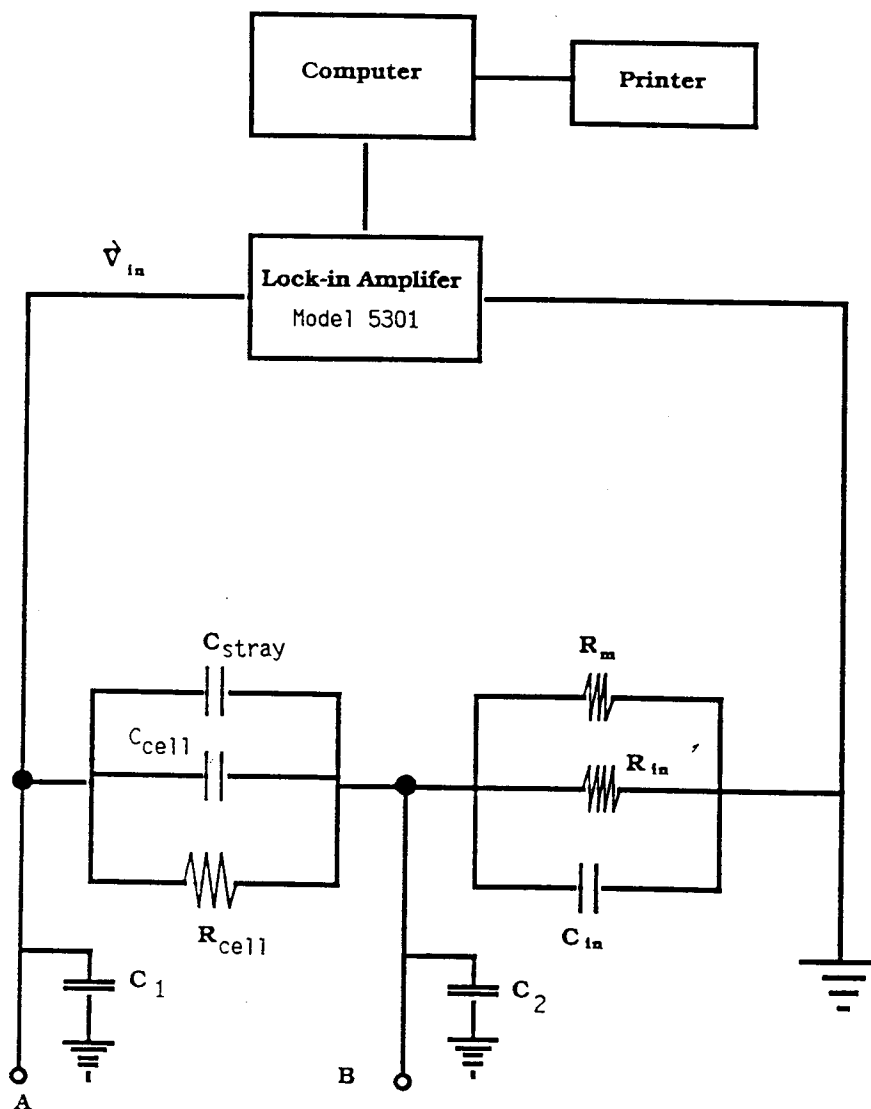


Figure 2.2a. Schematic diagram of equivalent circuit with stray capacitance and cable capacitance.

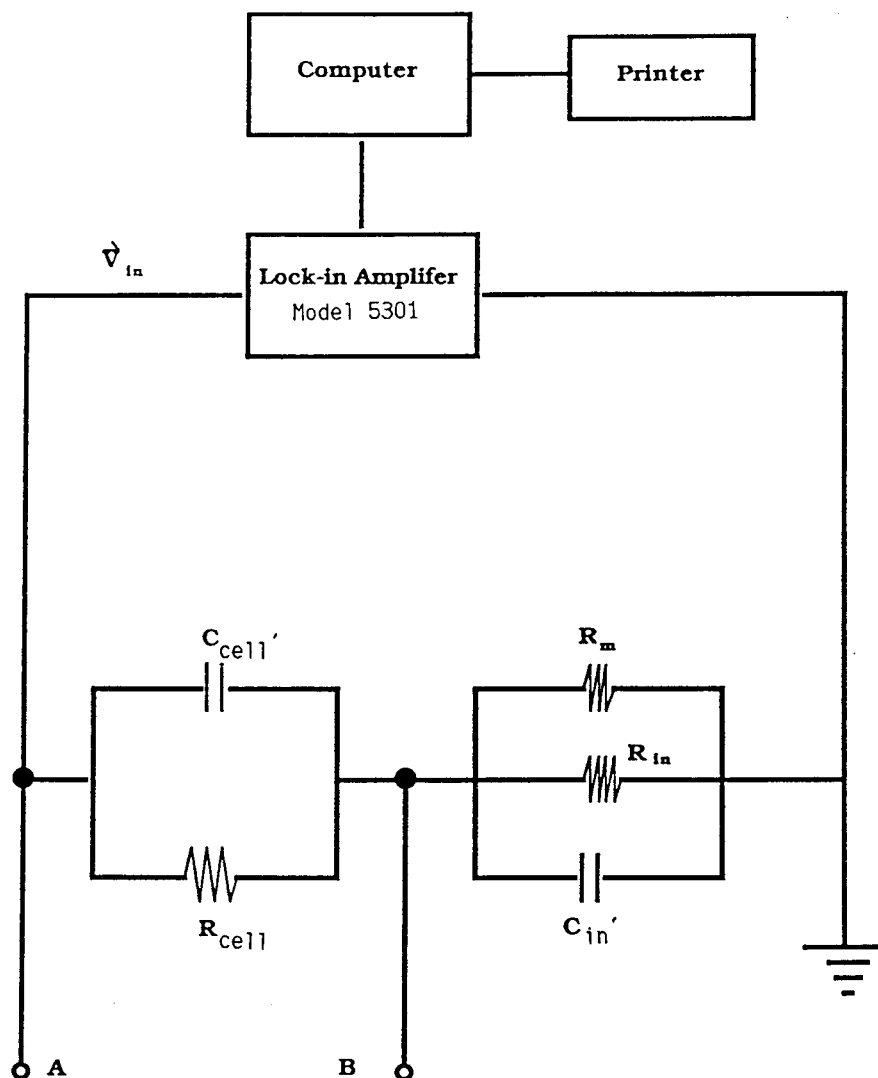


Figure 2.2b. Schematic diagram of equivalent circuit for calculation.

### Method for data analysis

Some of the circuit elements shown in Figure 2.2a can be combined into apparent circuit elements that are actually distinguishable in a set of measurements. Figure 2.2b shows a schematic diagram of this "reduced" equivalent circuit that was actually used for calculations.

The apparent cell capacitance,  $C_{cell}'$ , represents a parallel combination of the cell capacitance,  $C_{cell}$ , and the stray capacitance,  $C_{stray}$ , as expressed in Equation 2.4:

$$C_{cell}' = C_{cell} + C_{stray} \quad (2.4)$$

The apparent input capacitance,  $C_{in}'$ , represents a parallel combination of input capacitance,  $C_{in}$  (from manufacturer), and cable capacitance,  $C_2$ , as described in Equation 2.5:

$$C_{in}' = C_{in} + C_2 \quad (2.5)$$

The presence of  $C_1$  in Figure 2.2a has no effect, since, at the frequencies used in this study, the reactance associated with this capacitance is very large compared to the resistance of the cable and the output impedance of the oscillator. Thus any current passing through  $C_1$  would not load the test circuit at all.

The data analysis is broken into two sections. First the use of the equivalent circuit in Figure 2.2b to calculate  $R_{cell}$  and

$C_{cell}'$  is discussed. Then the determination of values for  $C_{stray}$ , and  $C_2$  (Figure 2.2a) will be discussed.

Determination of  $R_{cell}$  and  $C_{cell}'$ . Most of the quantities for the calculation are complex numbers. Therefore, it is necessary to review briefly the expression of the complex equations and the method of calculations.

A complex number is expressed in terms of its real component (the in-phase component), and its imaginary component (the out-of-phase component). Thus a complex impedance  $Z$  is expressed as:

$$Z = R - X_C j \quad (2.6)$$

where  $R$  is the real component (resistance) and  $X_C$  is the imaginary component (capacitive reactance), and  $j$  represents the complex number  $(-1)^{1/2}$ . If complex impedances, currents, and voltages are used in the usual equations for analysis of circuits, phase information is preserved, and resistance can be distinguished from reactance.

The values of  $R_{cell}$  and  $C_{cell}'$  are calculated from experimental data and the circuit in Figure 2.2b as follows. For simplicity, only complex equations will be described for derivation.

(i). The complex impedance of input circuit,  $Z_{in}$ , can be expressed from the parallel combination of  $R_m$ ,  $R_{in}$  and  $C_{in}'$ :

$$1/Z_{in} = [1/R_m + 1/R_{in}] + 1/X_{C_{in}'} j \quad (2.7)$$

(ii). The complex voltage at B,  $V_B$ , is calculated from the measured complex voltages,  $V_A$  and  $V_{A-B}$ , which are in series:

$$V_B = V_A - V_{A-B} \quad (2.8)$$

(iii). The complex current passing from point B to ground,  $i_B$ , can be easily calculated from Ohm's equation:

$$i_B = V_B / Z_{in} \quad (2.9)$$

Since the cell and the input circuit are connected in series, the complex current passing through the cell,  $i_{A-B}$ , and the complex current passing from B to ground should be equal in both amplitude and phase:

$$i_{A-B} = i_B \quad (2.10)$$

(iv). The complex impedance of the cell,  $Z_{cell}$ , is expressed as:

$$Z_{cell} = V_{A-B} / i_{A-B} \quad (2.11)$$

(v). Then the complex admittance of the cell,  $Y_{cell}$ , is obtained from the reciprocal of the impedance of the cell,  $Z_{cell}$ :

$$Y_{cell} = 1 / Z_{cell} \quad (2.12)$$

From  $Y_{cell}$ , the resistance  $R_{cell}$  and apparent capacitive reactance  $X_{Ccell}'$  of the cell can be obtained:

$$Y_{cell} = 1/R_{cell} + 1/X_{Ccell}' j \quad (2.13)$$

(vi). Finally, the apparent capacitance of the cell can be calculated:

$$C_{cell}' = 1 / (2 \pi f X_{Ccell}')$$
(2.14)

where the  $\pi$  is the constant 3.14159 and  $f$  is the frequency of the sine wave ( $V_A$ ).

In this study, the determination for each sample was carried out over a wide frequency range, e.g., from 5 Hz to 5 kHz for conductivity measurements, and from 5 Hz to 100 kHz for permittivity measurements. At each frequency, the computer recorded automatically the experimental data: frequency,  $f$ , and complex voltages,  $V_A$  and  $V_{A-B}$ , and calculated results:  $R_{cell}$  and  $C_{cell}'$ . Both determination and calculation were accomplished by a BASIC program, PC-5301L.BAS (Appendix I).

These calculations involved the simplified equivalent circuit in Figure 2.2b and the apparent capacitances  $C_{cell}'$  and  $C_{in}'$ . Next we discuss the full equivalent circuit in Figure 2.2a and the effects of  $C_2$  and  $C_{stray}$ . For reasons stated above the cable capacitance  $C_1$  has no effect.

Cable capacitance,  $C_2$ . Cable #2 connects the cell to the B-input of the instrument. The apparent capacitance in the input

circuit,  $C_{in}'$ , equals to the sum of the input capacitance from the amplifier,  $C_{in}$  (a known parameter from the manufacturer) and cable capacitance,  $C_2$  (an unknown parameter).

To calculate the value of  $C_2$ , a dummy cell with a low-inductance metal-film resistor was placed in the circuit. Relatively low values of  $R_{cell}$  ensure that the effect of  $C_{stray}$  is negligible. Under these conditions, the value calculated for  $R_{cell}$  by the procedure above should be independent of frequency. Then data are collected, and various values of  $C_{in}'$  are tried until  $R_{cell}$  does indeed become independent of frequency over the frequency range 5 Hz to 5 kHz.

Stray capacitance. Stray capacitance,  $C_{stray}$ , includes the capacitance across the leads of the cell, but excludes the capacitance due to the plates of the cell themselves. This capacitance is in parallel with the capacitance of the plates of the cell,  $C_{cell}$ , and the cell resistance  $R_{cell}$ . Therefore, the apparent capacitance across the cell,  $C_{cell}'$ , is actually a sum of the  $C_{cell}$  and the  $C_{stray}$  (Equation 2.4).

Two methods have been used in this study to calculate  $C_{stray}$ . In the first method, several low-inductance metal-film resistors with known values of resistance are used as test cells. The inductances of these resistors themselves are very small and negligible. The  $R_{cell}$  and  $C_{cell}'$  of the test cells are determined over the entire range of the frequency, and the value of  $C_{cell}'$  that is obtained from the measurements is considered to be the stray capacitance.

The second method for evaluation of  $C_{\text{stray}}$  is achieved by the relative permittivity study. Theoretically, the cell capacitance  $C_{\text{cell}}$  is related only to the permittivity of the medium and the cell constant, as expressed in Equation 2.2. However, during the measurement, the stray capacitance has to be taken into account. Thus, the apparent cell capacitance can be expressed as:

$$C_{\text{cell}}' = ( \epsilon \epsilon_0 A / l ) + C_{\text{stray}} \quad (2.15)$$

In this study, five organic solvents with known relative permittivities have been used as the standard solvents. The apparent cell capacitance,  $C_{\text{cell}}'$ , can be plotted as a function of the relative permittivity of the solvents. Thus the value of the  $C_{\text{stray}}$  can be obtained from the intercept of the plot, which is determined by a linear least-squares parameter optimization method. In order to increase the magnitudes of the cell capacitances,  $C_{\text{cell}}$ , over the magnitude of stray capacitance, a particular cell with small cell constant can be used.

The  $C_{\text{stray}}$  obtained from the two methods will be discussed in a later section.

## EXPERIMENTS

Materials and equipment. The solvent mixture used in the conductivity study was 1-octanol saturated with deionized water. The 1-octanol was analytical reagent from J.T. Baker Inc. The deionized water was from a Millipore Milli-Q system. The density and viscosity of the solvent mixture at 25 °C were  $0.8303 \text{ g cm}^{-3}$  and 7.275 cp as determined by pycnometer and capillary viscometer, respectively. The specific conductivity of the solvent mixture was in the range  $4 - 19 \text{ nS cm}^{-1}$ . The solute used in the experiments was potassium chloride purchased from EM Science. (The application of the technique described here with other salts is described in Chapter 3.)

The solvents used in the permittivity study were: 1-pentanol (analytical reagent) from Fluka Inc.; 1-octanol (analytical reagent) from J.T. Baker Inc.; hexane, ethyl acetate, and iso-propyl alcohols (spectrophotometry grade) from EM Science. All of the solvents were used as purchased; no further purification was done.

The cell used for the conductivity study was a Brinkmann Model EA 660-01 pipet cell with bright platinum electrodes. The cell constant was  $0.078 \text{ cm}^{-1}$  and the volume of the cell was approximately 2 mL.

For the permittivity study, a high-capacitance variable capacitor was used to increase the magnitude of the cell capacitance over the stray capacitance. The cell constant was  $0.00211 \text{ cm}^{-1}$  and the volume of the cell was approximately 60 mL. Both the capacitance and the resistance of the cell,  $C_{\text{cell}}$  and  $R_{\text{cell}}$ , were measured at 25 °C. The temperature was controlled by HAAKE G and HAAKE D1

thermostats. The cells and the other electronic components in the circuit, such as the current-measuring resistor ( $R_m$ ), were set in a shielding chamber made of aluminum screen to reduce electrical interference. The in-phase and out-of-phase components of voltage across the cell and the input circuit were determined with a Princeton Applied Research Model 5301 Lock-in Amplifier with a Model 5316 Preamplifier. The measurement and data analysis were controlled by a computer.

Sample preparations. The samples for the conductivity study were solutions of octanol saturated with aqueous KCl solutions. The samples were prepared as follows. The aqueous KCl solutions were prepared in the concentration range of 0.01 M to 1.00 M. The octanol was pre-equilibrated with water before contact with the aqueous KCl solution. This pre-equilibration step is essential as described in detail in Chapter 3. After the pre-equilibration, 10 mL of aqueous KCl solution and 10 mL of pre-equilibrated octanol were added into a 25-mL Corex glass centrifuge tube, and the tubes were tightly capped with Teflon-lined caps. Then solutions were agitated on a thermostatted shaker (New Brunswick Model G-24) at 500 RPM for 2 hours at 25 °C. Subsequently, the tubes were centrifuged at 11,000 G (10,000 RPM) by an IEC Model B-20A thermostatted centrifuge for 10 minutes to separate the two phases. After equilibration and phase separation, an aliquot of the octanol phase was transferred into the conductivity cell for the measurement. Approximately 6 mL were used for rinsing the cell and 2 mL for the measurement of  $R_{cell}$ .

The samples for the permittivity study were mixtures of water and 1-octanol, and water and 1-pentanol. The mole fractions of water in the mixtures were in the range 0.00 to 0.30. The samples were prepared by weight. After the samples were mixed, the densities of the samples were determined by pycnometer at 25 °C. The samples were then transferred into the cell for the measurement of  $C_{cell}$ . Besides the sample measurement, the capacitances of five organic solvents with known dielectric constants were also determined to obtain the calibration curve.

The samples were prepared and measured in triplicate for the conductivity experiments and in duplicate for the permittivity experiments.

Measurement procedures. The measurements and calculations of  $R_{cell}$  and  $C_{cell}$  were controlled by a computer with a BASIC program PC-5301L.BAS (Appendix I). After the measurement started, the instrument automatically waited 5 minutes for the solution to reach 25 °C. Then, an AC sinusoidal voltage signal from the oscillator output of the lock-in amplifier was sent out to the measurement system. The amplitude of the applied potential was set at 500 mV for all of the measurements. The range of AC frequencies was set from 5 to 5,000 Hz for the measurement of  $R_{cell}$  and 5 to 100,000 Hz for the measurement of  $C_{cell}$ , respectively. The complex voltage at the point A,  $V_A$ , and the complex voltage across the cell,  $V_{A-B}$ , as shown in the circuit (Figure 2.2a), were determined at each frequency by the phase-sensitive detector. The computer controlled the measurement frequency, the data collection, and the data analysis.

## RESULTS AND DISCUSSIONS

Verification of methods

Determination of the effective cable capacitance. The cable capacitance,  $C_2$  (see Figure 2.2a), was determined by the method described in the section on theory. The test cells used for the determination were metal-film resistors with values of 200 k $\Omega$ , 2.0, 5.0 and 10 M $\Omega$  with 1% tolerance. Figure 2.3 shows the results of this test. The open symbols indicate the  $R_{cell}$  calculated without inclusion of  $C_2$ . In this case, the total  $C_{in}'$  equals the instrument input capacitance  $C_{in}$ , which is 30 pF as reported by the manufacturer. The solid symbols represent the  $R_{cell}$  calculated with  $C_2 = 140$  pF,  $C_{in} = 30$  pF, and  $C_{in}' = 170$  pF.

As shown in Figure 2.3, with the inclusion of  $C_2$ ,  $R_{cell}$  is constant over the full range of frequency for all of the four test cells. Without  $C_2$ ,  $R_{cell}$  remains constant only at frequencies lower than 100 Hz and increases with frequency. This effect is stronger for the test cell with smaller resistance. The result in Figure 2.3 indicates that the correction of cable capacitance is essential if the values of measured  $R_{cell}$  are low. The value of  $C_2 = 140$  pF is used in all calculations.

Determination of  $C_{stray}$ . Two methods have been used for determination of the stray capacitance,  $C_{stray}$  (Figure 2.2a). In the first method, the  $C_{cell}'$  of "dummy" cells are considered to be the  $C_{stray}$ , as described in the previous section. For the four test cells with the resistances of 0.2, 2.0, 5.0, and 10 M $\Omega$ , the values of

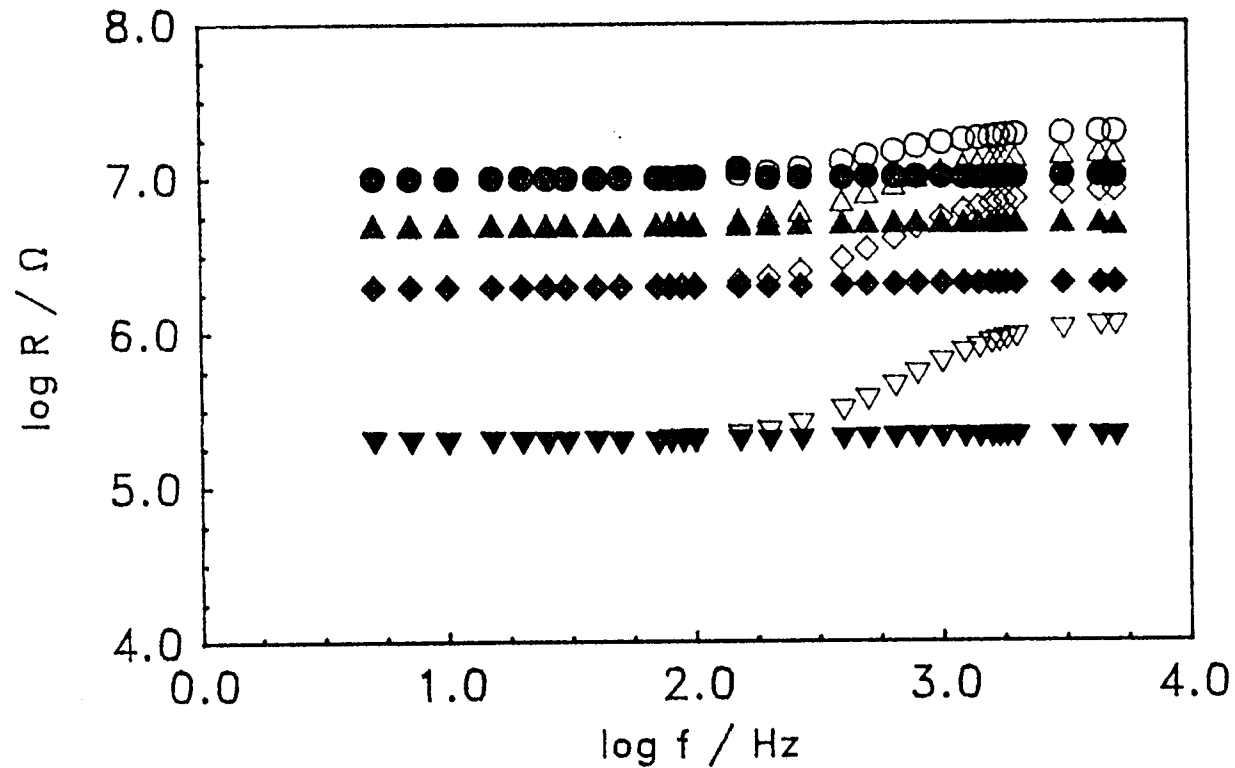


Figure 2.3. The frequency-dependence of the value of  $R_{cell}$  calculated for two values of  $C_{in}'$ . Solid symbols represent the  $R_{cell}$  which were determined with  $C_{in} = 30$  pF; and open symbols represent the  $R_{cell}$  which were determined with  $C_{in}' = 170$  pF. The resistances of the test cells are: (1) circle -  $10\text{ M}\Omega$ ; (2) triangle -  $5.0\text{ M}\Omega$ ; (3) diamond -  $2.0\text{ M}\Omega$ ; and (4) inverted triangle -  $200\text{ k}\Omega$ . The measuring resistance,  $R_m$ , was  $2.0\text{ M}\Omega$ .

the measured  $R_{\text{cell}}$  and the  $C_{\text{cell}}'$  after the correction of the cable capacitance are listed in Table 2.2. The typical value of the  $C_{\text{stray}}$  obtained from this method is 13 pF.

The second method for correction of  $C_{\text{stray}}$  is from calibration of the  $C_{\text{cell}}'$  vs. the dielectric constant  $\epsilon$  for certain organic solvents. Five organic solvents are used in this study. These are hexane, ethyl acetate, 1-octanol, 1-pentanol, and iso-propanol. The values of the  $C_{\text{cell}}'$  were determined by the technique described previously. The dielectric constants  $\epsilon$  for these solvents (Table 2.4) were quoted from the literature. Based on Equation 2.15, the  $C_{\text{stray}}$  is obtained to be 13 pF, from the intercept of the plot of the  $C_{\text{cell}}'$  vs. the  $\epsilon$ . The  $C_{\text{stray}}$  obtained from the two methods are consistent, although the geometries of the cells are different.

Frequency dependence of  $Z_{\text{cell}}$ ,  $X_{\text{cell}}$ , and  $R_{\text{cell}}$  for a test cell. The frequency dependence of the resistance  $R_{\text{cell}}$ , the capacitive reactance  $X_{\text{cell}}$ , and the impedance  $Z_{\text{cell}}$  of the test cell with a 2.0 M $\Omega$  resistor are illustrated in Figure 2.4. The  $R_{\text{cell}}$  is constant in the frequency range of 5 to 5,000 Hz. At frequencies less than 100 Hz, the impedance of the cell,  $Z_{\text{cell}}$ , is independent of the frequency and equal to  $R_{\text{cell}}$ . At higher frequencies,  $Z_{\text{cell}}$  begins to decrease with  $X_{\text{cell}}$ .

#### Determination of $R_{\text{cell}}$ of KCl in water-saturated octanol

Frequency dependence of  $R_{\text{cell}}$ . Octanol was saturated with aqueous solutions of KCl (0.01, 0.05, 0.1, 0.2, and 0.4 M) and was placed in the Brinkmann conductance cell. The value of  $R_{\text{cell}}$  was

Table 2.2. Values of  $R_{\text{cell}}$  and  $C_{\text{cell}}'$  for the test cells.

Test cell	$R^a$ $M\Omega$	$C_{\text{in}}'$ pF	$R_m$ $M\Omega$	$R_{\text{cell}}^b$ $M\Omega$	$C_{\text{cell}}'^c$ pF
1	0.2	170	2.0	$0.20 \pm 0.02$	$10.7 \pm 3.1$
2	2.0	170	2.0	$2.00 \pm 0.01$	$13.2 \pm 0.4$
3	5.0	170	2.0	$5.02 \pm 0.02$	$13.2 \pm 0.2$
4	10	170	2.0	$10.14 \pm 0.04$	$13.3 \pm 0.1$

<sup>a</sup>. The values of the resistances for the test cells are from the manufacturers.

<sup>b</sup>. These resistances,  $R_{\text{cell}}$ , were measured and calculated by the PC - lock-in amplifier system with correction for the cable capacitance ( $C_2 = 140$  pF).

<sup>c</sup>. The  $C_{\text{cell}}'$  were the average of capacitances determined in the frequency range of 1 - 5 kHz.

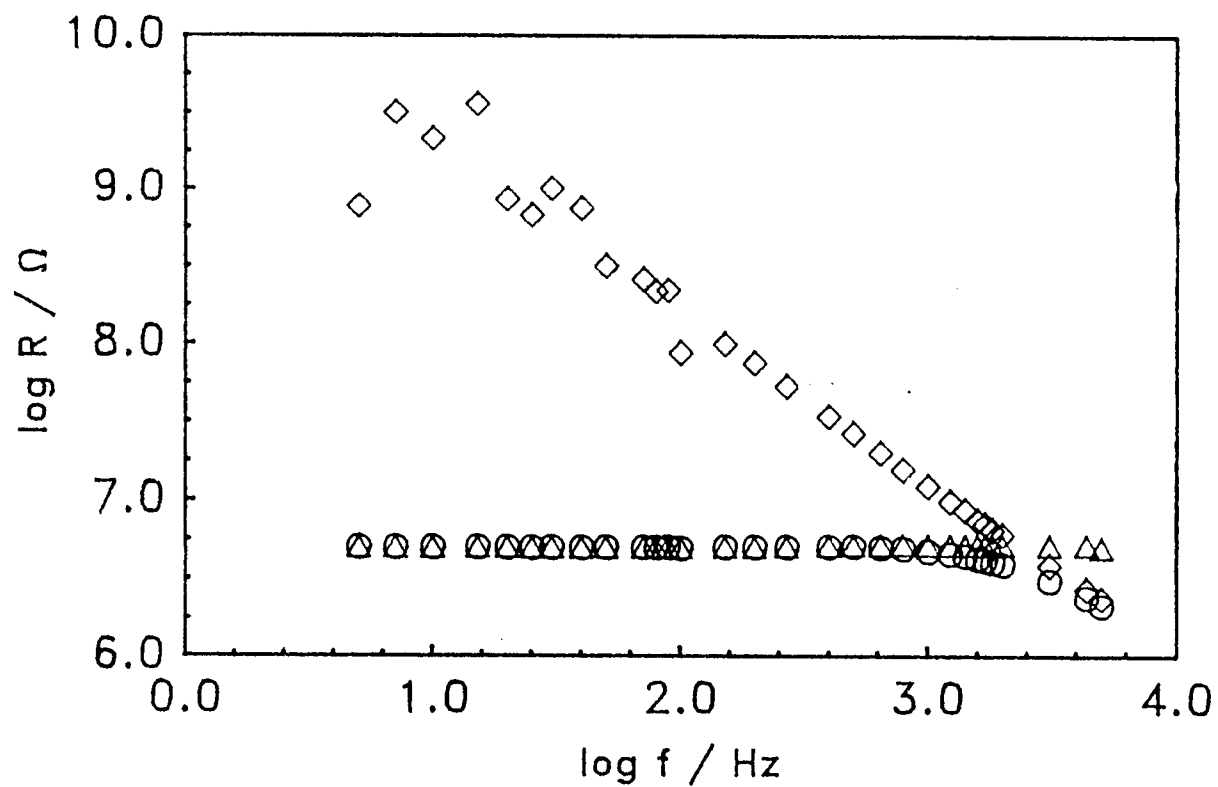


Figure 2.4. The frequency-dependence of  $R_{\text{cell}}$ ,  $X_{\text{Ccell'}}$ , and  $Z_{\text{cell}}$  for test cell ( $R_{\text{cell}} = 5.0 \text{ M}\Omega$ ). The symbols represent: triangle -  $R_{\text{cell}}$ ; diamond -  $X_{\text{cell}}$ ; and circle -  $Z_{\text{cell}}$ .  $R_{\text{m}} = 2.0 \text{ M}\Omega$ , and  $C_{\text{in'}} = 170 \text{ pF}$ .

determined over the frequency range of 5 Hz to 5000 Hz. Solution preparation and analysis was carried out in triplicate for all concentrations.

The average values of  $R_{cell}$  for four of the solution concentrations are shown as a function of frequency in Figure 2.5. Generally, the values of  $R_{cell}$  remain constant over the entire range of the frequency, especially at frequencies less than 100 Hz. These frequency independent resistances are considered to be the true values of resistances of the samples.

It is known that the contribution of double-layer capacitance,  $C_{edl}$ , to the equivalent circuit is more significant at lower frequencies. Our results show that the measured  $R_{cell}$  is very constant in the low frequency range, indicating that the reactance due to the  $C_{edl}$  is negligible compared to  $R_{cell}$ .

The values calculated for  $R_{cell}$  and  $C_{cell}$  are presented in Table 2.3 for the five concentrations of KCl. The values of  $C_{cell}$  are about 24 pF, corresponding to a reactance of 6.6 M $\Omega$  at 1000 Hz. The  $R_{cell}$  of each sample was measured in triplets with relative error generally less than 3%.

Comparison of the frequency dependence of  $X_{cell}$ ,  $R_{cell}$  and  $Z_{cell}$  of the conductance cell with octanol equilibrated with 0.01 M KCl is shown in Figure 2.6. The resistance remains constant at all frequencies from 5 to 5000 Hz. The parallel capacitive reactance  $X_{cell}$  decreases with the increase of the frequency and is equal to the resistance at about 1000 Hz. This result underscores the importance of using the low frequency range for high impedance samples.

Table 2.3. Values of  $R_{\text{cell}}$  and  $C_{\text{cell}}'$  for the samples of octanol saturated with KCl aqueous solutions.

KCl (w)	$C_{\text{in}}'$	$R_m$	$R_{\text{cell}}^a$	$C_{\text{cell}}'^b$
M	pF	M $\Omega$	M $\Omega$	pF
0.01	170	2.0	$5.27 \pm 0.32$	$23.6 \pm 0.3$
0.05	170	2.0	$2.68 \pm 0.05$	$24.1 \pm 0.3$
0.10	170	2.0	$1.45 \pm 0.03$	$24.6 \pm 0.7$
0.20	170	2.0	$0.96 \pm 0.03$	$24.5 \pm 1.2$
0.40	170	2.0	$0.55 \pm 0.00$	$24.7 \pm 1.1$

a. The resistances  $R_{\text{cell}}$  were measured and calculated by the PC - lock-in amplifier system with correction for the cable capacitance ( $C_2 = 140$  pF). The  $R_{\text{cell}}$  for each sample is the average of triplicate determination (solution preparation and analysis).

b. The  $C_{\text{cell}}'$  listed were determined and calculated in the frequency range of 1 - 5 kHz. The  $C_{\text{cell}}'$  for each sample is the average of triplicate determination (solution preparation and analysis).

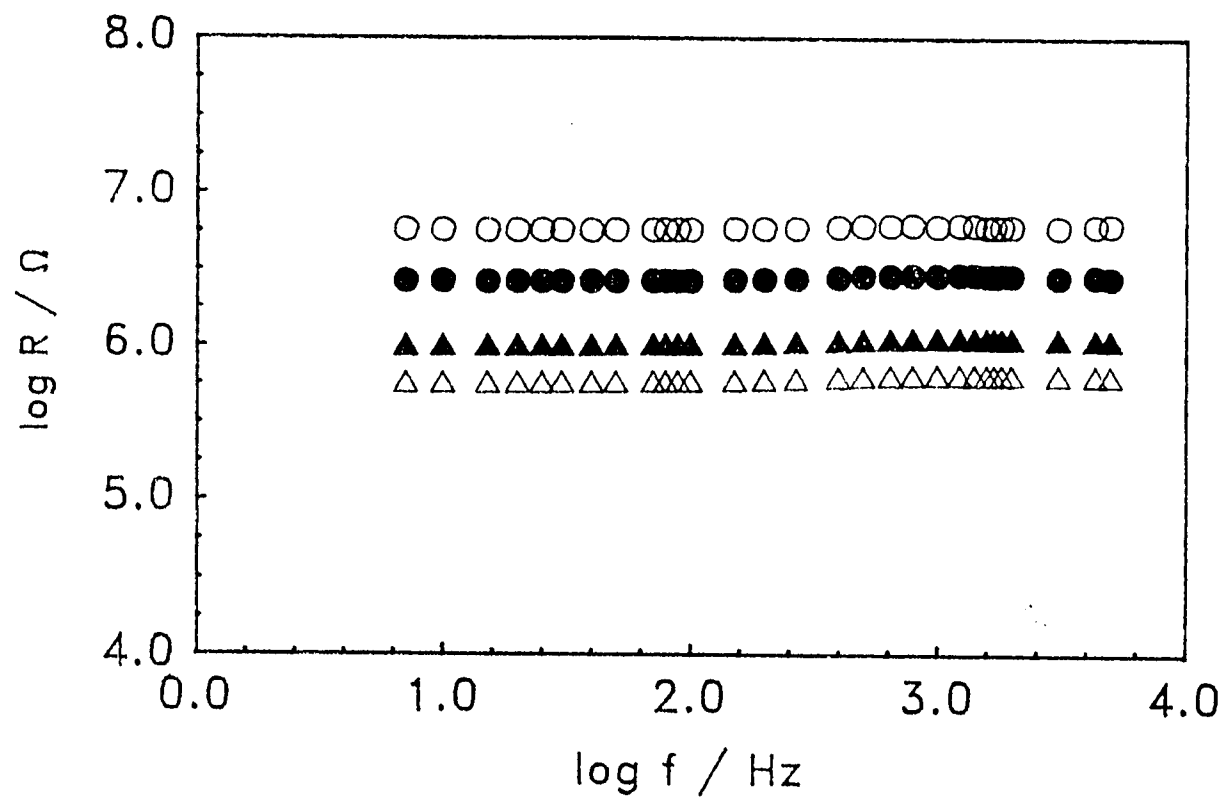


Figure 2.5. The frequency-dependence of  $R_{\text{cell}}$  for samples of octanol saturated with KCl aqueous solutions. The symbols represent the aqueous-phase concentrations of KCl: circle - 0.01 M; solid circle - 0.05 M; triangle - 0.20 M; and solid triangle - 0.40 M.  $R_m = 2.0 \text{ M}\Omega$ , and  $C_{\text{in}}' = 170 \text{ pF}$ .

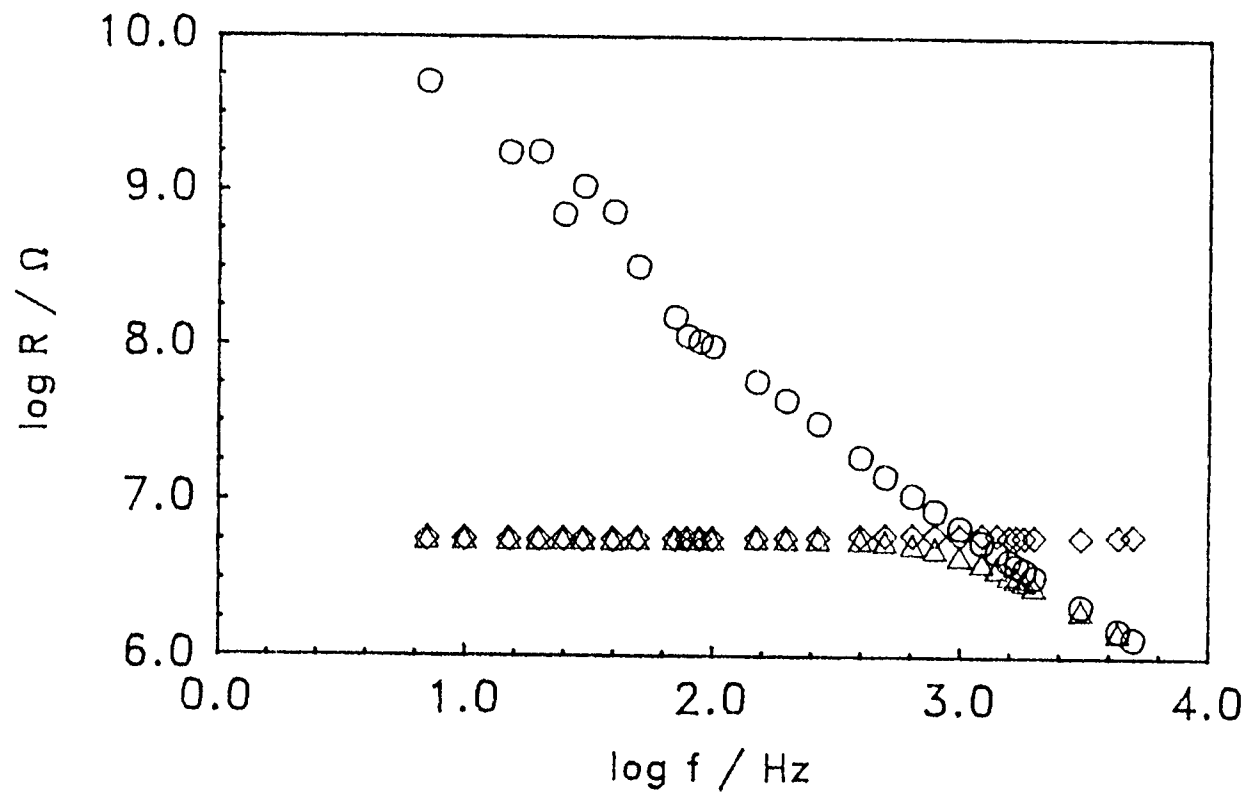


Figure 2.6. The frequency-dependence of  $R_{cell}$ ,  $X_{cell}'$ , and  $Z_{cell}$  for octanol saturated with 0.01 M aqueous KCl solutions: diamond -  $R_{cell}$ ; circle -  $X_{cell}'$ ; and triangle -  $Z_{cell}$ .  $R_m = 2.0 \text{ M}\Omega$ , and  $C_{in}' = 170 \text{ pF}$ .

Bright Pt vs. black Pt electrodes. Bright platinum electrodes have been used for the majority of the experiments. Platinum black electrodes were also tested by determining the time dependence of the  $R_{cell}$ . The test period was eight hours. The value of  $R_{cell}$  was measured at one-hour intervals for platinum black electrodes and one-and-one-half intervals for bright platinum electrodes. The power of the instrument was turned off between successive measurements.

Figure 2.7 shows the time dependence of  $R_{cell}$ . The sample for this test was octanol saturated with 0.01 M aqueous KCl solution. The value of  $R_{cell}$  determined by the bright platinum electrodes was generally stable during the 8-hour period of the test. However, the value of  $R_{cell}$  determined by the black platinum electrodes showed a dramatic decrease within the first 4 hours, and then reached a constant value. Figure 2.8 illustrates the result of the time-dependent test for the black platinum electrodes for different electrolyte concentrations. The result shows that the lower the concentration is, the more rapid the  $R_{cell}$  decreases with the time of the test.

It is surmised that the decrease of  $R_{cell}$  with time is due to the adsorption of electrolyte solutes on the surface of the black platinum electrodes, since the surface areas of these electrodes are large. It has also been suggested by Kratochvil and Yeager (1972) that bright platinum electrodes should be used for determination of conductance of high impedance nonaqueous solutions in order to reduce the effect of adsorption of solutes on the surfaces of the electrodes.

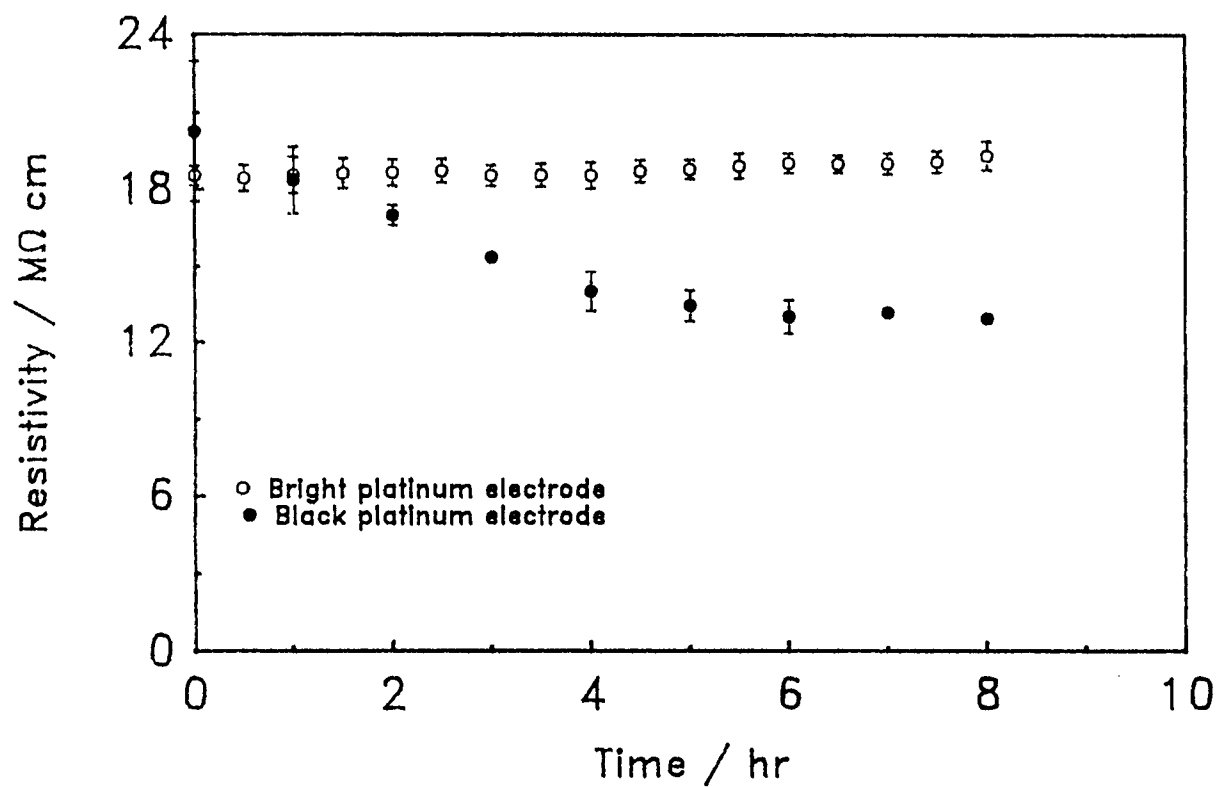


Figure 2.7. Time-dependence of resistivity,  $R_{cell}/(1/A)$ : a comparison of bright platinum electrodes with platinum black electrodes for octanol saturated with 0.01 M KCl aqueous solution.

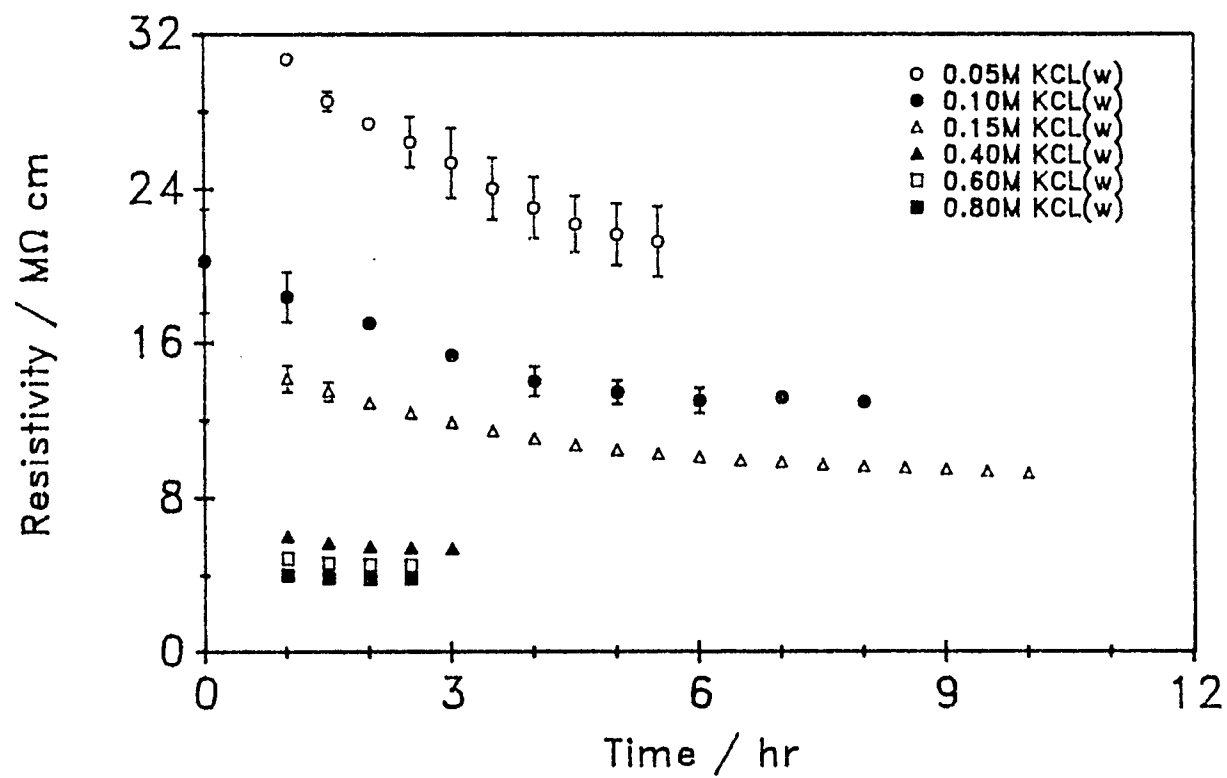


Figure 2.8. Time-dependence of resistivity,  $R_{\text{cell}}/(1/A)$ , determined by platinum black electrodes with octanol saturated with KCl aqueous solutions of: 0.05, 0.10, 0.15, 0.40, 0.60, and 0.80 M.

## Determination of permittivity of alcohol/water mixtures

### Apparent frequency dependence of the capacitance $C_{cell}'$ .

Dependence of the value of  $C_{cell}'$  on frequency in the range of 5 Hz to 100,000 Hz was investigated for both pure organic solvents and alcohol-water mixed solvents. The values of  $C_{cell}'$  as a function of frequency are shown in Figure 2.9 and 2.10.

As shown in the figures, the measured value of  $C_{cell}'$  appeared to increase with the decrease of frequency in the low frequency range. However, as indicated in Figure 2.11, this increase is not significant since at these frequencies the value of  $R_{cell}$  is much smaller than  $X_{C_{cell}}$ , and  $C_{cell}$  cannot be extracted reliably from the observed impedance.

As higher frequencies the value of  $C_{cell}'$  reaches a plateau. Frequency-independent  $C_{cell}'$  were observed in the frequency range from 1000 Hz up to 100,000 Hz for both the pure organic solvents (Figure 2.9) and the alcohol-water mixed solvents (Figure 2.10). These frequency-independent capacitances are considered to relate to the properties of the samples. In this study, all the values of  $C_{cell}$  reported were taken within this range.

A similar study on the dielectric constant of trifluoroacetic acid as a function of frequency was also reported by Dannhauser and Cole (1952). From their result, the apparent dielectric constant increased markedly with the decrease in the frequency as the frequencies were below 1 kHz. They concluded that the frequency independent values observed above several kilohertz are characteristics of the liquid.

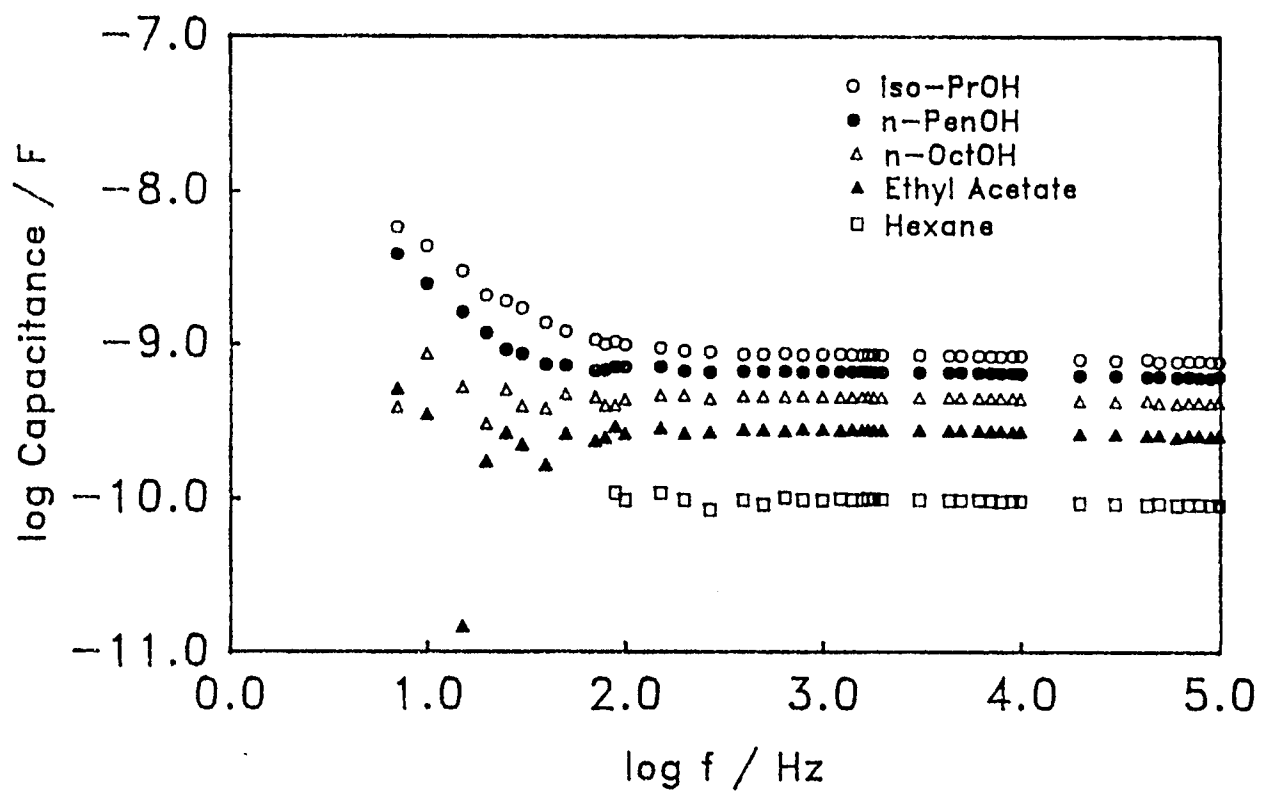


Figure 2.9. The frequency-dependence of  $C_{\text{cell}}'$  for some organic solvents.

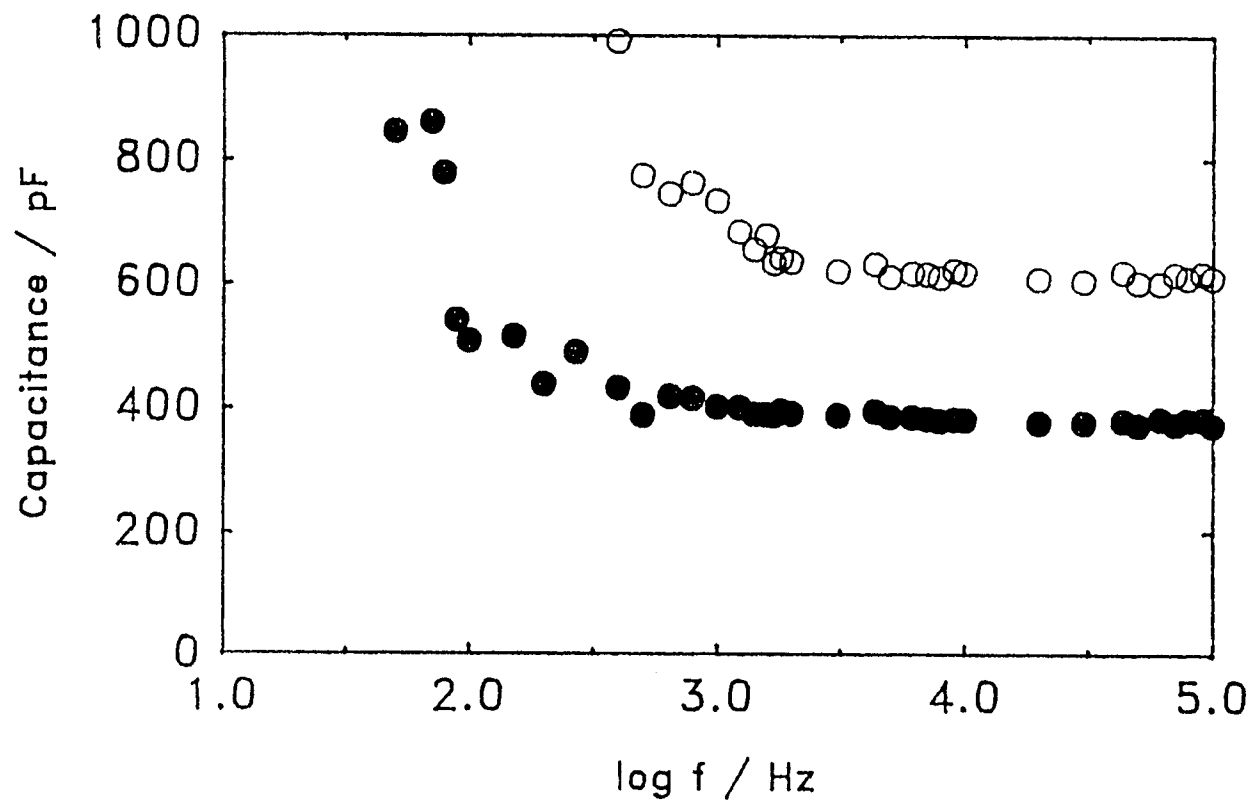


Figure 2.10. The frequency-dependence of  $C_{\text{cell}}'$  for mixed solvents. The symbols represent: open circle - 1-pentanol saturated with water ( $X_{\text{PenOH}} = 0.72$ ); and solid circle - 1-octanol saturated with water ( $X_{\text{OctOH}} = 0.73$ ).

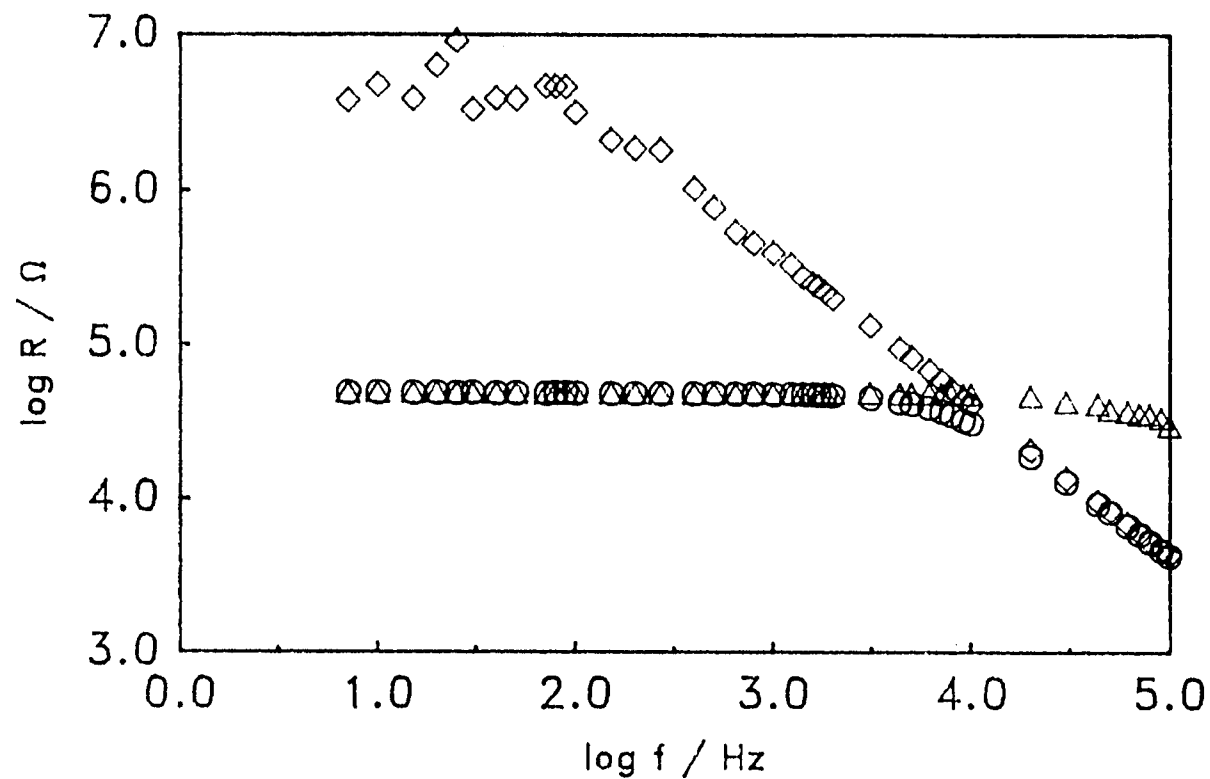


Figure 2.11. The frequency-dependence of  $R_{\text{cell}}$ ,  $X_{\text{cell}}'$ , and  $Z_{\text{cell}}$  for octanol saturated with water: triangle -  $R_{\text{cell}}$ ; diamond -  $X_{\text{cell}}'$ ; and circle -  $Z_{\text{cell}}$ .  $R_m = 10 \text{ k}\Omega$ ,  $C_{\text{in}}' = 170 \text{ pF}$ , and cell constant is  $0.00211 \text{ cm}^{-1}$ .

Calibration curve of  $C_{\text{cell}}'$  vs.  $\epsilon$ . Figure 2.12 shows the calibration curve of the measured  $C_{\text{cell}}'$  of the five organic solvents as a function of their relative permittivities,  $\epsilon$ . The linear relationship between  $C_{\text{cell}}'$  and  $\epsilon$  is described by Equation 2.15.

The parameters in Equation 2.15 have been determined by the linear squares parameter optimization method for the data in the plot. The stray capacitance  $C_{\text{stray}}$  is obtained from the intercept of the plot as 13 pF, which is consistent with the value of  $C_{\text{stray}}$  obtained from the test cell in the conductivity study.

From the slope of the plot, the cell constant ( $1/A$ ) of the cell is obtained to be  $0.00211 \text{ cm}^{-1}$ . An alternative method has also been used to determine the cell constant. In this method, the cell capacitance in the air was measured directly by a LC77 "AUTO-Z" Capacitor-Inductor Analyzer (from SENCORE Co.), and the cell constant obtained was  $0.00194 \text{ cm}^{-1}$ . The values of the cell constant from both methods are close.

The measured values of  $C_{\text{cell}}'$  of the alcohol-water mixtures are generally in the range of 90 to 900 pF. The precision was better than 0.2%. The dielectric constants of these mixtures, as listed in Table 2.4, were obtained from the  $C_{\text{cell}}'$  and the calibration curve.

Permittivities of pentanol-water and octanol-water mixtures.

This technique applied to determine the relative permittivities of 1-pentanol - water and 1-octanol - water mixed solvents. The mixed solvents were in the alcohol-rich range, that is mole fraction of

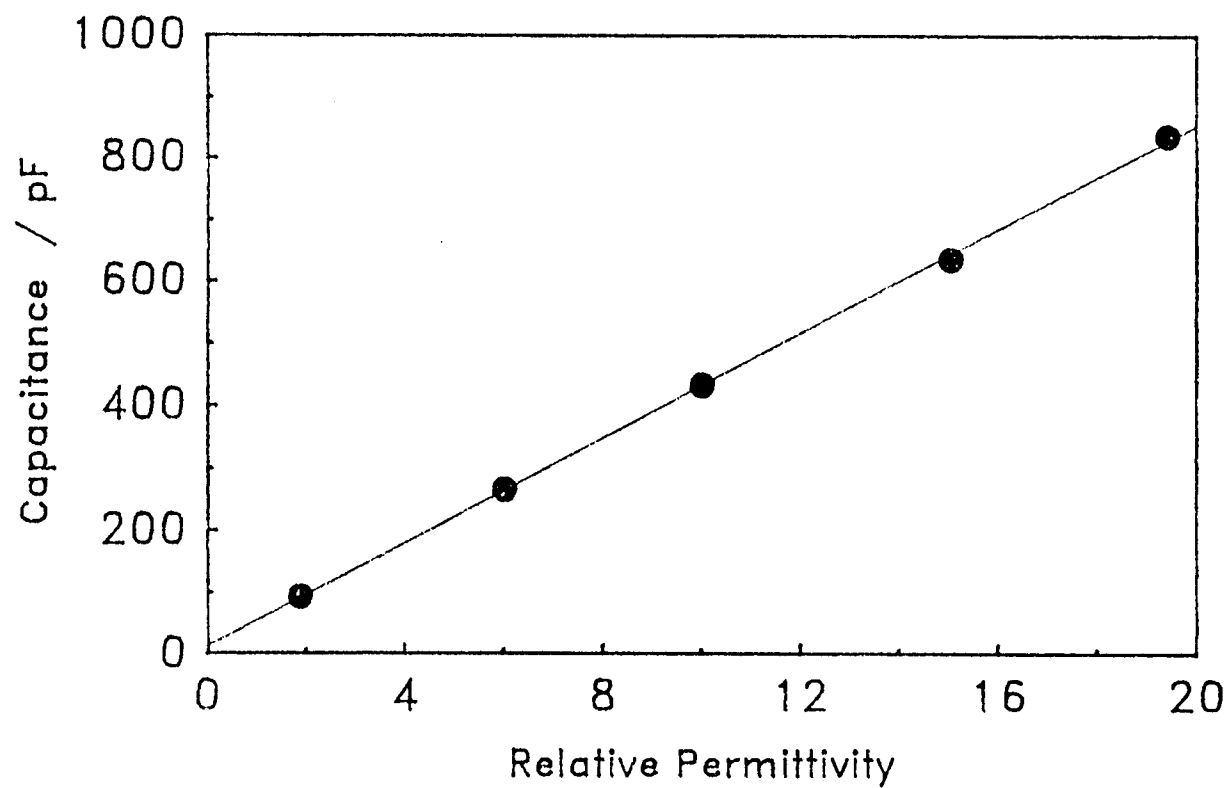


Figure 2.12. Calibration curve for determination of relative permittivity. The relative permittivities (the dielectric constant) of the solvents are given in Table 2.4.

Table 2.4. Relative permittivity and capacitance at 25 °C for some organic solvents and alcohol/water mixture.

Solvents	$\epsilon$	$C_{\text{cell}}^f$	
		(pF) Average	sd (n=3)
Hexane	1.088 <sup>b</sup>	94.23	1.15
Ethyl Acetate	6.02 <sup>a</sup>	266.65	0.06
1-Octanol	10.01 <sup>c</sup>	433.47	0.87
1-Pentanol	15.04 <sup>d</sup>	636.09	1.59
iso-Propanol	19.41 <sup>e</sup>	835.98	0.92
Octanol/Water	8.42 <sup>g</sup>	367.17	2.47

References:

- a. Riddick J. A. and W. B. Bunger, Organic Solvents, Wiley-Interscience, New York (1970).
- b. The  $\epsilon$  at 25 °C is calculated from the  $\epsilon$  at 20 °C and the temperature coefficient from Ref. a.
- c. Grunwald, E., K. C. Pan and A. Effio, J. Phys. Chem. (1976), 80, 2937.
- d. Evans, D. F. and P. Gardam, J. Phys. Chem. (1969), 73, 158.
- e. Dannhauser, W. and L. W. Bahe, J. Phys. Chem. (1964), 40, 3058.
- f. The  $C_{\text{cell}}^f$  were determined and calculated by PC - lock-in amplifier measurement system.
- g. The  $\epsilon$  for octanol saturated with water was obtained from the calibration curve.

alcohol ( $X_{\text{alcohol}}$ ) between 0.7 and 1.0, as shown in Figure 2.13.

The figure shows that the addition of water ( $\epsilon = 78.39$ ) to pentanol ( $\epsilon = 15.04$ ) results in a decrease in permittivity. A minimum permittivity is reached at  $X_{\text{PenOH}} \approx 0.82$ . Further increase in the mole fraction of water results in an increase in the permittivity of the mixed solvent. This result is in good agreement with the previous studies (D'Aprano, et al. 1979 and 1982; Sjoblom, 1979 and Sjoblom and Dyhr, 1981).

The permittivity of octanol-water mixed solvents also decreases with increasing the mole fraction of water, as shown in Figure 2.13. However, no minimum value of  $\epsilon$  was observed.

A pattern similar to the one shown in Figure 2.13 has also been observed for the mixtures of 1-hexanol, 1-heptanol, 1-octanol, 1-nonanol, 1-decanol and water by D'Aprano, et al. (1979 and 1982), and Sjoblom and Dyhr (1979 and 1981) .

The decrease of the dielectric constants with the increase of  $X_{\text{H}_2\text{O}}$  for the linear alcohol and water mixtures can be interpreted from two perspectives:

(i) Addition of a small amount of water into the long-chain alcohol may break the structure of the alcohol. It has been reported that the molecules in pure 1-octanol are associated each other through hydrogen bonding, forming chains with average lengths of 28 molecules (Grunwald et al. 1976). The interaction between water and alcohol molecules will break this alcohol self-association chain and make the alcohol solvent less structured.

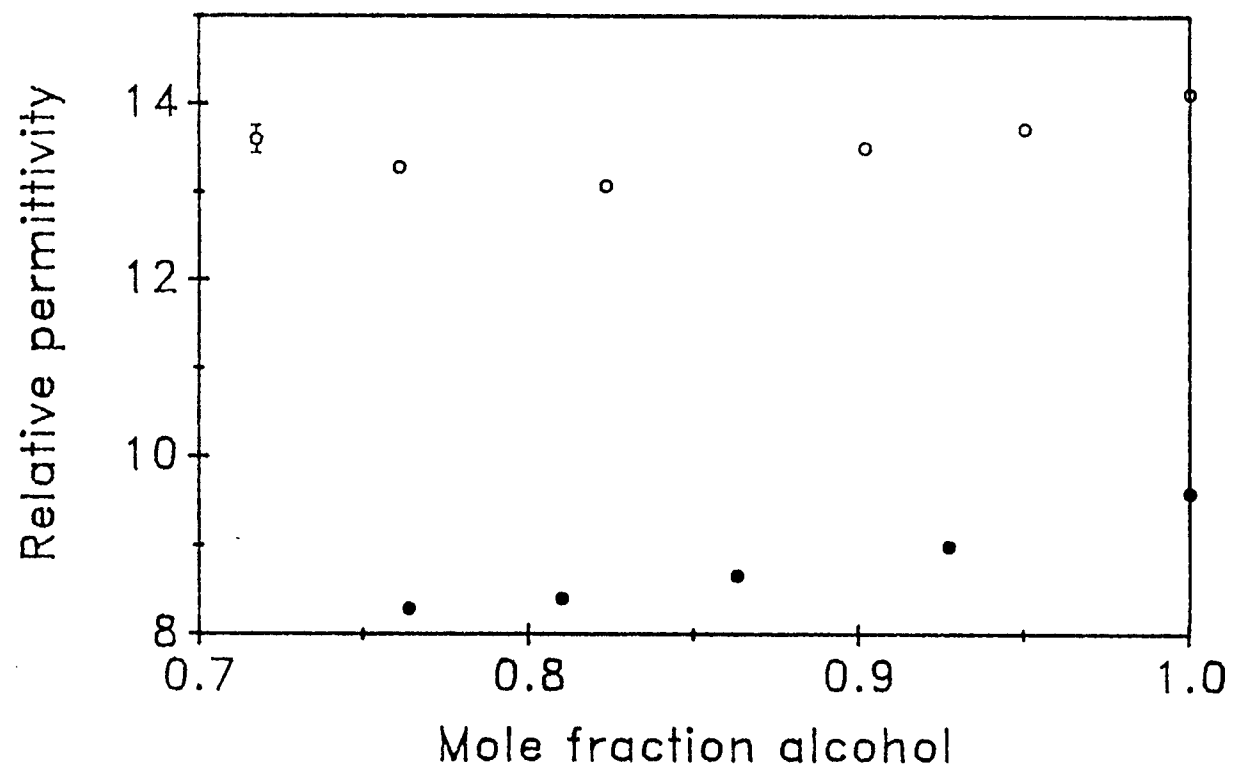


Figure 2.13. Relative permittivity as a function of mole fraction of alcohol for 1-pentanol - water (open circle) and 1-octanol - water (solid circle) mixtures.

(ii) The interaction between water and alcohol molecules may form some long-lived complexes through hydrogen bonding, for example, form water centered complexes with one water and four alcohol molecules. The formation of this water-centered tetrahedral complex will significantly decrease the dielectric constant of the mixture since the dipole moment of this complex is smaller than that of water (D'Aprano, et al. 1979 and 1982; and Sjoblom and Dyhr, 1979 and 1981).

We have compared the technique used in this study with those in published studies. From Sjoblom's study, the dipole moments of the alcohol-water mixtures were determined at a constant frequency of 2 MHz by a Dipolmeter. From D'Aprano's work, the capacitance of the mixtures were measured at 1 MHz using a bridge. The dielectric constants of the mixtures from both laboratories were calculated from the calibration curves which were obtained from the pure solvents with known  $\epsilon$ . Although a different technique was used in our determination, the results are in good agreement with theirs. This leads us to conclude that the PC - lock-in amplifier system can be used to determine the relative permittivities of nonaqueous media.

## CONCLUSIONS

A technique has been developed to determine the conductivity and permittivity of high-impedance solutions. Impedance measurements are obtained in the range from 5 Hz to 100,000 Hz. Frequency-independent solution resistances were observed at frequency less than 100 Hz. Frequency-independent capacitances were found at frequency larger than a few kilohertz. The resistance of samples can be determined up to 10 M $\Omega$  with precision better than 3%. The capacitance of the samples were determined in the range 90 - 900 pF with precision better than 0.2%.

## REFERENCES

- Bard, A. J.; Faulkner, L. R. "Electrochemical Methods"; by John Wiley & Sons, Inc. 1980, 316.
- Beronius, P.; Lindbaeck, T. Acta Chem. Scand. 1978, A32, 423-428.
- Broadwater, T. L. and Kay, R. L. J. Phys. Chem. 1970, 74, 3802-3812.
- Broadwater, T. L. and Douglas, R. T. J. of Soln. Chem. 1975, 4, 485-496.
- Braunstein, J. and Robbins, G. D. J. Chem. Educ. 1971, 48, 52.
- Dannhauser, W. and Cole, R. H. J. Phys. Chem. 1952, 56, 6105.
- D'Aprano, A.; Donato, D. I.; and Caponetti, E. J. of Soln. Chem. 1979, 8, 135.
- D'Aprano, A.; Donato, D. I.; and Agrigento, V. J. of Soln. Chem. 1982, 11, 259.
- DeSieno, R. P.; Greco, P. W.; and Mamajek, R. C. J. Phys. Chem. 1971, 75, 1722-1726.
- Doe, H.; Kitagawa, T.; Sasabe, K. J. Phys. Chem. 1984, 88, 3341-3345.
- Evans, D. F.; and Gardam, P. J. Phys. Chem. 1968, 72, 3281-3286.
- Evans, D. F.; and Gardam, P. J. Phys. Chem. 1969, 73, 158-163.
- Evans, D. F.; and Matesich, M. A. "The Measurement and Interpretation of Electrolytic conductance" in Techniques of Electrochemistry, Vol. II; Yeager, E. and Salkind, A. J. Eds.; Wiley: New York, 1973.
- Fang, J. and Venable, R. L. J. Coll. Interface Sci. 1987, 116, 269.
- Fuoss, R. M. J. Phys. Chem. 1978, 82, 2427.
- Goffredi, M. and Shedlovsky, T. J. Phys. Chem. 1967, 71, 2176-2181.
- Goffredi, M. and Shedlovsky, T. J. Phys. Chem. 1967, 71, 2182-2186.
- Grunwald, E.; Pan, K. C.; and Effio, A. J. Phys. Chem. 1976, 80, 2937.
- Hafez, A. M.; Ramadan, M. Sh.; and Sadek, H. Electrochimica Acta 1987, 32, 625-628.
- Hawes, J. L. and Kay, R. L. J. Phys. Chem. 1965, 69, 2420-2431.

- Highsmith, S. J. Phys. Chem. 1975, 79, 1456-1459.
- Huang, F. and Gilkerson, W. R. J. of Soln. Chem. 1983, 12, 161-170.
- Kay, R. L.; Zawoyski, C.; and Evans, D. F. J. Phys. Chem. 1965, 69, 4208-4215.
- Kissinger, P. T. and Heinemann, W. R. Laboratory Techniques in Electroanalytical Chemistry; Dekker, 1984.
- Kratochvil, B. and Yeager, H. L. "Conductance of Electrolytes in Organic Solvents", Topics in Current Chemistry, 1972, No. 27, 1.
- Matesich, M. A.; Nadas, J. A.; and Evans, D. F. J. Phys. Chem. 1970, 74, 4568-4573.
- Monica, M. D.; Ceglie, A.; and Acostiano, A. Electrochimica Acta 1984, 29, 161.
- Okubo, T. J. of Coll. Interfac. Sci. 1988, 125, 380-385.
- Ono, K.; Konami, H.; and Murakami, K. J. Phys. Chem. 1979, 83, 2665-2669.
- Papadopoulos, G. P. N. and Jannakoudakis, D. Electrochimica Acta 1985, 30, 431-433.
- Pilarczyk, M. and Klinszporn, L. Electrochimica Acta 1986, 31, 185-192.
- Riddick, J. A.; and Bunger, W. B. Organic Solvents; Wiley-Interscience: New York, 1970.
- Robison, R. A.; Stokes, R. H. Electrolyte Solutions; Butterworths: London, 1968.
- Salomon M. and Plichta, E. J. Electrochimica Acta 1985, 30, 113-119.
- Shedlovsky, T. and Kay, R. L. J. Phys. Chem. 1956, 60, 151-155.
- Sjoblom, J. Finn. Chem. Lett. 1979, 245.
- Sjoblom, J. and Dyhr, H. Acta Chemica Scandinavica A 1981, 35, 219.
- Spivey, H. O. and Shedlovsky, T. J. Phys. Chem. 1967, 71, 2165-2171.
- Tanaka, N. and Harada, K. Electrochimica Acta 1976, 21, 615.
- Tissier, M. and Douheret, G. J. of Soln. Chem. 1978, 7, 87-98.
- van Os, N. M.; Daane, G. J.; and Bolsman, T. A. B. J. Coll. Interfac. Sci. 1987, 115, 402-409.

Wellington, S. L. and Evans, D. F. J. of Soln. Chem. 1983, 12, 815-828.

Westall, J. C.; Johnson, C. A.; and Zhang, W. Environ. Sci. Technol. 1990, 24, 1803-1810.

## CHAPTER 3

THE DISTRIBUTION OF  $\text{LiCl}$ ,  $\text{NaCl}$ ,  $\text{KCl}$ ,  $\text{HCl}$ ,  $\text{MgCl}_2$  AND  $\text{CaCl}_2$   
BETWEEN OCTANOL AND WATER

## INTRODUCTION

The two-phase octanol-water system has been used extensively in environmental and medicinal chemistry as a reference system for the distribution of nonpolar organic compounds between aqueous and nonaqueous phases (Leo and Hansch, 1971; Lyman et al., 1982). Correlations have been made between octanol-water partition constants and properties such as solubility, chromatographic retention, soil-water or sediment-water distribution ratios, and bioavailability or bioconcentration factors (e.g., Karickhoff et al., 1979; Veith et al., 1980; Hansch and Dunn, 1972; Schellenberg et al., 1984).

Whereas the octanol-water reference system is most readily applicable for the distribution of nonpolar organic compounds, its applicability for ionogenic and ionic organic compounds is being investigated (Schellenberg et al., 1984; Westall et al., 1985; Johnson and Westall, 1990). However, the transfer of an organic ion from water to octanol requires the transfer of a counter-ion; thus the observed distribution ratio becomes dependent on the nature and concentration of counter-ions in the water. In most simple distribution experiments, the counter-ions are those of a simple inorganic salt or buffer. However, even for these ions, a systematic investigation of the distribution between octanol and water still has not been made.

As an initial step towards understanding the behavior of organic ions in the octanol-water system, a study was undertaken in this laboratory to elucidate (i) the distribution of simple salts between water and water-saturated octanol and (ii) the speciation of the salts

in water-saturated octanol. The experimental data for the distribution of LiCl, NaCl, KCl, HCl, MgCl<sub>2</sub> and CaCl<sub>2</sub> between octanol and water were obtained by Johnson (1987), and the data were interpreted in terms of a multicomponent equilibrium model by Westall et al. (1990). The contribution presented in this thesis is the confirmation of the speciation in the nonaqueous phase through a study of the conductivity of the nonaqueous phase.

All experiments in this study deal with octanol-water distributions; hence the term "octanol (or organic) phase" refers to water-saturated octanol and the term "water phase" refers to octanol-saturated water.

## THEORY

In this study the octanol-water distribution and speciation of the salts LiCl, NaCl, KCl, HCl, MgCl<sub>2</sub>, CaCl<sub>2</sub> are considered. The salts can be represented as MX and MX<sub>2</sub>, and possible reactions involved in the distribution of the salts between the two phases are represented in Table 3.1. Reactions 1 and 2 show free ions and ion pairs of the 1:1 salts in the octanol phase. Reaction 3 shows one possibility for triple-ion formation in the octanol phase. Reactions 4 - 6 show free ions and ion associates of the 1:2 salts in the octanol phase. Reactions 7 and 8 refer not to phase-transfer reactions, but to reactions in the octanol phase; these two reactions are not independent, but can be represented as a combination of the preceding reactions.

The central questions are, which of these reactions actually occur to a significant extent, and what are the equilibrium constants? These questions can be answered through two approaches: (i) by determination of the functional dependency (i.e., linear, quadratic, etc.) of the activity of the salts in the octanol phase on the activity of the salts in the water phase, and (ii) by determination of the conductivity of the octanol phase as a function of activity in the aqueous phase. The first approach was discussed by Westall et al. (1990). Here we present the basic theory for the calculation of the distribution equilibria in these multicomponent systems, which is required in the interpretation of the conductivity in the nonaqueous phase, and then examine the conductivity in detail.

Table 3.1. Distribution reactions of inorganic salts between octanol and water, and ion-pair formation reactions of inorganic salts in octanol. The overbar denotes a species in the organic phase.

<u>Distribution Equilibria</u>	<u>Equilibrium Constant</u>	<u>Reaction #</u>
$M^+ + X^- = \overline{M^+} + \overline{X^-}$	$K_1$	(1)
$M^+ + X^- = \overline{MX}$	$K_2$	(2)
$3 M^+ + 3 X^- = \overline{M_2X^+} + \overline{MX_2^-}$	$(K_3)$	(3)
$M^{2+} + 2 X^- = \overline{MX^+} + \overline{X^-}$	$K_4$	(4)
$M^{2+} + 2 X^- = \overline{MX_2}$	$K_5$	(5)
$M^{2+} + 2 X^- = \overline{M^{2+}} + 2 \overline{X^-}$	$(K_6)$	(6)
<u>Ion-pair Formation Reactions</u>		
$\overline{M^+} + \overline{X^-} = \overline{MX}$	$K_7$	(7)
$\overline{MX^+} + \overline{X^-} = \overline{MX_2}$	$K_8$	(8)

## Distributions

The discussion of distributions will be presented in two parts: (i) the numerical method for solving multicomponent equilibrium problems; and (ii) the calculation of activity coefficients for ions in the water and octanol phases.

Numerical method for multicomponent equilibria. A numerical method is used to solve the multicomponent chemical equilibrium problems. The basis of the method has been described in detail by Westall (1986), and the adaptation for two-phase equilibria is outlined here.

This method is based on the following definitions of components and species. Every chemical entity to be considered in a reaction at equilibrium is defined as a species. Then a set of components are chosen, such that every species can be written as the only product of a reaction in which only the components are reactants, and no component can be written as the product of a reaction in which only the other components are reactants. Thus the components are a complete and independent set of reactants, from which all of the species can be formed.

The relation between the free concentration of the components and the concentration of every species can be described through mass action equations in the following form:

$$C_i = K_i \prod X_j^{a(i,j)} \quad (3.1)$$

where  $C_i$  and  $K_i$  are the concentration and formation constant for the species  $i$ , the product is taken over all components  $j$ ,  $X_j$  is the concentration of component  $j$ , and  $a(i,j)$  is the stoichiometric coefficient of component  $j$  in species  $i$ . Here  $K_i$  is a "conditional constant", which is equal to the "infinite dilution constant,"  $K^\circ$ , corrected with the activity coefficients of the components and species,  $\gamma$ :

$$K_i = (K^\circ_i / \gamma_i) \prod \gamma_j^{a(i,j)} \quad (3.2)$$

The mole balance equations are formulated as

$$Y_j = \sum a(i,j) C_i - T_j \quad (3.3)$$

where the summation is taken over all species  $i$ ,  $T_j$  is the total (analytical) concentration of component  $j$  (determined from experiment) and  $Y_j$  is a difference function, that is, the difference between the total concentration which is calculated from the model and the  $T_j$ . The object is to find the set of  $X_j$  such that all  $Y_j = 0$ . For each component there is one unknown ( $X_j$ ) and one nonlinear equation (Equation 3.3). The set of equations is solved iteratively by Newton's method from an initial guess of the  $X_j$ .

Thus each multicomponent equilibrium problem is completely defined by the  $A$  matrix of stoichiometric coefficients  $a(i,j)$ ; the  $K$  vector of formation constants  $K_i$ , and the  $T$  vector of total concentrations  $T_j$ . These matrices and vectors are presented in

Table 3.2 for three systems considered in this study: (i) the simple 1:1 electrolytes LiCl, NaCl and KCl (Table 3.2a); (ii) the 1:2 electrolytes  $\text{MgCl}_2$  and  $\text{CaCl}_2$  (Table 3.2b); and (iii) HCl, for which the formation of triple ions may be significant (Table 3.2c). The components for this study include the metal ion and chloride ion in the aqueous phase, and the free chloride in the octanol. The phase ratio  $\Phi_D$  and the Donnan potential  $X_\Psi$  are also used as components in consideration of material balance and charge balance, respectively. The total concentration for these components are experimental parameters.

The concentrations for all of the species in the octanol phase are calculated by a computer program MICROQL (Westall, 1986). The mathematical formulations for these calculations are described in Table 3.2 a-c.

Activity and concentration of salts in water and octanol. The subject of activity coefficients was mentioned briefly in connection with Equation 3.2, and is handled here in detail.

The data in this work are reported in units of molar concentrations and activities, in order to facilitate comparison with most other data for octanol-water systems. However, to determine molar activities, it was necessary to convert molar concentrations to molal concentrations, use the established equations of Pitzer and Mayorga (1975) to calculate molal activities, and then convert these molal activities to molar activities. This procedure is described below.

The aqueous salt solutions were prepared volumetrically with known molar concentrations. The molar concentrations of the salts in

Table 3.2a. Mathematical formulation of the Donnan equilibrium model for distribution of LiCl, NaCl, and KCl between octanol and water<sup>a</sup>. The numbers in the table are the stoichiometric coefficients of the components in species, that is, the  $a(i,j)$  in Equation 3.1 - 3.3. The overbar denotes a species in the organic phase.

### Material Balance Matrix

Species	Components					
	$M^+$	$X^-$	$X_\Psi$	$\Phi_D$	$X_{Cl^-}$	K
$M^+$	1	0	0	0	0	1
$X^-$	0	1	0	0	0	1
$\overline{M^+}$	1	0	1	1	0	$K_1$
$\overline{X^-}$	0	1	-1	1	1	1
$\overline{MX}$	1	1	0	1	1	$K_2$
	$T_{M^+}^b$	$T_{X^-}^b$	$T_\sigma$	$T_\Phi$	$T_{Cl^-}^b$	

a. The distribution reactions are the Reactions 1 and 2 in Table 3.1.

b. The experimental data from Johnson (1987).

Table 3.2b. Mathematical formulation of the Donnan equilibrium model for distribution of  $\text{MgCl}_2$ , and  $\text{CaCl}_2$  between octanol and water<sup>a</sup>. The numbers in the table are the stoichiometric coefficients of the components in species, that is, the  $a(i,j)$  in Equation 3.1 - 3.3. The overbar denotes a species in the organic phase.

### Material Balance Matrix

Species	Components					
	$\text{M}^{2+}$	$\text{X}^-$	$\text{X}_\Psi$	$\Phi_D$	$\text{X}_{\text{Cl}^-}$	K
$\text{M}^{2+}$	1	0	0	0	0	1
$\text{X}^-$	0	1	0	0	0	1
$\overline{\text{MX}^+}$	1	1	1	1	1	$K_4$
$\overline{\text{X}^-}$	0	1	-1	1	1	1
$\overline{\text{MX}_2}$	1	2	0	1	2	$K_5$
	$T_{\text{M}^{2+}}^b$	$T_{\text{X}^-}^b$	$T_\sigma$	$T_\Phi$	$T_{\text{Cl}^-}^b$	

a. The distribution reactions are the Reactions 4 and 5 in Table 3.1.

b. The experimental data from Johnson (1987).

Table 3.2c. Mathematical formulation of the Donnan equilibrium model for the distribution of HCl between octanol and water<sup>a</sup>. The numbers in the table are the stoichiometric coefficients of the components in species, that is, the  $a(i,j)$  in Equation 3.1 - 3.3. The overbar denotes a species in the organic phase.

Material Balance Matrix

Species	Components					K
	$M^+$	$X^-$	$X_\Psi$	$\Phi_D$	$X_{Cl^-}$	
$M^+$	1	0	0	0	0	1
$X^-$	0	1	0	0	0	1
$\overline{M^+}$	1	0	1	1	0	$K_1$
$\overline{X^-}$	0	1	-1	1	1	1
$\overline{MX}$	1	1	0	1	1	$K_2$
$\overline{MX_2^-}$	1	2	-1	1	2	$K_3$
$\overline{M_2X^+}$	2	1	1	1	1	1
	$T_{M^+}^b$	$T_{X^-}^b$	$T_\sigma$	$T_\Phi$	$T_{Cl^-}^b$	

a. The distribution reactions are the Reactions 1, 2 and 3 in Table 3.1.

b. The experimental data from Johnson (1987).

these solutions were converted to molal concentrations through the equation:

$$m = c / (\rho - c M) \quad (3.4)$$

where  $m$  is the molal concentration,  $c$  is the molar concentration,  $\rho$  is the density of the solution [ $\text{kg dm}^{-3}$ ], and  $M$  is the molar mass of the salt [ $\text{kg mol}^{-1}$ ]. The density of the solutions was calculated from the equations of Soehnel and Novotny (1985).

From the molal concentration of the electrolyte, the molal mean salt activity coefficients,  $\gamma_{\text{ms}}^{\text{m}}$ , were calculated from the equations of Pitzer and Mayorga (1975) for binary electrolytes. The accuracy of this calculation was verified by comparison of the calculated activity coefficients to the experimental values published by Robinson and Stokes (1959), as shown in Figure 3.1.

The molal mean salt activities,  $a_{\text{ms}}^{\text{m}}$  were calculated from the molal concentrations and activity coefficients:

$$a_{\text{ms}}^{\text{m}} = m \gamma_{\text{ms}}^{\text{m}} \quad (3.5)$$

from which the molar mean salt activities,  $a_{\text{ms}}$ , were found through the relation (Robinson and Stokes, 1959):

$$a_{\text{ms}} = a_{\text{ms}}^{\text{m}} \rho^{\circ} \quad (3.6)$$

where  $\rho^{\circ}$  is the density of the pure solvent,  $0.997 \text{ kg dm}^{-3}$  for pure water at  $25^{\circ}\text{C}$  (Robinson and Stokes, 1959). Furthermore, the molar

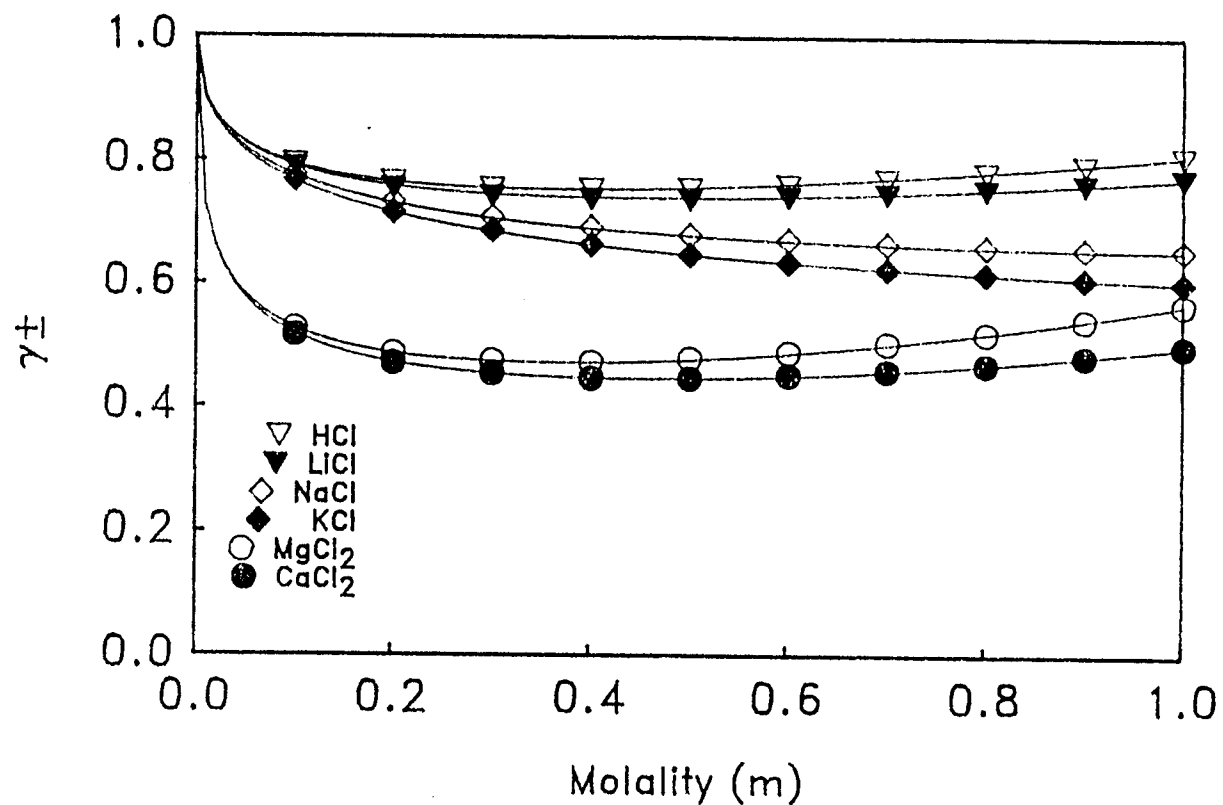


Figure 3.1. The molal mean activity coefficients,  $\gamma_{\text{ms}}^{\text{m}}$ , as a function of the molal concentration for binary electrolytes in water. The symbols represents the experimental values published by Robinson and Stokes (1959), and the lines were calculated from the equations of Pitzer and Mayorga (1975).

mean salt activity,  $a_{ms}$ , of a binary electrolyte  $MX_\nu$ , is related to the activities of the component ions by the equation:

$$a_{ms} = (a_M a_X^\nu)^{1/(1+\nu)} \quad (3.7)$$

Thus Equations 3.4 - 3.6 allow molar mean salt activities to be calculated from the molar mean salt concentrations.

## EXPERIMENTS

Materials. The octanol used in this study was Analyzed Reagent Grade from J.T. Baker Inc., used without further purification. Selected experiments were made to compare behavior of octanol as received, octanol purified by distillation, and octanol purified by extraction with water. While a significant difference in conductivity of the water-saturated octanol was detected, no significant difference was detected on the distribution of the inorganic salts between octanol and water. The deionized water was obtained from a Millipore Milli-Q system. The inorganic salts for this study were analytical grade (EM Science Co.) and used as received.

Conductivity of octanol saturated with aqueous salt solutions. The octanol used for the experiments was pre-saturated with deionized water before it was equilibrated with aqueous salt solutions. The previous study of Johnson (1987) in this laboratory found that, if octanol was not pre-saturated with water, the octanol phase could take up a large amount of water and change the aqueous-phase salt concentrations.

The aqueous salt solutions were prepared with concentrations in the range of 0.01 to 1.00 M. A 10-mL aliquot of the octanol saturated with water and 10 mL of aqueous solution were added into a 25-mL Corex glass centrifuge tube. The tubes were tightly sealed with Teflon-lined caps. The solutions were mixed for 2 hours at 500 RPM and 25 °C on a thermostatted shaker (New Brunswick Model G-24). After the samples were mixed, they were centrifuged for 10 minutes at 10,000

RPM and 25 °C by an IEC Model B-20A thermostatted centrifuge to separate the two phases.

The procedures for the determination of the extremely low conductivity of the water-saturated octanol solutions is described in Chapter 2, and is outlined here. After centrifugation, the octanol solution was added to a conductivity cell with bright planar platinum electrodes. The conductivity cell used was Brinkmann Model EA 660-01 pipet cell with a cell constant of  $0.078 \text{ cm}^{-1}$ . The sample was isolated from the atmosphere during the measurement and maintained at  $25 \pm 1 \text{ }^{\circ}\text{C}$ .

A sine wave of 500 mV p-p was imposed across a series combination of the conductivity cell and a measuring resistor of known resistance. The real and imaginary components of the voltage drop across the cell and measuring resistor were measured and recorded with a Princeton Applied Research Model 5301 Lock-in Amplifier with a Model 5316 Preamplifier. The system was controlled by a computer. The impedance of the conductivity cell was determined from an equivalent circuit that included stray capacitance, the current-measuring resistor, input impedance of the amplifier, and the conductivity cell. All of the experiments were carried out at several frequencies in the range of 5 to 5000 Hz. The constancy of the measured resistance at low frequencies (less than 100 Hz) indicates the absence of significant uncompensated stray capacitance. The cell resistances were typically on the order of 1-10 M $\Omega$ .

The entire procedure for determination of conductivity was carried out in triplicate for each aqueous salt solution. The relative error was less than 4%.

## RESULTS

The distribution of LiCl, NaCl, KCl. The concentrations of the 1:1 electrolytes LiCl, NaCl, and KCl in octanol, as a function of the molar mean salt activity in water, have been reported by Westall et al. (1990). The molar mean salt activity,  $a_{ms}$ , of a binary electrolyte  $MX_v$ , is related to the activities of the component ions by equation 3.7.

The experimental data for the distribution are interpreted in terms of Reactions 1 and 2 in Table 3.1, for which the mass action equations are (the overbar denotes a species in the organic phase):

$$a_M a_X K_1 = \bar{c}_M \bar{c}_X \quad (3.8)$$

$$a_M a_X K_2 = \bar{c}_{MX} \quad (3.9)$$

The constants  $K_1$  and  $K_2$  were determined by weighted nonlinear least squares parameter optimization (Westall et al., 1990), and are given in Table 3.3.

The presence of these species in the octanol phase is further substantiated by the dependence of the specific conductivity on the mean activity of the salt, as shown in Figure 3.2.

The specific conductivity of the solution was calculated from the concentrations of the free ions  $c_M = c_X = c_{M,X}$ , the equivalent conductivity of the ionic salt,  $\Lambda_{M,X}$ , and the background conductivity of the salt-free water-saturated octanol,  $\kappa^\circ$ :

Table 3.3 The equilibrium constants for distribution and ion-pair formation reactions<sup>a</sup>.

A. Monovalent cations

Electrolyte	$\log K_1$	$\log K_2$	$\log K_3$	$\log K_7$
LiCl	-7.36(0.04)	-2.74(0.01)		4.62(0.04)
NaCl	-7.71(0.04)	-3.16(0.01)		4.55(0.05)
KCl	-7.69(0.04)	-3.10(0.01)		4.59(0.02)
HCl <sup>b</sup>	-6.12(0.07)	-1.37(0.01)		4.75(0.03)
HCl <sup>c</sup>	-6.00(0.03)	-1.40(0.01)	-4.61(0.03)	4.60(0.04)

B. Divalent cations

Electrolyte	$\log K_4$	$\log K_5$	$\log K_8$
MgCl <sub>2</sub>	-7.49(0.02)	-3.62(0.02)	3.87(0.02)
CaCl <sub>2</sub>	-7.62(0.02)	-3.81(0.03)	3.81(0.03)

Reference:

<sup>a</sup>. Westall et al., 1990.

<sup>b</sup>. Species of HCl in octanol phase are free ions and ion pairs, determined for aqueous-phase concentration 0.01-0.2 M.

<sup>c</sup>. Species of HCl in octanol phase are free ions, ion pairs, and triple ions, determined for aqueous-phase concentration 0.01-1 M.

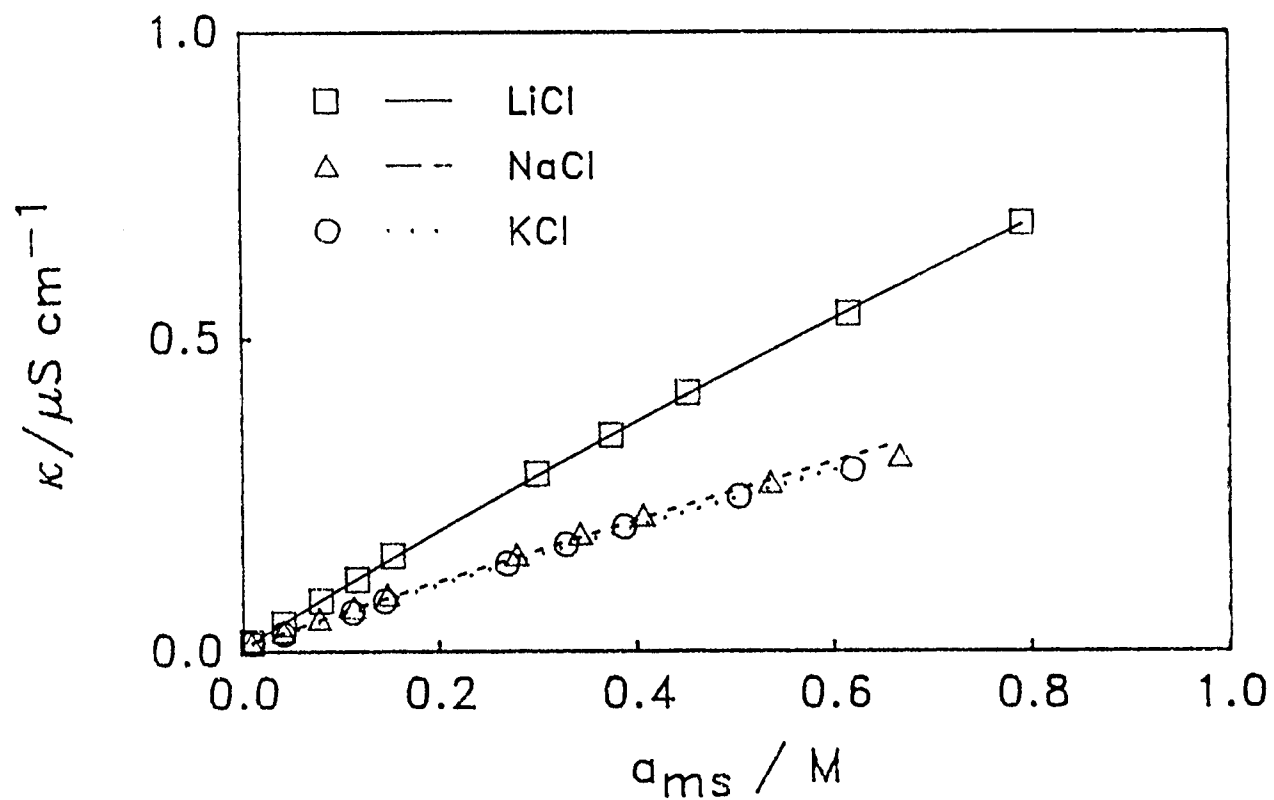


Figure 3.2. The specific conductivity of octanol that has been equilibrated with an aqueous salt solution of the indicated mean molar activity. The symbols represent the experimental data, and the lines are calculated from Equation 3.10, and the constants in Table 3.3 and 3.4.

$$\kappa = \bar{c}_{M,X} \Lambda_{M,X} + \kappa^{\circ} \quad (3.10)$$

For these simple electrolytes, the concentration of the ions  $c_{M,X}$  in octanol are linear functions of the mean salt activity in water (Equations 3.7-8). The equivalent conductivity of the salt was calculated as a function of concentration of free ions in the octanol through the Onsager equation (Robinson and Stokes, 1959; Bockris and Reddy, 1976):

$$\Lambda_{M,X} = \Lambda^{\circ}_{M,X} - \bar{c}_{M,X}^{0.5} S \quad (3.11)$$

where  $S$  is the Onsager slope, calculated from first principles and dependent on the the dielectric constant, the viscosity and temperature:

$$S = A + B \Lambda^{\circ}_{M,X} \quad (3.12)$$

For a 1:1 salt in water-saturated octanol, with  $\epsilon = 8.1$ ,  $\eta = 7.9$  cP, and  $T = 298.2$  K,  $A = 7.271 \times 10^{-5} \text{ S m}^2 \text{ mol}^{-1} (\text{mol m}^{-3})^{0.5}$ , and  $B = 2.186 \times 10^{-1} (\text{mol m}^{-3})^{0.5}$ .

In Equation 3.11 we use the very simple Onsager equation to calculate the equivalent conductivity of the salt as a function of concentration. This equation is generally recognized as being inadequate except at very low concentrations of salt. Therefore, we have calculated equivalent conductivity from the more rigorous model of Fuoss and Onsager (1959) for comparison. This model, with ion-size parameter 400 pm, yielded values of  $\Lambda_{M,X}$  that differed from those

of Equation 3.11 by about 1-2% at  $c_{M,X} = 10 \mu\text{M}$  and by about 10% at  $c_{M,X} = 100 \mu\text{M}$ . Thus Equation 3.11 appears to provide an acceptable estimate for  $\Lambda_{M,X}$  over a wide range of concentrations. The Fuoss-Onsager model was not pursued further since an additional adjustable parameter (ion size) is required, and the range and precision of the data are not sufficient for an analysis of conductivity per se.

The values of  $\Lambda^\circ_{M,X}$  and  $\kappa^\circ$  were determined from the data in Figure 3.2 by a weighted nonlinear least squares parameter optimization procedure and are presented in Table 3.4. The continuous lines in Figure 3.2 are calculated directly from Equations 3.8-12, and the constants in Tables 3.3 and 3.4.

The values obtained for the background conductivities of the salt-free water-saturated octanol,  $\kappa^\circ$ , generally varied between 5-10  $\text{nS cm}^{-1}$ , or about 25-50% of the conductivity of the solution with the lowest salt concentration. Further study to isolate the source of the background conductivity ( $\text{H}^+$ ,  $\text{OH}^-$ , impurities, or inappropriateness of the model) was not conducted. The values determined for  $\Lambda^\circ$  were not particularly sensitive to the value of  $\kappa^\circ$ .

For the salts LiCl, NaCl, and KCl, there is no evidence, nor any reason to suspect, that any species other than those represented in Reactions 1 and 2 are present in octanol. The data for both chloride concentration and conductivity can be explained very satisfactorily by these species.

Table 3.4. Conductivity of electrolytes in octanol saturated with water at 25 °C<sup>a</sup>.

A. Monovalent cations

Electrolyte	$\Lambda^\circ_{M,X}$ , S cm <sup>2</sup> mol <sup>-1</sup>	$\kappa^\circ$ , nS cm <sup>-1</sup>
LiCl	4.83(0.02)	5.4(0.5)
NaCl	3.96(0.02)	9.7(0.3)
KCl	3.73(0.03)	8.8(0.6)
HCl <sup>b</sup>	9.75(0.07)	
Electrolyte	$\Lambda^\circ_{M,X}$ , S cm <sup>2</sup> mol <sup>-1</sup>	$\Lambda^\circ_{M_2X, MX_2}$ , S cm <sup>2</sup> mol <sup>-1</sup>
HCl <sup>c</sup>	7.15	2.39

B. Divalent cations

Electrolyte	$\Lambda^\circ_{M,X}$ , S cm <sup>2</sup> mol <sup>-1</sup>	$\kappa^\circ$ <sup>d</sup> , nS cm <sup>-1</sup>
MgCl <sub>2</sub>	2.24(0.02)	18(0.2)
CaCl <sub>2</sub>	2.18(0.02)	15(0.1)

<sup>a</sup>. Westall et al., 1990.

<sup>b</sup>. Species of HCl in octanol phase are free ions and ion pairs.

<sup>c</sup>. Species of HCl in octanol phase are free ions, ion pairs, and triple ions.

<sup>d</sup>. The values of  $\kappa^\circ$  for the divalent cations are larger than expected for pure water-saturated octanol; values more consistent with pure water-saturated octanol are found if the species  $M^{2+}$  is included in the model. More experiments at low concentrations of  $MCl_2$  would be necessary to quantify this relation.

The distribution of HCl. The concentration of HCl in octanol equilibrated with aqueous solutions have been reported by Westall et al. (1990). The transfer of HCl from water to octanol is more favorable than that of LiCl, NaCl, and KCl. These data are interpreted in terms of Reactions 1 and 2, for which the equilibrium constants are in Table 3.3.

Since the total concentration of HCl in octanol is so high, the data have been considered in two sets: (i) the data for aqueous phase concentrations from 0 - 0.2 M in the aqueous phase, for which the assumption of unit activity coefficients in the octanol phase is justifiable; and (ii) the full dataset for aqueous phase concentrations from 0 - 1 M, for which the fit of the model to the data is satisfactory, but for which the assumption of unit activity coefficients in the aqueous phase is not strictly justifiable. The constants derived from the two sets of data are not greatly different, as can be seen in Table 3.3.

The dependence of conductivity on mean salt activity shown in Figure 3.3 for HCl differs qualitatively from the linear dependence seen for the other monovalent electrolytes in Figure 3.2. This dependence could be attributed to a significant change in the activity coefficients of species in the organic phase or to greater-than-pairwise ion association (that is, formation of species such as  $M_2X^+$ , and  $MX_2^-$ ), as discussed by Fuoss and Accascina (1959). However these questions will not be pursued further here on account of the uncertainties associated with the high concentrations of HCl in the organic phase and the limited amount of data.

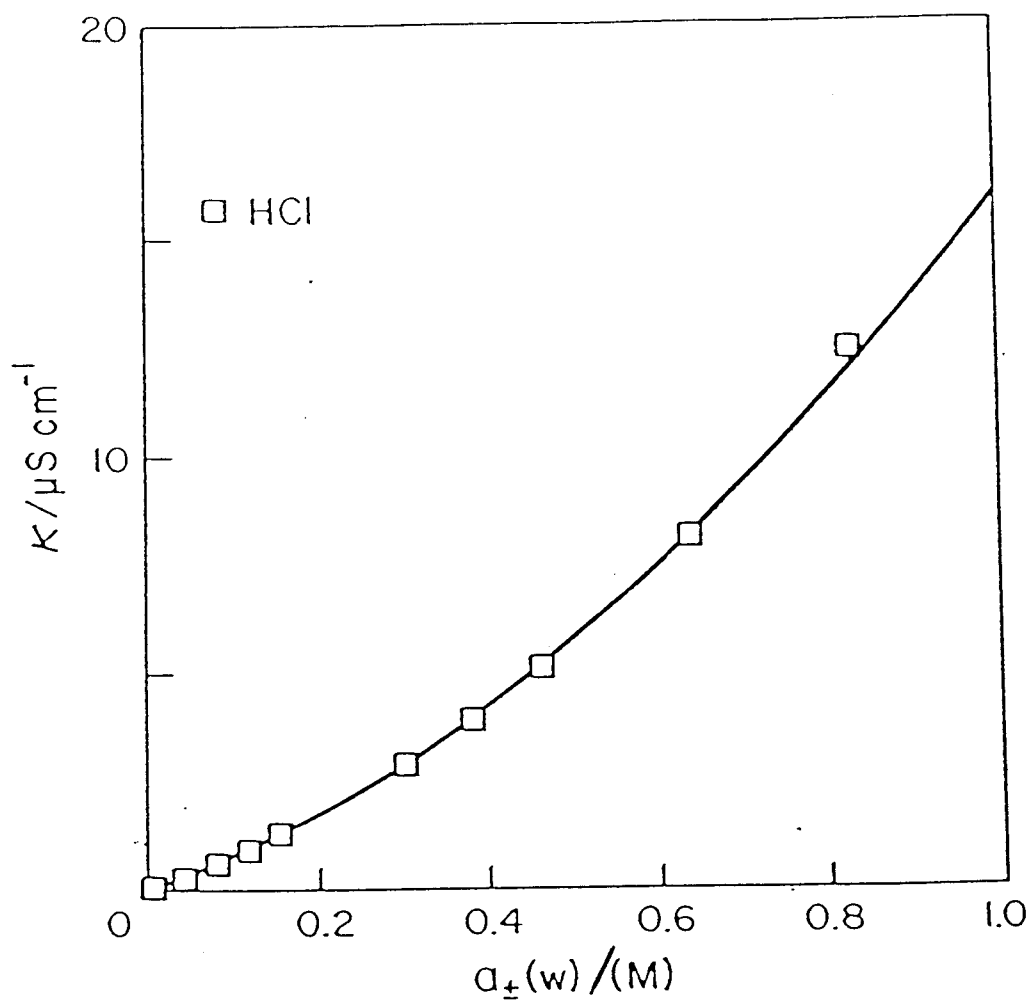


Figure 3.3. The specific conductivity of octanol that has been equilibrated with an HCl solution of the indicated mean molar activity. The symbols represent the experimental data, and the lines are calculated from Equation 3.10, and the constant in Table 3.3 and 3.4 in consideration of the presence of the triple ions in octanol.

In summary, I have reasonable confidence in the interpretation of the HCl distribution up to 0.2 M in the aqueous phase; to interpret the distribution at higher concentrations, more data are necessary.

The distribution of MgCl<sub>2</sub> and CaCl<sub>2</sub>. The concentrations of the 1:2 electrolytes MgCl<sub>2</sub> and CaCl<sub>2</sub> in octanol, as a function of their mean salt activities in aqueous solution, have been reported by Westall et al. (1990). These experimental data were interpreted in terms of Reactions 4 and 5 in Table 3.1, for which the mass action equations are

$$a_M a_X^2 K_3 = \bar{c}_{MX} \bar{c}_X \quad (3.13)$$

$$a_M a_X^2 K_4 = \bar{c}_{MX_2} \quad (3.14)$$

The constants  $K_3$  and  $K_4$  were determined by weighted nonlinear least squares parameter optimization (Westall et al., 1990), and are given in Table 3.3.

The conductivity data shown in Figure 3.4 further substantiate the predominance of the two ionic species,  $MX^+$  and  $X^-$ , in octanol. For these divalent metal chlorides, the concentrations in the octanol phase of  $c_{MX^+} = c_{X^-} = c_{MX,X}$  are found from Equations 3.7 and 3.13 to be proportional to the mean salt activity to the power 1.5. Hence the specific conductivity is expected to vary with the mean salt activity to the power 1.5 according to the equation (adjusted for variation in  $\Lambda$  with  $c$ ):

$$\kappa = \bar{c}_{MX,X} \Lambda_{MX,X} + \kappa^\circ \quad (3.15)$$

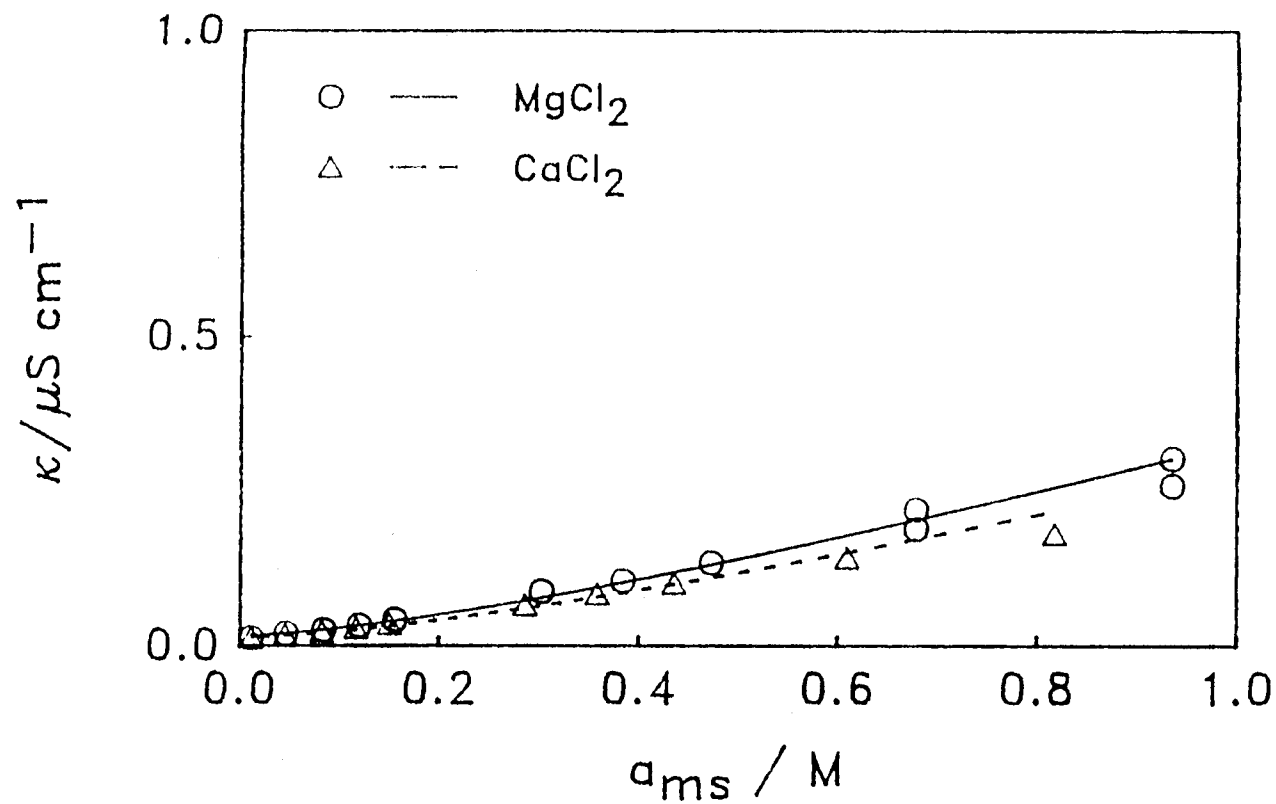


Figure 3.4. The specific conductivity of octanol that has been equilibrated with an aqueous salt solution of  $MgCl_2$  or  $CaCl_2$  with the indicated mean molar activity. The symbols represent the experimental data, and the lines are calculated from Equation 3.15, and the constants in Table 3.3 and 3.4 in consideration of the species of  $MX^+$  and  $X^-$  in octanol.

This dependence is seen in Figure 3.4. Values of  $\Delta^\circ$  for  $MX^+$ ,  $X^-$  and  $\kappa^\circ$  were determined from the data in Figure 3.4, with  $\Delta_{MX,X}$  calculated from Equation 3.11, and are presented in Table 3.4. The lines in Figure 3.4 were calculated from these constants and agree well with the data points.

For the salts  $MgCl_2$  and  $CaCl_2$ , the existence of the uncomplexed metal ion  $M^{2+}$  in octanol was considered. The equilibrium was represented by Reaction 6 in Table 3.1, for which the mass action equation is:

$$a_M a_X^2 K_5 = \bar{c}_M \bar{c}_X^2 \quad (3.16)$$

The correspondence of the model to the experimental data for the distribution of chloride was not improved by inclusion of this reaction. More experiments at lower concentrations of  $MX_2$  might yield more evidence for the species  $M^{2+}$ . We conclude that this species is not significant in the octanol phase equilibrated with 0.01 M  $MX_2$  in the water phase.

## DISCUSSION

Ion-pair formation. Ion-pair formation reactions in the octanol phase can be expressed by Reaction 7 and 8, as shown in Table 3.1. The ion-pair constants for these reactions can be calculated from the ratios of the distribution constants in terms of the Reactions 1 and 2, and 4 and 5.

Table 3.3 lists the equilibrium constants. The logarithms of the ion-pair formation constants in Table 3.3 are generally on the order of 4, indicating that ionic association of electrolytes in octanol is very strong. According to Bjerrum's model (Robinson and Stokes, 1959), the tendency for ion-pair formation of electrolytes in a solution strongly relies on the dielectric constant of the medium. The variation of the association constants with dielectric constants for 1:1 salts has been illustrated by Bockris and Reddy (1976). The ion-pair formation constants for KCl in ethanol ( $\epsilon = 24.55$ ) is only 1.98 (Kratochvil and Yeager, 1972) while in water-saturated octanol ( $\epsilon = 8.1$ ) it is 4.42. Thus, the strong electrolytes, corresponding to high dielectric solvent, would behave like weak electrolytes when they are dissolved in low dielectric solvents.

Another characteristic of the results are that the ion-pair constants for LiCl, NaCl, and KCl in octanol are too close to show any particular trend. However, for the same salts in ethanol, the ion-pair constants for Li, Na, and K chlorides were 1.43, 1.64, and 1.98, respectively (Kay and Evans, 1965), indicating that the tendency for ion-pair formation of these alkali-metal cations with same anion can be correlated to their ionic radius. Increasing in dielectric

property from ethanol to octanol not only increases the capability of ion association for these cations, but decreases the difference for these ions.

For the divalent salts, the ion-pair formation constants for  $\text{MgCl}^+$  and  $\text{CaCl}^+$  with  $\text{Cl}^-$  were found to be approximately 4, which is in the same order with the constants for the monovalent salts (Table 3.3). This indicates that the ions  $\text{MgCl}^+$  and  $\text{CaCl}^+$  in octanol may behave like monovalent species. Recently, Apelblat and Manzurola (1987) have studied the partition of  $\text{CaCl}_2$  in 1-octanol and water system at the aqueous  $\text{CaCl}_2$  concentration range of 0.2323 up to 6.71 m. They have found that the amount of water in octanol varies with the aqueous  $\text{CaCl}_2$  concentration. They conclude that  $\text{CaCl}_2(\text{H}_2\text{O})_5(\text{ROH})_5$  complex is present in octanol phase, but there is no further information about the ionic solvation or the structure of these complexes. From our results, however, at the aqueous salt activity lower than 0.8 M, the species of  $\text{CaCl}^+$  is the major form of  $\text{Ca(II)}$  in octanol, the species of  $\text{CaCl}_2$  is only predominate when the aqueous salt activity is larger than 0.8 M. Therefore, the results from this work only partially agree with Apelblat and Manzurola's data.

In consideration of the argument over the formation of triple ions, two questions should be answered: (i) is it possible to form triple ions in the octanol phase? (ii) how do we interpret conductance data with single ions and triple ions.

Bockris and Reddy (1976) suggested that triple ion formation should be considered in solvents for which the dielectric constant is less than 15. The evidence for formation of triple ions could be

supported by recent spectroscopic data (Bacelon et al., 1980) and computer simulations (Rossky et al., 1980). From this work, the parabolic dependence of conductivity in octanol on aqueous mean salt activity for HCl indicates that triple ions may exist in octanol, though the activity coefficient for HCl in octanol may need to be corrected since the concentration of ions in octanol is high.

In order to interpret conductivity data which involves triple ion formation, additional assumption have to be made (Fuoss, 1933) to simplify the problem. The most common assumption is that both  $M_2X^+$  and  $MX_2^-$  exist, and the triple ion formation constant for  $M_2X^+$  is equal to that for  $MX_2^-$ . Therefore, the concentrations for  $M^+$  and  $X^-$  are equal, and the concentrations for  $MX_2^-$  and  $M_2X^+$  are also equal. This is the assumption many people have used (Beronius and Lindback, 1978; Fuoss, 1933; and Sukhotin and Timofeeva, 1959), and here the same assumption was used to describe our conductivity data for HCl.

However, the assumption mentioned above may not be true. In order to interpret correctly conductivity data of an electrolyte solution which involves single ions, ion pairs, and triple ions, one has to deal with four different conducting species (different equivalent conductivity and different concentration). This problem, up to date, has not been solved. Recently, Grigo (1982) attempted to describe conductivity data for the systems LiBr in octanol and NaI in butanol with a model that only includes single ions and ion pairs so that the sticky problem with triple ions would be avoided. From the results of concentration distribution and conductivity for LiCl between octanol and water in this study, it is verified that there is

no evidence for existence of triple ions for LiCl in octanol phase.

Limiting equivalent conductivity. Limiting equivalent conductivities,  $\Lambda^\circ$  of the electrolytes in octanol saturated with water are shown in Table 3.4. The value of  $\Lambda^\circ$  for LiBr in octanol was obtained by Beronius (1978) and reported to be 3.921, which is very close to the data for LiCl (3.91), obtained from this work.

The limiting equivalent conductivity is related to the mobility of the ion, which is a function of charge and size of the ion and viscosity of the medium. Comparison of the  $\Lambda^\circ$  values may tell us the situation of ionic solvation. The order of  $\Lambda^\circ$  for the simple monovalent salts in octanol(w) is  $\text{LiCl} > \text{NaCl} > \text{KCl}$  (Table 3.4). This is the same order as the crystal radius of the cations.

However, the trends of the  $\Lambda^\circ$  for these electrolytes in water, methanol, and ethanol are  $\text{LiCl} < \text{NaCl} < \text{KCl}$  (Table 3.5), which means the hydration (or solvation) of  $\text{Li}^+$  is so strong that even changes the order of the size of ions. Obviously, the long alkyl chain octanol molecule is not favorable in the solvation of small inorganic ions, the ions in octanol might be bare without any solvation, or, since the solvent is octanol saturated with water, the ions might be hydrated by water. However, it is predicted that this hydration of ions in octanol is much weaker than that in water medium, and the extent of hydration for Li, Na, and K may be the same.

From conductivity results, the interpretation of HCl in octanol includes the contribution of single ions and triple ions, and the 1:2 electrolytes  $\text{MgCl}_2$  and  $\text{CaCl}_2$  in octanol includes only the contribution of the species  $\text{MX}^+$  and  $\text{X}^-$ . No strong evidence for the species  $\text{M}^{2+}$  in the nonaqueous phase was found.

Table 3.5. The limiting equivalent conductivities of the inorganic salts in water and alcohols at 25 °C.

	Water	Methanol	Ethanol	Propanol	Octanol(W)	
Viscosity(cP):	0.890 <sup>a</sup>	0.545 <sup>a</sup>	1.078 <sup>a</sup>	1.956 <sup>a</sup>	7.275 <sup>f</sup>	
$\epsilon$ :	78.39 <sup>a</sup>	32.70 <sup>a</sup>	24.55 <sup>a</sup>	20.33 <sup>a</sup>	8.1 <sup>f</sup>	
Electrolyte	$\Lambda^\circ$ <sup>b</sup>	$\Lambda^\circ$ <sup>c</sup>	$\Lambda^\circ$ <sup>c</sup>	$\Lambda^\circ$	$\Lambda^\circ$ (M,X)	$\Lambda^\circ$ (M2X,MX2)
HCl	426.16	193.2	81.7	29.81 <sup>d</sup>	7.15	2.39
LiCl	115.03	92.05	38.94		4.83	
NaCl	126.45	97.4	42.17	22.8 <sup>e</sup>	3.96	
KCl	149.86	104.9	45.42		3.73	

	Water	Octanol(W) <sup>f</sup>
Electrolyte	$\Lambda^\circ$ (1/2M,X)	$\Lambda^\circ$ (MX,X)
MgCl <sub>2</sub>	129 <sup>c</sup>	2.24
CaCl <sub>2</sub>	135.84 <sup>b</sup>	2.18

Reference:

- a. Marcus, 1985.
- b. Bard and Faulkner, 1980.
- c. Popovych and Tomkins, 1981.
- d. Goffredi and Shedlovsky 1967a.
- e. Goffredi and Shedlovsky 1967b.
- f. Data from this work. The relative permittivity of water-saturated octanol,  $\epsilon$ , was obtained with different calibration method which is described in Chapter 2.

## SUMMARY

The data for the distribution of LiCl, NaCl, KCl between water and water-saturated octanol phase are well explained by the species,  $M^+$ ,  $X^-$ , and  $MX$  in the nonaqueous phase. Values of ion-pair formation constants agree with those found in the literature.

For HCl the distribution data could be interpreted satisfactorily in terms of the species  $H^+$ ,  $X^-$ , and  $HCl$ , but the conductivity data indicate the presence of triple ions such as  $H_2Cl^+$  or  $HCl_2^-$ .

For  $MgCl_2$  and  $CaCl_2$ , the data are explained by  $MX^+$ ,  $X^-$ , and  $M_2X$  in the nonaqueous phase. No strong evidence for the species  $M^{2+}$  in the nonaqueous phase was found.

The limiting equivalent conductivities  $\Lambda_{M,X}^\circ$  for the Li, Na, and K chlorides are in the same order as the crystal radii of the cations. This result is different with the  $\Lambda_{M,X}^\circ$  of these salts in water and the alcohols with shorter alkyl chains.

## REFERENCES

- Apelblat, A. and Manzurola, E. Ber. Bunsenges. Phys. Chem. 1987, 91, 1387-1394.
- Bacelon, P.; Corset, J.; and de Loze, C. J. Solution Chem. 1980, 9, 129.
- Bard, A. J. and Faulkner L. R. Electrochemical Methods; 1980, John Wiley & Sons.
- Beronius, P. Acta Chem. Scand. A 1978, 32, 469-470.
- Beronius, P.; Lindbaeck, T. Acta Chem. Scand. A 1978, 32, 423-428.
- Bockris, J. O'M. and Reddy, A. K. N. Modern Electrochemistry 1. 1976, A Plenum/Rosetta Edition.
- Fuoss, R. M. and Kraus, C. A. J. Am. Chem. Soc. 1933, 55, 2387.
- Fuoss, R. M. and Accascina, F. Electrolytic Conductance 1959, Interscience: New York.
- Goffredi, M. and Shedlovsky, T. a: J. Phys. Chem. 1967, 71, 2182-2186. b: J. Phys. Chem. 71, 2176-2181.
- Grigo, M. J. of Solution Chem. 1982, 11, 529-537
- Hansch, C. and Dunn, W. J. III. J. Pharm Sci. 1972, 61, 1.
- Johnson, C. A. Department of Chemistry, Oregon State University. Experimental data, 1987.
- Johnson, C. A. and Westall, J. Environ. Sci. Technol. 1990, 24, 1869-1875.
- Karickhoff, S., Brown, D. S. Water Res. 1979, 13, 241-248.
- Kay, R. L.; Zawayski, C.; Evans, D. F. J. Phys. Chem. 1965, 69, 4208.
- Kratochvil, B. and Yeager H. L. Topics in Current Chemistry; 1972, No. 27.
- Leo, A. and Hansch, C. J. Org. Chem. 1971, 36, 1539-1544.
- Lyman, W. J. in Handbook of Chemical Property Estimation Methods; Lyman, W. J.; Rheel, W. F.; Rosenblatt, D. H., Eds.; McGraw Hill: New York, 1982, 2-40.
- Marcus, Y. Ion Solvation; 1985, Wiley-Interscience: London.
- Pitzer, K. S. and Mayorga, G. J. Phys. Chem. 1975, 77, 2300-2308.

Popovych, O. and Tomkins, R. P. T. Nonaqueous Solution Chemistry; 1981, Wiley-Interscience: New York.

Robinson, R. A. and Stokes, R. H. Electrolyte Solutions. 1959, Butterworths: London.

Rosky, P. J.; Dudowicz, J. B.; Tembe, B. L.; and Friedman, H. L. J. Chem. Phys. 1980, 73, 3372.

Schellenberg, K.; Leuenberger, C.; and Schwarzenbach, R. P. Environ. Sci. Technol. 1984, 18, 652-657.

Soehnel, O. and Novatny, P. Densities of Aqueous Solutions of Inorganic Substances; 1985, Elsevier: Amsterdam.

Sukhotin, A. M. and Timofeeva, Z. N. Zhur. Fiz. Khim. 1959, 33, 1602.

Veith, S. D.; Macek, D. J.; Petrocelli, S. R.; and Carroll, J. Aquatic Toxicology; Eaton J. G., Passish P. R., Hendricks A. C., Eds.; ASTM STP 707, 1980.

Westall, J. C.; Leuenberger, C.; Schwarzenbach, R. P. Environ. Sci. Technol. 1985, 19, 193-198.

Westall, J. C. FITEQL-A Computer Program for Determination of Chemical Equilibrium Constants from Experimental Data. Version 1.2. Report 86-01, Department of Chemistry, Oregon State University, Corvallis, OR, 1986.

Westall, J. C. MICROQL-A Chemical Equilibrium Program in BASIC. Version 2 for PC's. Report 86-02, Department of Chemistry, Oregon State University, Corvallis, OR, 1986.

Westall, J. C.; Johnson, C. A.; Zhang, W. Environ. Sci. Technol. 1990, 24, 1803-1810.

## CHAPTER 4

### METHODS FOR THE STUDY OF ADSORPTION OF SURFACTANTS ON ENVIRONMENTAL SORBENTS

## INTRODUCTION

The transport and fate of anionic, cationic, and nonionic surfactants in the environment is a matter of interest due to the large amounts of these compounds that are released into the environment in consumer products (Boethling et al., 1984; Games and Larson, 1982; Larson and Vashon, 1983).

In order to assess the environmental safety of surfactants, it is important to study the mechanisms of adsorption of surfactants and further understand the distribution and speciation of surfactants. It is the goal of this chapter to overview some of the general characteristics of the surfactants and describe the methods developed in this research to study the adsorption of the surfactants on environmental sorbents.

Properties of surfactants. Surfactants consist of two parts in their molecular structures: a hydrophilic head and a hydrophobic chain. These special structures give the distinguishable features for the behaviors of surfactants.

A remarkable characteristic of surfactants is their strong tendency to be adsorbed at various interfaces, such as air-water, oil-water, and solid-water, etc. They also reduce the interfacial energy of the systems (Rosen, 1978; Aveyard, 1984).

Another important property of surfactants is the formation of micelles. Micelle formation dramatically changes many physical properties of surfactant solutions such as surface tension, conductivity, equivalent conductivity, turbidity, and osmotic pressure

(Rosen, 1978; Hiemenz, 1986). The concentration at which the abrupt changes in the properties occur is known as the critical micelle concentration or CMC.

Adsorption of surfactants on pristine surfaces. In order to study the mechanisms of adsorption of surfactants on environmental sorbents (e.g. sediments, soils, aquifer materials, etc.), it is important first to understand the mechanisms of adsorption of surfactants on some pristine sorbents, since the surfaces of pristine sorbents are generally more homogeneous and better characterized. Table 4.1 summarizes the published studies on adsorption of anionic, cationic, and nonionic surfactants on a variety of pristine sorbents. Several excellent reviews are also available on this subject (Rosen, 1978; Hough and Rendall, 1983; Chander et al., 1983; Clunie and Ingram, 1983).

The electrostatic interaction has been observed for adsorption of alkylsulfonates and alkylbenzenesulfonates on alumina (Somasundaran and Fuerstenau, 1966; Dick et al., 1971; and Chander et al., 1983). Their results showed that the increase in the  $H^+$  concentration of the aqueous phase increased significantly the adsorption of the anionic surfactants on the sorbent. At the pH of the point of zero charge of the sorbent, the p. z. c., the adsorption trended to be zero. This result indicated that there was little specific interaction between the surfactants and the sorbent.

The hydrophobic interaction has also been observed for adsorption of ionic surfactants on pristine surfaces. An increase in the chain length of alkylbenzenesulfonate homologs increased the adsorption of these surfactants on alumina and kaolinite

Table 4.1. Studies of adsorption of surfactants on pristine sorbents.

Surfactant	Sorbents	Objective (effect factors)	Year	Investigator
<u>Anionic</u>				
C-12 LAS	alumina	isotherm, pH, I.S.	1966	Somasundaran, et al.
ABS and LAS	hydroxy Fe and Al gel	comparison	1968	Volk and Jackson
C-12 ABS	alumina	isomers, pH,	1971	Dick, et al.
C-12 ABS	A zeolite	isotherm	1981	Savitsky, et al.
C-9,10,12 ABS	alumina	isotherm, and	1982	Scamehorn, et al.
	kaolinite	chain length		
C-12 LAS and ABS	alumina	pH, I.S. isomers	1983	Chander, et al.
C-12 ABS	fibers	counter ions	1987	Sakata and Katayama
C-12 ABS	kaolinite	adsorption	1987	Siracusa, et al.
<u>Cationic</u>				
C-8,10,12,16 TMAB	latex	pH, I.S., and chain length	1971	Connor and Otteville
C-12, C-16 TMAB	silica	isotherm, pH, chain length	1974	Bijsterbosch
C-14 TMAC	zeolite A	isotherm	1981	Savitsky, et al.
C-16,18 DMDAC	zeolite A	isotherms, I.S.	1983	Schwuger, et al.
C-10 TMAB	silica gel	isotherm and heat of adsorption	1988	Woodbury and Noll
C-16 TMAB	silica gel	hemimicellization	1989	Gu and Huang
<u>Nonionic</u>				
C <sub>12</sub> E <sub>6</sub>	zeolite A	isotherm	1981	Savitsky, et al.
APE	activated C,	isotherm	1985	Narkis and Bella
PEO and PPO	latex	# of ethylene	1987	van den Boomgaard, et al.
	silica	and temperature		

Chander et al., 1983; and Scamehorn et al., 1982), whereas the increase in branching in the alkyl chain decreased the adsorption (Dick et al., 1971).

Some studies have been carried out for adsorption of surfactants over a wide concentration range to elucidate both the sorbate/sorbent interaction and sorbate/sorbate interaction. The adsorption isotherms were generally S-type with three distinguishable regions: the low surface coverage region, the hemimicelle formation region, and the plateau region. The mechanisms of adsorption in each region have been interpreted by Chander et al. (1983), Scamehorn et al. (1982), and Gu and Huang (1989). These S-type isotherms have been found for adsorption of cationic, anionic and nonionic on variety of pristine sorbents, such as silica, alumina, kaolinite, type A zeolite, and polystyrene latex (Gu and Huang, 1989; Savitsky et al., 1981; Schwuger et al., 1983; Chander et al., 1983; Scamehorn et al., 1982; and Mathai and Ottewill, 1966).

Adsorption of surfactants on heterogeneous materials. Although extensive studies have been done on the mechanisms of adsorption of surfactants on a variety of pristine sorbents, the adsorption of ionic and nonionic surfactants on environmental sorbents (e.g. sediments, soils, and aquifer, etc.) has received relatively little attention (Hand and Williams, 1987; Urano and Saito, 1984). It is probably due to the fact that surfaces of these environmental sorbents are extremely heterogeneous as compared with the surfaces of pristine sorbents. Some recent studies in this area are summarized in Table 4.2.

Table 4.2 Studies of adsorption of surfactants on natural materials.

Surfactant	Objective	Year	Investigator
<u>Anionic</u>			
branched ABS	degradation	1963	Robeck, et al.
LAS	effect of OC% and clay%	1966	Krishna Murti, et al.
branched ABS	isotherms	1970	Fink, et al.
ABS	field adsorption	1975	Reneau and Pettry
C-12ABS	biodegradation	1983	Larson
ABS	environmental fate, models	1983	Games
ABS	toxicity	1983	Lewis and Suprenant
C-12ABS	isotherms	1984	Urano and Saito
C-12ABS	isotherms, effect of OC%	1984	Urano and Murata
C-12ABS	toxicity	1984	Yamane, et al.
ABS	adsorption and desorption	1985	Matthijs, De Henau
ABS	accumulation	1985	McEvoy and Giger
branched ABS and SDS	fate in groundwater	1986	Thurman, et al.
C-12ABS	environmental fate of LAS	1986	Holysh, et al.
ABS	removal	1986	Sedlak and Booman
ABS	effect of chain length	1987	Hand and Williams
ABS, SDS	biodegradation	1987	Sales, et al.
ABS	degradation	1987	Scheunert, et al.
ABS	adsorption	1988	Brunner, et al.
<u>Cationic</u>			
C-18 TMAC	fate and distribution	1982	Games and Larson
TMAC, DMAC	biodegradation	1983	Larson
C-16 TMAC	toxicity	1983	Lewis and Suprenant
TMAC, DMAC	adsorption, degradation	1983	Larson and Vashon
TMAC, DMAC	fate and toxicity	1984	Boethling
<u>Nonionic</u>			
AE	biodegradation	1981	Larson and Games
AE	toxicity	1983	Lewis and Suprenant
APE	degradation and toxicity	1984	Giger, et al.
AE, APE	isotherms	1984	Urano and Saito
AE	toxicity	1984	Yamane, et al.
AE	biodegradation	1985	Turner, et al.
PEG	adsorption	1987	Podoll, et al.

Some of the areas of study have been biodegradation, bioaccumulation, and toxicity (Yamane et al., 1984; Sales et al., 1987; Lewis and Suprenant, 1983; Larson and Games, 1981; Turner et al., 1985). Another aspect is kinetics of adsorption and desorption.

Sorption equilibrium of LAS with natural materials was found to be relatively rapid and occur within 1 to 4 hours in the studies reported by Matthijs and De Henau (1985), and Hand and Williams (1987). For nonionic surfactants, however, the equilibration is relatively slow.

Experimental studies with LAS and branched chain alkylbenzenesulfonate with sediments (Urano et al., 1984; Matthijs and De Henau, 1985; Hand and Williams, 1987) and soils (Inoue et al., 1978) suggest that both hydrophobic and electrostatic interactions are important. The LAS adsorption was reported to be correlated highly to the organic matter content of the soils (Krishna Murti et al., 1966).

Adsorption of long-chain ( $C_{16}$  -  $C_{18}$ ) monoalkyl and dialkyl quaternary ammonium compounds (QAC's) has been investigated by Larson and Vashon (1983). Their results showed that adsorption of long-chain QAC's to river sediments depended on natural organic matter and other detergents in the system.

In comparison with the studies of adsorption of surfactants on pristine surface, the adsorption behavior of surfactants on natural materials was generally performed within a relatively narrow concentration range. The adsorption due to chain/chain association of the surfactants on the surfaces of environmental sorbents, namely the hemimicelle formation, has not been found in the literature.

The object of the following sections is to describe some of the methods we have developed in our study in the goal of understanding the mechanisms of adsorption of surfactants on environmental sorbents in terms of hydrophobic, electrostatic, and specific chemical interactions. Several methods used in the determination of adsorption of surfactants on different materials are described. The procedures used in quality control of the experiments are also discussed.

## EXPERIMENTAL METHODS

Table 4.3 outlines the major methods and tests which have been investigated in this study. This section includes the methods for pretreatment of sorbents, equilibration and phase separation in batch experiments, determination of  $^{14}\text{C}$  labeled surfactants in water, on sorbents, and on the walls of labware, and determination of pH of the aqueous samples. The method for clay mineral analysis and the tests for adsorption of surfactants on different laboratory materials will also be discussed.

Materials and equipment. Surfactants used in this study are homologs of alkylbenzene sulfonate (LAS), dodecyltrimethylammonium chloride (C-12 TMAC), and homologs of monoalkyl ethers of polyethylene glycol (AE). These surfactants and their formulas are listed in Table 4.4. The ionic surfactants, homologs of linear alkylbenzenesulfonate (LAS) and dodecyltrimethylammonium chloride (C-12 TMAC) were obtained from Procter and Gamble through the Soap and Detergent Association. The nonionic surfactants, homologs of alkyl ethers of poly(ethylene glycol), or "alcohol ethoxylates" (AE), were provided by Shell Research through the Soap and Detergent Association. The specific activity for these surfactants are given in Table 4.4. The radioactive purity for C-12 TMAC was relatively less than the other surfactants. It was reported to be 92% and verified by HPLC measurement in this lab. The standard solutions of  $^{14}\text{C}$  labeled surfactants were prepared in 95% ethanol and stored at temperature below 0 °C.

Table 4.3. Overview of the methods and tests on adsorption of surfactants.

No.	METHODS AND TESTS
1.	Pretreatment of environmental sorbents
2.	Qualitative analysis of clay minerals in the sorbents
3.	Adsorption of surfactants on different materials
4.	Determination of distribution ratio $D_c$
5.	Alternative procedures for analyzing adsorbed LAS on soils
6.	Method of determination of pH
7.	Control charts of calibrations

Table 4.4 Surfactants and characteristics.

Surfactant and formula	abbreviation	purity %	sp. act. Ci/mol
ANIONIC			
<u>linear alkylbenzenesulfonate</u> $C_nH_{2n+1}(C_6H_4)SO_3^-$ :			
sodium 4-(1-methylnonyl)benzenesulfonate	C-10 LAS	>99	1.46
sodium 4-(1-methylundecyl)benzenesulfonate	C-12 LAS	>99	13.4
sodium 4-(1-methyltridecyl)benzenesulfonate	C-14 LAS	>99	12.9
CATIONIC			
<u>linear alkyltrimethylammonium chloride</u> $C_nH_{2n+1}N(CH_3)_3Cl$ :			
dodecyltrimethylammonium chloride	C-12 TMAC	92	25
NONIONIC			
<u>monoalkylethers of poly(ethylene glycol)</u> $C_nH_{2n+1}(OCH_2CH_2)_mOH$ :			
$C_{13}H_{27}(OCH_2CH_2)_3OH$	$A_{13}E_3$	95 - 98	6.9
$C_{13}H_{27}(OCH_2CH_2)_6OH$	$A_{13}E_6$	95 - 98	21.3
$C_{13}H_{27}(OCH_2CH_2)_9OH$	$A_{13}E_9$	95 - 98	6.6

The environmental sorbents used in this study were from the "EPA" soil series and obtained through Professor John J. Hassett at the University of Illinois. Table 4.5 shows the properties of these sorbents. Deionized water used in all experiments was from a Millipore Milli-Q System, with a specific resistivity of 18 M $\Omega$  cm.

A thermostatted shaker (New Brunswick Model G-24) and thermostatted centrifuge (IEC Model B-20A) were used for batch equilibration and phase separation. The sorbent samples were oxidized with a Harvey Model 300 Oxidizer, and radioactivity was determined with a Beckman Model LS 7800 scintillation counter.

Clay mineral analysis. The composition of clay minerals in six environmental samples were analyzed qualitatively by x-ray diffraction. The procedure for clay mineral analysis consists of four steps: (i) preparation of clay suspension and slides; (ii) treatments of samples slides; (iii) scanning of x-ray diffraction spectra; and (iv) qualitative analysis of spectra.

Figure 4.1a shows schematically the procedures for preparation of clay suspension and slides. A 5.0 g sample of sorbent and 100 mL of filtered water were added into a beaker, and then sonicated for 10 minutes to disperse and disaggregate particles (Cell disruptor model 350 Sonifier<sup>R</sup>, Branson Sonic Power Co.). The supernatant was then poured into a 250 mL plastic centrifuge bottle and centrifuged for 1.5 minutes at 1000 RPM in order to sediment the clay. After centrifugation, excess water was decanted and the clays were resuspended in 10 mL of water. A 1-mL of the concentrated clay suspension was drawn into a plastic 100 mL syringe filled with 4 mL of K<sup>+</sup> or Mg<sup>2+</sup> charged cation exchange resin (Rexyn 101(H), Fisher

Table 4.5. Properties of environmental sorbents.<sup>a</sup>

soil	organic carbon %	sand %	silt %	clay %	CEC mmol/g	pH <sup>b</sup> (1:1)	pH <sup>c</sup> (1:20)	Surface area <sup>d</sup> m <sup>2</sup> /g
EPA-16	1.20	0.5	60.5	39.0	0.110	6.50	6.76	18
EPA-13	3.04	20.3	27.1	52.6	0.119	6.90	7.08	13
EPA-1	0.22	93.9	0	6.1	0.011	7.30	-	0.8
EPA-12	2.33	0	64.6	35.4	0.135	7.63	7.52	12
EPA-25	0.76	41.9	37.6	20.5	0.089	7.65	7.57	8

<sup>a</sup> Reported by Hassett et al., 1980.

<sup>b</sup> Solution was 0.01 M NaCl, 1 g soil to 1 mL solution.

<sup>c</sup> Solution was 0.01 M NaN<sub>3</sub>, 1 g soil to 20 mL solution.

<sup>d</sup> Determined courtesy of Jeff Fahey, Teledyne Wah-Chang, Albany, Oregon.

## Clay Mineral Analysis: Sample Preparation

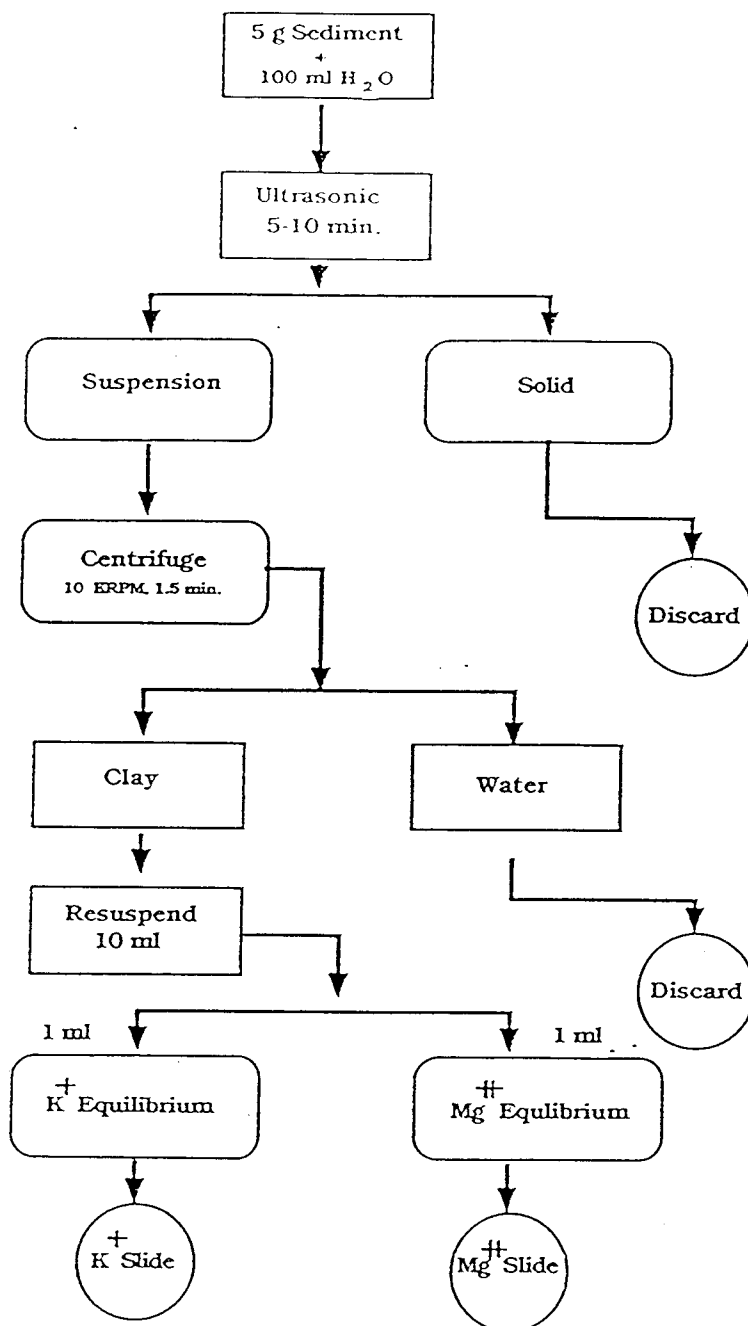


Figure 4.1a. Clay mineral analysis procedures: the preparation of sample suspensions.

## Clay Mineral Analysis: Treatment for X-ray Diffraction

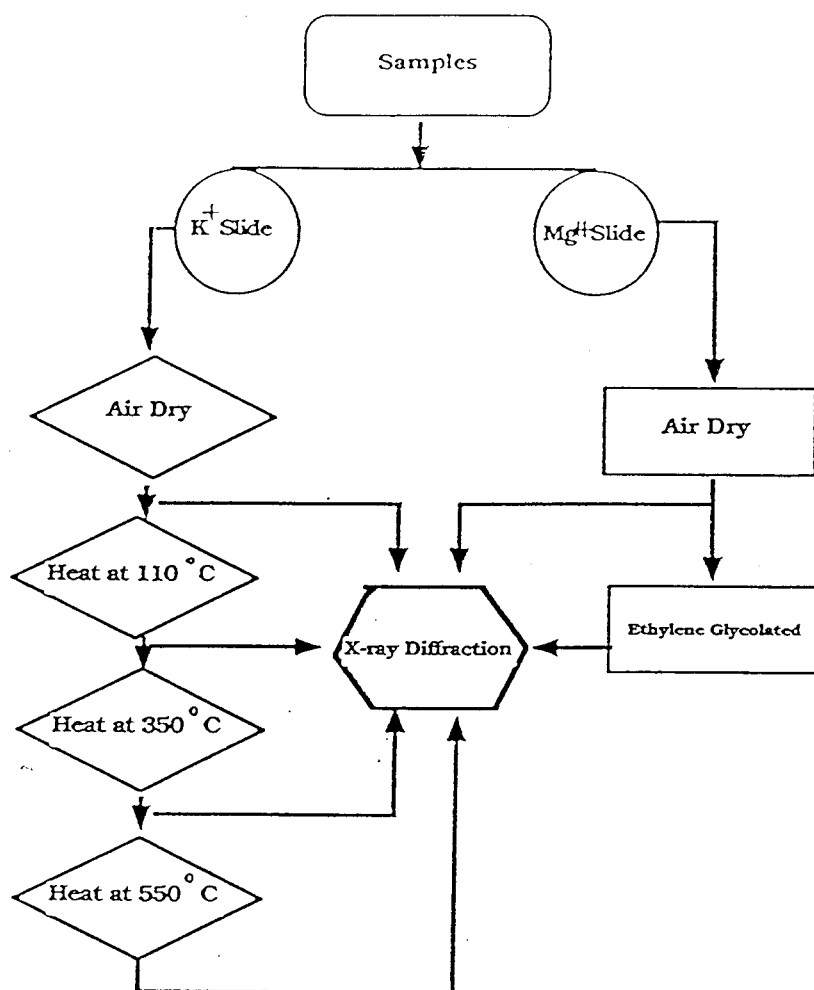


Figure 4.1b. Clay mineral analysis procedures: the treatment of sample slides for X-ray diffraction analysis.

Scientific Co.) and allowed to equilibrate with the resin for 1-2 minutes. The  $K^+$  or  $Mg^{2+}$  charged clay was then deposited onto a 1" diameter glass slide and allowed to air dry. After drying was complete, the slides were placed in a desiccator containing saturated  $Mg(NO_3)_2 \cdot 6H_2O$  (relative humidity = 54%) for 4 days.

For each sample, four sequential treatments were performed for the  $K^+$  slides: air dried, heat treated for 2 hours at 110°C, 350°C, and 550°C, respectively. The heat treatments were performed in a muffle furnace. Two treatments were performed for  $Mg^{2+}$  slides: air dried, and ethylene glycolated. For ethylene glycol treatment, the  $Mg^{2+}$  slide was placed in a desiccator which was filled previously with ethylene glycol (preheated to 70 °C), and the desiccator was placed in a 70 °C oven and heated for 1 hour.

As shown in Figure 4.1b, after each treatment, a scan of the spectrum was run on the slide using a PAD V X-ray diffraction instrument, manufactured by SCINTAG, Inc. A total of 6 spectra scans were run for each sample on the slides of  $K^+$  and  $Mg^{2+}$ . The ID of the runs were KAD, K110C, K350C, K550C, MGAD, MGGLY.

The last step of clay mineral analysis was to analyze the X-ray diffraction spectra of the samples. The information about this step is in Appendix II.

Pretreatment of the sorbents. The sorbents were washed before they were used in batch adsorption experiments. The purpose of this pretreatment step is to remove nonseparable materials (NSM) from the aqueous phase, since the adsorption or the association of surfactants on these nonseparable materials will affect significantly the determination of concentration distribution ratio of surfactants

between the sorbents and the aqueous phases (Gschwend and Wu, 1984). In this study, two methods were used for washing the sorbents: an individual-tube method and a large-volume method.

For the individual-tube method, as illustrated schematically in Figure 4.2a, a 0.05 - 1.0 g sample of the sorbent was added into a 25-mL Corex glass centrifuge tube, and then 20 mL of deionized water was added into the same tube. The slurry was mixed for 1 hour at 500 RPM at 25 °C on a shaker, and centrifuged for 10 minutes at 10,000 RPM at 25 °C to separate the two phases. The supernatant was then discarded. In the same way, the sorbents were washed subsequently eight times and then were ready for the batch experiments. The efficiency of this washing step was evaluated by determination of the UV absorbance of the supernatant after each washing step. In this study, the sorbents used for most of the adsorption experiments were treated by this method.

For the large volume method, as illustrated schematically in Figure 4.2b, 20 g of sorbents was added to a 250 mL plastic bottle, then 200 mL of water was added. The time for sample mixing and centrifugation was the same as the time for the individual method. After the sorbents were washed eight times, the wet sorbents were transferred to a porcelain crucible, and dried in an oven at 50 °C. The sorbents were weighed and dried alternately until the mass lost between the last two measurements was less than 1% of the total mass of the sorbent. After this step, the dry sorbents were ground slightly, mixed well, and ready for the batch experiment. The possibility that the grinding of the dry sorbent might change its properties was considered; however, experiments (to be discussed)

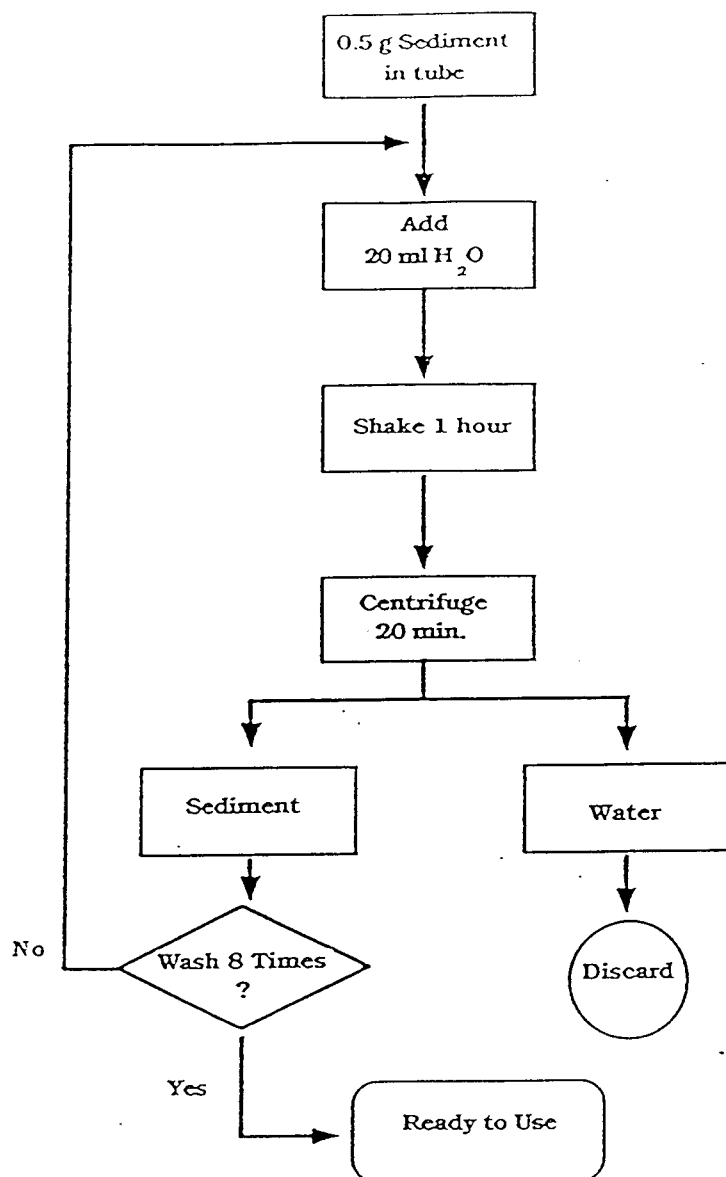


Figure 4.2a. The flow chart for the procedures of washing sorbents: an individual tube washing method.

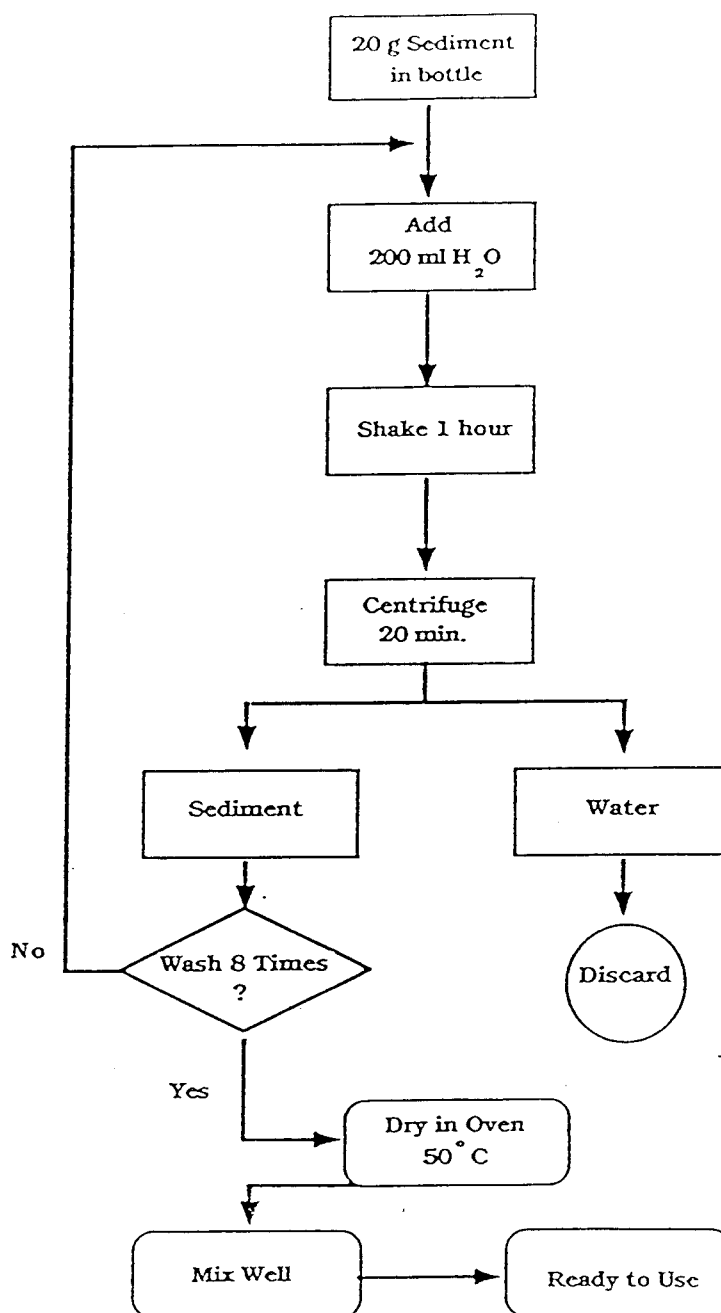


Figure 4.2b. The flow chart for the procedures of washing sorbents: a large volume washing method.

indicated no significant effect.

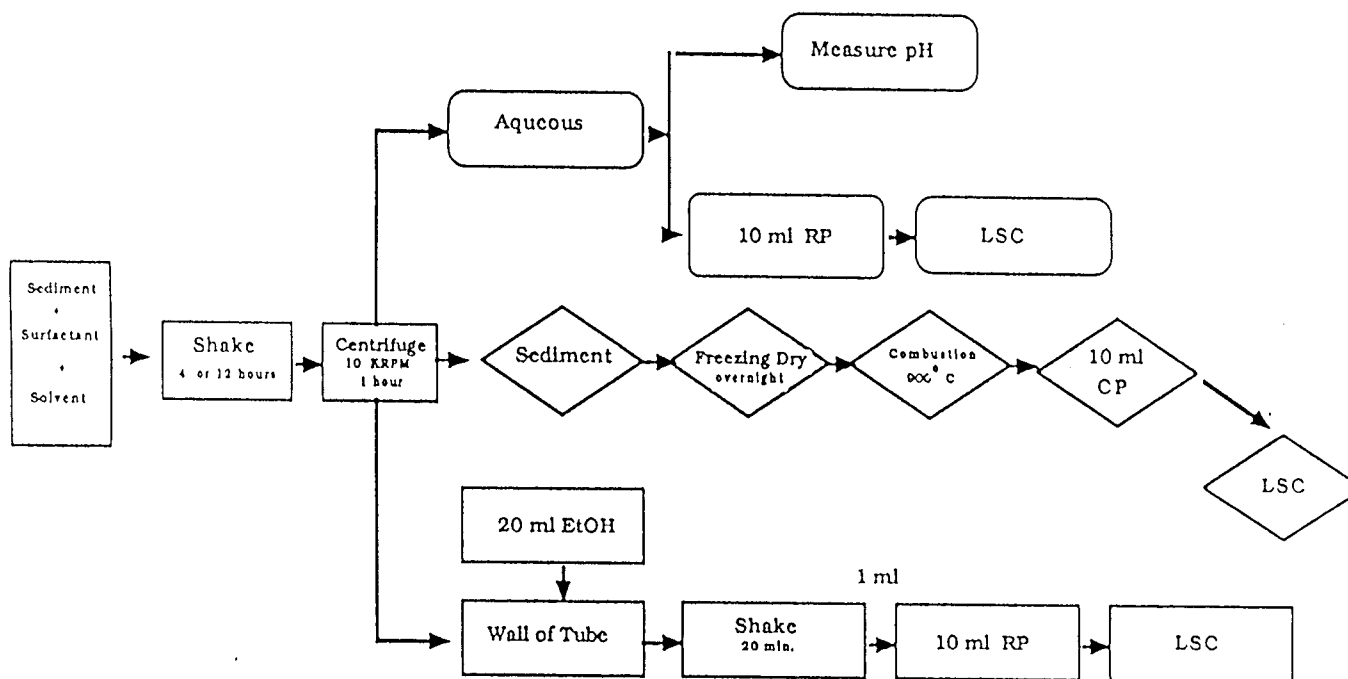
An experiment was performed to examine whether or not the method of washing the sorbent would affect the adsorption of the surfactant. No significant effect was seen, as will be discussed in a later section.

Determination of distribution ratio  $D_C$ . In this study, the concentration distribution ratio,  $D_C$ , is defined as the ratio of total concentration of a given surfactant on the sorbent to the total concentration of the surfactant in the aqueous phase, expressed by the equation

$$D_C = C(s) / C(w) \quad (4.1)$$

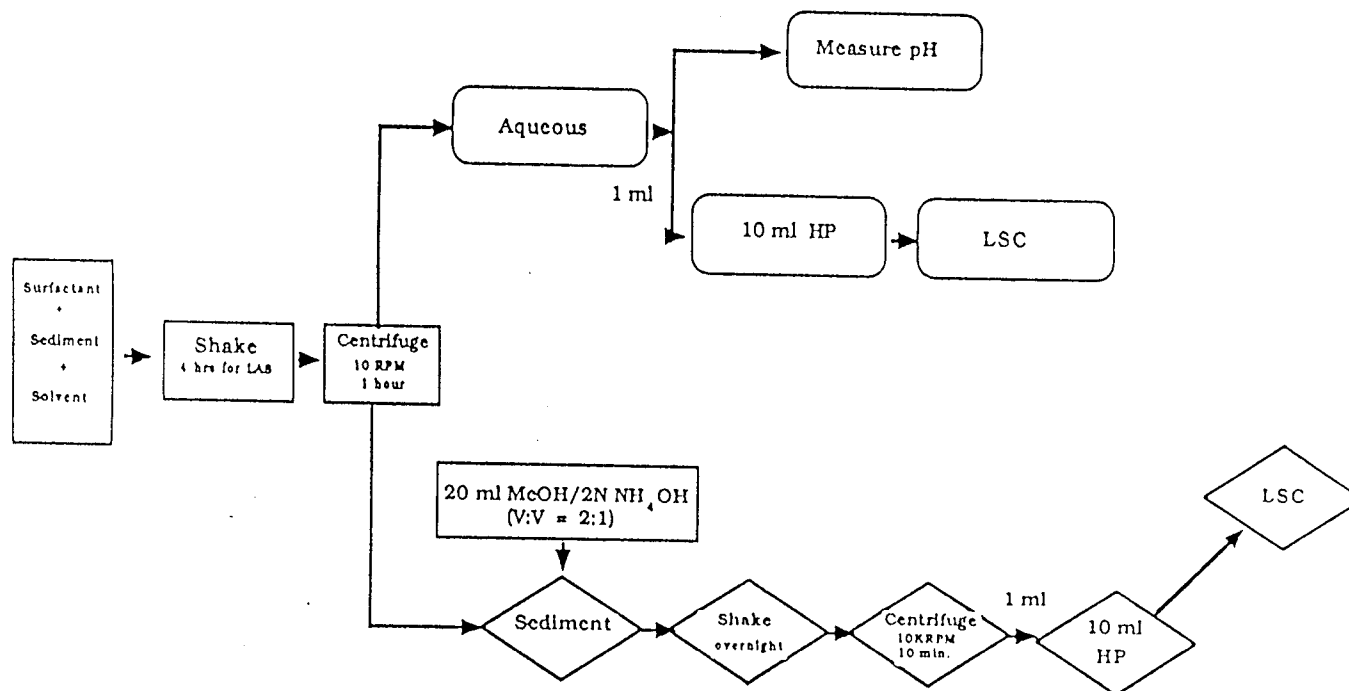
where  $C(s)$  and  $C(w)$  are the concentrations in sorbents and water in the units of mol/kg and mol/L, respectively.

The procedures for determining the distribution ratio ( $D_C$ ) of surfactants between the sorbents and the aqueous phases are illustrated in Figure 4.3a and described as follows. After the sorbents were washed eight times, 20 mL of 0.01 M  $\text{NaN}_3$  (or in some cases 0.01 M of  $\text{NaCl}$ ) solution was added into the tube containing the washed sorbents. A 10 - 100  $\mu\text{L}$  spike of standard solutions of  $^{14}\text{C}$  labeled surfactant, prepared in 95% ethanol, was added into each tube with a Hamilton syringe. The tubes were then capped tightly and agitated on a thermostatted shaker at 500 RPM at 25 °C. The previous experiments on the adsorption kinetics have verified that a four-hour equilibration was sufficient for adsorption of C-12 TMAC and LAS, and a 12 hours equilibration was needed for adsorption of  $A_{13}\text{E}_m$ .



Batch Adsorption Procedure I: Combustion Method

Figure 4.3a. The flow chart of the procedures for batch adsorption experiments: by a combustion method.



Batch Adsorption Procedure II: Extraction Method

Figure 4.3b. The flow chart of the procedures for batch adsorption experiments: by an extraction method.

After the batch adsorption equilibration, the samples were centrifuged at 11,000 G (10,000 RPM) for 1 hour at 25 °C to separate the two phases.

For aqueous sample analysis, a 0.2 - 1.0 mL aliquot of the aqueous solution was transferred directly into a scintillation vial containing 10 mL of Beckman HP/b scintillation fluid. The pH of the aqueous samples were then determined. The method for determination of the pH will be discussed in detail later. After that, excess aqueous sample was removed, and the wet sorbents samples were freeze dried directly in the tubes overnight. The tubes were weighed before and after the step of freeze drying to estimate how much water was left in the sorbents samples. For each sorbents sample, two subsamples of the sorbents (10 - 200 mg) were taken for combustion. Each subsample was transferred onto an combustion boat, weighed, and oxidized at 900 °C in an oxygen stream. The  $^{14}\text{CO}_2$  produced was trapped in a mixture of 5 mL Packard Carbo-sorb and 5 mL Packard Permafluor V scintillation liquid, and determined by liquid scintillation counting.

The amounts of surfactants adsorbed on the walls of the tubes were also determined by the following procedures. After removal of the sorbent samples for combustion, the excess sorbent samples were discarded, and the dust of the sorbents in the tubes were brushed out by cotton Q-tips. Then 20 mL of 95% ethanol was added into each tube, the tubes were shaken at 500 RPM at 25 °C for 20 minutes to rinse out the surfactants from the walls. After that, a 1-mL aliquot of the rinsing solution was delivered into a vial containing 10 mL of

Beckman HP/b scintillation fluid for determining the radioactivity.

For each sample, the material recovery was calculated as the ratio of the total activity founded in the water, the sorbents, and the wall to the total activity added.

For each experiment, the combustion recovery was evaluated to verify that the combustion oven operated properly. The procedure for this test is as follows: a spike (10 to 30  $\mu\text{L}$ ) of surfactant standard solution was added directly to a certain amount of sorbent on a combustion boat. This sample was then oxidized, and the combustion recovery was calculated to be the ratio of the activity found to the activity added.

Calibrations were determined for each experiment by adding various amounts (a spike of 10 to 50  $\mu\text{L}$ ) of surfactant standard solution into each phase and determining the activity. The concentrations of surfactants in each phase of the samples were then calculated from the measured activities and the calibration curves. The results of calibration, precision and material recovery will be summarized in next section.

Alternative procedure for analyzing LAS adsorbed on sorbent. For some experiments, an extraction method was used to extract the surfactants from the sorbents with a mixture of methanol and aqueous  $\text{NH}_4\text{OH}$  solution. The method will be described in detail in Chapter 7, and only be outlined here. The schematic description of the experimental procedure is in Figure 4.3b. In this method, after removal of excess water, the masses of the tubes were measured, then 20 mL of extraction solution with a 2:1 volume ratio of methanol and 2 N  $\text{NH}_4\text{OH}$  aqueous solution was added into each tube (Sales et al.,

1987). Then the samples were resuspended at 350 RPM at 25 °C on a thermostatted shaker for 15 hours. After this extraction step, the samples were centrifuged at 10,000 RPM at 25 °C for 10 minutes, then 1.0 mL of the liquid phase was transferred into a scintillation vial containing 10 mL of Beckman HP/b. It should be mentioned here that the amount of surfactants adsorbed on the walls cannot be determined if analysis is performed by this method.

Most of the experiments in this study were performed by the combustion method. The comparison of the extraction method with the combustion method for determination of the surfactants in the sorbents will be discussed in the section on results.

The method for determination of pH. The pH of the aqueous phase at equilibrium was determined at the temperature of 25 °C, controlled by a water circulation bath. An Orion Model 8102 Ross combination glass electrode and an Orion Model 701-A digital pH-mV meter were used. The cell was calibrated against pH 4 (phthalate), pH 7 (phosphate), and pH 10 (borate and carbonate) buffers from Micro Essential Laboratory, Brooklyn N.Y. In all of the cases the cell potential was recorded and pH calculated from the calibration equation

$$E = E^{\circ'} + k \log a_H^+ \quad (4.2)$$

where E is the measured cell potential,  $pH = - \log a_H^+$ , and  $E^{\circ'}$  and k are constants.

In this study, the values of the  $E^{\circ'}$  and the  $k$  obtained from each calibration performed on the different date were recorded to evaluate the long-term stability of the pH cell.

Determination of adsorption of surfactants on different materials. A set of experiments were performed to investigate the adsorption of C-12 TMAC and C-12 LAS on centrifuge tubes of different materials: glass, stainless steel, Teflon, polycarbonate, and polyethylene. The procedure for this test is as follows: a 10-mL aliquot of deionized water and a 100  $\mu$ L spike of C-12 TMAC or C-12 LAS stock solution was added into the centrifuge tube made out of the different materials, and the tubes were shaken at 500 RPM and 25  $^{\circ}$ C for 20 minutes. Then a 1-mL aliquot of the aqueous solution was transferred into a vial containing 10 mL of Beckman HP/b scintillation fluid, and the activity in the aqueous solution was determined by the counter. After this step, the extra aqueous solution was discarded, 10 mL of 95% ethanol was added into the tube, and the tubes were shaken at 500 RPM and 25  $^{\circ}$ C for 20 minutes to rinse the walls of the tubes. Then a 1-mL aliquot of the rinsing solutions was transferred into a vial containing 10 mL of HP/b scintillation fluid for determination of the activity. The percentage of surfactant adsorbed on the wall was calculated to be the ratio of the activity found in the rinsing solution to the activity added.

## VERIFICATION OF METHODS

Quality control

Efforts have been made to control the quality of the results for the adsorption experiments, as described in detail below.

Calibrations. Calibrations for the determination of surfactants in the water and on the sorbents were performed for each experiment. The calibrations were generally linear, as the examples shown in Figure 4.4a-c, for determination of C-10, C-12, and C-14 LAS. Figures 4.4b and c show the calibration curve for determination of LAS on the sorbent by the combustion method and by the extraction method, respectively.

A typical control chart is illustrated in Figure 4.5a-c for calibration of C-12 LAS obtained from 34 experiments which were conducted from 1986-1989. The averages of the slopes in aqueous phase and sorbents phase are  $30.6 \pm 1.2$  dpm/nM and  $29912 \pm 1320$  dpm/nmol, respectively. The average of the combustion recovery is  $98.0 \pm 1.6\%$ , indicating the combustion method is satisfactory for determination of surfactant adsorbed on the sorbents. The calibration information for all the seven surfactants used in this study are summarized in Table 4.6. The results indicate that the calibration methods are satisfactory.

Precision. The concentrations of surfactants adsorbed in the sorbents phase were determined in duplicate for each sample whether they were analyzed by the combustion method (a total of 491 samples

Table 4.6. Verification of analytical methods for batch adsorption experiments: the calibrations.

Surfactant	Combustion	Aqueous Phase <sup>a</sup>		Sorbent <sup>b</sup>	
	Recovery	Slope <sup>m</sup>	Slope <sup>c</sup>	Slope <sup>m</sup>	Slope <sup>c</sup>
	%	dpm/nM	dpm/nM	dpm/nmol	dpm/nmol
C-10 LAS	95.3 ± 2.1	3.30 ± 0.08	3.24	3181 ± 64	3241
C-12 LAS	98.0 ± 1.6	30.50 ± 1.15	29.81	29799 ± 1264	29815
C-14 LAS	96.8 ± 1.1	29.03 ± 0.47	28.64	27717 ± 1210	28638
A <sub>13</sub> E <sub>3</sub>	98.0 ± 0.9	15.15 ± 0.21	15.32	14892 ± 315	15318
A <sub>13</sub> E <sub>6</sub>	97.3 ± 1.8	48.88 ± 1.68	47.29	47194 ± 1382	47286
A <sub>13</sub> E <sub>9</sub>	97.6 ± 1.2	15.07 ± 0.72	14.65	14825 ± 520	14652
C-12 TMAC	101.2 ± 1.6 85.2 ± 3.5 <sup>c</sup>	54.44 ± 0.92	55.5	52529 ± 333	55500

<sup>a</sup> Slope<sup>m</sup> are determined from calibration curves and Slope<sup>c</sup> are calculated from the specific activities of surfactants listed in Table 4.1. For aqueous phase, the Slope<sup>c</sup> can be calculated:

$$\text{Slope}^c = \text{specific activity} \frac{(\text{Ci}) (2.22 \times 10^{12} \text{ dpm}) (1\text{mol}) (1\text{mL}) (1\text{L})}{(\text{mol}) (\text{Ci}) (10^9 \text{nmol}) (1000\text{mL})}.$$

<sup>b</sup> For sediment phase, Slope<sup>c</sup> can be calculated:

$$\text{Slope}^c = \text{specific activity} \frac{(\text{Ci}) (2.22 \times 10^{12} \text{ dpm}) (1\text{mol})}{(\text{mol}) (\text{Ci}) (10^9 \text{nmol})}.$$

<sup>c</sup> Some C-12 TMAC sorbent samples were analyzed by trapping the <sup>14</sup>CO<sub>2</sub> into 20 mL of 0.1M NaOH, in these cases the combustion recoveries are relatively low.

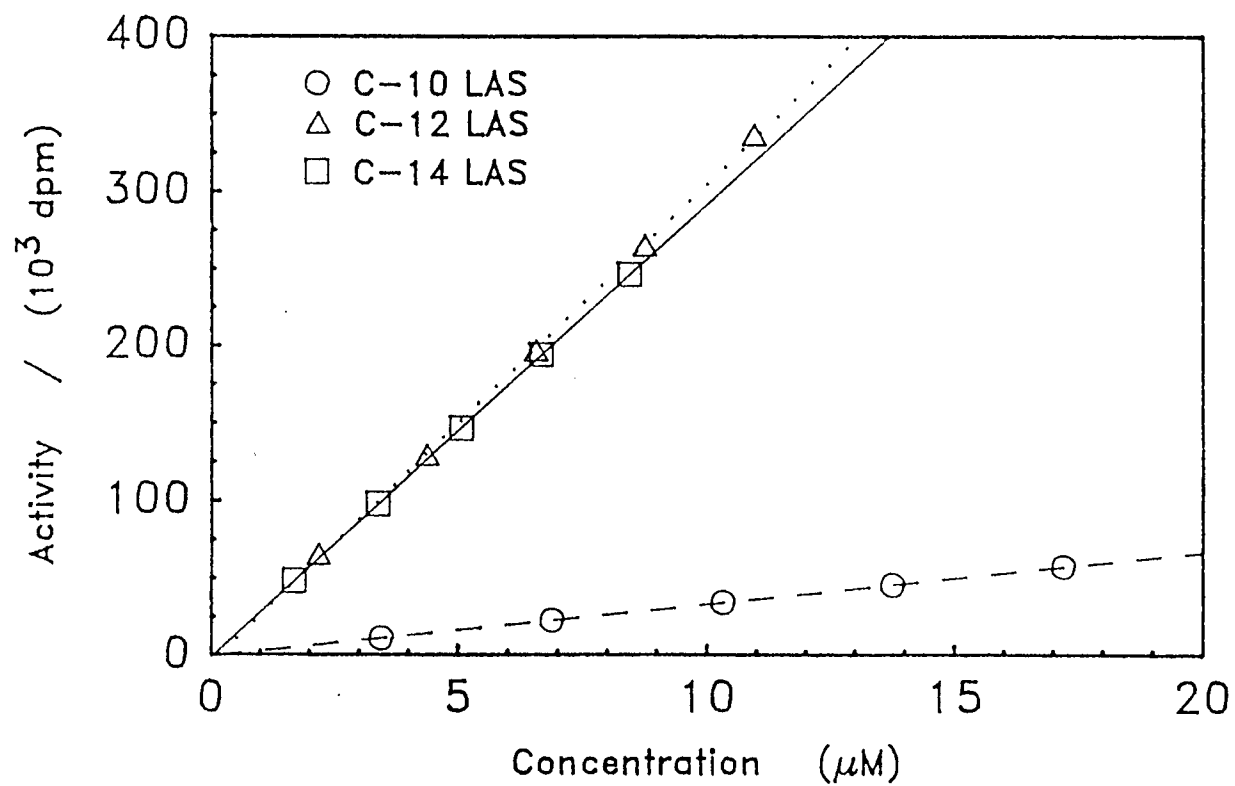


Figure 4.4a. Calibration curve for the determination of LAS in the aqueous phase, for 1 mL of sample delivered to scintillation vial.

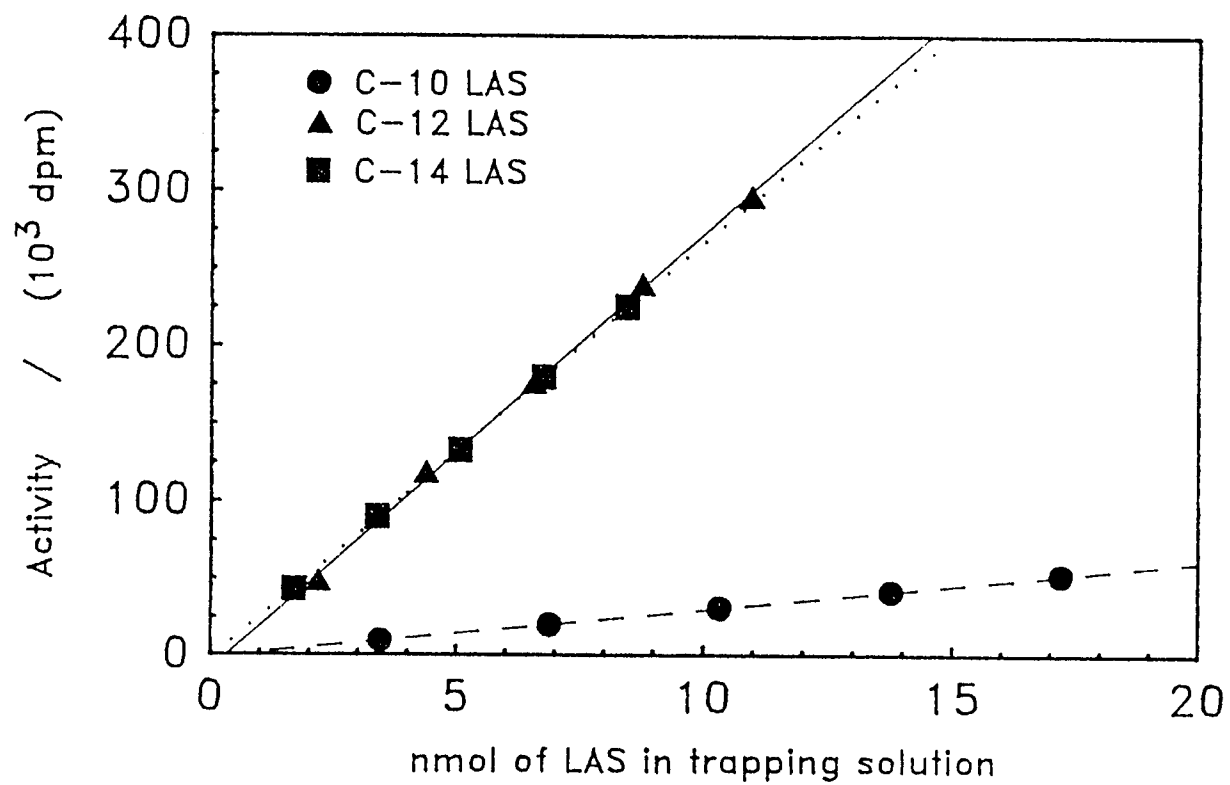


Figure 4.4b. Calibration curve for the determination of LAS in the sorbent phase by combustion method.

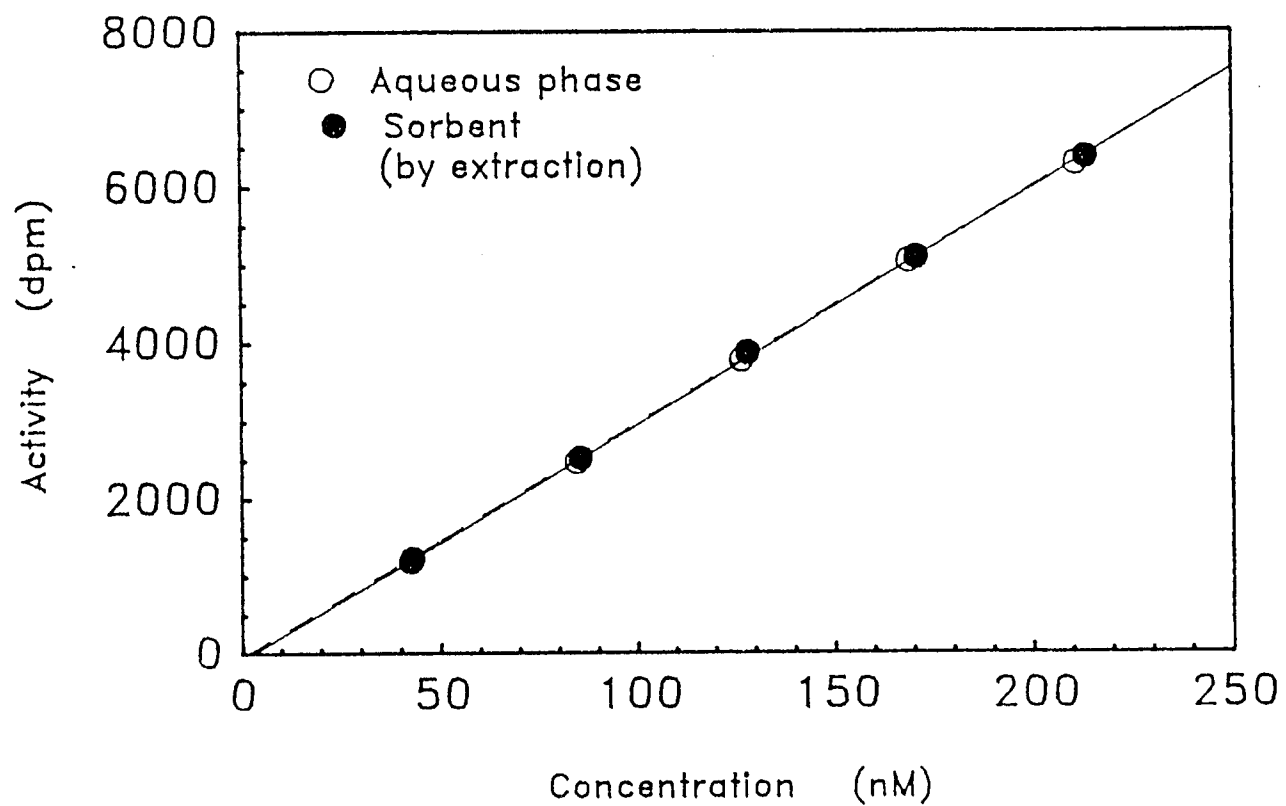


Figure 4.4c. Calibration curves for the determination of C-12 LAS in the aqueous and the sorbent phase by extraction method (1 mL of sample delivered to scintillation vial).

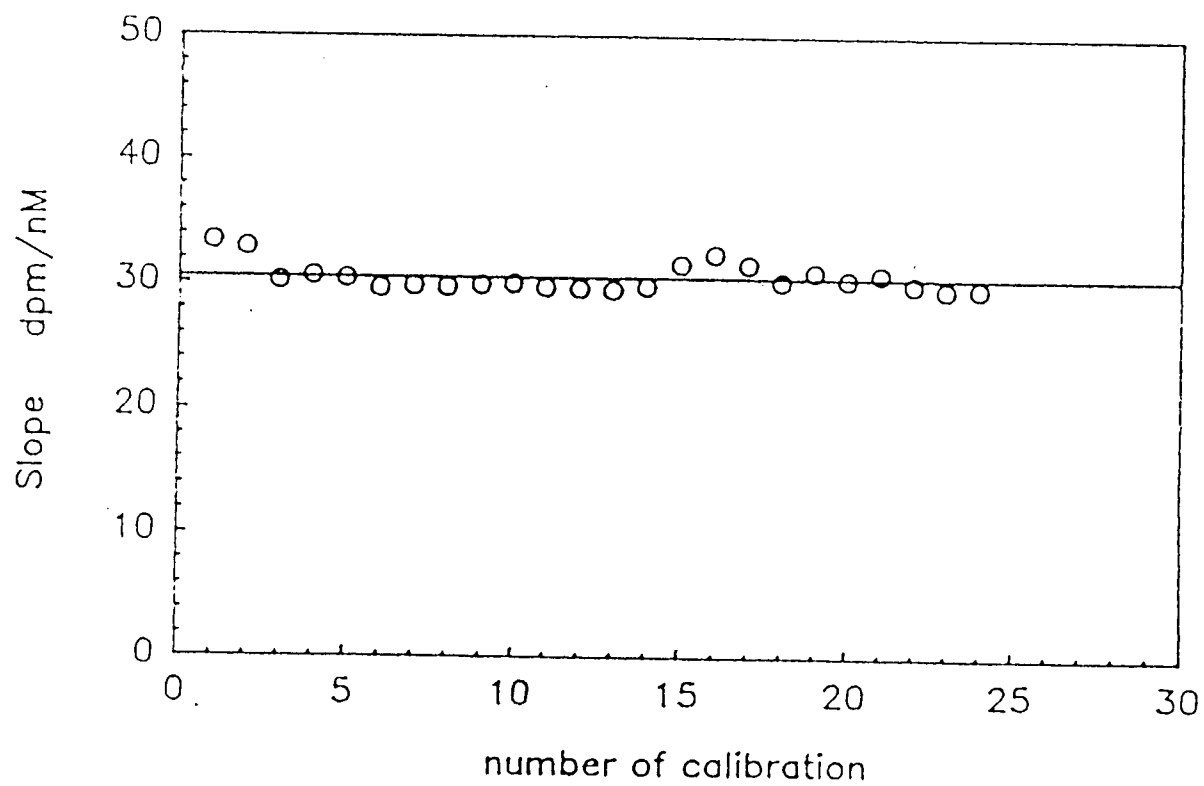


Figure 4.5a. Control charts for calibration of C-12 LAS in aqueous phase, based on 1 mL of sample delivered to scintillation vial.

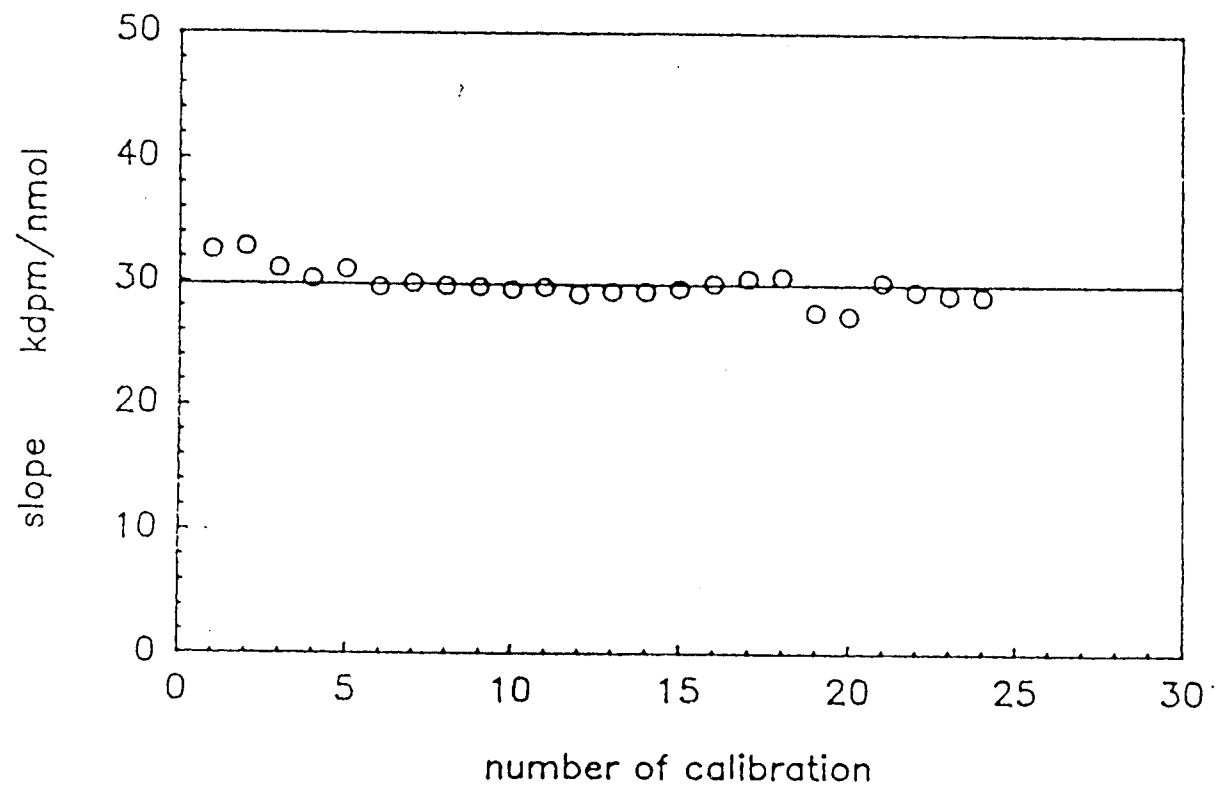


Figure 4.5b. Control charts for calibration of C-12 LAS in the sorbent phase.

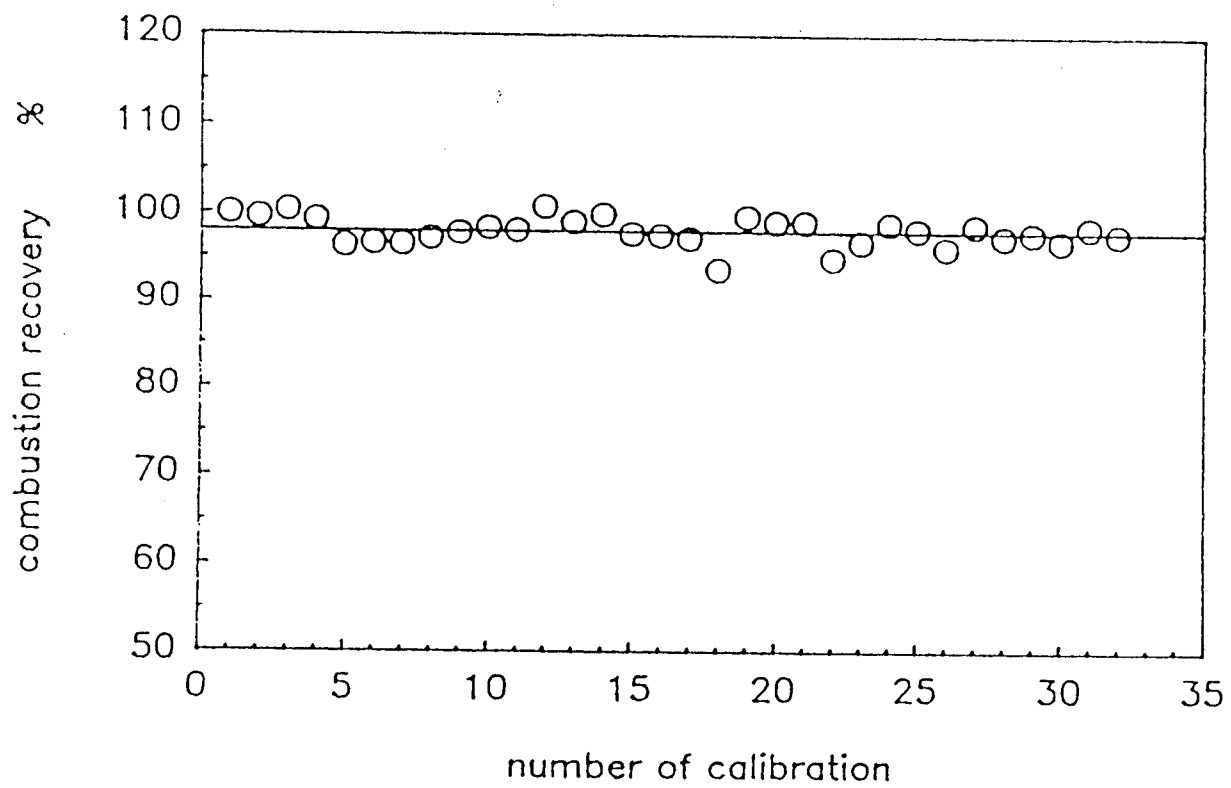


Figure 4.5c. Control charts for combustion recovery of C-12 LAS in the sorbent phase.

from 71 experiments) or by the extraction method (a total of 98 samples from 6 experiments). The precision (defined here as the absolute value of the difference between duplicate determinations divided by the average) for the sorbent samples was generally better than 5%. In addition, the reproducibility for the aqueous samples measurements (determined in duplicate) was tested for a total 114 samples from 8 experiments, and the precision was generally better than 4%. In this study, most of the adsorption experiments were performed over a low concentration range ( $C(w) < 1 \mu\text{M}$  and  $C(s) < 300 \text{ nmol/g}$ ). Therefore, the precision for determination is satisfactory.

Material recovery. The amounts of surfactants in the water, on the sorbents, and on the wall of the container (specifically for combustion experiments) were determined for each experiment. Table 4.7 gives the average of the material recoveries for each surfactant used in this study. For example, the value of average recovery for C-12 LAS is  $98.5 \pm 3.3\%$ , which was obtained from the determination of 291 samples of 34 experiments. The results in Table 4.7 show that the average recoveries for all of the surfactants are very close to 100% with a minimum of 94.8% and a maximum of 101.7%.

In order to monitor the long-term variation of the material recovery of the adsorption experiments, the material recovery from each individual experiment was recorded and plotted on a control chart. Figure 4.6a,b illustrates the control charts for LAS,  $A_{13}E_m$ , and C-12 TMAC. Each data point in the control chart represents the mean and standard deviation of the material recoveries for an individual experiment. The values of recoveries are generally scattered around the line of 100% in the range of 95 to 105%,

Table 4.7. Verification of analytical methods for batch adsorption experiments: the material recoveries.

Surfactant	# of Exp.	# of Samples	Material recovery %
C-10 LAS	5	40	$100.4 \pm 1.9$
C-12 LAS	34	291	$98.5 \pm 3.3$
C-14 LAS	5	40	$96.8 \pm 4.0$
A <sub>13</sub> E <sub>3</sub>	5	30	$94.8 \pm 4.1$
A <sub>13</sub> E <sub>6</sub>	14	90	$97.4 \pm 3.4$
A <sub>13</sub> E <sub>9</sub>	8	51	$99.1 \pm 2.0$
C-12 TMAC	6	47	$101.7 \pm 4.3$

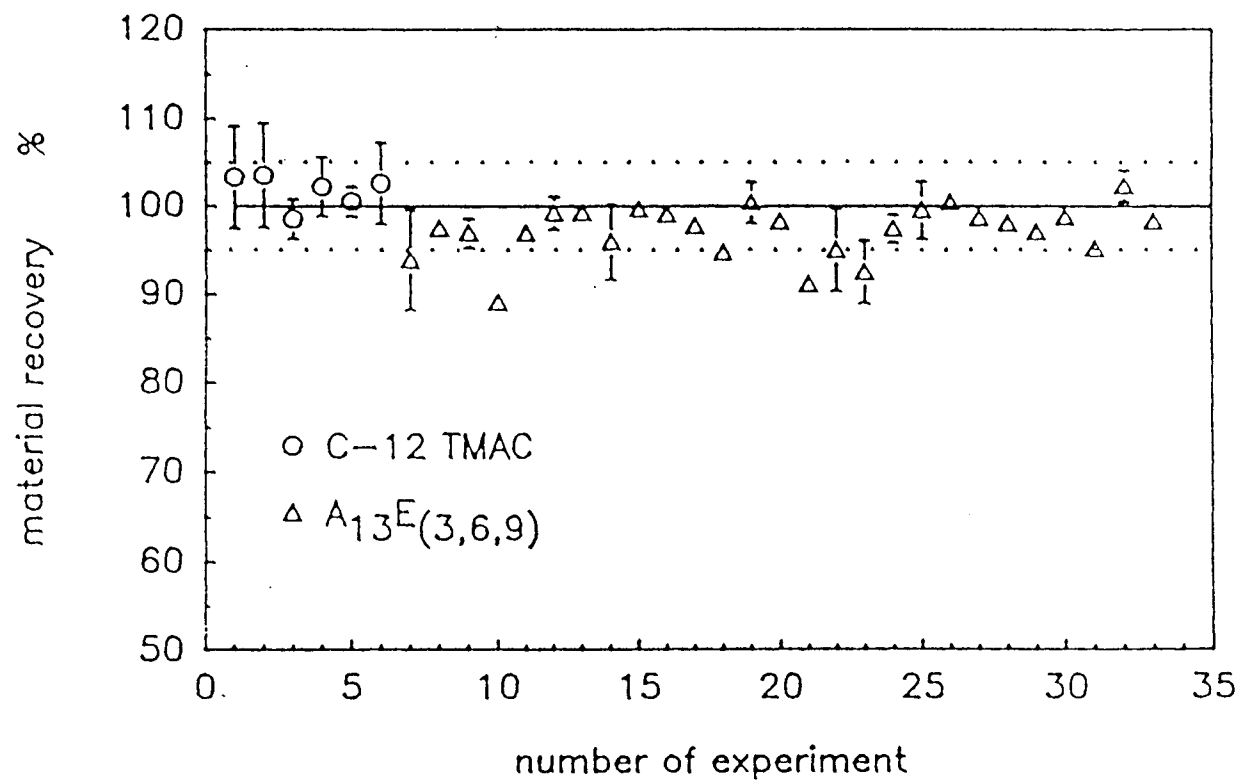


Figure 4.6a. Control charts for material recoveries of C-12 TMAC and A<sub>13</sub>E<sub>m</sub>.

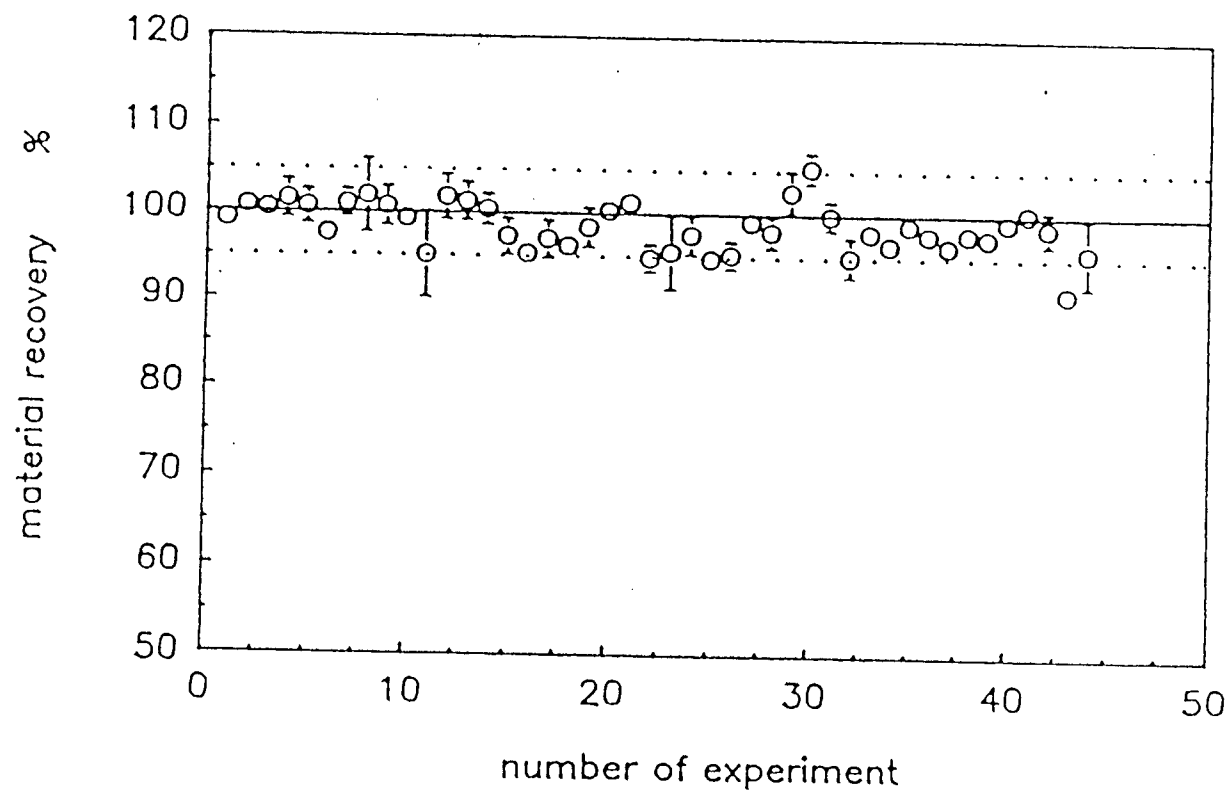


Figure 4.6b. Control charts for material recoveries of LAS.

indicating that the methods for the adsorption experiments are reliable and reproducible.

Control of pH. The pH electrode used in this study was calibrated for each experiment. The two parameters  $E^{\circ'}$  and  $k$  in Equation 4.2 were recorded from each calibration to evaluate the long-term stability of the cell. The control charts for  $E^{\circ'}$  and  $k$  are shown in Figure 4.7 a,b. The figures show that the values of  $E^{\circ'}$  and  $k$  obtained from different date are very consistent, indicating that the pH electrode is stable and the method for calibration of electrode is reliable.

#### Comparison of methods

##### Adsorption of C-12 LAS and C-12 TMAC on different materials.

The adsorption of surfactant on different materials is tabulated in Table 4.8a. The percentage recovery of the surfactants is in the range of 95 - 105%. For C-12 LAS, Corex glass showed the least affinity for absorption and stainless steel the most. For C-12 TMAC, Corex glass showed the greatest affinity and stainless steel the least. Teflon and polycarbonate tubes shows relatively little affinity for either C-12 LAS or C-12 TMAC.

The results indicate that different materials have different affinities to the surfactants. From these results, Corex glass tubes appear to be unsuitable for C-12 TMAC experiments. However, the significance of the wall as a sink is reduced if sorbents are included in the system. This situation is illustrated in Table 4.8b. The result shows that for C-12 TMAC, even with extremely high sorbents

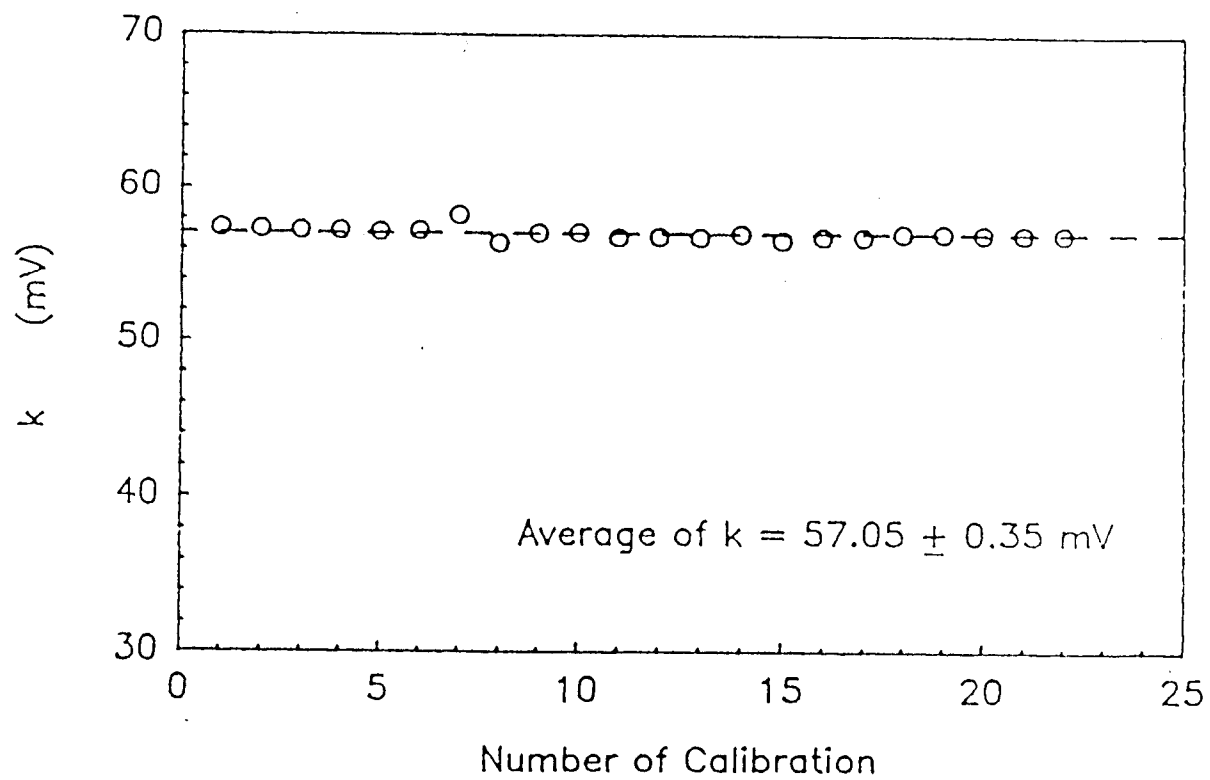


Figure 4.7a. A control chart for calibration of pH: the slope  $k$ .

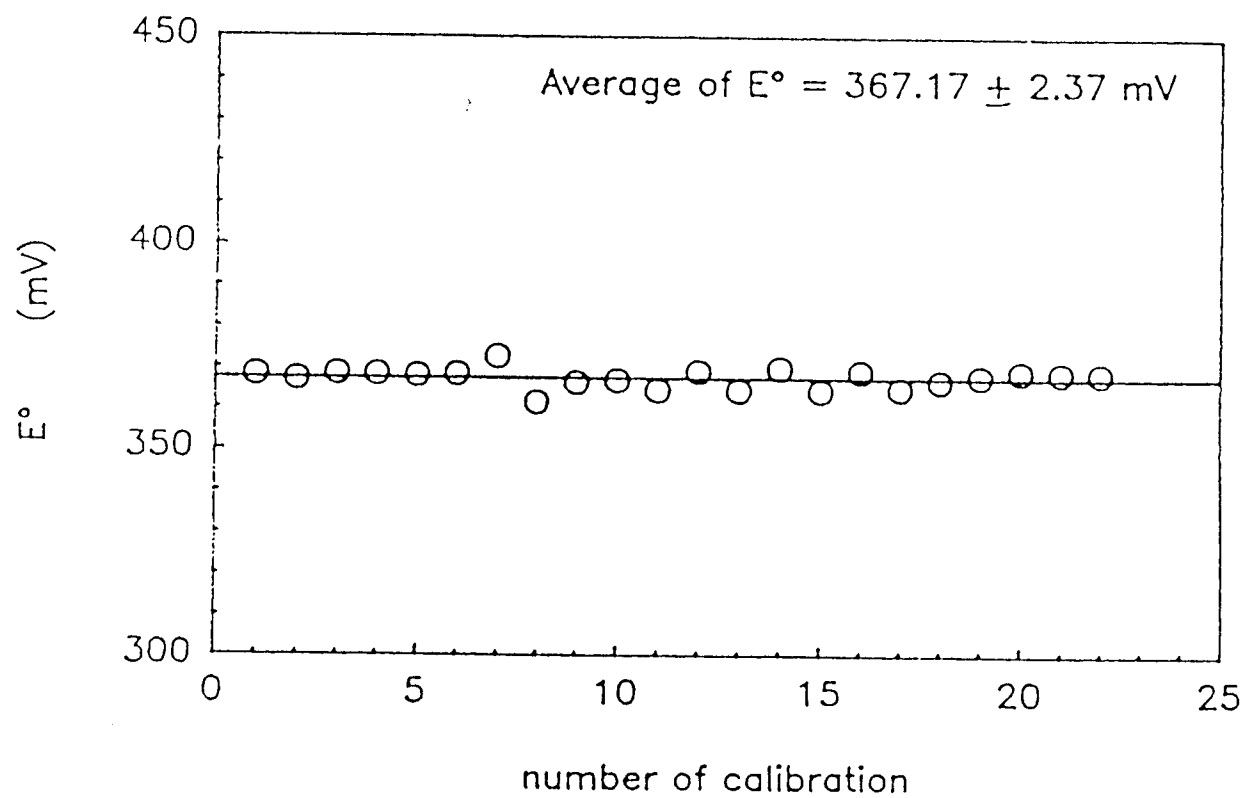


Figure 4.7b. A control chart for calibration of pH: the intercept  $E^\circ$ .

Table 4.8. Adsorption of surfactants on experimental materials.

a. In the absence of sorbents.

Surfactant	Material	Surfactant total nmol	Surfactant in water %	Surfactant on wall %	Recovery %
C-12 LAS	Stainless steel	6.36	59.0	39.0	98.6
	Teflon	6.36	93.6	1.8	95.4
	Polycarbonate	6.36	93.8	7.0	100.8
	Polyethylene	6.36	92.4	8.0	100.4
	Corex glass	10.08	97.4	2.1	99.5
C-12 TMAC	Stainless steel	32.42	91.4	9.8	101.2
	Teflon	32.42	94.5	1.6	96.1
	Polycarbonate	32.42	90.8	10.1	100.9
	Polyethylene	32.42	87.4	8.3	95.7
	Corex glass	22.34	83.2	14.7	97.9

b. In the presence of soil sorbents (Corex glass).

Surfactant	C <sub>s</sub> (v) g/mL	Surfactant total nmol	Surfactant in soil %	Surfactant in water %	Surfactant on wall %	Recovery %
C-12 TMAC	0	12.0		83.2	14.7	97.9
	0*	12.0		95.4	4.5	99.9
	0.0100	12.0	91.1	5.4	3.4	99.9
	0.0200	12.0	101.4	4.6	1.7	107.7
	0.0500	12.0	95.3	3.1	1.4	99.7
	0.1000	12.0	102.3	2.5	1.1	106.0

\* Liquid phase is ethanol solution.

concentrations, the adsorption of the C-12 TMAC on the wall of the Corex glass tube still cannot be eliminated, but the fraction of the total adsorbed to the walls is reduced to less than 5%. Based on the results of this test, all of the other batch adsorption experiments in this research were carried out in 25 mL Corex glass centrifuge tubes.

Methods for washing sorbent. The efficiency of washing sorbents for the removal of nonseparable materials (NSM) from the aqueous phase has been evaluated. The UV absorbance at 260 nm, symbolized as  $A_{260}$ , of the supernatant after each washing step was determined. The reason for selecting  $A_{260}$  is because many organic functional groups for humic substances in the soil or sorbents would give an UV absorbance at 260 nm, and it is presumed that the dissolved organic substances are the major fraction of the NSM.

The absorbance  $A_{260}$  as a function of  $C_s(w)$  with washing five times is shown in Figure 4.8. Two facts are depicted in the figure: (i) there is a linear relationship between  $A_{260}$  and the solid concentration, and (ii) the value of UV absorbance decreases significantly by the washing of the sorbent. Consequently, after washing eight times, the amount of NSM left in the aqueous phase must be very small.

The experiment above was conducted by the individual tube washing method. The efficiency for the washing of the sorbents by the large volume method was not determined directly by the determination of the UV absorbance. However, a test has been made to evaluate indirectly the efficiency of the large volume washing method. Figure 4.9 shows an isotherm for adsorption of C-12 LAS on the soil EPA-12. The first 10 data points of the isotherm were obtained with the sorbents which were

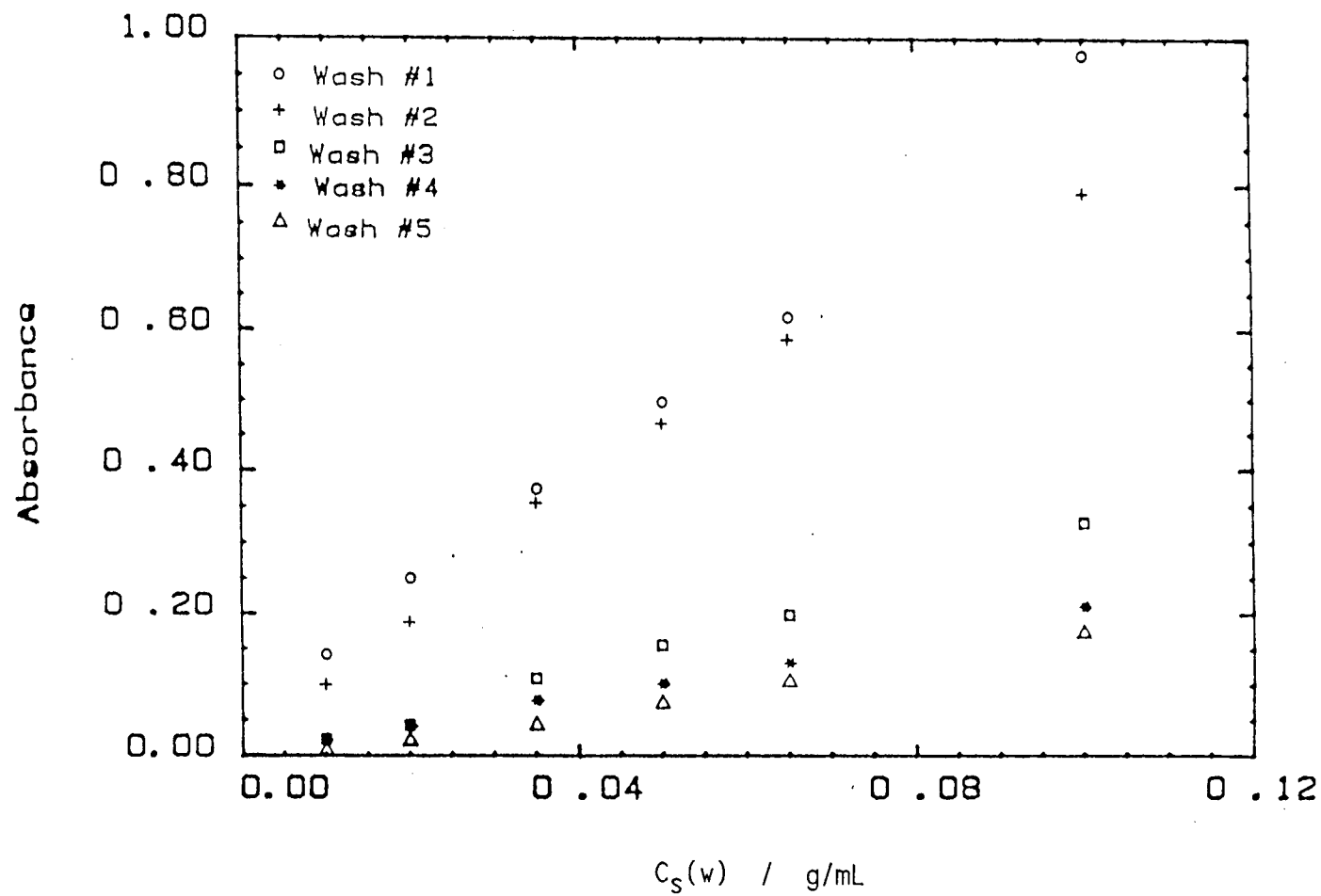


Figure 4.8. Test of washing times:  $A_{260}$  vs.  $C_S(w)$ .

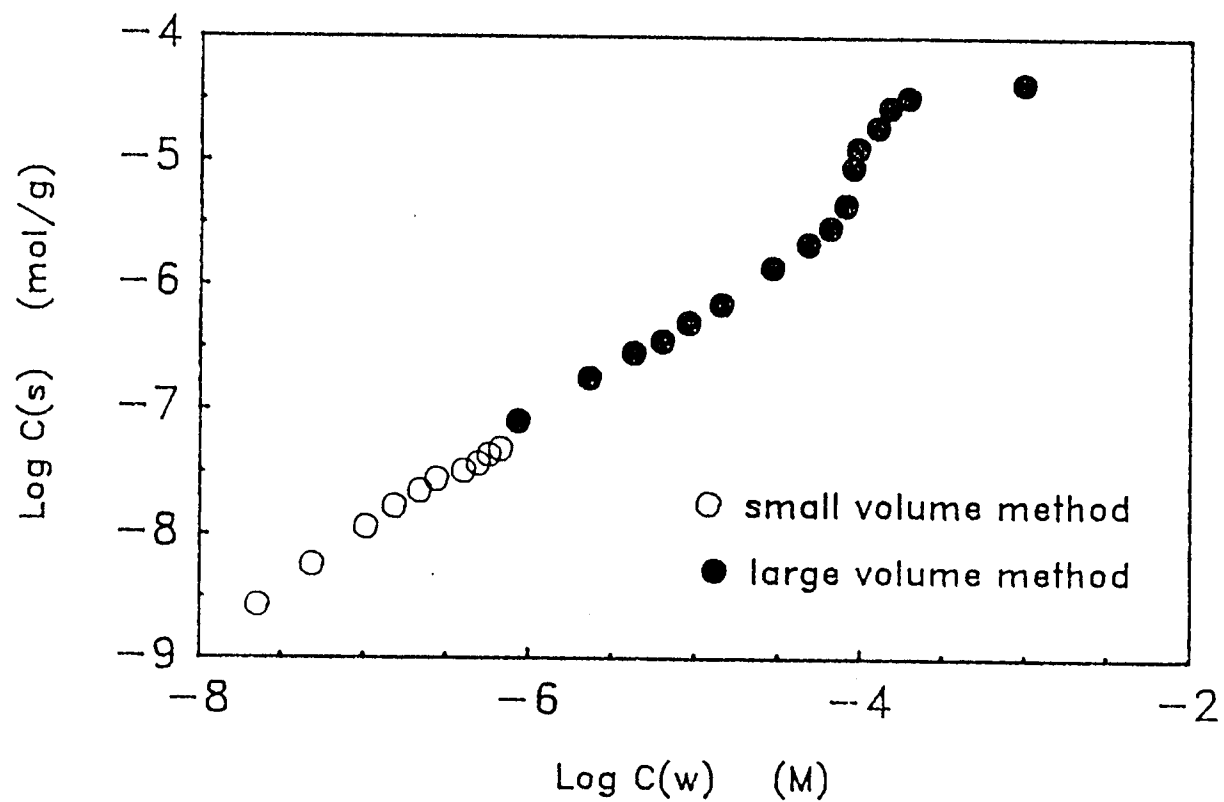


Figure 4.9. Comparison small vs. large volume washing methods.

washed by the individual tube method, whereas the other data points were obtained with the sorbents by the large volume method. The data show that there is no significant difference from the two washing methods. The advantage of large volume method is to save labor and time. On the other hand, the disadvantage is, as we already mentioned, that the method may affect the structure of sorbents since the dry sorbents were ground.

Methods for determination of C-12 LAS adsorbed on sorbent. Most of the experiments were carried out by the combustion method to determine the amount of surfactants adsorbed on the sorbents. The combustion method recoveries were very high, as shown in Table 4.6 and Figure 4.5c. For experiments performed at low concentrations ( $C(w)$  from nM to  $\mu M$  and  $C(s)$  from a few nmol/g to 300 nmol/g), the combustion technique works extremely well. This method also allows analysis of surfactants adsorbed on the wall of tubes.

The extraction method was also used to analyze surfactants adsorbed on sediments (Sale, et al., 1987, Hand, et al., 1986). In one experiment, three methods were used to analyze C-12 LAS in the sorbent samples: combustion, extraction, and concentration difference ( $C_0(w) - C(w)$ ). Figure 4.10 shows that there was no significant difference in C-12 LAS adsorption on surface by these three methods. The advantage of the extraction method is the speed and convenience of performance. However, the adsorption of surfactant on the wall can not be determined by this method. It should be mentioned that the aqueous concentrations used in this experiment were from 2.9  $\mu M$  up to 2.1 mM, which is higher than most of other experiments. Therefore, the adsorption on the tube wall is negligible in this range.

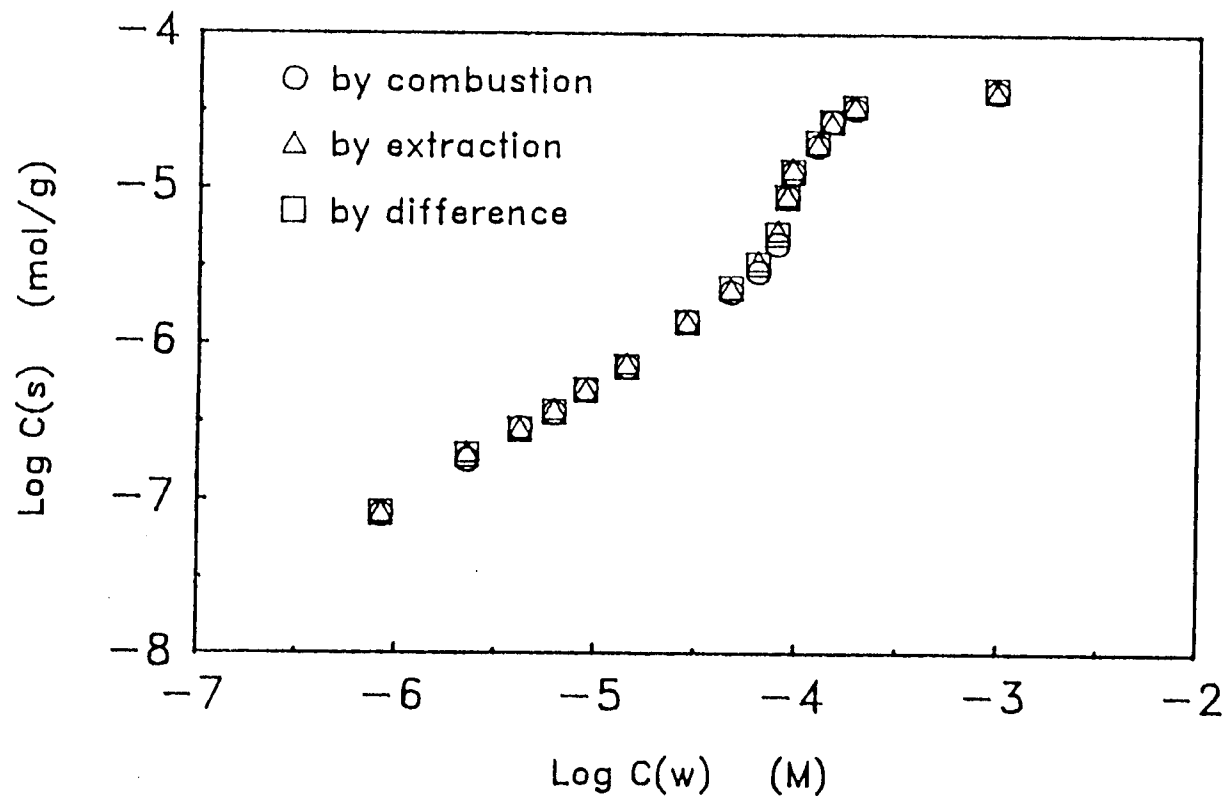


Figure 4.10. Comparison of combustion vs. extraction and concentration difference methods for analysis of C-12 LAS adsorbed on soil sorbent EPA-12.

## SUMMARY

The previous studies from the literature on the adsorption of surfactants on pristine and natural sorbents have been reviewed in this chapter. Another objective of this chapter is to describe the experimental methods used in this study for adsorption of surfactants on the natural sorbents. The verification of experimental methods, the quality control of the experimental data, and the comparison of different methods are also included in the chapter.

In this study, four control charts were maintained to record the day-to-day information about analytical procedures, that is, the calibrations, the combustion recovery, the total recovery, and the stability of the pH electrode. There was no significant variation in the control charts. The total recovery for the batch experiments is generally in the range of 95% to 105%. The precisions for analysis of  $^{14}\text{C}$  labeled surfactants in the aqueous and the sorbent phases are better than 4% and 5%. These results verified that the experimental methods are satisfactory.

The individual-tube washing method and the large-volume washing method have been used for the pretreatment of the sorbents. No significant differences were observed for adsorption of LAS on the sorbent when it was prepared by the two methods. The combustion and extraction methods for the determination of the LAS in the sorbent phase have also been compared. No significant difference was observed for the adsorption isotherms of C-12 LAS on EPA-12 when the sorbent was prepared by the two methods.

## REFERENCES

- Aveyard, R. "Adsorption at the Air/Liquid, Liquid/Liquid, and Solid/Liquid interfaces" in Surfactants; Tadros, Th. F. Ed.; Academic Press: London; 1984, 153-173.
- Bijsterbosch, B. H. J. Coll. Interface Sci. 1974, 47, 186-198.
- Boethling, R. S.; Water Res. 1984, 18, 1061-1076.
- Brunner, P. H.; Capri, S.; Marcomini, A.; Giger, W. Water Res. 1988, 22, 1465-1472.
- Clunie, J. S.; Ingram, B. T. "3. Adsorption of Nonionic Surfactants" in Adsorption from Solution at the Solid/Liquid Interface; Parfitt, G. D.; Rochester, C. H., Eds.; Academic Press: New York, 1983, 105-152.
- Chander, S.; Fuerstenau, D. W.; Stigter, D. "Adsorption from Solution"; Ottewill, R. H., Rochester, C. H., Eds; Academic Press: New York. 1983. 197-210.
- Connor, P. and Ottewill, R. H. J. Coll. Interface Sci. 1971, 37, 642-651.
- Dick, S. G.; Fuerstenau, D. W.; Healy, T. W. J. Coll. Interfac. Sci. 1971, 37, 595-602.
- Fink, D. H.; Thomas, G. W.; Meyer, W. J. Journal WPCF. 1970, 42, 265-271.
- Games, L. M.; Larson, R. J. Environ. Sci. Technol. 1982, 16, 483-488.
- Games, L. M. "Practical Applications and Comparisons of Environmental Exposure Assessment Models" In Aquatic Toxicology and Hazard Assessment: Sixth Symposium, ASTM STP 802; Bishop, W. E., Cardwell, R. D., Heidolph, B. B. Eds.; American Society for Testing and Materials: Philadelphia, 1983, 282-299.
- Giger, W.; Brunner, P. H.; Schaffner, C. Science 1984, 225, 623-625.
- Gschwend, P. M.; Wu, S-C. Environ. Sci. Technol. 1985, 19, 90-96.
- Gu, T.; Huang, Z. Colloids and Surfaces 1989, 40, 71-76.
- Hand, V. C.; Williams, G. K. Environ. Sci. Technol. 1987, 21, 370-373.
- Hiemenz, P. C. Principles of Colloid and Surface Chemistry 2nd Ed., Marcel Dekker Inc.: New York and Basel, 1986.
- Holysh, M.; Paterson, S.; Mackay, D.; Bandurraga, M. M. Chemosphere 1986, 15, 3-20.

Hough, D. B.; Rendall, H. M. "6. Adsorption of Ionic Surfactants" in Adsorption from Solution at Solid/Liquid Interface; Patfitt, G. D.; Rochester, C. H. Eds.; Academic Press: New York, 1983, 247-319.

Inoue, K.; Kaneko, K.; Yoshita, M. Soil Sci.: Plant Nutr. 1978, 24, 91-102.

Krishna Murti, G. S. R.; Volk, V. V.; Jackson, M. L. Soil Sci. Soc. Amer. Proc. 1966, 30, 685-688.

Larson, R. J. Residue Reviews 1983, 85, 159-171.

Larson, R. J.; Vashon, R. D. "Chapter 38 Adsorption and Biodegradation of Cationic Surfactants in Laboratory and Environmental System" in Developments in Industrial Microbiology; Vol. 24, Nash III, C. H. and Underkofler, L. A. Eds; 1983.

Larson, R. J.; Games, L. M. Environ. Sci. Technol. 1981, 15, 1488-1493.

Lewis, M. A.; Suprenant, D. Ecotoxicology and Environmental Safety 1983, 7, 313-322.

Mathai, K. G.; Ottewill, R. H. a: Trans. Faraday Soc. 1966, 62, 750-759; b: Trans. Faraday Soc. 1966, 62, 759-769.

Matthijs, E.; De Henau, H. Tenside Detergents 1985, 22, 299-304.

McEvoy, J.; Giger, W. Naturwissenschaften. 1985, 72, 429-431.

Narkis, N.; Bella, B. Water Res. 1985, 19, 815-824.

Podoll, R. T.; Irwin, K. C.; Brendlinger, S. Environ. Sci. Technol. 1987, 21, 562-568.

Reneau, R. B. Jr.; Pettry, D. E. J. Environ. Qual. 1975, 4, 370-375.

Robeck, G. G.; Cohen, J. M.; Sayers, W. T.; Woodward, R. L. Journal WPCF. 1963, 35, 1225-1236.

Rosen, M. J. "Surfactants and Interfacial Phenomena"; 1978, John Wiley & Sons.

Sakata, K.; Katayama, A. J. Coll. Interface Sci. 1988, 123, 129-135.

Sales, D.; Quiroga, J. M.; Gomez-Parra, A. Bull. Environ. Contam. Toxicol. 1987, 39, 385-392.

Savitsky, A. C.; Wiers, B. H.; Wendt, R. H. Environ. Sci. & Tech. 1981, 15, 1191-1196.

Scamehorn, J. F.; Schechter, R. S.; Wade, W. H. J. Coll. Interfac. Sci. 1982, 85, 463-501.

Scheunert, I.; Vockel, D.; Schmitzer, J. Chemosphere 1987, 16, 1031-1041.

Schwuger, M. J.; von Rybinsk, W.; Krings, P. "Adsorption from Solution"; Ottewill, R. H.; Rochester, C. H.; Smith, A. L., Eds.; Academic Press: New York, 1983, 185-196.

Sedlak, R. I.; Booman, K. A. SDA Annual Convention. 1986.

Siracusa, P. A.; Somasundaran, P. J. Coll. Interface Sci. 1987, 120, 100-109.

Somasundaran, P.; Fuerstenau, D. W. J. Phys. Chem. 1966, 70, 90-96.

Thurman, E. M.; Barber, L. B. Jr.; LeBlanc, D. Journal of Contaminant Hydrology 1986, 1, 143-161.

Turner, A. H.; Abram, F. S.; Brown, V. M.; Painter, H. A. Water Res. 1985, 19, 45-51.

Urano, K.; Saito, M. Chemosphere 1984, 13, 285-292.

Urano, K.; Saito, M.; Murata, C. Chemosphere 1984, 13, 293-300.

van den Boomgaard, Th.; Tadros, Th. F.; Lyklema, J. J. Coll. Interface Sci. 1987, 116, 8-16.

Volk, V. V.; Jackson, M. L. Journal WPCF 1968, 40, 205-213.

Woodbury, G. W. Jr.; Noll, L. A. Colloids and Surfaces 1988, 33, 301-319.

Yamane, A. N.; Okada, M.; Sudo, R. Water Res. 1984, 18, 1101-1105.

## CHAPTER 5

ADSORPTION OF ALKYL ETHERS OF POLY(ETHYLENE GLYCOL)  
ON ENVIRONMENTAL SORBENTS

## INTRODUCTION

Monoalkyl ethers of poly(ethylene glycol), known as "alcohol ethoxylates," are used widely in consumer and industrial products (Rosen, 1978; Greek and Layman, 1990). The chemical formula of this class of nonionic surfactants is  $C_nH_{2n+1}(OCH_2CH_2)_mOH$ , which we represent as  $A_nE_m$ . These surfactants are bioactive because of their tendency to interact with cell membranes (Florence et al., 1984). They are observed to have moderately high levels of toxicity to fish (Turner et al., 1985) and aquatic invertebrates (Lewis and Suprenant, 1983).

However, few studies have been made on the adsorption of nonionic surfactants on environmental sorbents (e.g. sediments, soils, aquifer materials, etc.). Several questions arise: (i) to what extent is sorption to environmental sorbents governed by the hydrophobic part of the molecule, and to what extent by the polar part? (ii) what are the important properties of surfactant, sorbent, and solution, that affect adsorption? The focus of this study is to investigate the adsorption of a homologous series of monotridecyl ethers of poly(ethylene glycol) ( $A_{13}E_m$ , with  $m = 3, 6, 9$ ) on environmental sorbents with different properties. The effects of  $Ca^{2+}$  concentration in solution and the salt ( $NaN_3$ ) concentration in solution have also been studied.

In general, the adsorption of surfactants can be separated into the ranges of low and high surface coverages. At low surface coverage, adsorption is mainly due to the interactions between the surfactant and the sorbent. At high surface coverage, e.g. at the

aqueous concentration near the critical micelle concentration (the CMC) of the surfactant, sorbate-sorbate interactions also become important. In this study, the adsorption of  $A_{13}E_m$  homologs was investigated at low surface coverage ( $C(w) < 650$  nM and  $C(s) < 300$  nmol/g) to elucidate the sorbate-sorbent interaction.

## EXPERIMENTS

Materials and equipment. The nonionic surfactants used in this study were the homologs of monotridecyl ethers of poly(ethylene glycol)  $A_nE_m$  ( $m = 3, 6, 9$ ), which were obtained through the Soap and Detergent Association from Shell Research. The specific activities of the surfactants were 6.9, 21.3, and 6.6 mCi/mmol, for  $A_{13}E_3$ ,  $A_{13}E_6$ , and  $A_{13}E_9$ , respectively. The radiochemical purities, were 95 - 98%, as determined by HPLC. The standard solutions of  $^{14}C$  labeled surfactants were prepared in 95% ethanol and stored in refrigerator at the temperature less than 0 °C.

The environmental sorbents used in this study were from the "EPA" soil series and obtained through Professor John J. Hassett at the University of Illinois. The physical and chemical properties of the sorbents are listed in Table 4.5. The compositions of clay mineral in the sorbents were analyzed qualitatively by x-ray diffraction method, and the results are reported in Appendix II (Table II.2). The deionized water used in all experiments was from a Millipore Milli-Q System, with specific resistivity of 18 M $\Omega$  cm.

A thermostatted shaker (New Brunswick Model G-24) and thermostatted centrifuge (IEC Model B-20A) were used for the batch equilibration and phase separation. Sorbent samples were oxidized with a Harvey Model 300 Oxidizer, and radioactivity was determined with Beckman Model LS 7800 scintillation counter.

Determination of distribution ratio  $D_c$ . In this study, the concentration distribution ratio,  $D_c$ , is defined as the ratio of total concentration of surfactant in sorbent phase to the total

concentration of the surfactant in aqueous phase, expressed by equation

$$D_c = C(s) / C(w) \quad (5.1)$$

where  $C(s)$  and  $C(w)$  are the concentrations of surfactant in sorbent and water in the units of mol/kg and mol/L, respectively.

The procedures for determination of the concentration ratio  $D_c$  have been described in detail in Chapter 4, and will only be outlined in this chapter. The sorbents were washed with deionized water 8 times by the individual tube method. Then 20 mL of 0.01 M  $\text{NaN}_3$  solution and a spike of 10 - 100  $\mu\text{L}$  of  $A_{13}E_m$  standard solution was added into each tube, and the slurries were agitated on a thermostatted shaker at 500 RPM at 25 °C for 12 hours. Subsequently, the tubes were centrifuged at 11,000 G (10,000 RPM) for 1 hour at 25 °C to separate the aqueous and the sorbent phases.

After centrifugation, a 0.2 - 1.0 mL aliquot of the aqueous sample was transferred into a scintillation vial containing 10 mL of Beckman HP/b scintillation fluid for determining the activity in the aqueous phase. The activities of labeled surfactants in the sorbent phase were determined by the combustion method, as described in Chapter 4. In addition, the amount of surfactants adsorbed on the walls of the tubes were also determined, and the material recovery for each sample was calculated from the ratio of the total activity found to the total activity added.

The concentration of  $A_{13}E_m$  in the aqueous and sorbent phases were calculated from the measured activities and the corresponding calibration curves.

## RESULTS AND DISCUSSION

Adsorption of  $A_{13}E_6$  on different soil sorbents. The adsorption isotherms of  $A_{13}E_6$  on four different soil sorbents were determined to examine the effect of sorbent properties on the adsorption. Figure 5.1 shows the surfactant adsorbed as a function of aqueous surfactant concentration. Although the experiments were performed at low concentration of nonionic surfactant, all of the four isotherms are nonlinear. The results were fitted very well by Freundlich isotherm:

$$C(s) = K C(w)^n \quad (5.2)$$

The parameters in Equation 5.2, which were determined for the data in Figure 5.1, are in Table 5.1. The values of  $n$  are all less than 1, in the range of 0.78 - 0.85. The highest fractional surface coverage from this work is 0.013, calculated from the surface area of EPA-12 and the limiting surface area of  $0.95 \text{ nm}^2$  for the saturation of adsorption of  $A_{12}E_6$  on carbon black (Koganovskii et al., 1974). Therefore, the experiments were performed far from surface saturation of  $A_{13}E_6$  (if surface coverage is assumed to be uniform), and the sorbate-sorbate interaction is not important to interpret nonlinearity of isotherms. The nonlinearity of isotherms in this work is mainly due to the heterogeneity of the adsorption sites of the surface.

The magnitudes of Freundlich isotherm parameter,  $K$ 's for  $A_{13}E_6$  are larger than the  $K$ 's for adsorption of anionic

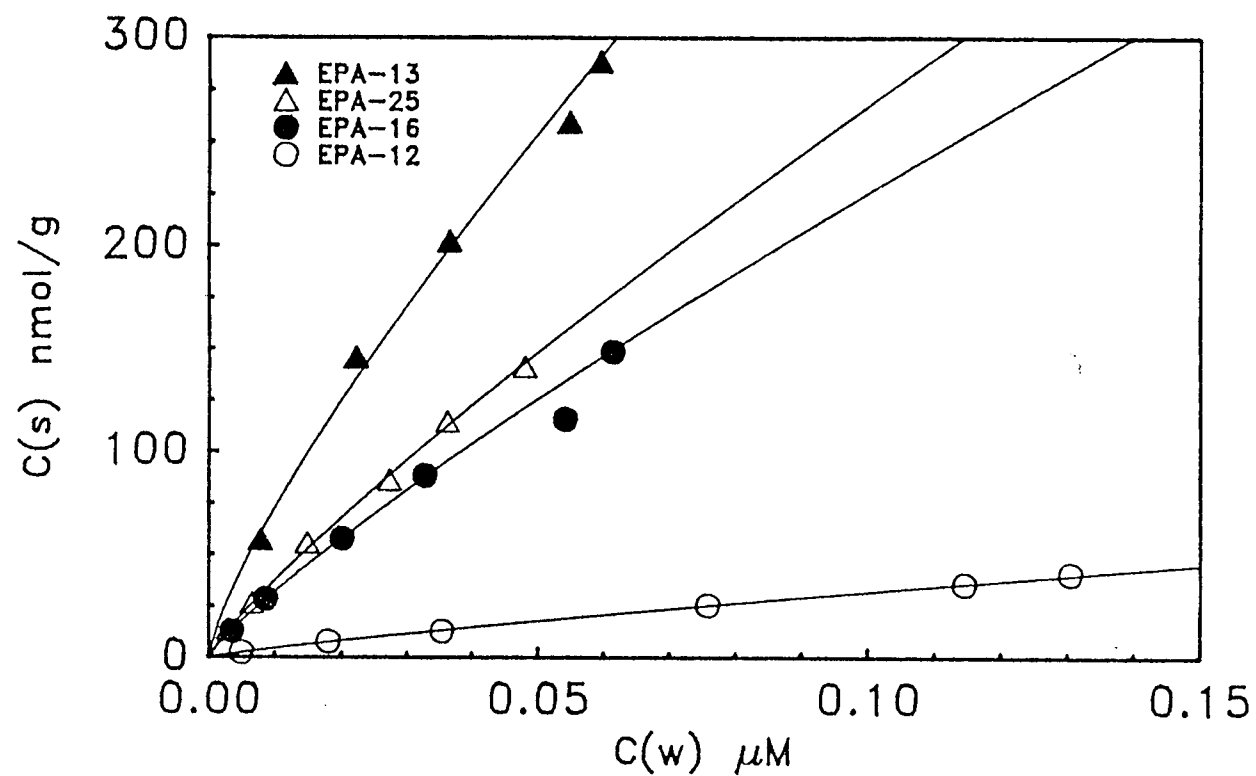


Figure 5.1. Adsorption isotherms of  $A_{13}E_6$  on different sorbents at 0.024 g/mL in 0.01 M  $NaN_3$ ; The curves were calculated from parameters of the Freundlich isotherm (Table 5.1).

Table 5.1. Adsorption Isotherms of  $A_{13}E_6$  on different soil sorbents ( $C_s(w) = 0.024$  g/L) in 0.01 M  $NaN_3$ . Values of parameters are determined from Freundlich model.

Sorbent	Freundlich <sup>a</sup>	
	K	n
EPA-13	$2.6 \times 10^3$	0.89
EPA-25	$1.9 \times 10^3$	0.82
EPA-16	$1.6 \times 10^3$	0.80
EPA-12	$2.2 \times 10^2$	0.77

<sup>a</sup> Freundlich equation:  $C_i(s) = K C_i(w)^n$ ; concentration  $C_i(w)$  in nmol/mL, concentration  $C_i(s)$  in nmol/g. Data from Figure 5.1.

surfactants (C-12 LAS) on the same series of soil sorbents (see Chapter 6). This is because the presence of the electrostatic repulsion between the LAS and the negatively charged surface is unfavorable to the adsorption of the anionic surfactants.

Urano et al. (1984) have found that the adsorption by sediments of one AE and one alkylphenol ethoxylate (APE) increased nonlinearly with increasing concentration of surfactants (with Freundlich isotherm parameter,  $n = 1.4$ ), and the adsorption tended to increase with increasing organic carbon content of the sorbent. In this study, however, the adsorption of  $A_{13}E_6$  on different soil sorbents does not correspond to the fraction of organic carbon of the sorbents. The order of fraction of organic carbon is EPA-13 > EPA-12 > EPA-16 > EPA-25 (see Table 4.5), whereas the affinity of adsorption of  $A_{13}E_6$  is in the order EPA-13 > EPA-25  $\geq$  EPA-16  $\gg$  EPA-12.

This result is also different from adsorption of the anionic surfactant, (dodecylbenzenesulfonate, C-12 LAS) on the same series of the soil sorbents. The order of the adsorption affinity of C-12 LAS does correspond to the order of fraction of organic carbon of the sorbents. Also, the adsorption of C-12 LAS on EPA-12 is much stronger than that on EPA-25 and EPA-16 (Chapter 6). The comparison above indicates that some properties of soil sorbents might favor the adsorption of  $A_{13}E_m$  on EPA-16 and EPA-25, but not LAS.

The order of affinity of adsorption for  $A_{13}E_6$  did not correspond to the surface area of the sorbents (Table 4.5), either. However, the order of affinity for adsorption of  $A_{13}E_6$  might be related to the quantities of swelling clays which are present in

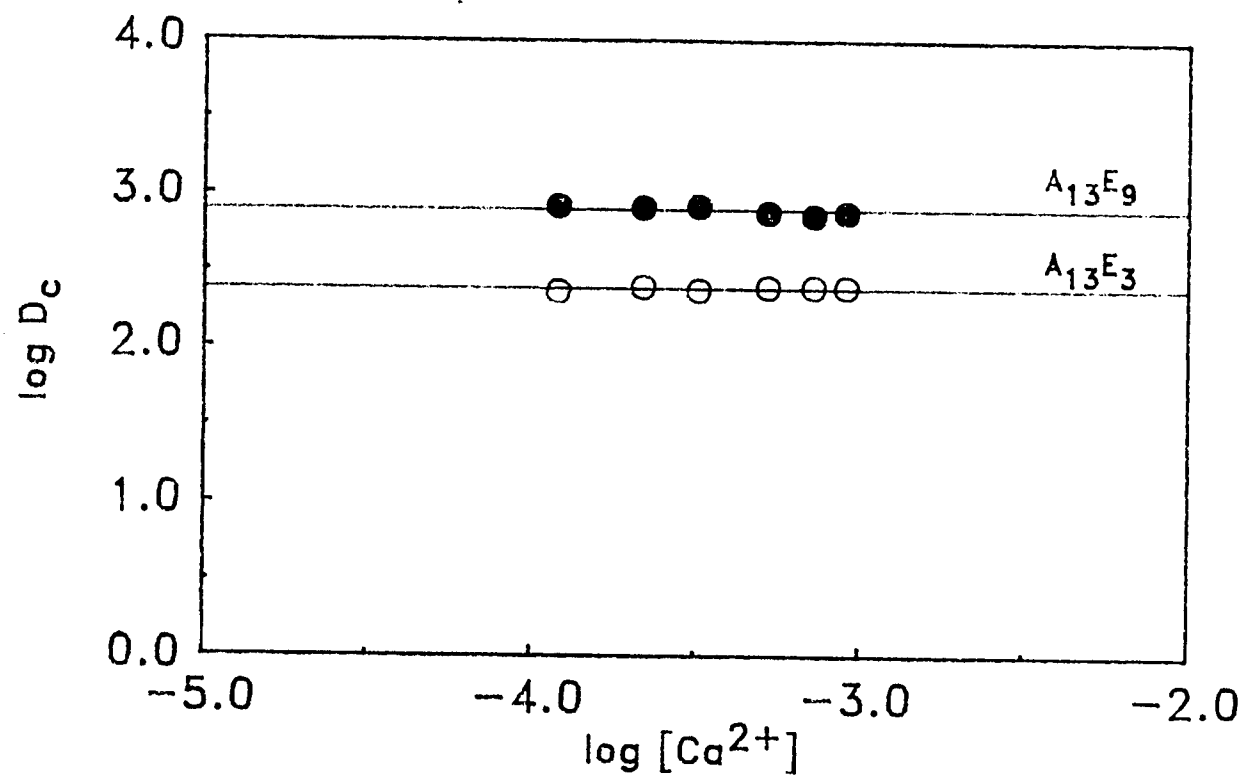


Figure 5.2. Effect of added  $Ca^{2+}$  on adsorption of  $A_{13}E_m$ . The  $\log D_c$  of  $A_{13}E_3$  and  $A_{13}E_g$  on soil sorbent EPA-12 at 0.011 g/mL in 0.01 M  $NaN_3$  as a function of the logarithm of concentration of  $Ca^{2+}$  added to the solution.

sorbents: EPA-16 and EPA-25 contain large amounts of smectite and vermiculite, but EPA-12 does not (Table II.2). Smectite is a general term for swelling clays; montmorillonite and vermiculite are specific types of smectites. It has been found that swelling clays intercalate AE's but not anionic surfactants (Law and Kunze, 1966; Platikanov et al., 1976). Podoll and coworkers (1987) found that the adsorption of poly(ethylene glycols) to natural sediments was related to the fraction of montmorillonite + vermiculite, and not directly to fraction organic carbon, for all system studied.

The effect of added  $\text{Ca}^{2+}$  on adsorption of  $\text{A}_{13}\text{E}_m$ . The adsorption of  $\text{A}_{13}\text{E}_3$  and  $\text{A}_{13}\text{E}_9$  on the sorbent EPA-12 was determined as a function of  $\text{Ca}^{2+}$  concentration in the aqueous phase. Figure 5.2 illustrates the observed distribution ratio,  $D_c$ , of the two homologs, as a function of  $\text{Ca}^{2+}$  concentration. As shown in the figure, the addition of  $\text{Ca}^{2+}$  in the system has no significant effect on the adsorption of these nonionic surfactants on the natural sorbent. The result suggests that even though the addition of divalent cations such as  $\text{Ca}^{2+}$  into the sorbent-water system may change the electrical charge of the surface, this change does not affect the adsorption of these nonionic surfactants. Thus, the electrostatic interaction between the sorbate and the sorbent is insignificant for the adsorption of the  $\text{A}_{13}\text{E}_m$  on the natural sorbent.

The addition of  $\text{Ca}^{2+}$  shows a different effect on the adsorption of anionic surfactant such as linear alkylbenzenesulfonate (LAS) on the same sorbent (EPA-12). A large increase in the distribution ratio  $D_c$  with the increase in  $\text{Ca}^{2+}$  has been observed

for adsorption of LAS homologs on EPA-12 (Chapter 6). This increase in  $D_c$  is attributed to the specific interaction of the  $\text{Ca}^{2+}$  ions on the negatively charged surface resulting in a positively charge sorption site which is more favorable to adsorption of LAS. This result will be described in Chapter 6.

The effect of salt concentration on adsorption of  $A_{13}E_m$ .

The experiments with variable  $\text{NaN}_3$  concentration were performed with  $A_{13}E_3$  and  $A_{13}E_9$  homologs to examine the effect of salt concentration on the adsorption of  $A_{13}E_m$ . Small but measurable changes in  $D_c$  with ionic strength were observed in this study, and the effect is different for the two homologs. The logarithm of  $D_c$  as a function of  $\text{NaN}_3$  is shown in Figure 5.3. For  $A_{13}E_9$ ,  $D_c$  decreases as  $\text{NaN}_3$  concentration increases, whereas for  $A_{13}E_3$ ,  $D_c$  increases with the increase of  $\text{NaN}_3$  concentration. The effects are more pronounced for ionic strengths between 0.01 and 0.1 M for both homologs. The processes causing these two different types of effects are not clear.

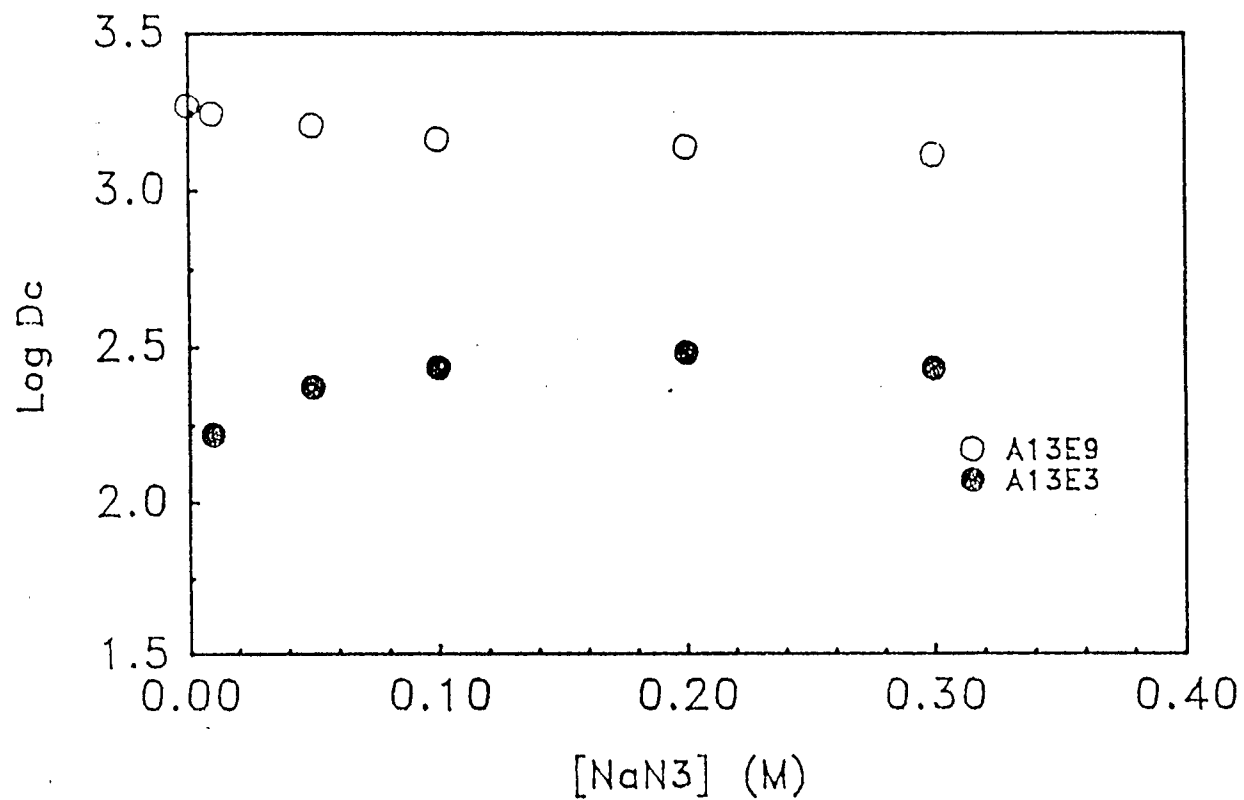


Figure 5.3. Effect of added NaN<sub>3</sub> on adsorption of A<sub>13</sub>E<sub>m</sub>. The log D<sub>c</sub> of A<sub>13</sub>E<sub>3</sub> and A<sub>13</sub>E<sub>9</sub> on soil sorbent EPA-12 at 0.025 g/mL in 0.01 M NaN<sub>3</sub> as a function of the logarithm of concentration of NaN<sub>3</sub> added to the solution.

## SUMMARY

The nonionic surfactants  $A_{13}E_m$  were strongly adsorbed on the soil sorbents. Adsorption isotherms of  $A_{13}E_6$  is well expressed by Freundlich model. The affinity of the adsorption of  $A_{13}E_6$  on the different sorbents does not correspond to the order of fraction of organic carbon for the sorbents. The results might be interpreted by clay mineral composition of the sorbents, particularly swelling clay composition. The addition of  $Ca^{2+}$  has no effect on the adsorption of  $A_{13}E_m$ , which indicates that the electrostatic interaction is insignificant. An increase in salt concentration decreases the adsorption of the  $A_{13}E_9$  homolog, but increases the adsorption of the  $A_{13}E_3$  homolog. The interpretation of this effect is not clear.

## REFERENCES

- Florence, A. T.; Tucker, I. G.; Walters, K. A. in "Effect of Structure on Performance in Various Application"; Rosen, M. J., ed.; ACS: Wash. D. C., 1984; 189-208.
- Greek, B. F.; Layman, P. L. Chem. Eng. News 1990, 68, 37-60.
- Koganovskii, A. M.; Klimenko, N. A.; Tryasorukova, A. A. Colloid Journal of USSR (in English); 1974, 36, 790-792.
- Law, J. P.; Kunze, G. W. Soil Sci. Soc. Amer. Proc. 1966, 30, 321-327.
- Lewis, M. A.; Suprenant, D. Ecotoxicol. Environ. Safety. 1983, 7, 313-322.
- Platikanov, D.; Weiss, A.; Lagaly, G. Colloid Polymer Sci. 1977, 255, 907-915.
- Podoll, R. T.; Irwin, K. C.; Bredlinger, S. Environ. Sci. Technol. 1987, 21, 562-568.
- Rosen, M. J. "Surfactants and Interfacial Phenomena"; John Wiley & Sons: New York, 1978, 17-22.
- Turner, A. H.; Abram, F. S.; Brown, V. M.; Painter, H. A. Water Res. 1985, 19, 45-51.
- Urano, K.; Saito, M.; Murata, C. Chemosphere 1984, 13, 293-300.

## CHAPTER 6

ADSORPTION OF LINEAR ALKYL BENZENESULFONATES  
ON ENVIRONMENTAL MATERIALS

## INTRODUCTION

Linear alkylbenzenesulfonates (LAS) are anionic surfactants. They are used in large quantities in industrial and consumer products and enter the environment primarily through wastewater and sludge. Even though these compounds are reasonably degradable and not particularly toxic, the magnitude of the quantities in use require that possible effects of these compounds in the environment should be investigated thoroughly.

In the environment, LAS is not adsorbed as strongly as the corresponding alkylbenzenes, on account of the repulsion of the anion by the negative charge present at most environmental surfaces. LAS is more likely to be associated with surfaces in environments with high amounts of suspended solids, such as in wastewater treatment plants. LAS has been found to accumulate in sewage sludge, especially sludge that has been treated anaerobically (McEvoy and Giger, 1985; Giger et al., 1984). LAS may accumulate in sediments as well, particularly at waste-water-discharge or sludge-disposal sites. The environmental concentrations of surfactants have not been surveyed as intensively as those of other compounds.

Studies of biotoxicity of cationic, anionic, and nonionic surfactants show great variability. Lewis and Suprenant (1983) reported that the 48-hour  $LC_{50}$  values for LAS and D. Magna were in the range of 1.8 - 5.6 mg/L. Toxicities of surfactants also depend on their speciation in test systems. Furthermore, it is likely that interactions among anionic and cationic surfactants in wastewater may lead to significant reduction in toxicity from the value predicted

from consideration of the toxicity of either species by itself.

Imboden and Schwarzenbach (1985) have discussed the role of chemical speciation in affecting transport and fate of organic chemicals in natural waters.

The adsorption of ionic organic compounds, such as LAS, has received relatively little attention (Hand and Williams, 1987). Our approach to the study of adsorption of LAS is to identify the important properties of solutes, sorbents, and solvents that influence adsorption of organic compounds to natural materials, and to describe equilibrium distributions in terms of hydrophobic, electrostatic, and specific chemical interactions.

Experimental studies with LAS and branched chain alkylbenzenesulfonates with sediments (Urano et al., 1984; Matthijs and De Henau, 1985; Hand and Williams, 1987) and soils (Krishna Murti et al., 1966; Inoue et al., 1978) suggest that both hydrophobic and electrostatic interactions are important. The contribution of hydrophobic interactions to adsorption is demonstrated best by the dependence of adsorption on alkyl chain length of LAS to sediments (Hand and Williams, 1987) and to alumina (Dick et al., 1971). The importance of hydrophobic mechanisms are also suggested by the correlation of adsorption with the fraction of organic carbon of sediments in the the study of Urano and coworkers (1984). However, other studies have shown that organic carbon is not the only important property of sorbents for adsorption of anionic surfactants (Krishna Murti et al., 1966; Inoue et al., 1978; Matthijs and De Henau, 1985; Hand and Williams, 1987).

The effect of electrostatic interactions on the energy of adsorption is suggested by the dependence on pH of adsorption of LAS on soils (Inoue et al., 1978), alumina (Dick et al., 1978), and clays (Siracusa and Somasundaran, 1986). The significance of electrostatic effects are also seen when the adsorption of LAS is compared to that of neutral and cationic surfactants on the same sediments (Urano et al., 1984; Westall et al., 1989). In those studies, the extent of adsorption of anionic surfactants on predominantly negatively charged sediments was found to be lower than that of similarly sized neutral compounds and much lower than that of cationic organic compounds. Various models have been employed to describe the electrostatic interactions of ionic species with charged surfaces and phases (Westall et al., 1985; Westall, 1986, 1987.). Electrostatic models have yet to be applied to adsorption of hydrophobic ionic organic compounds with sediments or soils. However, a Donnan distribution model has been successfully applied to describe some aspects of the association of LAS with vinylon and acetate fibers (Sakata and Katayama, 1987; 1988), which are organic polyelectrolytes whose properties resemble those of natural geopolymers in some respects.

In this investigation we have examined the adsorption of pure LAS homologs on five characterized environmental sorbents, as a function of properties of the surfactant, characteristics of the sorbents, and composition of the solutions.  $^{14}\text{C}$ -labeled homologs were used to facilitate experimentation at low (sub  $\mu\text{M}$ ) concentrations and surface coverages.

## THEORY

Partition constant  $K_p$  and distribution ratio  $D_c$ . In this study we distinguish between an operational concentration distribution ratio,  $D_c$  [(mol/g) / (mol/mL)], which is based on the total concentration of all forms a component in the operationally defined aqueous phase and sorbent, and  $K_p$  [(mol/g) / (mol/mL)], which refers to a partition constant for a single species. The value of  $D_c$  is defined

$$D_c = \Sigma C_j(s) / \Sigma C_j(w) \quad (6.1)$$

where the summation is over all forms of a component  $j$  (free ion, ion pair, organic complex, etc.),  $C_j(s)$  is the concentration of  $j$  associated with the sorbent [mol g<sup>-1</sup>] and  $C_j(w)$  is the concentration of  $j$  in solution phase [mol mL<sup>-1</sup>].

Adsorption of nonpolar hydrophobic compounds. The sorption of nonpolar hydrophobic organic compounds (HOC) to soils and sediments has been shown to involve nonspecific, hydrophobic interactions, and observed distributions can be predicted reasonably well from the solutes hydrophobicity, and the organic carbon content of the sorbent (Karickhoff et al., 1979; Chiou et al., 1979; Schwarzenbach and Westall, 1981). The partition constant  $K_p$  of a nonpolar organic compound between a natural sorbent and water can be described in terms of a property of the compound (the octanol-water partition constant,  $K_{ow}$ ) and a property of the sorbent (the fraction of organic carbon,  $f_{oc}$ ):

$$\log K_p = a \log K_{ow} + b + \log f_{oc} \quad (6.2)$$

This equation is applicable to a wide range of compounds and sorbents from a number of different sources (sewage sludge, sediments, aquifer material, etc.) A very simplified interpretation of this phenomenon is that the organic matter in natural sorbents from many sources is more or less similar in its ability to accommodate nonpolar compounds, and the hydrophobicity, or the water's inability to accommodate the compounds, drives the adsorption reaction. A more rigorous explanation of hydrophobic interactions related to sorption in the environment is given by Westall (1984).

Adsorption of hydrophobic ionic compounds. The study of adsorption of nonpolar compounds has been extended to include hydrophobic ionizable organic compounds (HIOC's), in particular, chlorophenols (Westall et al., 1985). The mechanism proposed for the transfer of the organic compound from water to the sorbent, and the effect of pH and ionic strength on this transfer, have been discussed by Westall (1985).

For the compounds in this study we expect a significant contribution to adsorption energy both from hydrophobic and ionic interactions. Thus the contribution of chain length is to be expected, as well as the ionic contribution. One way to represent the various contributions is through the equation:

$$\log D_c = a \log [i] + b n + c \quad (6.3)$$

where  $[i]$  is the solution concentration of surface-potential determining ions, such as  $\text{Ca}^{2+}$ ,  $n$  is the number of methylene units in the alkyl chain, and  $a$ ,  $b$  and  $c$  are the adjustable parameters.

The a term corresponds to an ionic contribution, the b term reflects the hydrophobic interaction, and c is a constant.

Isotherms. In this study, many of the isotherms are nonlinear in contrast to the generally linear isotherms observed for nonpolar hydrophobic organic compounds at similar concentrations. The two isotherms used to represent the data in this study are the Freundlich isotherm and the virial (or electrostatic) isotherm. The Freundlich equation is

$$C_i(w)^n K = C_i(s) \quad (6.4)$$

where K and n are constants. The Freundlich equation is simple and describes almost all of our data very well. In principle it has a mechanistic basis as a summation of Langmuir isotherms with a distribution of  $\ln K$ 's (Sposito, 1986); however in practice there is a great deal of covariance between experimentally determined values of K and n, and differences in energies of adsorption for different materials are not readily found from the Freundlich constants. Also the limit of  $C_i(s) / C_i(w)$ , as  $C_i(w)$  approaches zero, is undefined for  $n < 1$ . Thus we consider the Freundlich isotherm most convenient for empirical representation of our data, but of little use for mechanistic questions.

The virial (electrostatic) equation (Delahay, 1965) is

$$C_i(w) \exp[-b C_i(s)] K = C_i(s) \quad (6.5)$$

where b and K are constants. This isotherm is formally equivalent to

an adsorption model involving adsorption of charged species to a charged surface, with the electrostatic energy of interaction described by a Helmholtz, or constant capacitance model of the electric double layer. This electrostatic model is explained in detail in Table 6.1. The virial isotherm does have a mechanistic basis, the ratio  $C_i(s) / C_i(w)$  does approach a finite limit as  $C_i(w)$  approaches zero, and interpretation of differences in adsorption energies in terms of differences in values of  $K$  is meaningful.

Table 6.1. Electrostatic model for adsorption.

---

Mass action equation for adsorption of charged species:

$$C_R(w) \exp[-z_R F \Psi / RT] K = C_R(s) \quad (1)$$

Boltzmann factor for electrostatic energy, expressed as  $\Delta \log K$ :

$$\Delta \log K = [-z_R F \Psi / RT \ln 10] \quad (2)$$

Surface charge:

$$\sigma = F C_R(s) / s \quad [C \text{ m}^{-2}] \quad (3)$$

Surface potential:

$$C = \frac{\sigma}{\Psi} \quad [F \text{ m}^{-2}] \quad (4)$$


---

where<sup>a</sup>:

C	interfacial capacitance	F m <sup>-2</sup>
C <sub>i</sub> (s)	concentration of ion i on the surface	mol kg <sup>-1</sup>
C <sub>i</sub> (w)	concentration of ion i in solution	mol m <sup>-3</sup>
F	Faraday constant	C mol <sup>-1</sup>
K	adsorption constant	m <sup>3</sup> kg <sup>-1</sup>
R	ideal gas constant	J mol <sup>-1</sup> K <sup>-1</sup>
s	specific surface area	m <sup>2</sup> kg <sup>-1</sup>
T	temperature	K
z <sub>i</sub>	charge on ion i	
σ	surface charge	C m <sup>-2</sup>
Ψ	surface potential	V

---

<sup>a</sup> All quantities are specified here in S.I. units; other units are sometimes defined and used in the text.

## EXPERIMENTAL METHODS

Materials and equipment. The homologs of C-10, C-12, and C-14 LAS used in this study were originally synthesized by New England Nuclear and obtained through the Soap and Detergent Association from Procter and Gamble. The compounds were uniformly ring labeled with  $^{14}\text{C}$ . The specific activities of C-10, C-12, C-14 LAS were 1.46, 13.4 and 12.9 Ci/mol, respectively. The radiochemical purity of the compounds was greater than 99%, as determined by HPLC. The purity was routinely verified during the course of the study. Original and spiking standard solutions of labeled LAS were in methanol or 95% ethanol, and stored at temperature  $< 0^\circ\text{C}$ .

The soil sorbents that were used in this study exhibited a wide range of physical and chemical properties (Table 4.5). They were provided by Professor John J. Hassett of the University of Illinois. Procedures for characterization of the sorbents are discussed by Hassett et al., 1980. In addition, the specific surface area was determined by single point BET (Fahey, 1987) and clay mineralogy was qualitatively analyzed by X-ray diffraction (see Appendix II).

The deionized water used in all experiments was from a Millipore Milli-Q System, with specific resistivity usually approaching  $18\text{ M}\Omega\text{ cm}$ .

For equilibration and phase separation, a thermostatted shaker (New Brunswick Model G-24) and thermostatted centrifuge (IEC Model B-20A) were used. Sorbent samples were oxidized and labeled compounds were converted to  $^{14}\text{CO}_2$  with a Harvey Model 300 Oxidizer. Radioactivity was determined with a Beckman Model LS 7800

scintillation counter.

Determination of distribution ratios. Adsorption of LAS on sorbents was studied through equilibration of LAS solutions with sorbents in batch experiments. The procedures for determination of distribution ratio,  $D_C$ , have been described in detail in Chapter 4, and will only be outlined in this chapter. The sorbents (0.050 - 1.0 g) were washed with deionized water 8 times by the individual tube method. Then a 20-mL aliquot of electrolyte solution (0.01 M  $\text{NaN}_3$  or in some case 0.01 M  $\text{NaCl}$ ) and a spike of 10 - 200  $\mu\text{L}$  of LAS in 95% ethanol were added into each tube, and the slurries were agitated on a thermostatted shaker at 500 RPM at 25 °C for 4 hours. Aqueous and sorbent phases were then separated by centrifugation at 11,000 G at 25 °C for 1 hour.

After centrifugation, a 0.2 - 1.0 mL aliquot of the aqueous sample was transferred into a scintillation vial containing 10 mL of Beckman HP/b scintillation fluid for determining the activity in the aqueous phase. The activities of labeled surfactants in the sorbent phase were determined by the combustion method, as described in Chapter 4. In addition, the amount of surfactants adsorbed on the walls of the tubes were also determined, and the material recovery for each sample was calculated from the ratio of the total activity found to the total activity added. The concentration of LAS in the aqueous and sorbent phases were calculated from the measured activities and the corresponding calibration curves.

The distribution of LAS as a function of  $\text{Ca}^{2+}$  concentration was determined by adding  $\text{CaCl}_2$  to the 0.01 M  $\text{NaN}_3$  solution to yield final concentrations of  $\text{Ca}^{2+}$  between 0.10 and 1.0 mM. In other

experiments the background concentrations of Ca(II) and other elements that dissolve from the sorbents during equilibration were analyzed by inductively coupled plasma emission spectrometry on a Jarrel-Ash ICAP-9000 spectrometer.

## RESULTS

Adsorption of C-12 LAS on different soil sorbents. A set of experiments was run to investigate the adsorption of LAS on different sorbents and to attempt to establish the properties of sorbents (Table 4.5) that influence the adsorption of LAS. Isotherms for adsorption of C-12 LAS on the four sorbents are shown in Figure 6.1a. The isotherms cover the low adsorption range with surface coverage less than 0.036%. The experimental data have been interpreted based on the Freundlich isotherm and the electrostatic isotherm models. These parameters are given in Table 6.2. Isotherms for all sorbents did appear to approach linearity towards very low concentrations, as shown in Figure 6.1b; It is noted, however, that the intercepts of the linear isotherms are not strictly zero. The linear adsorption constants are given in Table 6.2. The distribution ratio from Freundlich isotherms increases as the fraction of organic carbon of the sorbents increases. However, the relationship between  $K$  and  $f_{oc}$  is not linear.

Effect of  $Ca^{2+}$  on the adsorption of LAS. The distribution ratio of LAS homologs on sorbent EPA-12, as a function of  $[Ca^{2+}]$ , is shown in Figure 6.2. The experiment was performed in the region of a near-linear adsorption isotherm. The addition of  $Ca^{2+}$  clearly enhances adsorption. The parameters  $a$ ,  $b$ , and  $c$  determined from fit of Equation 6.3 to the data in Figure 6.2 are given in Table 6.3. This effect is even slightly greater than that of  $H^+$ , which is calculated from the data of Chen and Westall (1988).

Table 6.2. Adsorption Isotherms of C-12 LAS on different soil sorbents (0.024 g/L) in 0.01 M  $\text{NaN}_3$ . Values of parameters from Freundlich and electrostatic models.

Sorbent	Freundlich <sup>a</sup>		Electrostatic <sup>b</sup>		Linear <sup>c</sup>	
	K	n	K [mL/g]	C [F/m <sup>2</sup> ]	K [mL/g]	b [nmol/g]
EPA-13	$2.0 \times 10^2$	0.89	$2.9 \times 10^2$	0.071	$2.6 \times 10^2$	0.3
EPA-12	$6.9 \times 10^1$	0.82	$1.3 \times 10^2$	0.027	$1.0 \times 10^2$	0.6
EPA-16	$4.5 \times 10^1$	0.80	$8.6 \times 10^1$	0.012	$6.6 \times 10^1$	0.7
EPA-25	$3.7 \times 10^1$	0.77	$6.9 \times 10^1$	0.023	$6.0 \times 10^1$	0.0

- <sup>a</sup> Freundlich equation:  $C_i(s) = K C_i(w)^n$ ; concentration  $C_i(w)$  in nmol/mL, concentration  $C_i(s)$  in nmol/g. Data from Figure 6.1a.
- <sup>b</sup> Electrostatic equation:  $C_i(w) \exp[-b C_i(s)] K = C_i^i(s)$ , with  $b = F^2 / RT C s$ . See Table 6.1 for explanation of symbols. Data from Figure 6.1a.
- <sup>c</sup> Linear isotherm:  $C_i(s) = K C_i(w) + b$ . Data from Figure 6.1b.

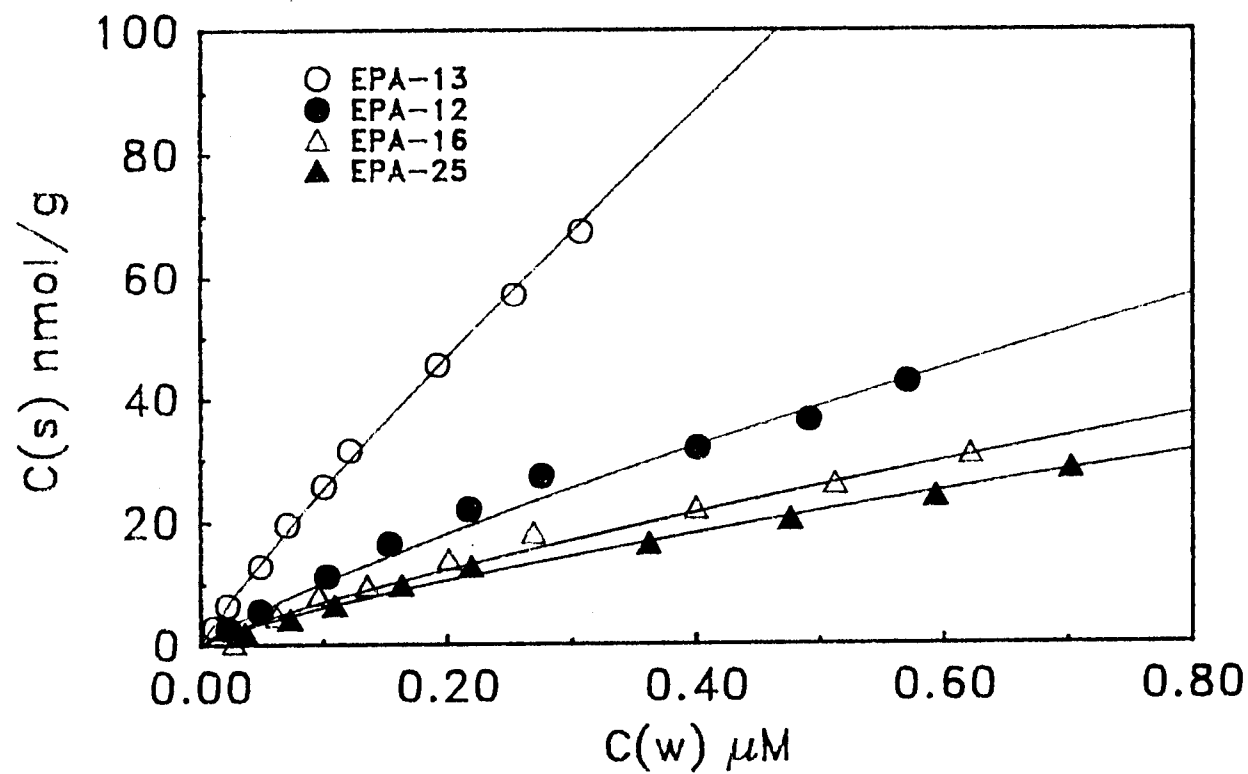


Figure 6.1a. Adsorption isotherms of C-12 LAS on different sorbents at higher concentrations of C-12 LAS. The isotherms are nonlinear. The curves were calculated from the parameters of the Freundlich isotherm (Table 6.2); curves calculated from the electrostatic model (not shown) have virtually the same appearance.

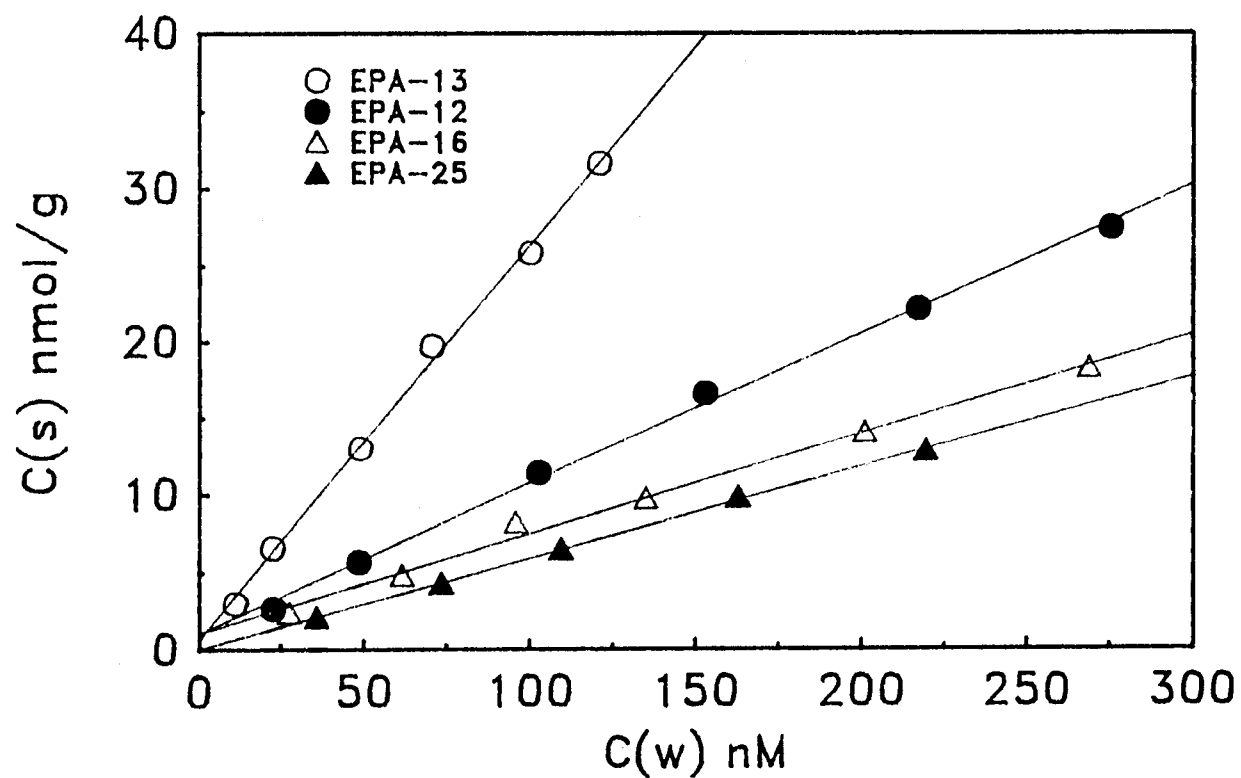


Figure 6.1b. Adsorption isotherms of C-12 LAS on different sorbents at lower concentrations of C-12 LAS. The isotherms approach linearity, although the intercept is not zero. The curves were calculated from the linear isotherm (Table 6.2).

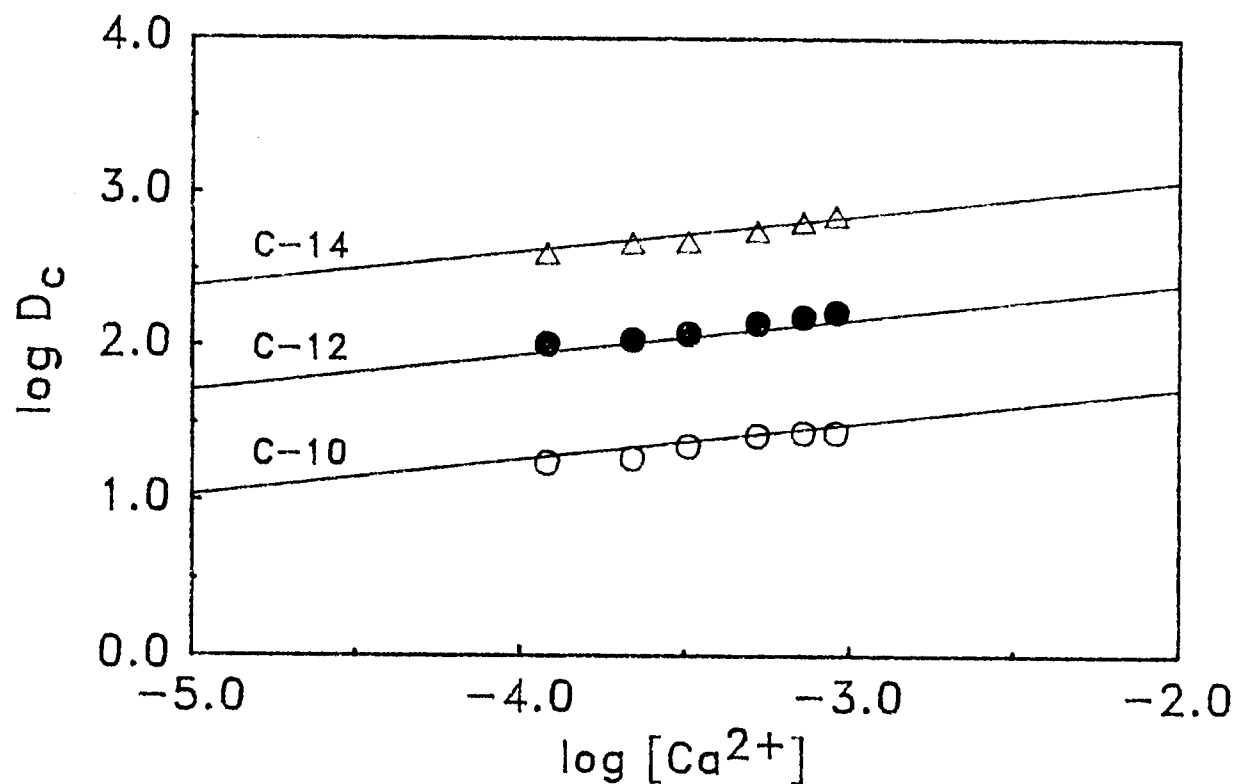


Figure 6.2. Effect of added  $\text{Ca}^{2+}$  on adsorption of LAS. The  $\log D_c$  of C-10, C-12, C-14 LAS on sorbent EPA-12 at 0.094 g/mL in 0.01 M  $\text{NaN}_3$  as a function of the logarithm of concentration of  $\text{Ca}^{2+}$  added to the solution. The lines were calculated from Equation 6.3 (written for  $\text{Ca}^{2+}$  instead of  $i$ ) and the parameters of Table 6.3. The concentration of LAS in water ranged from  $C(w) = 36 - 251$  nM, and on the surface from  $C(s) = 4 - 26$  nmol/g.

Table 6.3. Effect of  $H^+$  and  $Ca^{2+}$  on  $D_c$  of LAS homologs on EPA-12 in 0.01 M  $NaN_3$ .

Parameter for Equation:  $\log D_c = a \log [i] + b n_{-CH_2-} + c$

Ion	a	b	c
$H^+$	0.17	0.38	-1.3
$Ca^{2+}$	0.23	0.34	-1.2

Note:

The parameters of effect of  $H^+$  were determined from the data of Chen and Westall (1988), the experiments ran with EPA-12 in 0.01 M  $NaN_3$  at  $C_s(w) = 0.048$  g / mL.

The experiments for effect of  $Ca^{2+}$  ran with EPA-12 in 0.01 M  $NaN_3$  at  $C_s(w) = 0.094$  g / mL.

Isotherms of C-12 LAS on EPA-12 at different sorbent concentrations. In an effort to clarify the effect of the concentration of solids on the observed concentration distribution ratio, a series of isotherms of C-12 LAS on sorbent EPA-12 were obtained with different concentrations of solid in water. The results are shown in Figure 6.3, and experimental data are fit well by Freundlich equation (the K and n obtained are listed in Table 6.4).

It is shown that the concentration of solids did affect the adsorption of LAS, which increases the observed concentration distribution ratio as  $C_s(w)$  increases. The results may be partially explained by a model which incorporates the increase in concentration of  $Ca^{2+}$  with the increase in solids concentration.

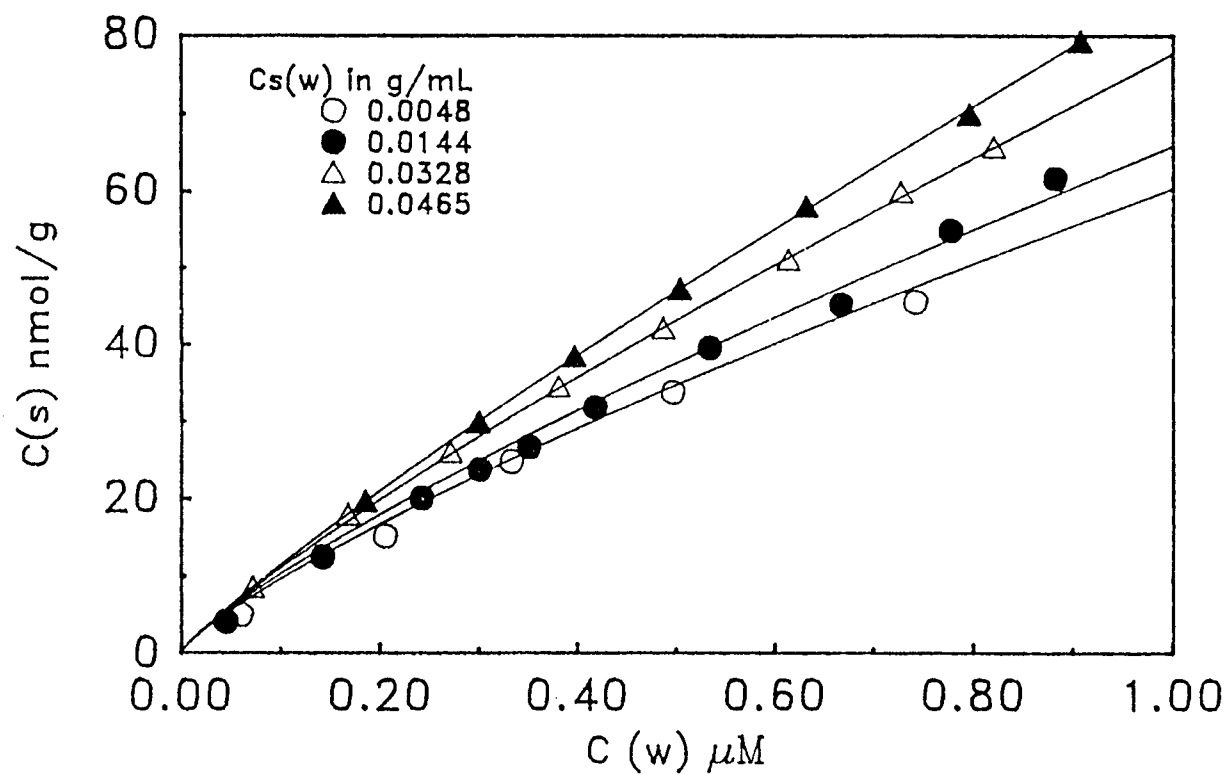


Figure 6.3. Adsorption isotherms of C-12 LAS on sorbent EPA-12 at different ratios of sorbent to solution: 0.0048, 0.0144, 0.0328, 0.0465 g/mL in 0.01M  $\text{NaN}_3$ . Curves calculated from parameters of the Freundlich isotherm (Table 6.4).

Table 6.4. Adsorption Isotherms of C-12 LAS on EPA-12 in 0.01 M  $\text{NaNO}_3$  with different solid concentrations. Values of parameters from Freundlich Model.

Sorbent	$C_s(w)$	Freundlich			$[\text{Ca}^{2+}]^c$
	[g/mL]	$K_p^b$	$SD_{Kp}$	n	[uM]
EPA-12	0.0048 <sup>a</sup>	60	0.2	0.80	70
EPA-12	0.0144 <sup>a</sup>	66	0.2	0.81	130
EPA-12	0.0328	78	0.6	0.85	268
EPA-12	0.0465	86	0.2	0.88	325

Note:

a. The ionic strength for these two isotherms were 0.01 M  $\text{NaCl}$ .

b. In Figure 6.3, the units of  $C(s)$  and  $C(w)$  are  $\text{nmol/g}$  and  $\mu\text{M}$ , respectively. Thus the unit of  $K_p$  can be obtained as following:

$$\begin{aligned}
 K_p &= \frac{(\text{nmol} / \text{g})}{(\mu\text{mol} / \text{L})} = \frac{(\text{nmol} / \text{g})}{(\mu\text{mol} / \text{L}) (\text{L} / 10^3 \text{ mL})} = \frac{(\text{nmol} / \text{g})}{(\text{nmol} / \text{mL})} \\
 &= \frac{\text{mL}}{\text{g}}
 \end{aligned}$$

## DISCUSSION

We have studied the effects of LAS chain length,  $[\text{Ca}^{2+}]$ , sorbent type, and solids concentration. The experimental results allow us to answer the following questions: (i) what are the driving forces for adsorption of LAS on natural sorbents? (ii) why are the isotherms nonlinear? (iii) how do the properties of the sorbents affect adsorption? (iv) what is difference between adsorption of LAS on natural materials and on pristine oxides or clays?

Adsorption energy of LAS

The driving force for adsorption of LAS can be analyzed as contributions from three primary components: (i) hydrophobic interactions, (ii) specific interactions with surface functional groups, and (iii) electrostatic interactions. Even for homogeneous sorbents, such a separation of energies into discrete components is generally indeterminate; for heterogeneous natural sorbents the problem is much more difficult. However, such a mechanistic approach does ultimately aid in understanding adsorption and the sensitivity of adsorption to variations in environmental conditions.

Hydrophobic interactions. Hydrophobic interactions literally refer to the tendency of water to expel the solute molecule. However, in assessing the magnitude of the hydrophobic effect in a sorption reaction, one must also consider the tendency of the sorbing phase to

accept the molecule expelled by the aqueous phase. The net tendency for sorption is the difference between these two effects.

Two questions arise with respect to hydrophobic interactions and sorption of LAS: (i) the effect of the alkyl chain length; and (ii) the sorption of alkylbenzene sulfonate compared to analogous alkylbenzenes.

The effect of alkyl chain length can be seen in Figures 6.2. The difference in  $\log K$  for adsorption of the C-10, C-12, and C14 homologs is equivalent  $\Delta \log K \approx 0.4$  per  $-\text{CH}_2-$  group. This value obtained here is similar to the value of  $\Delta \log K = 0.45$ , reported by Hand and Williams (1987) (as the multiplicative factor 2.8) for adsorption of LAS on a series of natural materials, and  $\Delta \log K = 0.44$  reported by Dick et al. (1971) (as  $\Delta G^\circ$  of 600 kcal / mol) for adsorption of LAS onto oxides. Furthermore this value is similar to that of a  $-\text{CH}_2-$  group on the solubility of a nonpolar hydrophobic compound in water, as demonstrated by the fragment of  $\Delta \log K = 0.50$  reported by Lyman (1982).

The fact that the energy of adsorption per  $-\text{CH}_2-$  group is similar for many different sorbents is noteworthy. It implies that the energies of interactions of the  $-\text{CH}_2-$  group with the different sorbents are similar, or simply that the differences in interactions with the sorbents are small compared to the differences in the hydrophobic interactions with water.

The second question involves the contribution of the hydrophobic alkyl benzene and the ionic sulfonate group. The  $\log K$  for adsorption of dodecylbenzene can be estimated by many methods; in any case it is several orders of magnitude greater than that of dodecylbenzene

sulfonate. The difference can be attributed to the tendency of the sulfonate group both to enhance the solubility of the dodecylbenzene in water and to repel the molecule from negatively charged surfaces. It is difficult to assess the relative magnitudes of the processes without further information on the behavior of the fragments themselves.

Specific interactions with surface functional groups. Specific interactions with surface functional groups were not investigated extensively in this study, but some information is available from this study and the literature. Four types of results which could be interpreted as evidence for specific interactions have been reported: (i) correlation of adsorption of LAS with sesquioxide content of natural sorbents (Inoue et al., 1986; Krishna Murti et al., 1966); (ii) enhancement of adsorption of LAS with increase in solution  $\text{Ca}^{2+}$  concentration; (iii) enhancement of adsorption of LAS with increase in solution  $\text{H}^+$  concentration; and (iv) competition in adsorption of LAS by  $\text{SO}_4^{2-}$  and  $\text{HPO}_4^{2-}$  (Inoue et al., 1986). Similar results have been reported for the adsorption of sulfate on natural materials (e.g., Nodvin et al., 1986; Singh, 1984; Chao et al., 1965).

The correlation of the degree of LAS adsorption with Fe and Al oxide content of sorbents is consistent with ligand exchange reactions of LAS with surface  $=\text{FeOH}$  and  $=\text{AlOH}$  groups. We have no information on these data for our sorbents.

The enhancement of adsorption of LAS by  $\text{Ca}^{2+}$  could be interpreted as (i) a complexation of LAS by  $\text{Ca}^{2+}$ , and preferential adsorption of the positively charged complex to the negatively charged LAS; (ii) adsorption of  $\text{Ca}^{2+}$  and neutralization of the negative

surface charge, without any specific interaction with LAS. Similarly the competing effects of the anions could be thought of as specific competition in ligand exchange reactions at oxide surfaces, or as a non-specific electrostatic interaction.

How difficult is it to distinguish specific from non-specific effects? For these natural heterogeneous adsorbents, it is extremely difficult to separate clearly the specific and nonspecific effects. It is likely that both contribute to the total energy of adsorption. Towards the goal of a comprehensive quantitative model for adsorption of LAS, it is very important to distinguish between the two mechanisms. However, at this time, some arbitrary division of energy into specific and nonspecific components must be made. With the data available in this study, we assess the energy of interaction in terms of an electrostatic model, to set some limits.

Electrostatic interactions. The electrostatic interactions arise when the ions of one charge accumulate at the surface in preference to ions of the other charge; a separation of charge and an electrostatic energy result. With respect to the origin of the surface charge two questions arise: (i) to what extent is the surface charge due to ionogenic functional groups of the natural sorbent (for example, carboxylic acid groups of organic matter or hydroxyl groups of oxides or minerals), and (ii) to what extent is the surface charge due to adsorption of LAS itself?

With respect to arrangement of the surface charge and counter charge two questions arise: (i) to what extent is the interface planar (that is, charge and counter charge arranged in opposing planes) and amenable to description by a classical planar electric double layer

model; and (ii) to what extent do the counter ions penetrate the plane of the the surface charge, creating effectively a Donnan phase at the surface?

Finally, with respect to the distribution of charge in the plane of the surface of the sorbent, the question is: (i) to what extent is the distribution of LAS over the surface uniform, and (ii) to what extent does sorption take place in particularly energetic islands.

All of these questions cannot be answered in this study, but they guide our discussion.

Contribution of LAS to total surface charge. To answer the first question, an upper bound to the contribution of the adsorbed LAS to the total electrostatic energy at the surface can be estimated by applying the electrostatic model in Table 6.1 to the isotherms in Figure 6.1a, as follows: express the electrostatic energy in the mass action equation for adsorption (Table 6.1, Equation 1) as the equivalent change in the logarithm of the adsorption constant,  $\Delta \log K$  (Table 6.1, Equation 2); calculate  $\Delta \log K$  by converting adsorption density to charge density (Table 6.1, Equation 3), taking a lower bound on interfacial capacitance to compute surface potential from surface charge density (Table 6.1, Equation 4), and then calculating the change in adsorption constant from the Boltzmann factor for the surface potential (Table 6.1, Equation 2).

The maximum concentration of C-12 LAS on the surface of EPA-12 (Figure 6.1a) was 40 nmol/g. The surface area of EPA-12 was determined to be 13 m<sup>2</sup>/g. The absolute minimum for the interfacial capacitance is 0.2 F m<sup>-2</sup>, as computed from the Gouy Chapman equation for a perfectly planar interface in 0.01 M 1:1 electrolyte at the

potential of zero charge (Bard and Faulkner, 1980). For these charged, nonplanar interfaces, the capacitance can be greater, up to apparent values of  $1 \text{ F m}^{-2}$ . From these data and the equations in Table 6.1, the value of  $\Delta \log K$  is calculated to be 0.006 for C-12 LAS. The interfacial capacitances are only in the range of  $0.012 - 0.071 \text{ F m}^{-2}$  for the adsorption of C-12 LAS on the four sorbents (Table 6.2). Thus we conclude that at these low surface concentrations, the LAS acts a spectator in an electrostatic atmosphere determined by other ions. Another way of expressing this result is that the surface charge density due to LAS is so low that it is easily countered by the relatively high concentrations of ions in solution. Of course, this explanation is subject to the condition that the LAS is relatively uniformly distributed over the surface of the sorbent.

The conclusion that LAS contributes little to the total surface charge in these experiments aids in interpreting the nonlinearity of isotherms, as discussed below. This conclusion is further confirmed by the result of electrophoresis experiments, which will be described in Chapter 7.

Nonlinearity of isotherms. This apparent absence of an electrostatic effect is significant for the linear-nonlinear appearance of the isotherms in Figure 6.1a and 6.1b. According to the analysis presented above, the transition from linear to nonlinear appearance of the isotherms cannot be attributed to electrostatic energy. Another cause of nonlinearity of isotherms is the saturation of a fixed number of surface sites, as is expressed by the Langmuir isotherm. If all sites on the surface are uniform with respect to

affinity for LAS, this saturation would not begin to occur until surface concentrations were relatively high and the fractional surface coverage begins to approach a few percent. If the sites are heterogeneous with respect to affinity for LAS, sites of higher affinity and lower concentrations would begin to saturate and cause nonlinearity at relatively lower surface concentrations.

For nonpolar hydrophobic compounds, isotherms are typically linear up to relatively high surface concentrations, indicating that the surface is relatively uniform in its affinity for the HOC, i.e., that no group of sites begins to be significantly saturated. In contrast, isotherms for adsorption of LAS become nonlinear at relatively low surface concentrations, suggesting that, if electrostatic effects are ruled out, there are some sites of low concentration with high affinity for LAS that do become saturated. Since similar effects are not observed for nonpolar hydrophobic compounds, the sites of high affinity and low concentrations must be attributed to specific interactions of the sulfonate group with the surface.

A monolayer of cubic packed sulfonate groups based on the diameter of 0.59 nm for the sulfonate head, given by Somasundaran and Fuerstenau, (1966) on a perfectly uniform surface area of  $10 \text{ m}^2 \text{ g}^{-1}$  would result in an adsorption density of  $4.8 \times 10^{-6} \text{ mol m}^{-2}$  or  $48 \text{ } \mu\text{mol g}^{-1}$ ; the adsorption density in these experiments are clearly far below this limit, for uniformly distributed LAS.

Adsorption of C-12 LAS on different soil sorbents. Three properties were of particular interest: organic carbon content, pH, and surface area, as determined directly or estimated from the size distribution among sand, silt, and clay size classes. The properties of the sorbents are listed in Table 4.5. Organic carbon ranges from 0.2 to 3 %, the pH ranges from 6.7 to 7.6, and the size distribution ranges from virtually all sand to virtually no sand.

These experiments were designed to allow comparisons to be made on the relative intensity of adsorption for different sorbents. Adsorption isotherms of C-12 LAS on these sorbents are shown in Figure 6.1. All isotherms were obtained with 0.025 g/mL of the sorbent in 0.01 M  $\text{NaN}_3$ . All isotherms are reasonably linear in the lower concentration range (Figure 6.1b) and nonlinear over the wider concentration range (Figure 6.1a). Hand and Williams (1987) report linear isotherms for both mixed C-10 LAS and mixed C-14 LAS in experiments run at constant concentration of sediments in water, and roughly the same concentrations of surfactants on the surface and in solution as those used in these experiments.

In view of the nonlinearity of these isotherms at higher concentrations, there is no simple way to compare quantitatively the energy of adsorption of LAS to the different materials. However, a very simple qualitative comparison can be made. (The conclusions from this comparison must be used carefully due to the relatively small number of experiments and the relatively large number of factors, some of which are themselves correlated to some degree.) Inspection of the isotherms shows that the distribution of surfactant between the sorbent and water, per unit mass of sorbent, decreases in the order

EPA-13 > EPA-12 > EPA-16  $\approx$  EPA-25 > EPA-1. This order corresponds to the order of organic carbon content of the material. A very weak correlation of adsorption energy with organic carbon content of sediment has been seen by Hand and Williams (1987) and Urano et al. (1984). For these heterogeneous sorbents, correlations with surface area are not observed.

Although the influence of the pH on the distribution of LAS between water and a single sorbent is easy to establish, it is clear from these data that the solution pH alone does not dominate the partition energy. There is virtually no correlation of the order of adsorption energies with solution pH and some notable exceptions (EPA-12, for example).

Since the fraction of these sorbents in the clay size fraction correlates relatively well with the organic carbon content, an assessment of the relative impact of these factors is difficult.

A comparison between the isotherms of EPA-16 and EPA-25 is particularly interesting. The isotherms are virtually identical, but all factors (organic carbon, pH, and size fraction) would appear to favor adsorption to EPA-16.

Several researchers have found a correlation between sesquioxide content of the sorbent and adsorption of sulfonate and inorganic ions such as sulfate and phosphate (Inoue et al., 1986; Krishna Murti et al., 1966). Since no data on sesquioxides (i.e. extractable iron and aluminum) are available for the sorbents in this study, this relationship cannot be pursued.

A more rigorous comparison of these data is probably not warranted, although several possibilities exist, including

nonparametric and parametric methods. Among the parametric methods are comparison of  $D_c$  at similar  $C_i(s)$  or at similar  $C_s(w)$ , whichever is thought to be the major source of nonlinearity.

Effect of the ratio of solids to liquid in the slurry. An apparent dependence of the concentration distribution ratio on the ratio of solids to liquid in the slurry has been reported frequently for batch adsorption studies (Di Toro, 1985). Some of the factors which can contribute to this phenomenon are: (i) dependence of solution composition (concentration of NSM or species truly dissolved) on amount of solids in the solution; (ii) slow adsorption or desorption kinetics; (iii) particle aggregation; or (iv) variation of  $D_c$  with nonlinear isotherms.

In view of the fact that the isotherms are known to be nonlinear in this study, the isotherms themselves, at various ratios of solid to liquid in the slurry, are compared in Figure 6.3. Although many explanations could be invoked to explain the differences among the isotherms, we begin with one that is to a great extent independently verifiable: the concentration of  $Ca^{2+}$  in solution varies with the amount of solid, and the value of  $D_c$  varies with concentration of  $Ca^{2+}$ .

We have shown (Figure 6.2) that  $\Delta \log D_c / \Delta \log [Ca^{2+}] \approx 0.23$  for C-12 LAS and EPA-12 at concentrations of LAS on the sorbent less than 30 nmol/g. In other experiments we determined the concentration of  $Ca^{2+}$  as a function of amount of EPA-12 in 0.01 M  $NaN_3$ : we found  $d \log [Ca^{2+}] / d \log C_s(w) \approx 0.66$ , for EPA-12 in 0.01 M  $NaN_3$  over the range of  $C_s(w)$  from 0.005 to 0.01 g/mL. This variation was more or less consistent with ion exchange between

$\text{Na}^+$  from solution and  $\text{Ca}^{2+}$  from the surface, as determined from charge balance in solution. From these data we can calculate the variation in  $D_c$  with  $C_s(w)$  that is attributable to variation in  $\text{Ca}^{2+}$ :

$$\frac{d \log D_c}{d \log C_s(w)} = \frac{d \log D_c}{d \log [\text{Ca}^{2+}]} \frac{d \log [\text{Ca}^{2+}]}{d \log C_s(w)} = 0.15 \quad (6.6)$$

Finally we estimated the variation in apparent  $D_c$  among the different isotherms in Figure 6.3: we defined  $D_c^{\text{eff}}$  as the slope of the Freundlich isotherm evaluated at  $C(s) = 20 \text{ nmol / g}$ :

$$D_c^{\text{eff}} = \partial C(s) / \partial C(w) |_{C(s) = 20 \text{ nmol/g}} \quad (6.7)$$

The magnitude of the variation in  $D_c^{\text{eff}}$  with  $C_s(w)$  was determined experimentally by this method and found to be  $d \log D_c^{\text{eff}} / d \log C_s(w) = 0.15$ , for  $C(s) = 20 \text{ nmol/g}$ .

Thus this explanation based on effect of  $[\text{Ca}^{2+}]$  works very well for the low-concentration, near-linear segments of the isotherms. At higher concentrations the variation of  $D_c^{\text{eff}}$  with  $C_s(w)$  is stronger. To investigate these regions, more experiments would have to be performed with very close control of solution composition. Furthermore, a conceptual model for the nonlinearity of the isotherms would have to be invoked.

The point to be made is that many mechanisms can contribute to the apparent dependence of  $D_c$  on  $C_s(w)$ . To interpret this effect mechanistically requires the utmost attention to all experimental conditions.

## SUMMARY

The objective of this study was to elucidate the adsorption of LAS to natural sorbents in terms of the hydrophobic, specific chemical, and electrostatic interactions. Sorption of LAS was determined as a function homolog,  $\text{Ca}^{2+}$  concentration in solution, sorbent type, and concentration of solids. Evidence for both hydrophobic and specific or electrostatic interactions was seen. Isotherms were generally nonlinear, and the data were represented well by Freundlich or electrostatic isotherms; the data were not represented well by the simple (one-site) Langmuir isotherm. Comparisons of apparent distribution ratios for linear portions of the isotherms showed:  $d \log D_c / d \log n_{-\text{CH}_2-} \approx 0.4$ ;  $d \log D_c / d \log [\text{Ca}^{2+}] \approx 0.23$ . The value of  $D_c$  for different sorbents seemed to correlate most closely with the  $f_{oc}$  of the sorbents. The effect of increasing concentration of solids was increasing values of  $D_c$ ; this effect could be explained partially by the increase in  $\text{Ca}^{2+}$  concentration in solution.

## REFERENCES

- Bard, A.; Faulkner, L. Electrochemical Methods. 1980, Wiley: New York.
- Chao, T. T.; Harward, M. E.; Fang, S. C. Soil Sci. 1965, 99, 104-108.
- Chen, H.; Westall, J. C. Department of Chemistry, Oregon State University. Experimental data, 1988.
- Chiou, C. T.; Peters, L. J.; Freed, V. H. Science 1979, 206, 831-832.
- Delahay, P. Double Layer and Electrode Kinetics. 1965, Wiley Interscience: New York.
- Dick, S. G.; Fuerstenau, D. W.; Healy, T. W. J. Coll. Interface Sci. 1971, 37, 595-602.
- Di Toro, D. M. Chemosphere. 1985, 14, 1503-1538.
- Fahey, J. Experimental data of specific surface area of the sorbents, 1987.
- Giger, W.; Brunner, P. H.; Schaffner, C. Science 1984, 225, 623-625.
- Hand, V. C.; Williams, G. K. Environ. Sci. Technol. 1987, 21, 370-373.
- Hassett, J. J.; Means, J. C.; Banwart, W. L.; Wood, S. G. Sorption Properties of Sediments and Energy-Related Pollutants. U.S. Environmental Protection Agency, Report EPA-600/3-80-041, National Technical Information Service, Springfield, VA. 1980.
- Imboden, D. M.; Schwarzenbach, R. P. in Chemical Processes in Lakes, W. Stumm, Ed., Wiley, New York, 1985.
- Inoue, K.; Kaneko, K.; Yoshida, M. Soil Sci. Plant Nutr. 1978, 24, 91-102.
- Karickhoff, S. W., Brown, D. S.; Scott, T. A. Water Res. 1979, 13, 241-248.
- Krishna Murti, G. S. R.; Volk, V. V.; Jackson, M. L. Soil. Sci. Soc. Amer. Proc. 1966, 30, 685-688.
- Lewis, M. A.; Suprenant, D. Ecotoxicology and Environmental Safety 1983, 7, 313-322.
- Lyman, W. J. in Handbook of Chemical Property Estimation Methods. Lyman, W. J.; Reel, W. F.; Rosenblatt, D. H., Eds.; McGraw Hill: New York, 1982, 2-40.
- Matthijs, E.; De Henau, H. Tenside Detergents 1985, 22, 299-304.

- McEvoy, J.; Giger, W. Naturwissenschaften 1985, 72, 429-431.
- Nodvin, S. C.; Driscoll, C. T.; Likens, G. E. Soil Sci. 1986, 142, 69-75.
- Sakata, K.; Katayama, A. J. Coll. Interface Sci. 1987, 116, 177-181.
- Sakata, K.; Katayama, A. J. Coll. Interface Sci. 1988, 123, 129-135.
- Schwarzenbach, R. P.; Westall, J. Environ. Sci. Technol. 1981, 15, 1360-1367.
- Singh, B. R. Soil Sci. 1984, 138, 346-353.
- Siracusa, P. A.; Somasundaran, P. J. Coll. Interface Sci. 1986, 114, 184-193.
- Somasundaran, P.; Fuerstenau, D. W. J. Phys. Chem. 1966, 70, 90-96.
- Sposito, G. The Surface Chemistry of Soils. 1986. Oxford University Press: New York.
- Urano, K., Saito, M. Murato, C. Chemosphere 1984, 13, 293-300.
- Westall, J. Properties of Organic Compounds in Relation to Chemical Binding in Biofilm Processes in Ground Water Research, The Ecological Research Committee of the NFR, Stockholm. pp 65-90. 1984
- Westall, J.; Leuenberger, C.; Schwarzenbach, R. P. Environ. Sci. Technol. 1985, 19, 193-198.
- Westall, J. in Geochemical Processes at Mineral Surfaces, Davis, J.; Hayes, K., Eds.; Symposium Series No. 323, American Chemical Society, Washington, D.C. 1986.
- Westall, J. in Aquatic Surface Chemistry, W. Stumm, Ed., Wiley: New York, 1987.
- Westall, J.; Chen, H.; Zhang, W.; Brownawell, B. Report in preparation, 1989.

## CHAPTER 7

ADSORPTION OF LINEAR ALKYL BENZENESULFONATES (LAS)  
AT THE PARTICLE-WATER INTERFACE:  
A STUDY OF ISOTHERMS AND ELECTROPHORETIC MOBILITIES

## INTRODUCTION

It is well known that the electrophoretic mobility ( $\mu$ ) and the calculated zeta potential ( $\zeta$ ) of colloidal particles can be used to elucidate the mechanisms of adsorption. An excellent review correlating adsorption isotherms and  $\zeta$ -potentials has been given by Chander et al., (1983) for adsorption of alkylsulfonates and alkylbenzenesulfonates on alumina. Vilcu and Olteanu (1975) have correlated the adsorption of cationic surfactants on silica and alumina with the electrophoretic mobility of the particles. Sieglaff and Mazur (1960 and 1962) have studied the electrophoretic mobility of polystyrene latex in solutions of aliphatic acids ( $C_8$  to  $C_{16}$ ) to elucidate the effect of chain length on adsorption. Keesom and co-workers (1988) have used the zeta-potential data to interpret quantitatively the adsorption of cationic and anionic surfactants on a hydrophobic-surface polycarbonate membrane. The surfaces mentioned above are all pristine or "model" surfaces, which are relatively homogeneous with known properties. However, few studies have been made for adsorption of ionic surfactants on environmental sorbents (e.g. sediments, soils, aquifer materials, etc.), which are more heterogeneous and more difficult to characterize.

The study of adsorption of ionic surfactants on natural particles through zeta potential is difficult due to the heterogeneity of the surface. The goal of this study is to correlate isotherms and electrophoretic mobilities to elucidate the relative contributions of hydrophobic and electrostatic interactions to the adsorption of anionic surfactants on environmental sorbents.

The surfactants used in this study were three homologs of alkylbenzenesulfonates: 4-(1-methylnonyl)benzenesulfonate, 4-(1-methylundecyl)benzenesulfonate, and 4-(1-methyltridecyl)benzenesulfonate, abbreviated as C-10 LAS, C-12 LAS, and C-14 LAS. The adsorption isotherms were obtained as a function of chain length of the LAS, and the pH and the salt concentration of the aqueous solutions. The previous study, described in Chapter 6, addresses the adsorption of LAS over low-surface-coverage range to elucidate sorbate-sorbent interactions. The experiments in this study, however, were performed over a wider concentration range (the aqueous phase concentration from nM up to mM), at which sorbate-sorbate interactions are significant, too. Both the isotherm experiments and the electrophoretic mobility experiments were performed under the same experimental conditions.

## THEORY

Electrical double layer, electrophoretic mobility, and zeta potential. When a solid is immersed in an electrolyte solution, there will exist electric charges on surface of the solid and charges in the solution which is adjacent to it. There will be a tendency for these charges to distribute themselves in a nonuniform way at the interface. This uneven distribution of the charges will cause an electric potential difference across the interface. The arrangement of charged species and oriented dipoles (e.g. water molecules) existing at solid/liquid interface is called the electrical double layer, abbreviated as EDL (Hunter, 1986). In fact, the phenomenon of the electrical double layer exists at most interfaces.

The electrostatic interaction with the double layer is one of the major contributions to the energy of adsorption of an ionic surfactant on the charged surface of a particle. Thus it is necessary to review the theory of the EDL and to understand how the surface charge changes during the adsorption of charged species.

A schematic diagram for the structure of the electrical double layer at a solid-liquid interface is presented in Figure 7.1. In this example, the surface is negatively charged. The "double layer" can be described in terms of three planes or layers: the inner Helmholtz plane (IHP), the outer Helmholtz plane (OHP), and the diffuse layer. In the inner Helmholtz plane, the ions are generally adsorbed by specific interactions, e.g. interactions of the ions with inorganic and organic functional groups on the surface. In the outer Helmholtz plane, the solvated ions interact with the charged surface through

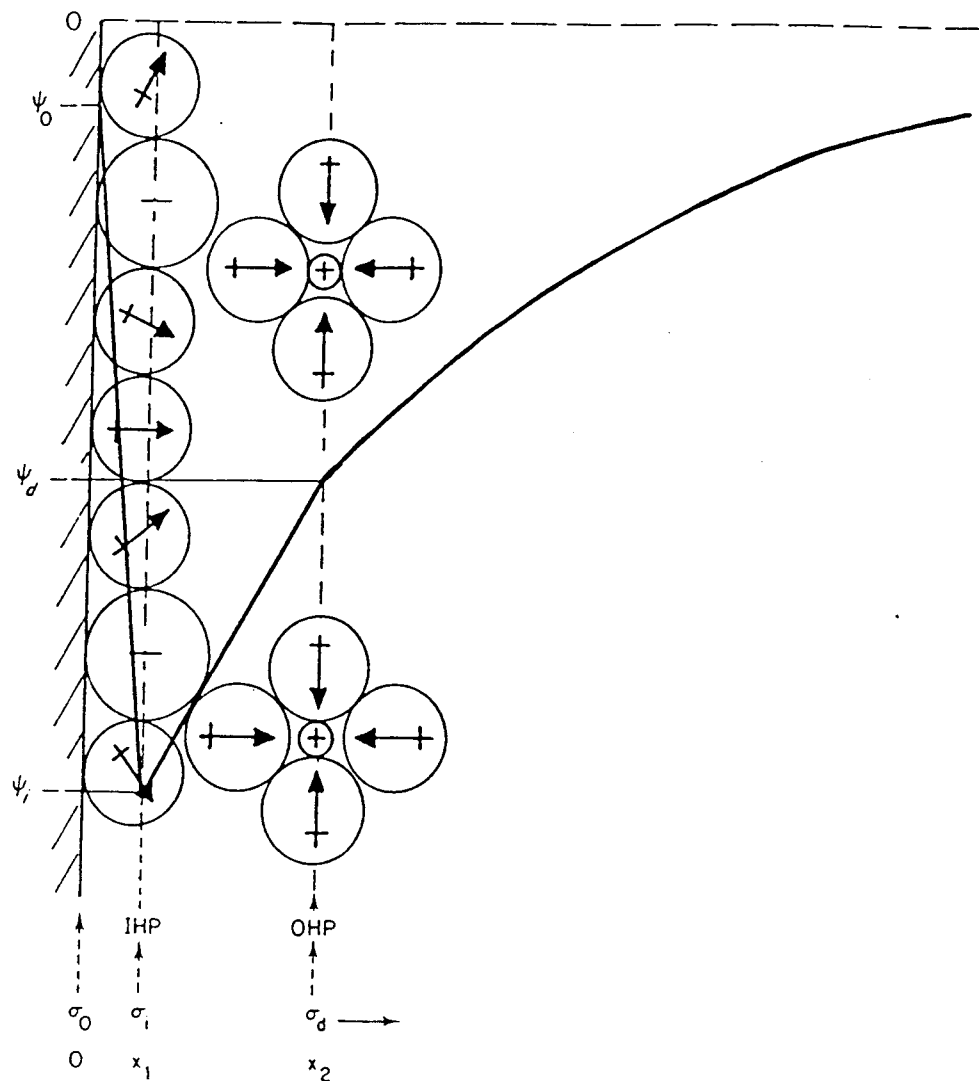


Figure 7.1. The electrical double layer at solid/liquid interface.  
Source: Reproduced (without permission) from Hunter, 1986.

long-range electrostatic forces. The diffuse layer is defined as the region from the OHP to the bulk of solution, at which the net charge equals zero (Bard and Faulkner, 1980).

When a charged colloidal particle moves in an electrolyte solution, the surrounding solution will move with the particle: the greater the distance from the particle, the smaller the velocity of the solution, until the velocity of the solution equals zero. Thus, in actuality, the velocity decreases continuously with distance from the particle. However, this velocity gradient is often treated discontinuously. It is presumed that there exists an imaginary surface, within which the solution moves with the velocity of the particle, and outside of which the solution is stationary. This surface is called the plane of shear and is commonly considered to be at the OHP (Hough and Rendall, 1983), although there is no real theoretical justification for this practice. The electric potential at the shear plane is named the zeta potential ( $\zeta$ ). The zeta potential can be used as a probe to evaluate the electrical environment at the surface of colloid particles during adsorption of ions, and thus to understand further the adsorption energy and adsorption processes (Hough and Rendall, 1983; Hunter, 1986; and Hiemenz, 1985).

The  $\zeta$ -potential is actually an operational parameter derived from the electrophoretic mobility of the particles, whereas the mobility is an experimental parameter which can be found from the equation (Hiemenz, 1986):

$$\mu = \frac{v}{E} \quad (7.1)$$

where  $\mu$  is the mobility, ( $\mu\text{m s}^{-1}$ ) / ( $\text{V cm}^{-1}$ ),  $v$  is the measured velocity of the charged particle ( $\mu\text{m s}^{-1}$ ) and  $E$  is the strength of applied electric field ( $\text{V cm}^{-1}$ ).

The equations used to convert the electrophoretic mobility into  $\zeta$ -potential depend on the size and shape of the colloidal particles. The critical factor in these equations is the value of  $\kappa a$ , where  $\kappa$  is the inverse of the thickness of the double layer (Bard and Faulkner, 1980, p. 506) and  $a$  is the radius of the particles.

For large (i.e.,  $\kappa a > 200$ ) spherical particles, the  $\zeta$ -potentials are calculated generally through the Smoluchowski equation (Hunter, 1986):

$$\zeta = \frac{\mu \eta}{\epsilon} \quad (7.2)$$

where  $\eta$  and  $\epsilon$  are the viscosity and dielectric constant of the medium, and  $\zeta$  is the zeta potential. For water at 25 °C,  $\eta/\epsilon$  equals to 12.83 with units of  $\text{mV } \mu\text{m}^{-1} \text{ s V cm}^{-1}$ .

For small (i.e.  $\kappa a < 0.1$ ) spherical particles, the Hückel equation can be used (Hiemenz, 1985):

$$\mu = \frac{\epsilon \zeta}{6 \pi \eta} \quad (7.3)$$

For spherical particles with intermediate sizes (i.e.  $0.1 < \kappa a < 200$ ), the Henry equation is generally used (Wiersema et al., 1966):

$$\mu = \frac{\epsilon \zeta [1 + f(\kappa a)]}{6 \pi \eta} \quad (7.4)$$

where  $f(\kappa a)$  is the correction factor.

For particles with nonspherical shapes, the conversion of measured mobility into  $\zeta$ -potential is more complicated. Particularly for natural particles with quite irregular sizes and shapes, it is practically impossible to justify a suitable equation for conversion of the measured  $\mu$  to the  $\zeta$ -potential. Thus the results from this study are generally presented as mobilities instead of  $\zeta$ -potentials, unless specifically the  $\zeta$ -potential is needed. When the  $\zeta$ -potential is needed, the Smoluchowski equation is used, based on the following considerations.

For a colloidal particle with radius of 1  $\mu\text{m}$  in an aqueous electrolyte (1:1) solution of 0.01 M at 25  $^{\circ}\text{C}$ , the value of  $\kappa a$  is calculated to be 329. We presume that the average size of the natural-sorbent particles is not smaller than 1  $\mu\text{m}$ , thus the Smoluchowski equation is more appropriate for calculation of the  $\zeta$ -potential.

The mechanisms of adsorption and S-type isotherm. For adsorption of ionic surfactants over a wide concentration range, S-type isotherms, as shown in Figure 7.2 (Chander et al., 1983), have been observed on a variety of sorbents such as alumina, kaolinite, and zeolite (Somasundaran and Fuerstenau, 1966; Dick et al., 1971; Scamehorn et al., 1982; Savitsky et al., 1981). As shown in the figure, the S-type isotherm consists of three distinct regions, as described below.

In Region I, the surfactant is adsorbed by ion exchange between the chloride ions and the sulfonate ions. Since adsorption occurs by ion exchange, the surface charge and the  $\zeta$ -potential do not vary

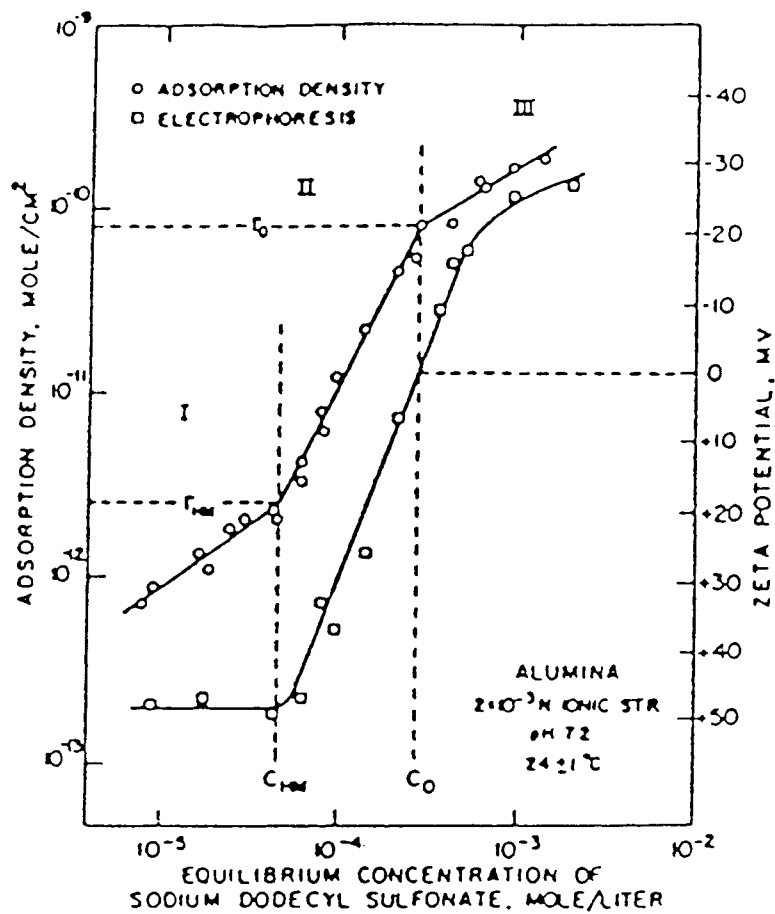


Figure 7.2. Adsorption density of dodecyl sulfonate ions on alumina and the zeta potential of alumina as a function of the concentration of sodium dodecyl sulfonate.  
Source: Reproduced (without permission) from Chander et al., 1983.

over this range. The constancy of charge and potential has been verified by study of electrophoretic mobility, also shown in Figure 7.2 (Somasundaran and Fuerstenau, 1966).

In Region II, adsorption occurs on the surface through hydrophobic chain-chain interactions between the adsorbed molecules. This process results in a sudden increase in the slope of the adsorption isotherm. In this region ion exchange is not the predominant mechanism; as a result the surface charge becomes more negative and causes a dramatic decrease in the zeta potentials, as seen in Figure 7.2. The aggregation of surfactants on the surface which occurs as a result of chain-chain interaction is called hemimicelle formation (Somasundaran and Fuerstenau, 1966). The concentration of surfactant at which the sudden increase in adsorption starts to occur is named as hemimicelle concentration, the HMC.

In Region III, owing to the electric repulsion between adsorbed surfactant ions, the slope of the adsorption isotherm decreases. The increase in adsorption terminates when the concentration of surfactant in solution reaches the critical micelle concentration, CMC, above which a plateau region occurs. At this point, the activity of the surfactant in solution no longer increases with increase in total surfactant concentration.

Scamehorn et al. (1982) introduced a patchwise adsorption model to interpret the S-type adsorption of alkylbenzenesulfonates on alumina and kaolinite. In this theory, shown in Figure 7.3 a-b, the adsorption in Region I is also linear. However, the molecules are considered to orient horizontally on the surface. The adsorption sites in Region II are heterogeneous. The surface is comprised of

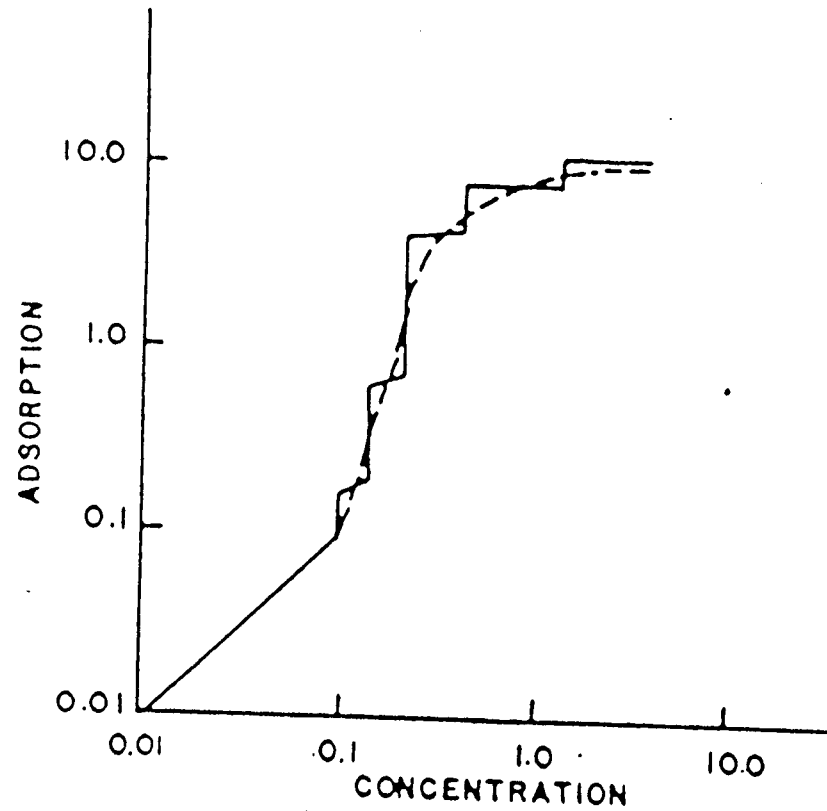


Figure 7.3a. Schematic description of S-type isotherm by patchwise adsorption model.  
Source: Reproduced (without permission) from Scamehorn et al., 1982.

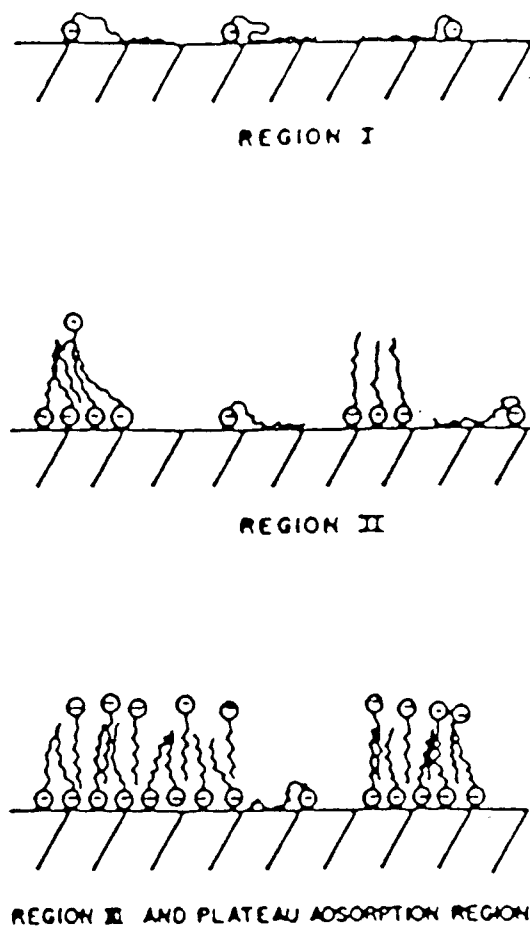


Figure 7.3b. Configuration of adsorbed anionic surfactant molecules.  
Source: Reproduced (without permission) from Scamehorn et al., 1982.

different patches. In each patch the energies of the adsorption sites are uniform, but in different patches the energies of the sites are different. The simultaneous bilayer adsorption occurs in Region II until the system reaches the CMC. The bilayer adsorption range is actually the region of hemimicelle formation, as described by Somasundaran and Fuerstenau (1988). The explanation for Region III (the plateau region) is the same as it is in the theory by Fuerstenau.

Both the theories interpreted well the S-type isotherm for adsorption of ionic surfactants on mineral surfaces from aqueous solutions. However, there is some limitation for applying these theories to interpret adsorption of surfactants on natural sorbents. Since the surface of the sorbent is extremely heterogeneous, even the adsorption in Region I is not linear (confirmed by experimental results from this study). The adsorption processes must be very complicated in this case.

Methods for calculation of aggregation number,  $n_H$ . Two approaches have been used in this study to estimate the aggregation number of hemimicelles, i.e. the number of surfactant molecules in a hemimicelle, symbolized as  $n_H$ . The first approach was proposed by Chander et al. (1983), and the second by Gu et al. (1987, 1988, and 1989). In general, the values of  $n_H$  from both methods are determined from the adsorption isotherms in the range of hemimicelle formation (Region II).

In the approach of Chander et al., (1983), the  $n_H$  is actually the slope of Freundlich isotherm in Region II, i.e. the slope of a plot of  $\log \Gamma$  vs.  $\log C_M(w)$ , in which  $\Gamma$  and  $C_M(w)$  are the surface

density ( $\text{mol m}^{-2}$ ) and aqueous concentration ( $\text{mol L}^{-1}$ ) of surfactants. A simple method can be used to derive this relationship, as described below.

The reaction of  $n_H$  monomers in solution to form a hemimicelle on the surface can be represented as:



where  $M(w)$  and  $H(s)$  represent the monomers of surfactant in solution and the hemimicelles of surfactant on the surface. At equilibrium of hemimicellization, the mass action equation can be expressed as:

$$C_H(s) = K C_M(w)^{n_H} \quad (7.6)$$

where  $C_H(s)$  is the surface concentration of hemimicelles,  $C_M(w)$  is the aqueous concentration of the monomers, and  $K$  is the equilibrium constant. The units used commonly for the surface and aqueous concentration are  $\text{mol kg}^{-1}$  and  $\text{mol L}^{-1}$ , respectively.

The surface concentration for hemimicelles cannot be determined directly from experiment, thus it is necessary to convert the  $C_H(s)$  to some experimentally measurable parameter such as the total surface concentration of surfactants  $C_T(s)$  in  $\text{mol kg}^{-1}$ . Chander et al. (1983) assumed that the surface concentration of monomers is very small and negligible in Region II since the hemimicelle formation is predominant. Based on this assumption, the relationship between the surface concentration of hemimicelles and the total surface concentration of surfactants can be expressed:

$$C_H(s) = \frac{C_T(s)}{n_H} \quad (7.7)$$

From Equation 7.6 and 7.7,

$$C_T(s) = n_H K C_M(w)^{n_H} \quad (7.8)$$

Equation 7.8 in logarithmic form is:

$$\log C_T(s) = \log(n_H) + \log K + n_H \log C_M(w) \quad (7.9)$$

A combination of the two constant terms in Equation 7.9 yields

$$\log C_T(s) = K' + n_H \log C_M(w) \quad (7.10)$$

Therefore, the aggregation number of surfactants in a hemimicelle can be obtained from the slope of a plot of log total surface concentration,  $\log C_T(s)$ , versus log concentration of monomers in solution,  $\log C_M(w)$ , as shown in Equation 7.10.

For many surface chemistry studies, it is more appropriate to express surface "concentrations" as an area-specific quantity,  $\Gamma$  ( $\text{mol m}^{-2}$ ), rather than a mass-specific quantity,  $C(s)$  ( $\text{mol kg}^{-1}$ ), as we have done. The difference between  $\Gamma$  and  $C(s)$  is only a constant factor:

$$\Gamma = \frac{C_T(s)}{s} \quad (7.11)$$

where the  $s$  is specific area of the sorbent in units of  $\text{m}^2 \text{kg}^{-1}$ .

In this case,

$$\log \Gamma = K'' + n_H \log C_M(w) \quad (7.12)$$

where  $K''$  includes the term of specific area  $s$  from conversion.

In this study, the surface of the natural sorbent is heterogeneous, therefore, it is better to use  $C_T(s)$ , which is closer to what we measured, to represent our data. The change from  $C_T(s)$  to  $\Gamma$  only changes the value of the intercept in Equations 7.10 and 7.12, but does not change the slope, which is  $n_H$ .

Chander et al. (1983) have used an alternative method to derive a similar relationship between the  $n_H$ ,  $\Gamma$ , and  $C_M(w)$ , as described in Equation 7.12. However, their derivation will not be discussed here.

The second approach was proposed by Gu and co-workers (Gao et al., 1987; Gu et al., 1988; and Gu and Huang, 1989). This approach is based on the assumptions that, at the onset of hemimicelle formation: (i) all surfactant molecules are adsorbed as monomers; (ii) each adsorbed monomer is the nucleus for a hemimicelle; (iii) no other nuclei will form. Thus the adsorption density at the onset of hemimicelle formation,  $\Gamma_{HM}$ , is equal to the number density of hemimicelles at any point in Region II (Figure 7.2). With  $\Gamma_{HM}$  known, the average aggregation number can be found from the ratio of the total surface density of surfactant,  $\Gamma$ , to the surface density of hemimicelles,  $\Gamma_{HM}$ . At  $\Gamma_{CMC}$ , the surface density at which the surfactants start to form micelles in the bulk solution and the

plateau region (Region III) of isotherm starts, the average aggregation number,  $n_H$ , can be obtained from the equation:

$$n_H = \Gamma_{CMC} / \Gamma_{HM} \quad (7.13)$$

where  $\Gamma_{CMC}$  and  $\Gamma_{HM}$  are in units of  $\text{mol m}^{-2}$ .

The aggregation number,  $n_H$ , can also be expressed by the surface concentration:

$$n_H = \frac{C_{CMC}(s)}{C_{HM}(s)} \quad (7.14)$$

where  $C_{CMC}(s)$  and  $C_{HM}(s)$  are the total surface concentrations at which micelles start to form in the bulk solution and hemimicelles start to form on the surface, respectively, in unit of  $\text{mol kg}^{-1}$ .

In this study, the aggregation numbers of hemimicelle,  $n_H$  are calculated by the methods of both Chander et al. and Gu et al. The comparison of the results of  $n_H$  from the two methods will be described in detail in the discussion section.

## EXPERIMENTS

Materials. The three homologs of linear alkylbenzenesulfonates, abbreviated as C-10 LAS, C-12 LAS, and C-14 LAS were obtained through the Soap and Detergent Association from Procter and Gamble Co. Each homolog was received in two forms: unlabeled and uniformly ring-labeled with  $^{14}\text{C}$ . The compounds were purified by preparative HPLC before use. The radiochemical purity was  $> 97\%$  for all three homologs. The standard solutions of unlabeled surfactants were prepared in  $0.01\text{ M NaN}_3$  and stored at  $4\text{ }^\circ\text{C}$ . The standard solutions of labeled surfactants were prepared in  $95\%$  of ethanol and stored at temperature less than  $0\text{ }^\circ\text{C}$ .

The sorbent used for this study was soil EPA-12 obtained through Professor John J. Hassett at the University of Illinois. The sorbent is  $2.33\%$  organic carbon,  $64.6\%$  silt, and  $35.4\%$  clay, as reported by Hassett (1980). The specific surface area is  $12\text{ m}^2/\text{g}$ , as reported by Fahey (1987).

Analytical-grade sodium azide (MC&B Co.) was used as a biostat and electrolyte. Analytical-grade NaOH and HCl (Fisher Scientific Co.) were used to adjust pH. Deionized water from a Millipore Milli-Q system was used for all solutions.

Adsorption isotherms. Six isotherms for adsorption of LAS on the sorbent were determined as a function of homologs, pH, and salt concentration. The experimental procedures consisted of four steps: (i) batch sorption equilibration; (ii) separation of the aqueous and sorbent phases; (iii) determination of pH of the aqueous phase; and (iv) determination of the LAS in the aqueous phase and sorbent. The

experimental procedures are described in detail in Chapter 4, and are only summarized briefly in this chapter.

First, the sorbent was washed with deionized water 8 times by a large-volume washing method to remove non-separable material (NSM) from the aqueous phase. The procedure and the purpose for this washing step are described in detail in Chapter 4 of the thesis. Then 0.5 g of the washed and dried sorbent was combined with 20 mL of 0.01 M  $\text{NaN}_3$ . To these slurries were added spikes of  $^{14}\text{C}$  labeled LAS, diluted with unlabeled LAS, to yield final concentrations of LAS between 1  $\mu\text{M}$  to 2 mM. These slurries were agitated at 500 RPM and 25 °C for 4 hours to allow equilibration, and then centrifuged for an hour at 10,000 RPM and 25 °C to separate the two phases. In separate experiments, it was established that 4 hours was sufficient for equilibration.

After centrifugation, 1 mL of aqueous sample was delivered into a vial containing 10 mL of Beckman HP/b scintillation fluid. The pH of the aqueous phase was then determined, and the extra aqueous solution was discarded. The method for control of pH in the experiments will be discussed in a separate section.

The amount of LAS adsorbed on the sorbent was determined by an extraction method (Sale et al., 1987). A 20-mL aliquot of the extraction solution (2:1 (v/v) methanol (HPLC grade from Fisher Scientific Co.) and 2N  $\text{NH}_4\text{OH}$ ) was added into the tubes. The samples were resuspended on a shaker at 350 RPM and 25 °C for 15 hours and then centrifuged at 10,000 RPM and 25 °C for 10 minutes. A 1.0-mL aliquot of the supernatant was subsequently transferred into a vial containing 10 mL of Beckman HP/b scintillation fluid.

A calibration for determination of LAS in the water and on the sorbent was performed for each experiment. The procedure is as follows: various amounts (20 to 100  $\mu\text{L}$ ) of  $^{14}\text{C}$  labeled LAS were spiked into the vials containing 10 mL of scintillation fluid and 1 mL of deionized water or 1 mL of the methanol- $\text{NH}_4\text{OH}$  extraction solvent. Each calibration solution was prepared in duplicate to evaluate the reproducibility. The radioactivities of these standard solutions were then determined and the calibration curves for each type of sample were obtained. It should be mentioned here that a real blank, which should be prepared under the same procedures as the sample preparation except the addition of LAS, was not done in this study. Therefore, the effect of extracted organics on the determination of LAS of the sorbent samples is unknown.

The  $^{14}\text{C}$  labeled LAS in the aqueous and the sorbent samples was also determined in duplicate. The total concentrations of LAS in the water and on the sorbent were then obtained from the calibration curves and the ratio between the labeled and unlabeled LAS which were added into the system. The material recovery for each sample was calculated as the ratio of the total activity found to the total activity added. In this study, the total activity found was calculated only from the aqueous and sorbent samples, because the amount of LAS adsorbed on the wall could not be determined by extraction method.

The precision and material recovery of the extraction method, and a comparison of the extraction method to other methods have been discussed in detail in Chapter 4 and will not be included in this chapter.

Electrophoretic mobilities. The procedure for determining the mobilities consists of three steps: (i) batch sorption equilibration; (ii) preparation of sample suspensions for mobility measurements; and (iii) determination of the mobility, as described in the flow chart in Figure 7.4. The control of the pH for these experiments will be discussed in a separate section.

The batch adsorption step for both the mobility experiments and the isotherm experiments were conducted under the same conditions, except no labeled LAS added into the system for the mobility study. The procedure for this step has been described in the previous section, and will not be included here.

Since the sorbent concentration used in these experiments was quite high, typically about  $0.025 \text{ g mL}^{-1}$ , the sample suspensions obtained directly from the batch adsorption step were too turbid to be used for determining the electrophoretic mobilities. Thus a suitable method was needed to dilute the suspensions. The dilution method should be able to reach these goals: (i) the diluted suspensions should be suitable for mobility determination; (ii) the aqueous and sorbent concentrations of LAS, as well as the solution compositions, (for example, pH and salt concentration), should remain the same after this dilution step; (iii) the diluted suspensions obtained from the method should be able to reflect the heterogeneity of the particle sizes of the original suspensions.

Two methods have been tested for the purpose: the incomplete centrifugation method and the complete centrifugation plus dilution method.

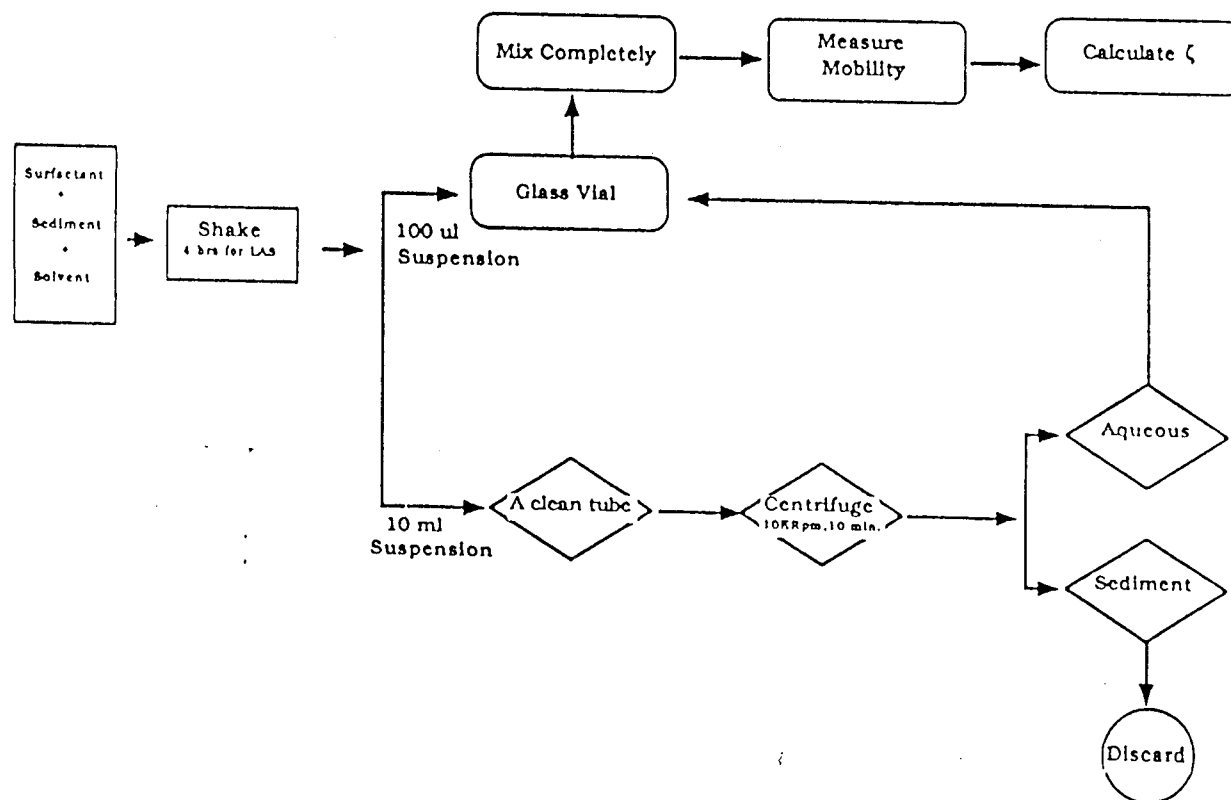


Figure 7.4. A flow chart of the procedures for determination of zeta potentials.

In the incomplete centrifugation method, the original suspensions were centrifuged for 2 minutes at 1,000 RPM; after this step, most of the sorbent particles were settled at the bottom of the tubes, and the suspensions obtained were suitable for the measurement. The disadvantage of this method is that the particles left in the suspensions are all fine particles which cannot represent the heterogeneity of the particle sizes of the original samples.

In the complete centrifugation plus dilution method, a portion of 100  $\mu$ L of the original suspension was first transferred into a glass vial, the suspension left was then centrifuged for 10 minutes at 10,000 RPM and 25  $^{\circ}$ C to separate the two phases completely. The supernatant was subsequently transferred into the vial containing a small portion of the original suspension for dilution. Then the samples were mixed well and ready for use. The suspension prepared in this way can reach the three goals mentioned above. Therefore, the complete centrifugation plus dilution method was used for the mobility experiments to dilute the suspensions.

The electrophoretic mobilities of the colloidal particles were determined by a Rank Brothers Mark II particle microelectrophoresis apparatus. A vertical flat cell with a pair of black platinum electrodes was used for this determination. The movement of the particles under the electric field were easily observed on the screen of a monitor (Philips Model LDH 2107/01). The mobilities of the particles were obtained from the measured velocity and applied electric field through Equation 7.1. The mobility recorded for each sample was an average of the mobilities of 20 different particles.

Before the equipment was used for the sample measurement, several calibrations were done to ensure that the equipment was operating properly and that the measurement was being carried out at the stationary level (described below) of the flat cell. The temperature of the water bath in which the electrophoretic mobility cell was immersed was controlled electronically at  $25 \pm 1$  °C. The voltmeter on the apparatus was calibrated by a Fluke 8020B Multimeter. No significant difference in the readings was found. The scale of the camera was calibrated by a "stage micrometer" from Graticules Ltd, and one unit on the scale of the camera was found to be 180 micrometers. The distance between the two electrodes,  $l$ , was determined by ruler as approximately 4.0 cm. Thus the strength of electric field  $E$  can be calculated from the interelectrode distance and the DC potential applied. The electric field was set in the range of 9.0 to 10.0 V  $\text{cm}^{-1}$ .

The most important calibration for this work is to determine the stationary level of the flat cell. As we know, when an electrophoretic cell is filled with an aqueous solution, the inner walls of the cell are usually negatively charged. Near the walls is a positive counter charge of mobile ions surrounded by solvent. Under the influence of the applied electric field, the positive charges move towards the negative electrode, causing the solvent near the walls to flow in that direction; at hydrodynamic steady state, an equal and opposite flow of solvent in the center of the cell results. The important point is that the velocity of the solvent is not uniform across a cross-section of the cell. Only at certain levels of the cell is the solvent is stationary. Only when the observed velocity

of a colloid particle is measured at these stationary levels, is the observed velocity equal to the electrophoretic velocity of the particle.

For a flat cell, the position of stationary level can be related to the parameters of the cell through Komagata equation (Komagata, 1933):

$$\frac{s}{d} = 0.500 - 0.0833 + \left[ \left[ \frac{32}{\pi^5} \right] \left[ \frac{d}{l} \right] \right]^{1/2} \quad (7.15)$$

where  $d$  and  $l$  are the width and height of the flat cell in the cross section,  $s$  is the distance of stationary level from the inner wall of the cell. In this study, the value of  $d$  is 0.882 mm, determined from this work, the value of  $l$  equals to 10 mm from manufacturer, thus  $s$  is calculated to be 0.160 mm.

In this study, the position of the stationary level calculated from Equation 7.15 was confirmed by determination of the mobility of a standard colloid suspension at that level. This standard suspension is the suspension of carboxylate modified hydrophilic latex (from Interfacial Dynamics Co. with the supplier part number of 10-36-23), prepared in 0.01 M NaCl and pH 7 aqueous solution. The size of the particles is  $0.865 \mu\text{m} \pm 5.3\%$ . The mobility of this standard colloid suspension was found to be  $-3.38 \pm 0.01 (\mu\text{m/s}) / (\text{V/cm})$ , measured from three individual experiments conducted on different date. This result is in good agreement with the mobility reported by manufacture, which is  $-3.42 (\mu\text{m/s}) / (\text{V/cm})$  at 25 °C. Therefore, the method used for calibration of the stationary level is reliable.

The reproducibility for determination of the mobilities was tested by measuring the mobilities of blank samples for each individual experiment performed on different dates. The blank suspensions were prepared in the same way as the sample suspensions except that no LAS added into the system. The mobility of the blank samples from the three experiments was  $-2.17 \pm 0.17$  ( $\mu\text{m/s}$ ) / ( $\text{V/cm}$ ) with the pH of  $7.30 \pm 0.02$ , indicating that the method used in this study was reproducible.

Figure 7.5 a,b illustrates the precision of measured electrophoretic mobilities and the zeta potentials calculated by Smoluchowski equation. The overall precision was generally better than 8% from total 38 samples of the three experiments. These results are in good agreement with those reported in the literature (Shaw, 1969).

Control of pH. Three isotherms for adsorption of C-12 LAS on the natural sorbent were determined at different pH values: 4.94, 7.31, and 8.89. The control of pH for these experiments was achieved according to the following procedure.

After 0.5 g of dried and washed sorbent and 20 mL of 0.01 M  $\text{NaN}_3$  were added into a 25 mL Corex glass centrifuge tube, a spike of 120  $\mu\text{L}$  of 1.0 N HCl or 30  $\mu\text{L}$  of 1N NaOH was added into the tube for the isotherms at pH 4.94 and pH 8.89, respectively. For the isotherm at pH 7.31, neither acid nor base was added. Then  $^{14}\text{C}$  labeled and unlabeled C-12 LAS were added into the slurry. After adsorption equilibration, centrifugation, and removal of 1 mL of aqueous sample for determination of LAS, as described in detail in the previous section, the pH values of the aqueous samples were determined by an

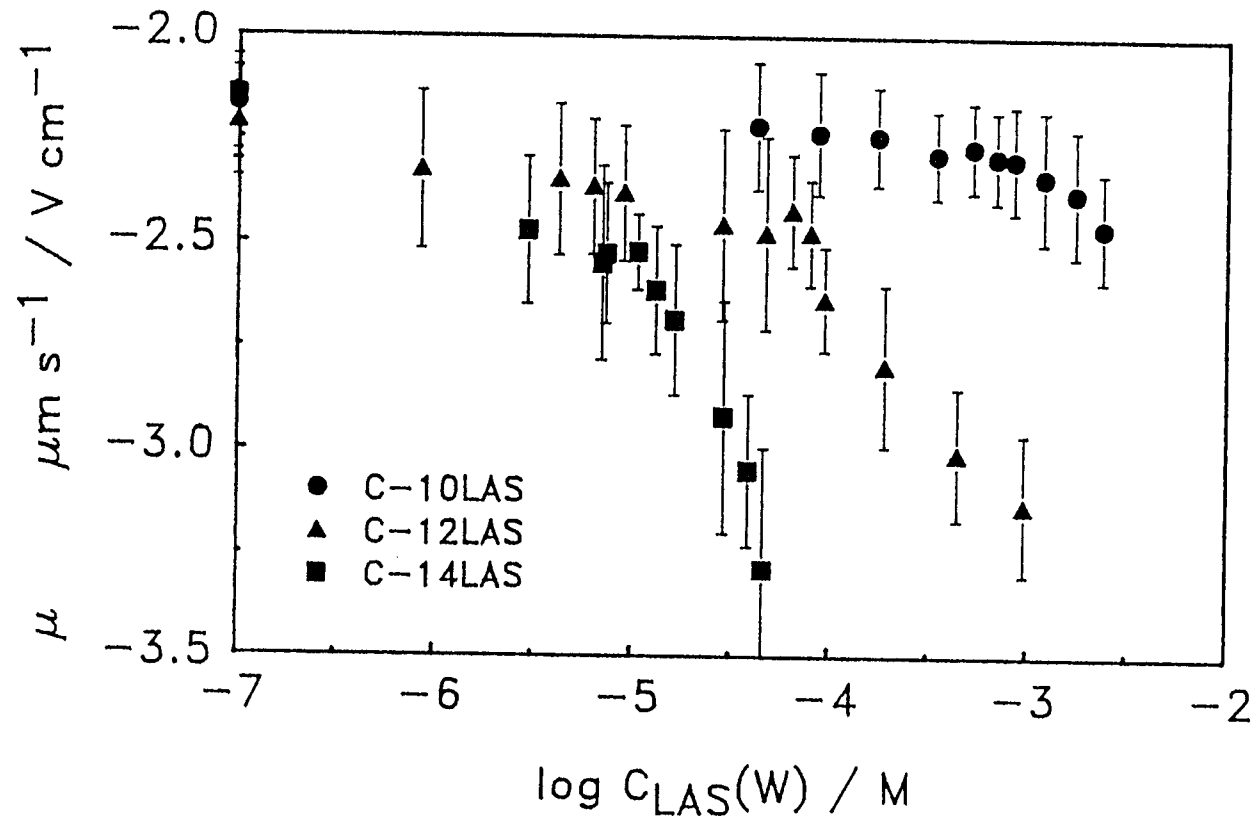


Figure 7.5a. Precision of  $\mu$  measurements.

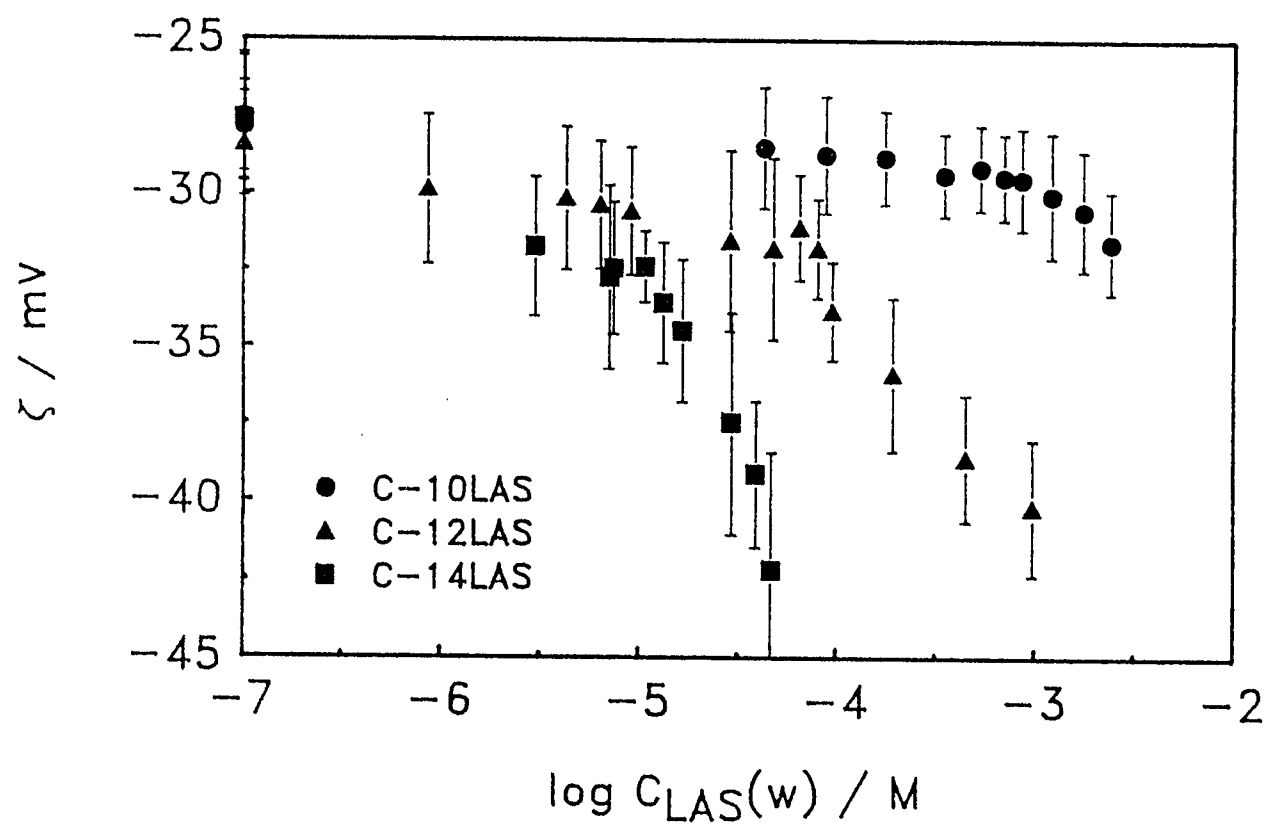


Figure 7.5b. Precision of  $\zeta$  measurements.

Orion Model 8102 Ross combination glass electrode and an Orion Model 701-A digital pH-mV meter. The temperature for pH measurement was controlled at  $25.0 \pm 0.1$  °C by a water circulation bath.

Before sample measurements, the pH electrode was calibrated against pH 4 (phthalate), pH 7 (phosphate), and pH 10 (borate and carbonate) buffers from Micro Essential Laboratory, Brooklyn N.Y. In all of the cases the cell potentials were recorded and pH calculated from the calibration equation

$$E = E^{\circ'} + k \log a_H^+ \quad (7.16)$$

where  $E$  is the measured cell potential,  $pH = -\log a_H^+$ , and  $E^{\circ'}$  and  $k$  are constants.

It should be mentioned here that the pH values of the samples for these experiments were determined after four hour batch equilibration and one hour centrifugation. The previous work from Chen (1988) has indicated that the pH of the aqueous phase for a given sample varied during the process of the four hour equilibration, and the upper limit of variation in pH was 0.51 pH unit. Thus, it might be a problem to represent the pH of the system by the pH data obtained from this work. The better way to obtain the pH is to determine the pH's of the sample before and after the sorption equilibration and report the range of the two pH data, as described by Chen (1988).

## RESULTS

Effect of chain length on adsorption of LAS. Figure 7.6 shows the adsorption isotherms of C-10, C-12, and C-14 LAS homologs on the sorbent in 0.01 M  $\text{NaN}_3$  at constant sorbent concentration ( $C_s(w) = 0.025 \text{ g/mL}$ ). The homologs with longer chain length adsorbed more strongly, indicating that the hydrophobic interaction plays an important role for the adsorption.

The isotherms were generally S-shape, consisting of three distinct regions. In Region I, the adsorption was not linear for all the three isotherms, and the Freundlich isotherm slopes in the log-log scale, listed in Table 7.1, were 0.881, 0.826, and 0.812 for C-10, C-12, and C-14 LAS, respectively. In Region II, hemimicelle formation was observable for adsorption of C-12 and C-14 LAS but rather indistinct for C-10 LAS. In Region III, a plateau in the adsorption isotherms was observed for C-10 and C-12 LAS but rather indistinct obviously for C-14 LAS. We presume that a plateau range for C-14 LAS was not observed because the concentration range selected was not high enough.

Effect of chain length on mobility of sorbent particles. Figure 7.7 a,b shows the effect of chain length of the LAS homologs on the electrophoretic mobilities ( $\mu$ ) of the colloidal particles. The experiments were conducted under the same conditions as the corresponding isotherms. All the mobilities obtained in this work were negative values, indicating that the surface was negatively charged.

The mobilities of the natural sorbent particles as a function of

Table 7.1. The effect of chain length, pH, and ionic strength on the parameters  $K_p$  and  $n$  of the Freundlich isotherm in Region I and the aggregation numbers  $n_H$  in Region II for adsorption of LAS on soil EPA-12.

Surfactant	$C_s(w)$	I.S.	pH	$K_p^a$	$n^a$	$n_H^b$	$n_H^c$
C-10LAS <sup>d</sup>	0.0248	0.01	$7.56 \pm 0.07$	26	0.88		
C-12LAS <sup>d</sup>	0.0245	0.01	$7.31 \pm 0.03$	77	0.83	4	18
C-14LAS <sup>d</sup>	0.0245	0.01	$7.36 \pm 0.03$	307	0.81	4	42
C-12LAS <sup>e</sup>	0.0245	0.01	$4.94 \pm 0.04$	232	0.84	4	28
C-12LAS <sup>e</sup>	0.0245	0.01	$8.89 \pm 0.14$	82	0.87	2	27
C-12LAS <sup>f</sup>	0.0245	0.001	$7.20 \pm 0.15$	50	0.82	2	25

<sup>a</sup> Freundlich equation:  $C_i(s) = K_p C_i(w)^n$ ; concentration  $C_i(w)$  in mol/L, concentration  $C_i(s)$  in mol/kg.

<sup>b</sup>  $n_H$  is aggregation number of surfactant ions in a hemimicelle, calculated by Chander's method (Chander et al., 1983).

<sup>c</sup>  $n_H$  is aggregation number of surfactant ions in a hemimicelle, calculated by Gu's method (Gu et al., 1987).

<sup>d</sup> Data from Figure 7.6.

<sup>e</sup> Data from Figure 7.9.

<sup>f</sup> Data from Figure 7.10.

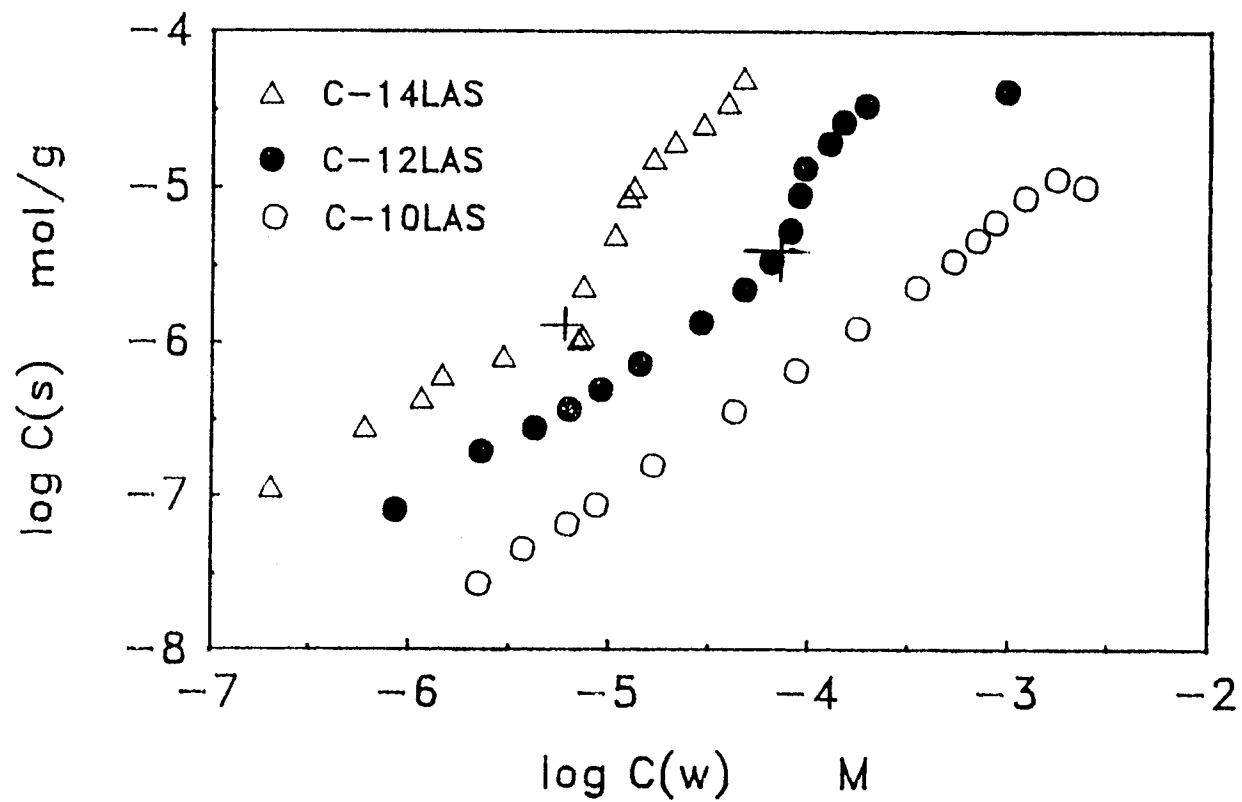


Figure 7.6. Effect of chain length on adsorption of LAS on EPA-12. The marks indicate divisions between Regions I, II, III, which were used to calculate Freundlich and hemimicelle parameters in Table 7.1.

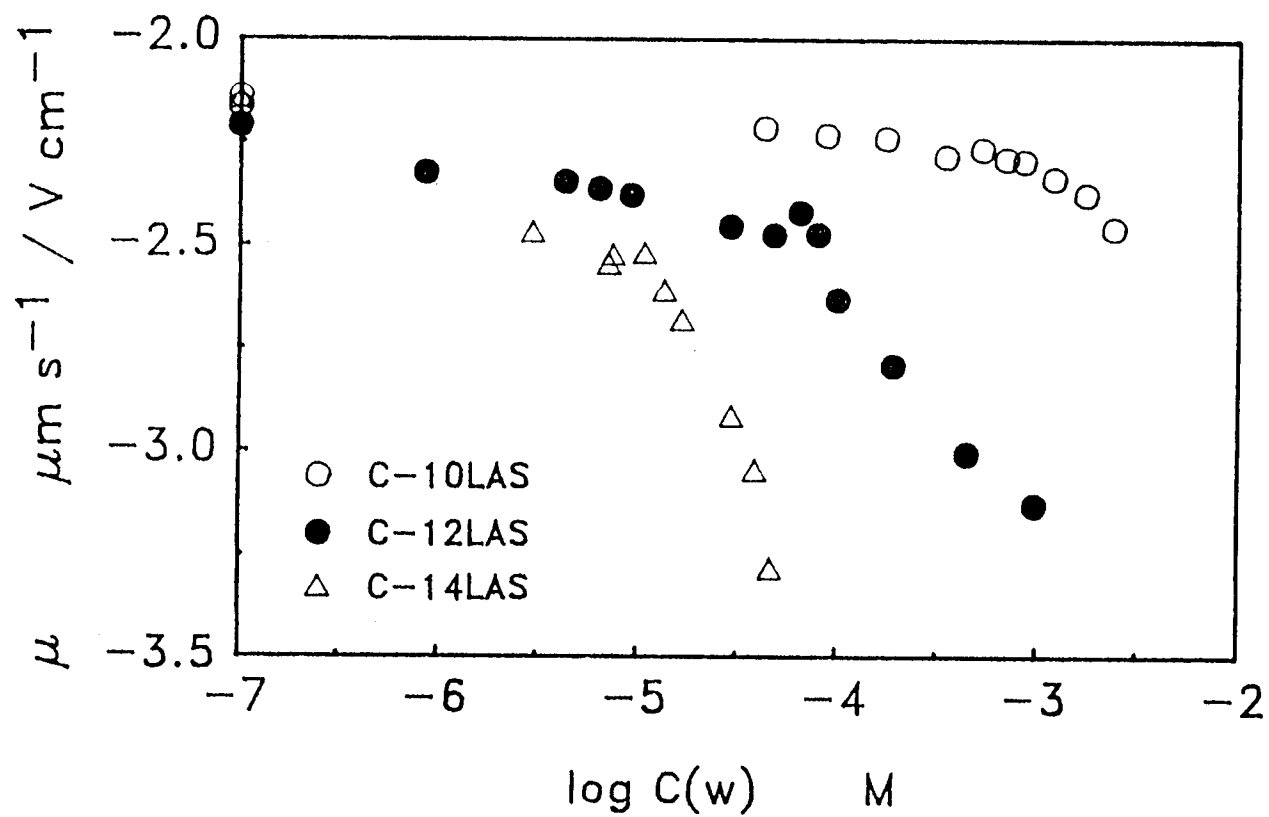


Figure 7.7a. Electrophoretic mobility of the sorbent EPA-12 particles as a function of aqueous concentration of C-10, C-12, and C-14 LAS.

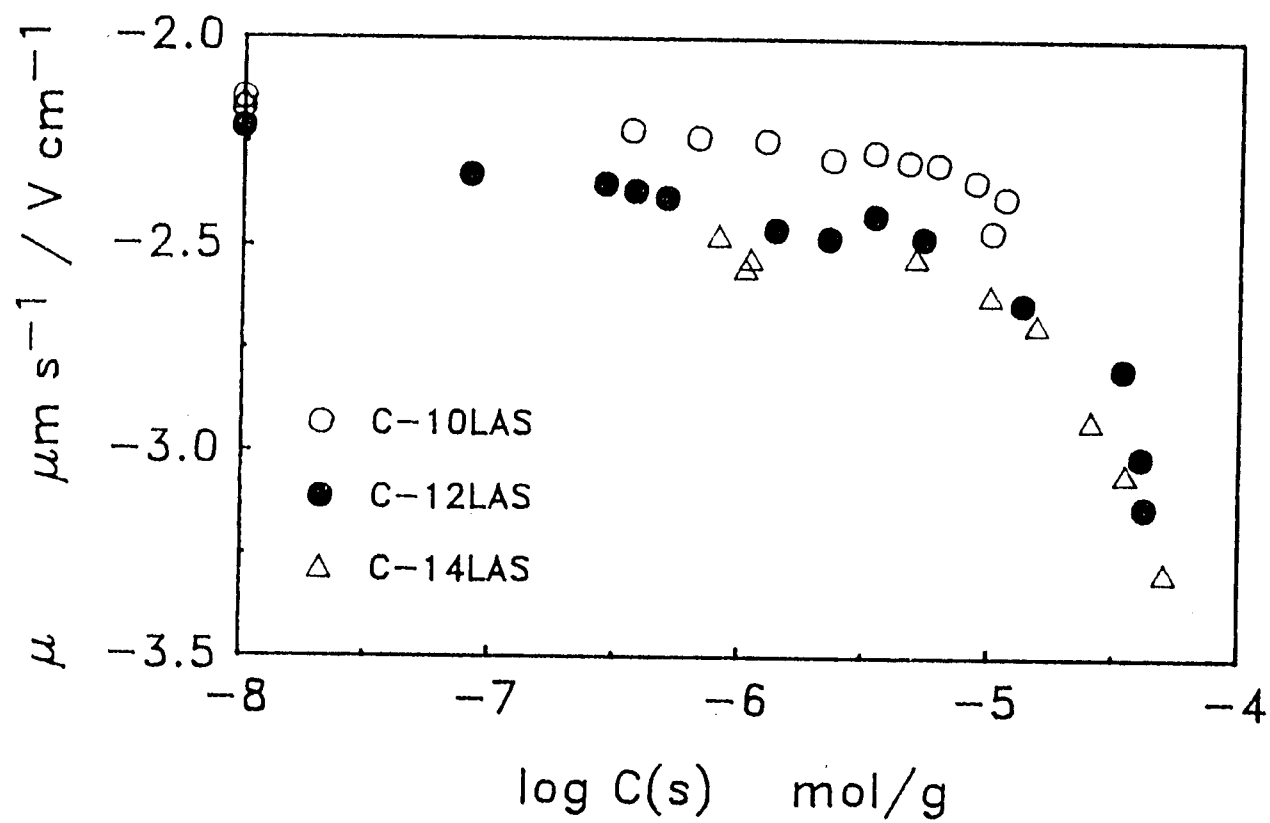


Figure 7.7b. Electrophoretic mobility of the sorbent EPA-12 particles as a function of surface concentration of C-10, C-12, and C-14 LAS.

the concentrations of LAS in the aqueous phase and on the sorbent, are plotted in Figure 7.7 a,b. For both the C-12 LAS and C-14 LAS the plots of  $\mu$  vs. either  $C(w)$  or  $C(s)$  exhibit the same two regions, Region I and Region II, as seen for the isotherms in Figure 7.6. For the C-10 LAS the two regions are not distinguishable; the isotherm reflects this behavior as well. In Region I, the mobilities become slightly more negative with increasing concentrations of all three homologs. The interpretation of this result will be included in the discussion section. In Region II, the mobilities become much more negative with hemimicelle formation.

Figure 7.7 b shows that the mobilities at the same surface concentration are very close for C-12 and C-14 LAS. This result indicates that, as the surface is covered by the same amount of ions of the surfactant homologs, the influence of these ions on the electrical circumstance of the surface is the same despite the differences in chain lengths. The electrophoretic mobility of C-10 LAS is higher than that of C-12 and C-14 LAS at the same surface concentration. This difference may be due to some systematic error, such as an error in determination of the stationary level for the mobility measurements. However, such a systematic error does not affect conclusions about the change in mobility with surfactant concentrations, since concentrations were varied without readjustment of the instrument.

Effect of pH on adsorption of C-12 LAS. In order to study the effect of pH on adsorption isotherms of ionic surfactants, it is very important to maintain the pH constant over the entire range of isotherms. However, this experimental condition is often difficult

to achieve. The first step in this study was to examine the variation of pH over the entire range of the isotherms for adsorption of C-12 LAS on the natural sorbent. The results in Figure 7.8 a-c show that the sorption of LAS had little effect on the pH of the aqueous phases, and the pH values were approximately invariant over the entire range of the isotherms at pH 4.94 and 7.31. For the isotherm at 8.89, there were not enough pH data taken to determine an effect.

Figure 7.9 shows the three isotherms determined at different pH values. The isotherms were all S-type. The decrease in pH of the aqueous phase increased significantly the adsorption of C-12 LAS over the entire concentration range of the investigation. In Region I, the adsorption of C-12 LAS was nonlinear. The  $n$  values from the Freundlich equation, listed in Table 7.1, were 0.841, 0.826, and 0.869 for the isotherms at pH of 4.94, 7.31 and 8.89, respectively. Formation of hemimicelles (Region II) was observed in the isotherms determined at all three pH values. The presence of Region III was not obvious for the isotherms at pH 4.94 and 8.89, probably due to the lack of data.

Effect of salt concentration on adsorption of C-12 LAS. Figure 7.10 gives the adsorption isotherms of C-12 LAS determined under two different  $\text{NaN}_3$  concentrations, in order to elucidate the effect of the salt concentration on the adsorption. Both isotherms were S-type. The nonlinear adsorption was observed in Region I with the  $n$  values of Freundlich isotherms about 0.8, as listed in Table 7.1. The adsorption of C-12 LAS in Region I and Region II increased significantly with salt concentration. The plateau range (the Region III) was observed for both isotherms.

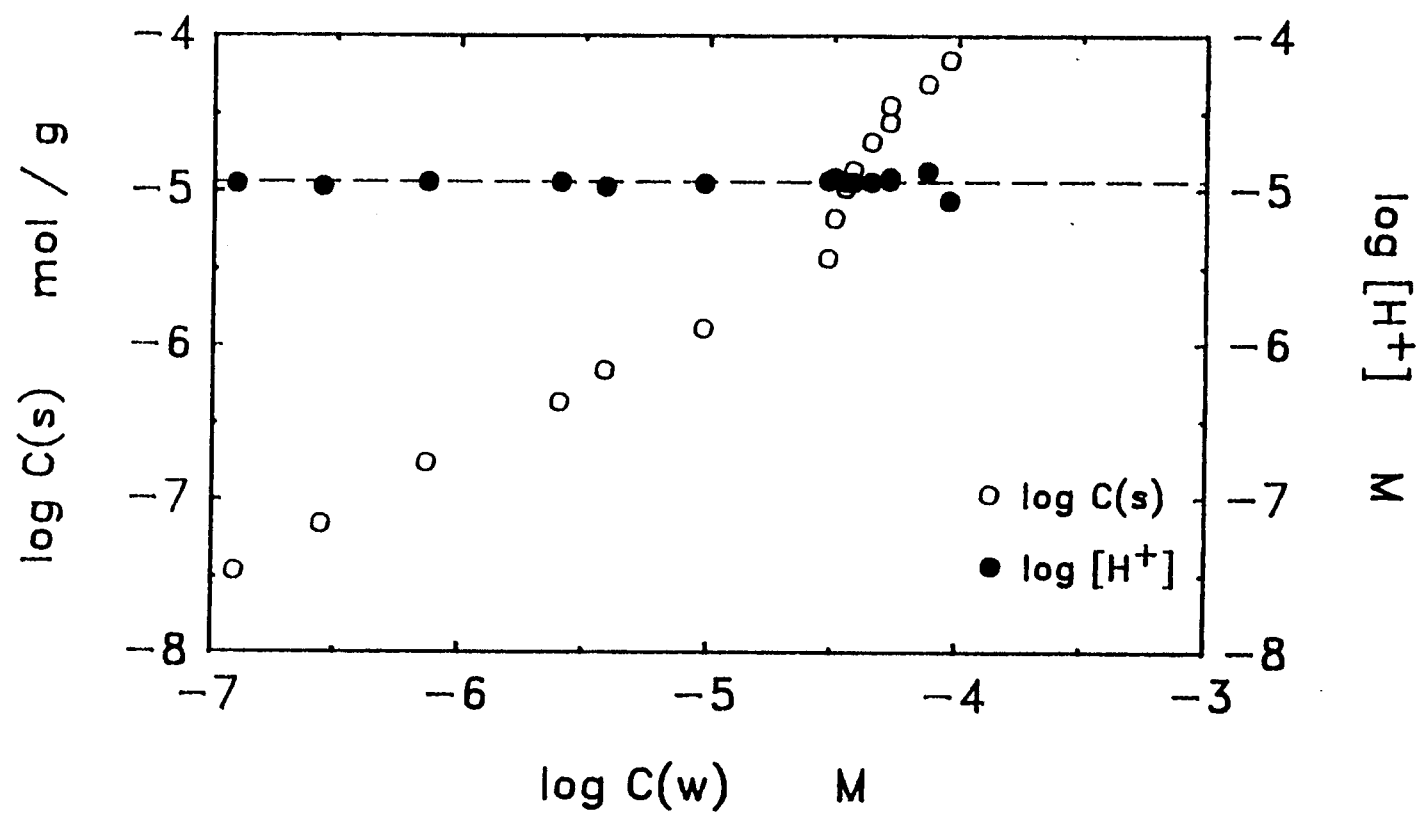


Figure 7.8a. Control of pH for adsorption isotherm of C-12 LAS on soil EPA-12 at pH  $4.94 \pm 0.04$ .

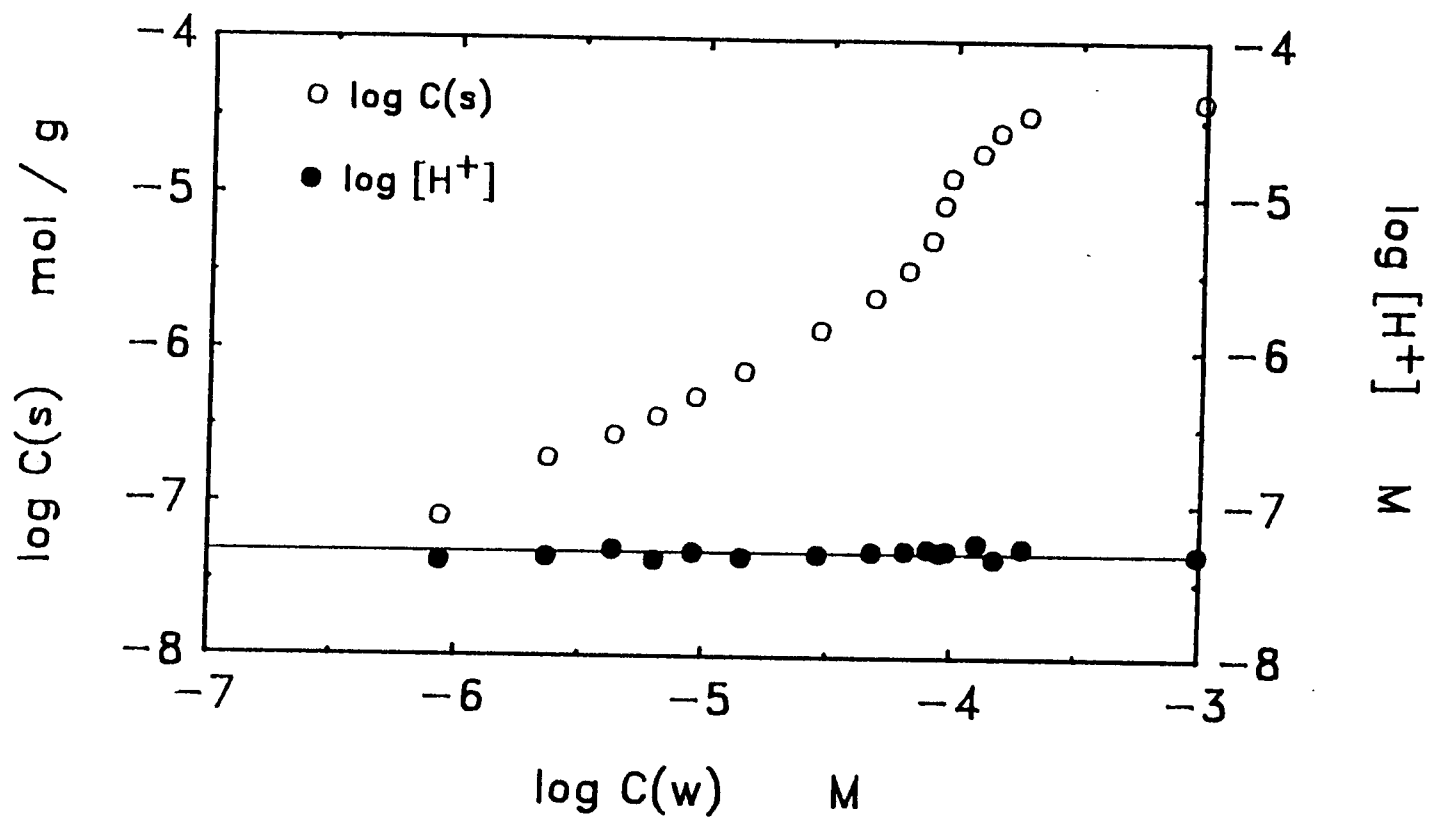


Figure 7.8b. Control of pH for adsorption isotherm of C-12 LAS on soil EPA-12 at pH of  $7.31 \pm 0.03$ .

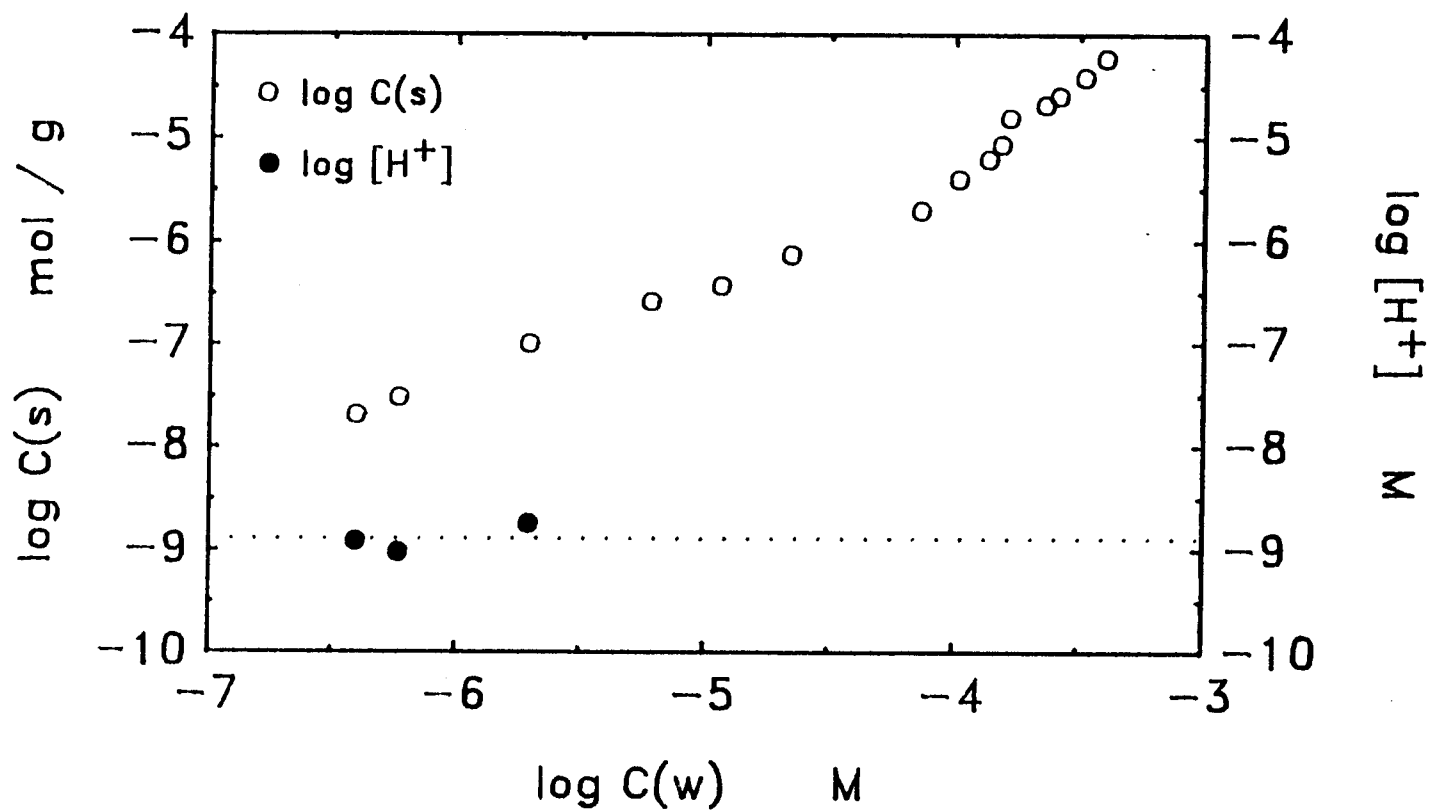


Figure 7.8c. Control of pH for adsorption isotherm of C-12 LAS on soil EPA-12 at pH of  $8.89 \pm 0.14$ .

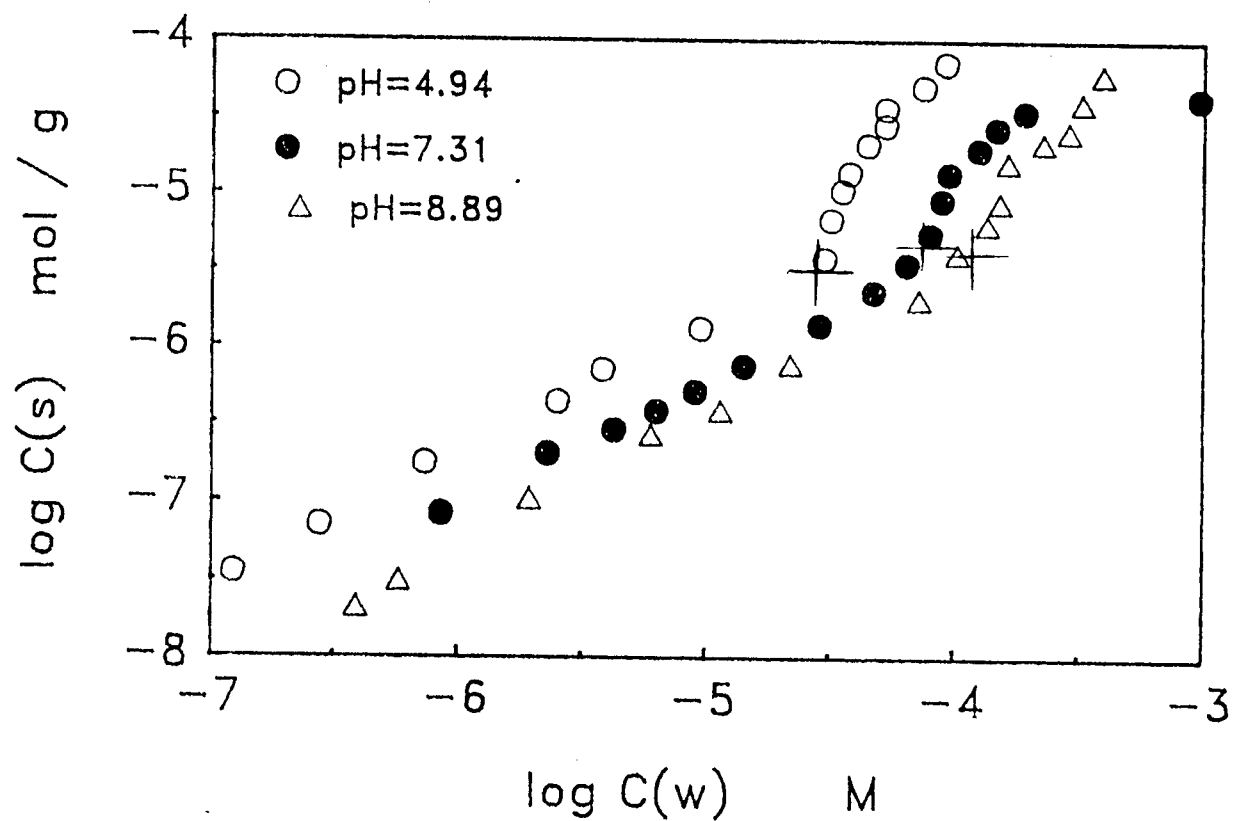


Figure 7.9. Adsorption isotherms of C-12 LAS on soil EPA-12 at  $C_s(w) = 0.0245 \text{ g/mL}$  in  $0.01 \text{ M NaNO}_3$  at different pH: 4.94, 7.31, and 8.89. Marks indicate divisions between Regions I, II, III, which were used to calculate Freundlich and hemimicelle parameters in Table 7.1.

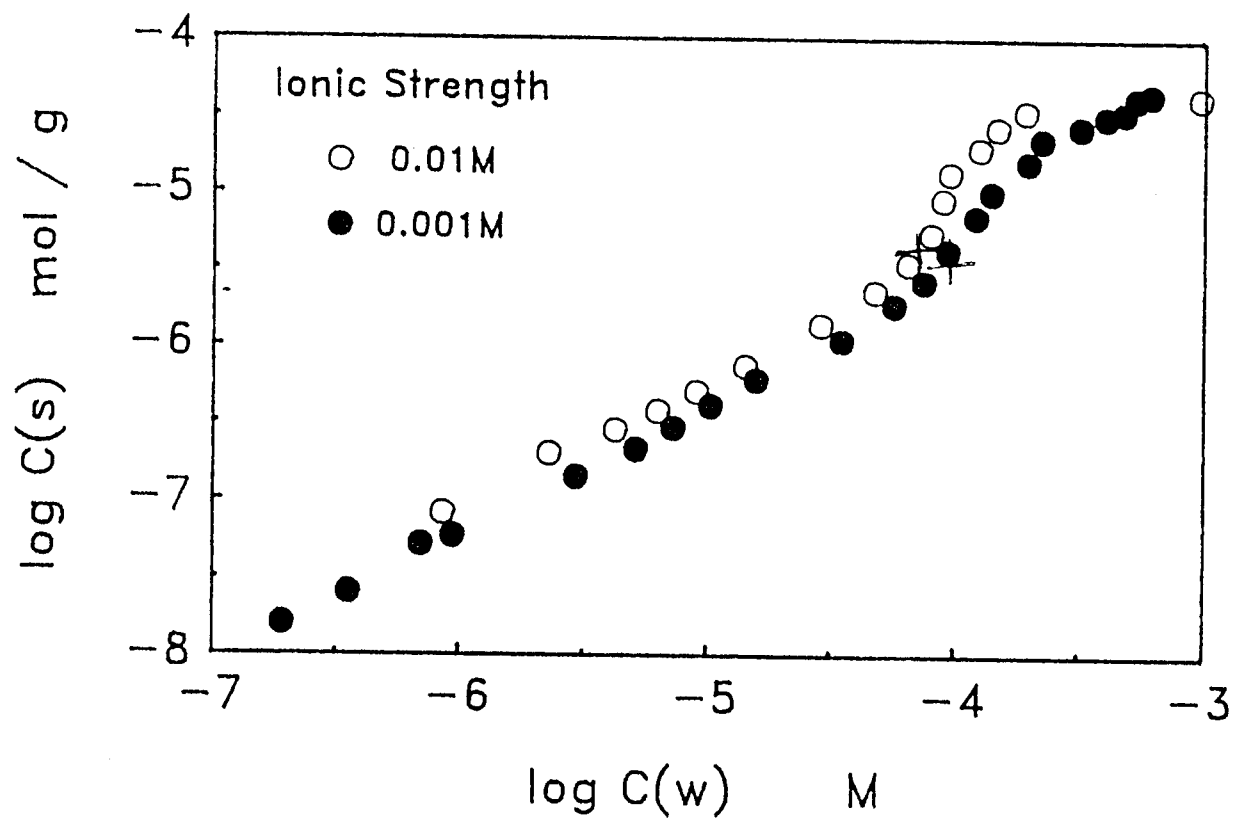


Figure 7.10. Adsorption isotherms of C-12 LAS on soil EPA-12 at  $C_s(w) = 0.0245$  g/mL in 0.01 M  $\text{NaNO}_3$  and 0.001 M  $\text{NaNO}_3$ . Marks indicate divisions between Regions I, II, III, which were used to calculate Freundlich and hemimicelle parameters in Table 7.1.

## DISCUSSION

S-type isotherms on pristine and environmental sorbents

The isotherms for adsorption of LAS on the environmental sorbents used in this study are typically S-type. This type of isotherm has been found for adsorption of ionic surfactants on a variety of sorbents such as alumina, silica, kaolinite, zeolite, and latex (Fuerstenau and Wakamatsu, 1975; Gu and Huang, 1989; Scamehorn et al., 1983; Savitsky et al., 1981; and Connor and Ottewill, 1971). While sorption of surfactants can be described by relatively simple mechanisms on these pristine sorbents, sorption of surfactants onto natural sorbents is much more complicated. The adsorption of LAS and branched chain alkylbenzenesulfonates on environmental sorbents (e.g., sediments and soils) has been studied by Urano et al., (1984) and Hand and Williams, (1987). However, extensive studies of mechanisms of adsorption of ionic surfactants on these heterogeneous sorbents have not been reported.

Several questions have motivated this study: what causes the negatively charged LAS to be adsorbed onto the negatively charged surface? why is the isotherm nonlinear on the natural material, although the surface coverage is quite low? and what factors affect the formation of hemimicelles of LAS on the environmental sorbent? We answer these questions in terms of the sorbate-sorbent and sorbate-sorbate interactions described in the following sections.

### Adsorption of LAS: sorbate-sorbent interactions

Negatively charged LAS being adsorbed on negatively charged surface. The net surface charge of the sorbent was found to be negative in the entire range of the isotherms from the result of electrophoretic mobility study (Figure 7.7 a, b). According to Coulomb's law, there exists electric repulsion between the sorbate and sorbent particles. Then what is the driving force which causes this adsorption. We interpret the result from two types of interactions: (i) specific interaction between LAS and the sorbent mediated by some divalent cations (e.g.,  $\text{Ca}^{2+}$ ) in the system; (ii) hydrophobic interaction, or the tendency for the LAS ions to remove themselves from the aqueous phase onto the sorbent surface.

An increase in concentration of  $\text{Ca}^{2+}$  in the system will increase the adsorption of anionic surfactants. This effect has been observed by van Senden (1968) and from the previous work described in detail in Chapter 6. This type of adsorption may be due to specific interaction of  $\text{Ca}^{2+}$  ion on the negatively charged surface yielding a positively charged sorption site which is more favorable to adsorption of LAS.

The increase in adsorption with increasing chain length of LAS, shown in Figure 7.6, confirmed the presence of a hydrophobic interaction. The hydrophobic interaction is favorable for adsorption of LAS.

It has also been observed through zeta potential studies that the negatively charged dodecylsulfonates were absorbed significantly on negatively charged polycarbonate membranes (Keesom et al., 1988).

The authors interpreted that the adsorption energy from hydrophobic interaction was great enough to overcome the coulombic repulsion energy between the surface carboxylate group and the surfactant head group. Thus, if the sorbent is hydrophobic or containing some hydrophobic sorption sites, the hydrophobic interaction plays an important role for adsorption of ionic surfactants. This interaction is strong enough to overcome the coulombic repulsion between sorbate and sorbent.

Quantification of electrostatic energy in Region I. The electrostatic interaction in the adsorption of ionic surfactants can be expressed through the following equation:

$$C_R(w) \exp \left[ \frac{-z_R F \Psi}{RT} \right] K_{\text{eff}} = C_R(s) \quad (7.17)$$

where  $C_R(s)$  and  $C_R(w)$  are the concentrations of LAS on the sorbent and in the aqueous phase, in the units of  $\text{mol kg}^{-1}$  and  $\text{mol L}^{-1}$ , respectively,  $\Psi$  is the surface potential in units of V,  $z_R$  is the charge of surfactant ion,  $T$  is temperature in K,  $F$  is the Faraday constant in  $\text{C mol}^{-1}$ ,  $K_{\text{eff}}$  adsorption constant in  $\text{L kg}^{-1}$ , and  $R$  is the gas constant in  $\text{J mol}^{-1} \text{K}^{-1}$ .

If we assume that the changes in the zeta potential,  $\zeta$ , can be used to represent the changes in the surface potential,  $\Psi$ , then the Boltzmann factor for electrostatic energy can be described by the term  $\Delta \log K$ , where:

$$\Delta \log K = \frac{-z_R F \Delta \zeta}{RT \ln 10} \quad (7.18)$$

The changes in the apparent distribution ratio  $D_C$ , determined from isotherm experiments, can be used to represent the changes in the total energy for adsorption of LAS on the sorbent. As we already mentioned in the previous chapter, the  $D_C$  can be expressed as:

$$D_C = C_R(s) / C_R(w) \quad (7.19)$$

For simplicity, the symbols  $C(s)$  and  $C(w)$  will be used instead of the  $C_R(s)$  and  $C_R(w)$ .

The objective of this work is to assess the contribution of electrostatic energy to the total energy for adsorption of LAS on the natural sorbent, through comparison of the  $\Delta \log K$  obtained from the  $\zeta$ -potential experiments and the  $\Delta \log D_C$  obtained from the isotherm experiments.

In this study, the changes in the  $\zeta$ -potential,  $\Delta \zeta$ , are calculated by subtracting the  $\zeta$ -potential of the first data point (at the lowest  $C(w)$  or  $C(s)$  of Figure 7.6 a,b) from the  $\zeta$ -potentials of the other data points. Then values of  $\Delta \log K$  are calculated from  $\Delta \zeta$  with Equation 7.18. The  $\Delta \log D_C$  are also calculated by subtracting the  $\log D_C$  of the first data point from the  $\log D_C$  of the other data points.

A comparison of  $\Delta \log K$  and  $\Delta \log D_C$  as a function of  $\log C(s)$  is shown in Figure 7.11 a,b for adsorption of C-10 and C-12 LAS on the

sorbent. The data were taken from the low-surface-coverage range (Region I), to elucidate the interactions between surfactants and the surface.

Figure 7.11 a, b shows that the value of  $\Delta \log D_c$  decreases more rapidly than the value of  $\Delta \log K$ , as the surface concentration of LAS increases. We interpret this result from several points of view.

First of all, the small change in the  $\Delta \log K$  with respect to the large change in the  $\Delta \log D_c$  indicates that the energy from the electrostatic interaction contributes only a small fraction to the total energy for adsorption of LAS on the natural sorbent. The values of the slopes of the plots in Figure 7.11 a,b, (i.e.,  $d \Delta \log K / d \log C(s)$  and the  $d \Delta \log D_c / d \log C(s)$ ), are listed in Table 7.2. From these slopes, the ratios of  $d \Delta \log K / d \log C(s)$  to  $d \Delta \log D_c / d \log C(s)$  are calculated to be 16.5% and 17.2% for C-10 LAS and C-12 LAS, respectively; in other words, the change in  $\zeta$ -potential accounts for about 15% of the change in  $\log D_c$ .

This explanation is based on the assumption that the change in the  $\zeta$ -potential,  $\Delta \zeta$ , can be used to represent the change in the surface potential,  $\Delta \Psi$ . However, the validity of this assumption warrants examination.

The plane of shear, at which the potential is named the zeta potential, may be far away from the surface. Therefore, it may be a problem to represent the change in surface potential  $\Delta \Psi$  by the change in zeta potential  $\Delta \zeta$ . It has been observed from the experiments that the change in the value of  $\Delta \zeta$  is very small; perhaps the  $\Delta \Psi$  is greater.

Table 7.2. Parameters of Figure 7.12 a, b.

Surfactant	Parameters <sup>a</sup>			
	$\frac{d \Delta \log D_c}{d \log C(s)}$	$\frac{d \Delta \log K}{d \log C(s)}$	$\frac{\Delta \zeta^{\text{exp.}}}{d \log C(s)}$	$\frac{\Delta \zeta^{\text{calc.}}}{d \log C(s)}$
	(mL g <sup>-1</sup> ) / (mol g <sup>-1</sup> )		mV / (mol g <sup>-1</sup> )	
C-10 LAS	- 0.109	- 0.018	- 1.0	- 6.4
C-12 LAS	- 0.157	- 0.027	- 1.6	- 9.3

<sup>a</sup> the vales of  $\Delta \zeta^{\text{calc.}} / d \log C(s)$  are calculated, based on the assumption that the adsorption of LAS is due to only electrostatic interaction, therefore the value of  $d \Delta \log D_c / d \log C(s)$  equals the value of  $d \Delta \log K / d \log C(s)$ .

The relationship between  $\Delta \log K$  and  $\Delta \zeta$  is shown by Equation 7.18.

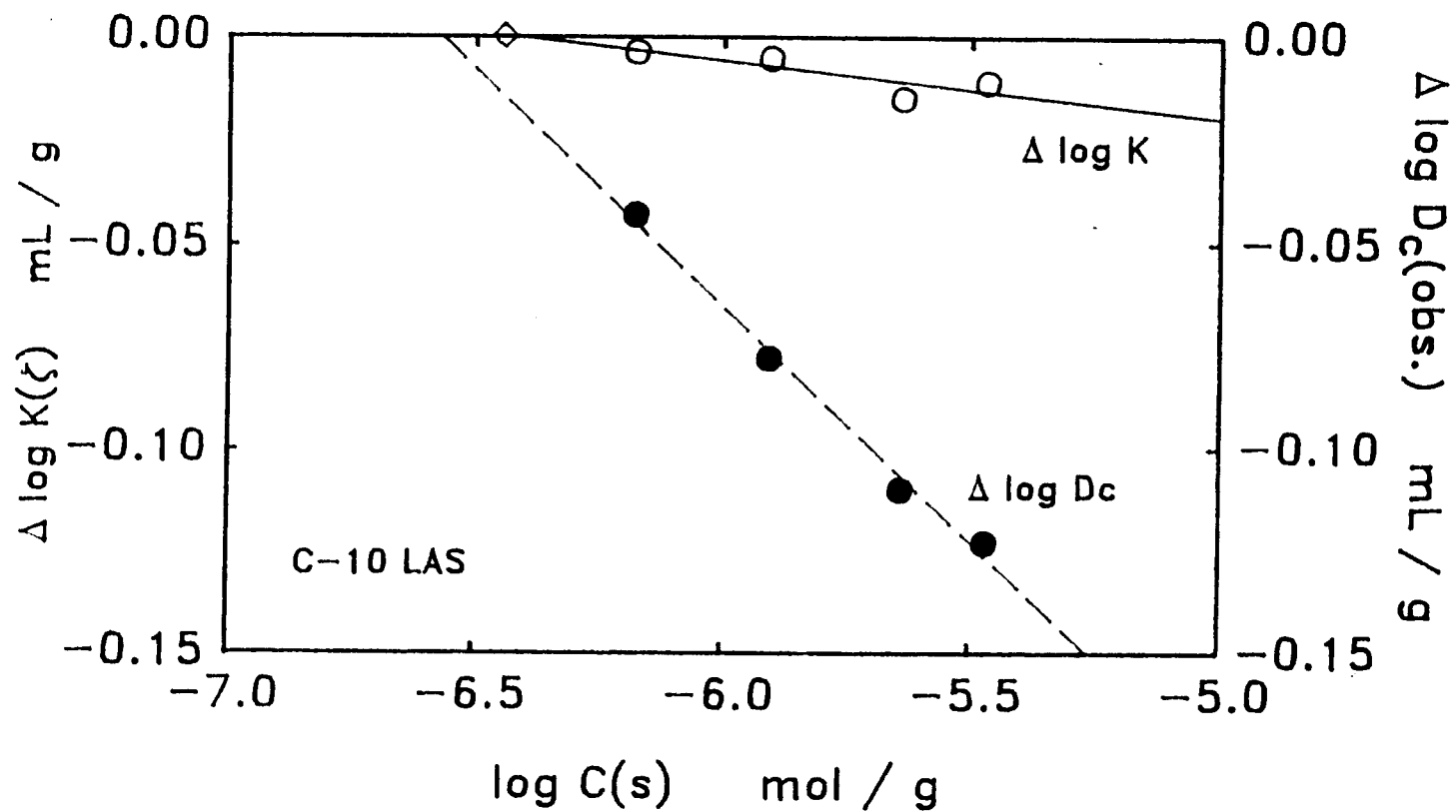


Figure 7.11a. A comparison of  $\Delta \log K$  vs.  $\Delta \log D_c$  for C-10 LAS.

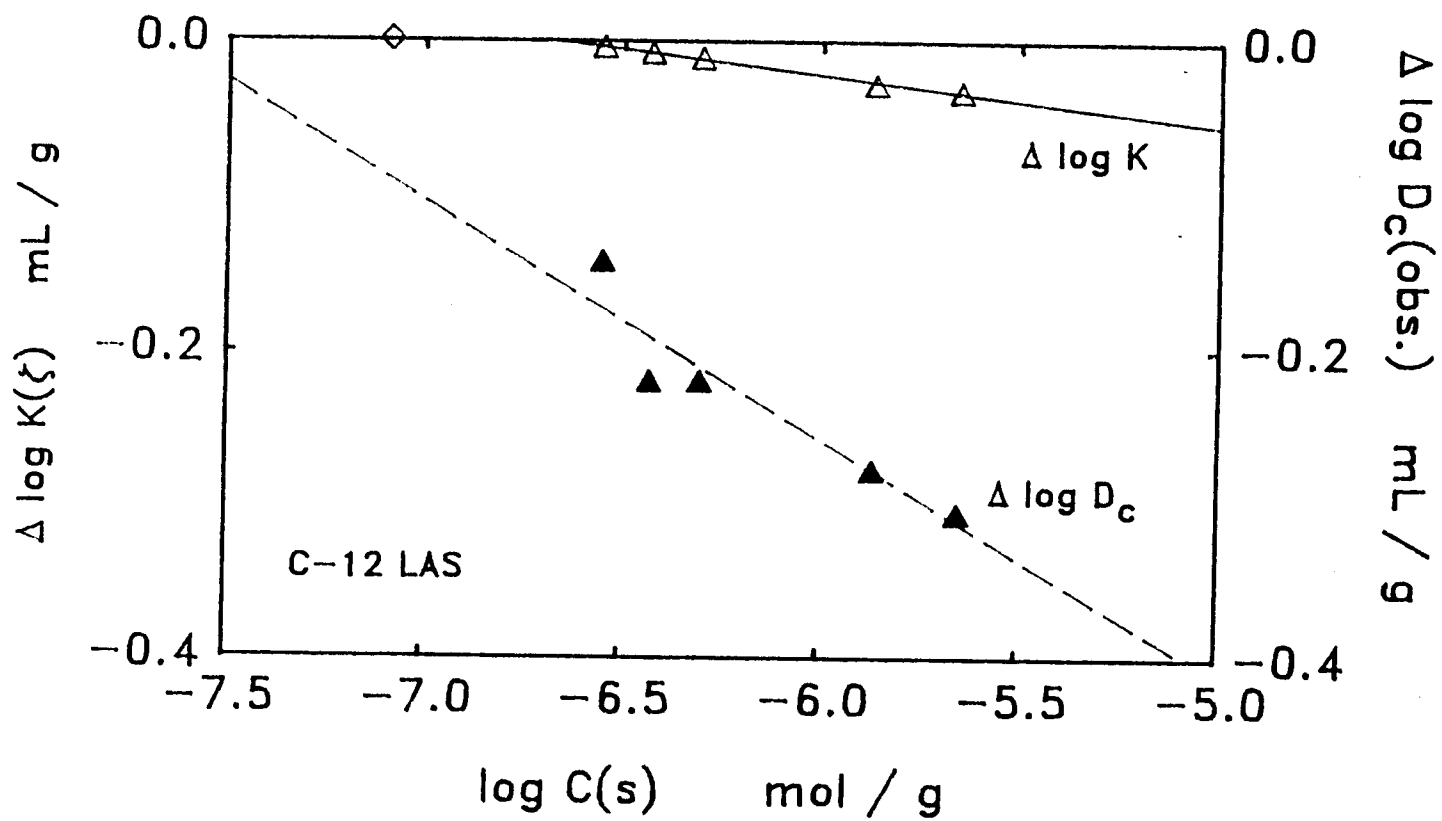


Figure 7.11b. A comparison of  $\Delta \log K$  vs.  $\Delta \log D_c$  for C-12 LAS.

If the change in  $\log D_c$  were due solely to the electrostatic interaction, the value of  $d \Delta \Psi / d \log C(s)$  would have to be -6.4 mV and -9.3 mV for C-10 and C-12 LAS, respectively; the values of  $d \Delta \zeta / d \log C(s)$  seen in Figure 7.11 a,b, are only -1.0 mV and -1.6 mV for C-10 and C-12 LAS.

Thirdly, we interpret the dramatic decrease in  $\Delta \log D_c$  with increasing  $\log C(s)$  as being due to the heterogeneity of the natural sorbent. This effect also causes the isotherms to be nonlinear at lower surface coverage (Region I). We will discuss this effect in detail in the following section.

Nonlinearity of isotherms. Nonlinear adsorption was found at the low-coverage region (Region I) of the isotherms. This result is contrary to adsorption of ionic surfactants on pristine surfaces, on which the linear isotherm was typically observed. We interpret the nonlinearity of isotherms as a result of the heterogeneity of the surface for the environmental material. Variety of sorption sites exist on the surface of the natural sorbent. The LAS ions will prefer to be adsorbed first on some high-energy sorption sites and saturate those sites, and then be adsorbed on low-energy sites. Thus, nonlinear isotherm is observed.

### Adsorption of LAS: sorbate-sorbate interactions

Hemimicelle formation. Hemimicelle formation, as indicated by the abrupt increase in adsorption at certain solution concentration range of LAS (Region II), was observed on all the isotherms, although it was almost not distinguishable for the isotherm of C-10 LAS, as shown in Figure 7.6. It has been interpreted that hemimicelles form as two-dimensional aggregations on the surface of the sorbent through chain/chain association of surfactants (Somasundaran and Fuerstenau, 1966; Chander et al., 1983; and Hough and Rendall, 1983).

Many factors affect the formation of hemimicelles on a surface, for example, chain length and functional group of the surfactant, pH and ionic strength of the solution, and properties of the surface. In this section, the hemimicelle formation of LAS on the environmental sorbent will be interpreted in consideration of these factors.

$C_{HM}(w)$  and  $\Gamma_{HM}$ . The symbols  $C_{HM}(w)$  and  $C_{HM}(s)$  represent the aqueous and surface concentration at which hemimicelle formation starts. These points for the formation of hemimicelles of LAS on the natural sorbent are marked on the isotherms shown in Figure 7.6, 7.9 and 7.10. Surface adsorption density  $\Gamma_{HM}$  ( $\text{mol m}^{-2}$ ), which is commonly used in the literature, is calculated from  $C_{HM}(s)$  and the specific area of the sorbent.

The effects of chain length, pH and salt concentration on the  $C_{HM}(w)$  and  $\Gamma_{HM}$  are illustrated in Figure 7.12 a-c for adsorption of alkylbenzenesulfonates on the natural sorbent. The concentration of onset of hemimicelle formation for C-10 LAS on the natural sorbent

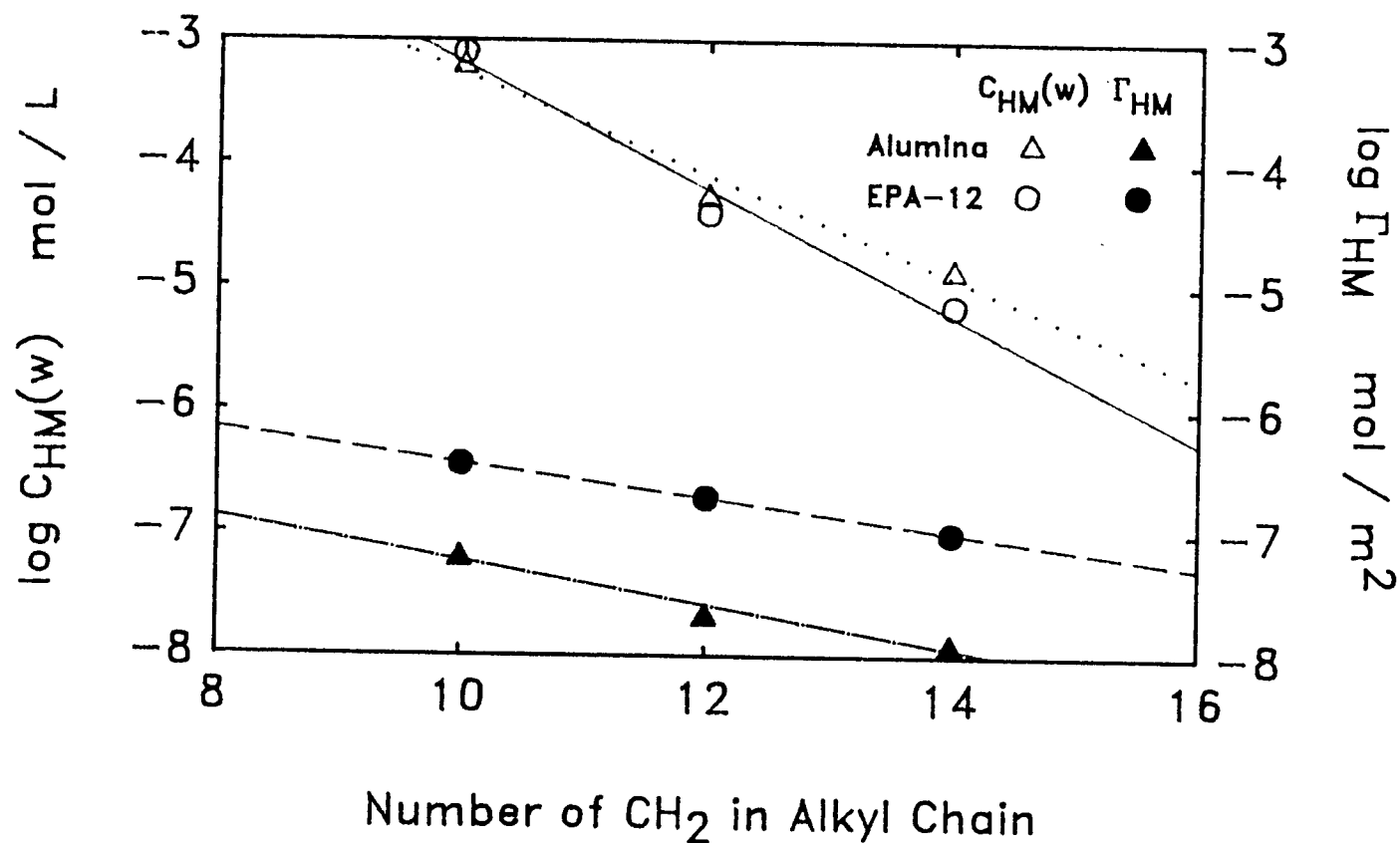


Figure 7.12a. Effect of chain length on hemimicelle formation: a comparison of  $\log C_{HM}(w)$  and  $\log \Gamma_{HM}$  for adsorption of dodecylbenzenesulfonate on EPA-12 (from this work), and adsorption of dodecylsulfonate on alumina (from Chander et al., 1983).

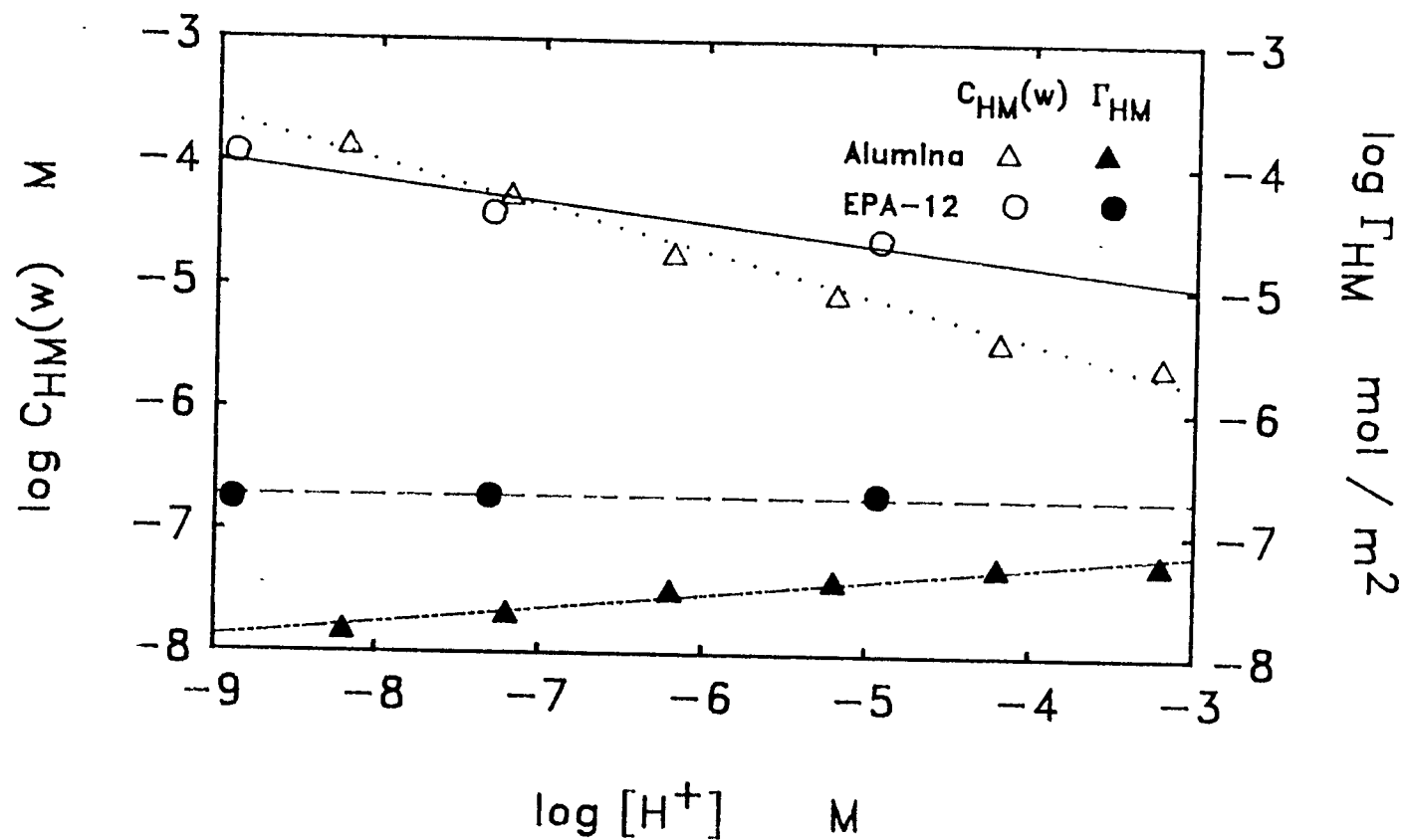


Figure 7.12b. Effect of pH on hemimicelle formation: a comparison of  $\log C_{HM}(w)$  and  $\log \Gamma_{HM}$  for adsorption of dodecylbenzenesulfonate on EPA-12 (from this work), and adsorption of dodecylsulfonate on alumina (from Chander et al., 1983).

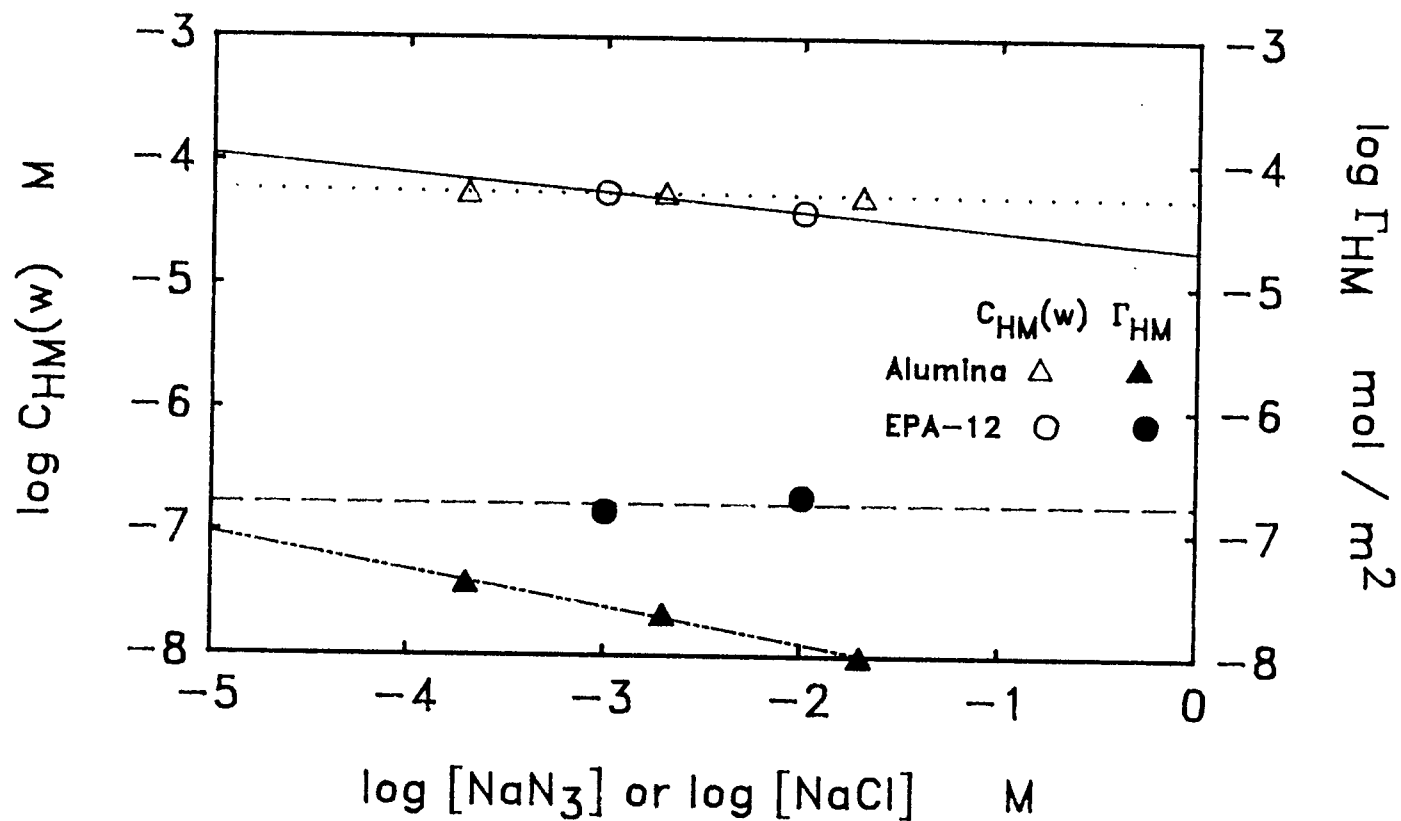


Figure 7.12c: Effect of salt concentration on hemimicelle formation: a comparison of  $\log C_{\text{HM}}(\text{w})$  and  $\log \Gamma_{\text{HM}}$  for adsorption of dodecylbenzenesulfonate on EPA-12 (from this work), and adsorption of dodecylsulfonate on alumina (from Chander et al., 1983).

is not very distinct (Figure 7.6), and the value selected for  $C_{HM}(w)$  for C-10 LAS is somewhat subjective.

A similar study has been made by Fuerstenau and co-workers for adsorption of alkylsulfonates on a pristine sorbent, alumina, as a function of chain length (Wakamatsu and Fuerstenau, 1968), pH (Fuerstenau and Wakamatsu, 1975), and salt concentration (Fuerstenau and Healy, 1967). These studies are reviewed by Chander et al. (1983). The data of  $C_{HM}(w)$  and  $\Gamma_{HM}$  from their studies are also plotted in Figure 7.12 a-c for comparison.

An increase in chain length shows a trend towards a decrease in both  $C_{HM}(w)$  and  $\Gamma_{HM}$  on the two types of sorbents (Figure 7.12a). This effect is similar to the influence of chain length on the CMC of surfactant homologs in solution. We attribute this effect to the stronger chain-chain association on the surface for the longer chain homolog, which causes the hemimicelle formation to start at lower aqueous concentrations and lower surface densities.

An increase in concentration of  $H^+$  in solution decreases the  $C_{HM}(w)$ , and the effect seems stronger on alumina than on the natural sorbent (Figure 7.12b). This decrease in  $C_{HM}(w)$  can be attributed to the increase in surface potential which is more favorable to adsorb anionic surfactants. The  $\Gamma_{HM}$  on alumina shows a significant increase with increasing  $H^+$  concentration. The  $\Gamma_{HM}$  on the natural sorbent, however, shows independence on the pH. We will discuss this difference later.

An increase in salt concentration yields no difference on  $C_{HM}(w)$  for dodecylsulfonate on alumina (Figure 7.12c, from the isotherms reported by Fuerstenau and Healy, 1967) and on  $C_{HM}(w)$  for

dodecylbenzenesulfonate on the natural sorbent (Figure 7.10 and Figure 7.12c). We have no clear explanation for this effect. The surface density  $\Gamma_{HM}$  on alumina shows a significant decrease as the salt concentration increases. This effect can be attributed to the effect of salt concentration on the aggregation of adsorbed surfactant ions to form the hemimicelles; this effect is similar to the effect of salt on the formation of micelles in bulk solutions (Chander et al., 1983). For adsorption of C-12 LAS on the natural sorbent, the change in  $\Gamma_{HM}$  with the salt concentration is insignificant.

In summary, the variation in the hydrophobic factors such as chain length of the sulfonates shows a large and similar effect on  $\Gamma_{HM}$  for both sorbents, whereas the variation in the electrostatic factors such as pH or salt concentration of the solutions seem only to show a large effect on  $\Gamma_{HM}$  for the pristine sorbent, but a small effect for the natural sorbent. This difference may be due to the different properties of the two type sorbents. For the pristine sorbent, the adsorption process can be considered as occurring on a two-dimensional surface, on which the electrostatic interaction within the double layer plays an important role for adsorption of ionic surfactants. However, for the natural sorbent, the adsorption may take place in three dimensions. In this case, the changes in electrostatic interaction seem to be relatively less important with respect to the changes in the hydrophobic interaction for adsorption of LAS on the natural sorbent.

Another observation from Figure 7.12 a-c is that the absolute values of  $\Gamma_{HM}$  on the natural sorbent are generally larger than the values of  $\Gamma_{HM}$  on alumina. Two reasons may cause this difference:

i) there might be an error in determining the specific surface area of the natural sorbent, and the real surface area for the soil EPA-12 may be larger than  $12 \text{ m}^2 \text{ g}^{-1}$ ; ii) the anionic surfactants used in Fuerstenau's studies are homologs of alkylsulfonates, but in our study the surfactants are the homologs of alkylbenzenesulfonates. The benzene rings in the structure of the alkylbenzenesulfonates may cause the changes in the apparent distribution ratio  $D_c$  for the adsorption so as to the surface densities  $\Gamma_{HM}$  for the hemimicelle formation.

Aggregation number of hemimicelle,  $n_H$ . As described in the section on theory, the aggregation number of a hemimicelle,  $n_H$ , can be obtained by two methods: (i) the method by Chander et al. (1983), in which  $n_H$  is the slope of a linear plot of  $\log \Gamma$  vs.  $\log C(w)$  in Region II of the S-shape isotherm; and (ii) the method by Gu et al. (1987, 1988), in which  $n_H$  is the ratio between the surface densities  $\Gamma_{CMC}$  and  $\Gamma_{HM}$  of the isotherm.

In this study, the  $n_H$  for alkylbenzenesulfonates on the natural sorbent are calculated by both methods, and the results are listed in Table 7.1. In general, the values of  $n_H$  from the method by Gu et al. are much larger than the values of  $n_H$  from the method by Chander et al. This may be caused by improper assumptions of Chander's method, in which the surface concentration of surfactants adsorbed as monomer is assumed to be very small and negligible. The aggregation number of a micelle,  $n_M$ , was found to be 54 for sodium dodecylsulfonate in water at 40 °C, and the value of  $n_M$  was 71 for sodium dodecylsulfate in water at 23 °C (Tartar and Lelong, 1955). Thus the values of aggregation number of hemimicelle  $n_H$  from Gu's method seem more reasonable.

Table 7.3 gives the  $\eta_{HM}$  for alkylsulfonates on alumina (Chander et al., 1983) and the  $\eta_H$  for alkylpyridinium on silica gel (Gu et al., 1987 and 1988). Our  $\eta_H$  values, which are shown in Table 7.1, are in the similar range of Chander's and Gu's  $\eta_H$  data for the surfactants with same chain length.

It should be mentioned here that in this study the values of  $\eta_H$  obtained through Equation 7.14 is calculated from the ratio of the  $C_{MAX}(s)$  to  $C_{HM}(s)$ . The  $C_{MAX}(s)$  is the maximum surface concentration observed from the isotherms, since the plateau region of some isotherms was not distinguishable. This substitution of  $C_{CMC}(s)$  by  $C_{MAX}(s)$  may cause some problem about the accuracy of the  $\eta_H$ .

Table 7.3. The aggregation number,  $n_H$ , of ionic surfactants on pristine surfaces.

Surfactant <sup>a</sup>	Sorbent	Salt Conc.	pH	$n_H$
Chander et al. (1983)				
<u>Effect of chain length:</u>				
C-10 LAS	alumina	0.002 M NaCl	7.2	2
C-12 LAS	alumina	0.002 M NaCl	7.2	2
C-14 LAS	alumina	0.002 M NaCl	7.2	2
C-16 LAS	alumina	0.002 M NaCl	7.2	7
<u>Effect of pH:</u>				
C-12 LAS	alumina	0.002 M NaCl	3.2	2
C-12 LAS	alumina	0.002 M NaCl	4.2	2
C-12 LAS	alumina	0.002 M NaCl	5.2	2
C-12 LAS	alumina	0.002 M NaCl	6.2	2
C-12 LAS	alumina	0.002 M NaCl	8.2	2
<u>Effect of Ionic strength:</u>				
C-12 LAS	alumina	0.02 M NaCl	7.2	2
C-12 LAS	alumina	0.002 M NaCl	7.2	2
C-12 LAS	alumina	0.0002M NaCl	7.2	2
Gu et al. (1987)				
<u>Effect of chain length and types of salt and surfactant:</u>				
C-12 PYRB	silica gel	water		12
C-14 PYRB	silica gel	water		13
C-14 PYRB	silica gel	0.01 M NaBr		18
C-14 PYRB	silica gel	0.01 M NaCl		14
C-14 PYRC	silica gel	water		6
C-14 PYRC	silica gel	0.01 M NaBr		14
C-14 PYRC	silica gel	0.01 M NaCl		10

<sup>a</sup>. The abbreviation of LAS, PYRB and PYRC are represented as linear alkylsulfonate, alkylpyridinium bromide and alkylpyridinium chloride, respectively.

## SUMMARY

The adsorption isotherms of LAS on the natural sorbent EPA-12 has been observed as S-type from this study. Hemimicelle formation was distinguishable for most of the isotherms, determined as a function of chain length, pH, and ionic strength. For C-10 LAS, the hemimicelle formation was not readily distinguishable. The adsorption in Region I was nonlinear with the  $n$  value of Freundlich isotherm about 0.8. The nonlinearity is attributed to the heterogeneity of the surface. The zeta potential study indicated that the negatively charged LAS molecules were adsorbed on the negatively charged surface.

The onset of hemimicelle formation,  $\Gamma_{HM}$ , on the natural sorbent was compared to published data for a pristine sorbent. The variation in the hydrophobic factors such as chain length of the sulfonates shows a large and similar effect on  $\Gamma_{HM}$  for both sorbents, whereas the variation in the electrostatic factors such as pH or salt concentration of the solutions seem only to show a large effect on  $\Gamma_{HM}$  for the pristine sorbent, but a small effect for the natural sorbent. This difference may be due to the different properties of the two type sorbents. For the pristine sorbent, the adsorption process can be considered as occurring on a two-dimensional surface, on which the electrostatic interaction within the double layer plays an important role for adsorption of ionic surfactants. However, for the natural sorbent, the adsorption may take place in three dimensions. In this case, the changes in electrostatic interaction seem to be relatively less important with respect to the changes in

the hydrophobic interaction for adsorption of LAS on the natural sorbent.

The aggregation number of hemimicelle,  $n_H$  for LAS on the natural sorbent are obtained by the methods from Chander et al. and Gu et al.

## REFERENCES

- Bard A. J.; Faulkner, L. R. Electrochemical Methods. John Wiley & Sons, 1980.
- Chander, S.; Fuerstenau, D. W.; Stigter, D. "On Hemimicelle Formation at Oxide/Water Interfaces" in Adsorption from Solution; Ottewill, R. H.; Rochester, C. H.; Smith, A. L.; Eds.; Academic Press: New York, 1983.
- Chen, H. Department of Chemistry, Oregon State University. Experimental data, 1988.
- Connor, P.; Ottewill, R. H.; J. Colloid Interface Sci. 1971, 37, 642-651.
- Dick, S. G.; Fuerstenau, D. W.; Healy, T. W.; J. Colloid Interface Sci. 1971, 37, 595-602.
- Fahey, J. Experimental data of specific surface area of the sorbents, 1987.
- Fuerstenau, D. W.; Healy, T. W. "The Adsorption of Alkyl and Alkylary Sulfonates on Polar Solids", report to Federal Water Pollution Control Administration, University of California, Berkeley, 1967.
- Fuerstenau, D. W.; Wakamatsu, T.; Faraday Discussions of the Chemical Society, 1975, 59, 157-168.
- Gao, Y.; Du, J.; Gu, T. J. Chem. Soc. Faraday Trans 1 1987, 83, 2671-2679.
- Gu, T.; Gao, Y.; He, L. J. Chem. Soc. Faraday Trans 1 1988, 84, 4471-4473.
- Gu, T.; Huang, Z.; Colloids and Surfaces 1989, 40, 71-76.
- Hand, V. C.; Williams, G. K.; Environ. Sci. Technol. 1987, 21, 370-373.
- Hassett, J. J.; Means, J. C.; Banwart, W. L.; Wood, S. G. Sorption Properties of Sediments and Energy-Related Pollutants. U.S. Environmental Protection Agency, Report EPA-600/3-80-041, National Technical Information Service, Springfield, VA. 1980.
- Hiemenz, P. C. Principles of Colloid and Surface Chemistry. 2nd Ed., Marcel Dekker, Inc: New York and Basel, 1986.
- Hough, D. B.; Rendall, H. M. "6. Adsorption of Ionic Surfactants"; in Adsorption from Solution at Solid/Liquid Interface; Patfitt, G. D.; Rochester, C. H. Eds.; 1983.

- Hunter, R. J. Zeta Potential in Colloid Science. Academic Press: New York, 1986.
- Keesom, W. H.; Zelenka, R. L.; Radke C. J. J. Colloid Interface Sci. 1988, 125, 575-585.
- Komagata, S. Researches Electrotech. Lab. Tokyo. Comm. No. 348. 1933.
- Rosen, M. J. "Relationship of Structure to Properties in Surfactants: III. Adsorption at the Solid-Liquid Interface from Aqueous Solution"; in Surfactants and Interfacial Phenomena; 1978.
- Sales, D.; Quiroga, J. M.; Gomez-Parra, A.; Environ. Sci. Technol. 1987, 39, 385-392.
- Savitsky, A. C.; Wiers, B. H.; Wendt R. H. Environ. Sci. Technol. 1981, 15, 1191-1196.
- Scamehorn, J. F.; Schechter, R. S.; Wade, W. H. J. Colloid Interface Sci. 1982, 85, 463-478.
- Shaw, D. J.; Electrophoresis 1969, Academic Press, New York and London.
- Sieglauff, C. L.; Mazur J. J. Colloid Sci. 1960, 15, 437.
- Sieglauff, C. L.; Mazur J. J. Colloid Sci. 1962, 17, 66-85.
- Somasundaran, P.; Fuerstenau, D. W. J. Phys. Chem. 1966, 70, 90-96.
- Tartar, H. V.; Lelong, A. L. M. J. Phys. Chem. 1955, 59, 1185.
- Urano, K.; Saito, M. Chemosphere 1984, 13, 285-292.
- Urano, K.; Saito, M.; Murata, C. Chemosphere 1984, 13, 293-300.
- van Senden, K. G.; Koning, J. Fette Seifen Anstrichm. 1968, 70, 36.
- Vilcu, R.; Olteanu, M.; Revue Roumaine de Chimie 1975, 20, 1041-1060.
- Wakamatsu, T.; Fuerstenau, D. W. Adv. Chem. Ser. 1968, 79, 161.
- Wiersema, P. H.; Loeb, A. L.; Overbeek, J. Th. J. Colloid Interface Sci. 1966, 22, 78.

## CHAPTER 8

## CONCLUSIONS

A technique has been developed to determine the conductivity of high-impedance nonaqueous electrolyte solutions and the relative permittivities of alcohol/water mixtures. A conductivity cell was in series with the current-measuring resistor. The complex voltage across the cell and the resistor are determined by a lock-in amplifier. The resistance of the cell is calculated according to the equivalent circuit, which includes the impedance of the cell, the impedance of the input circuit, and the stray capacitance. The measurements can be performed over a frequency range from 5 Hz to 5 kHz for conductance determination and from 5 kHz to 100 kHz for capacitance determination.

The frequency-independent resistance for the samples of octanol saturated with KCl aqueous solutions were observed at frequencies less than 100 Hz, and the measurement can be made up to 10 M $\Omega$  with precision better than 3%. Frequency-independent capacitances were observed for 1-pentanol - water and 1-octanol - water at frequencies larger than a few kHz, and measurements can be made in the range 90 - 900 pF with precision better than 0.2%.

This technique has been applied to study the speciation and distribution of inorganic salts between octanol and water. In this

study, the experimental data (from Johnson, 1987) were used for the aqueous phase concentrations of the salts between 0.01 M and 1 M. The speciation in the nonaqueous phase was consistent with the conductivity of the nonaqueous phase as determined by the technique developed in this study.

Distribution of LiCl, NaCl, and KCl between the two phases are well explained by the species,  $M^+$ ,  $X^-$ , and  $MX$  in the nonaqueous phase. For HCl, the distribution data could be interpreted satisfactorily in terms of the species  $H^+$ ,  $Cl^-$ , and  $HCl$ . But the conductivity data also suggest the presence of triple ions such as  $H_2Cl^+$  or  $HCl_2^-$ . For  $MgCl_2$  and  $CaCl_2$ , the data are explained by  $MX^+$ ,  $X^-$ , and  $M_2X$  in the nonaqueous phase. No evidence has indicated for the presence of the species  $M^{2+}$  in the nonaqueous phase.

The adsorption of anionic surfactants LAS on the soil sorbent materials has been investigated in terms of the hydrophobic, specific chemical and electrostatic interactions. Sorption of LAS was performed in two concentration domains: low concentration range, in which the interactions between the surfactant and the surface of the sorbents are addressed; and high concentration range (near the CMC of the surfactants), in which the interactions between the surfactants molecules are also significant. The effects of chain length of LAS,  $Ca^{2+}$  concentration in solution, sorbent type, and concentration of solids on the adsorption are evaluated.

Evidence has been shown for both hydrophobic and specific or electrostatic interactions at lower concentrations. The isotherms

were generally nonlinear, and the data were represented well by both the electrostatic model and the Freundlich model in the low adsorption range. Addition of  $\text{Ca}^{2+}$  into the system significantly enhanced the adsorption of LAS. This effect can be interpreted as the formation of LAS- $\text{Ca}^+$  complex either on the surface or in solution. The electrostatic attraction between this positively charged complex and negatively charged sorbent surface will increase the  $D_c$  of LAS. Comparisons of apparent distribution ratios for linear portions of the isotherms showed:  $d \log D_c / d \log n_{\text{-CH}_2^-} \approx 0.4$ ;  $d \log D_c / d \log [\text{Ca}^{2+}] \approx 0.23$ . The value of  $D_c$  for different soils seemed to correlate most closely with the  $f_{oc}$  of the sorbents. The effect of solid concentrations  $C_s(w)$  on adsorption of LAS, therefore, could be correlated to the  $\text{Ca}^{2+}$  concentration in aqueous suspensions.

Hemimicelle formation for the LAS, near the CMC, was observed at the higher concentration on natural sorbent material. Study also shows that  $\text{H}^+$ , ionic strength in solution and the hydrophobic chain length of the LAS homologs would affect the tendency of this formation. In order to understand the mechanism of adsorption, zeta potentials of the colloidal particles were determined corresponding to the isotherms of LAS homologs on sorbent EPA-12 in 0.01 M  $\text{NaN}_3$ . The values of zeta potentials were generally negative in the range of -27 to -43 mV. Good correlation has been observed for the zeta potential data and the corresponding isotherms.

The adsorption of nonionic surfactants  $A_{13}E_m$  on the sorbents were investigate at lower concentration range ( $C(w) < 650 \text{ nM}$  and  $C(s) < 300 \text{ nmol/g}$ ) to focus the surfactant-surface interactions. The

results show that  $A_{13}E_m$  adsorbed strongly to natural sorbents, and their affinities for the same sorbents were intermediate between anionic and cationic surfactants containing similar alkyl chain length. In contrast to LAS, the addition of  $Ca^{2+}$  has no effect on adsorption of  $A_{13}E_m$  on the sorbent. Increasing ionic strength of the solutions decreases adsorption of the  $A_{13}E_9$ , but increases adsorption of the  $A_{13}E_3$ . Affinity of adsorption of  $A_{13}E_6$  homolog on different sorbents does not correspond to the order of  $f_{oc}$  for the sorbents. These results may be interpreted by the clay mineral composition of the sorbents, particularly swelling clay composition. Adsorption isotherms of  $A_{13}E_6$  on the sorbents were generally nonlinear and expressed well by the Freundlich model.

In summary, investigations have been carried out in this study to elucidate the mechanisms of two processes: (i) distributions of inorganic compounds between octanol and water and (ii) adsorption of surfactants on environmental sorbent materials. The principal goal is generally achieved.

## BIBLIOGRAPHY

- Apelblat, A. and Manzurola, E. Ber. Bunsenges. Phys. Chem. 1987, 91, 1387-1394.
- Aveyard, R. "Adsorption at the Air/Liquid, Liquid/Liquid, and Solid/Liquid interfaces" in Surfactants; Tadros, Th. F. Ed.; Academic Press: London; 1984, 153-173.
- Bacelon, P.; Corset, J.; and de Loze, C. J. Solution Chem. 1980, 9, 129.
- Bard, A. J.; Faulkner, L. R. "Electrochemical Methods"; by John Wiley & Sons, Inc. 1980, 316.
- Beronius, P. Acta Chem. Scand. A 1978, 32, 469-470.
- Beronius, P.; Lindbaeck, T. Acta Chem. Scand. 1978, A32, 423-428.
- Bijsterbosch, B. H. J. Coll. Interface Sci. 1974, 47, 186-198.
- Bockris, J. O'M. and Reddy, A. K. N. Modern Electrochemistry 1. 1976, A Plenum/Rosetta Edition.
- Boethling, R. S.; Water Res. 1984, 18, 1061-1076.
- Braunstein, J.; Robbins, G. D. J. Chem. Educ. 1971, 48, 52.
- Broadwater, T. L. and Kay, R. L. J. Phys. Chem. 1970, 74, 3802-3812.
- Broadwater, T. L. and Douglas, R. T. J. of Soln. Chem. 1975, 4, 485-496.
- Brunner, P. H.; Capri, S.; Marcomini, A.; Giger, W. Water Res. 1988, 22, 1465-1472.
- Carroll, D. "Clay Mineral: A Guide to Their X-ray Identification", THE GEOLOGICAL SOCIETY OF AMERICA, INC. (1970).
- Chander, S.; Fuerstenau, D. W.; Stigter, D. "Adsorption from Solution"; Ottwill, R. H., Rochester, C. H., Eds; Academic Press: New York. 1983. 197-210.
- Chao, T. T.; Harward, M. E.; Fang, S. C. Soil Sci. 1965, 99, 104-108.
- Chen, H.; Westall, J. C. Department of Chemistry, Oregon State University. Experimental data, 1988.
- Chiou, C. T.; Peters, L. J.; Freed, V. H. Science 1979, 206, 831-832.

- Clunie, J. S.; Ingram, B. T. "3. Adsorption of Nonionic Surfactants" in Adsorption from Solution at the Solid/Liquid Interface; Parfitt, G. D.; Rochester, C. H., Eds.; Academic Press: New York, 1983, 105-152.
- Connor, P. and Ottewill, R. H. J. Coll. Interface Sci. 1971, 37, 642-651.
- Dannhauser, W. and Cole, R. H. J. Phys.Chem. 1952, 56, 6105.
- D'Aprano, A.; Donato, D. I.; and Caponetti, E. J. of Soln. Chem. 1979, 8, 135.
- D'Aprano, A.; Donato, D. I.; and Agrigento, V. J. of Soln. Chem. 1982, 11, 259.
- Delahay, P. Double Layer and Electrode Kinetics. 1965, Wiley Interscience: New York.
- DeSieno, R. P.; Greco, P. W.; and Mamajek, R. C. J. Phys. Chem. 1971, 75, 1722-1726.
- Dick, S. G.; Fuerstenau, D. W.; Healy, T. W. J. Coll. Interfac. Sci. 1971, 37, 595-602.
- Di Toro, D. M. Chemosphere. 1985, 14, 1503-1538.
- Doe, H.; Kitagawa, T.; Sasabe, K. J. Phys. Chem. 1984, 88, 3341-3345.
- Evans, D. F.; and Gardam, P. J. Phys. Chem. 1968, 72, 3281-3286.
- Evans, D. F.; and Gardam, P. J. Phys. Chem. 1969, 73, 158-163.
- Evans, D. F.; Matesich, M. A. "The Measurement and Interpretation of Electrolytic Conductance" in Techniques of Electrochemistry; Vol. II; E. Yeager and Salkind, A. J. Eds.; Wiley: New York, 1973, Chap. 1.
- Fahey, J. Experimental data of specific surface area of the sorbents, 1987.
- Fang, J. and Venable, R. L. J. Coll. Interface Sci. 1987, 116, 269.
- Fink, D. H.; Thomas, G. W.; Meyer, W. J. Journal WPCF. 1970, 42, 265-271.
- Florence, A. T.; Tucker, I. G.; Walters, K. A. in "Effect of Structure on Performance in Various Application"; Rosen, M. J., ed.; ACS: Wash. D. C., 1984; 189-208.
- Fuerstenau, D. W.; Healy, T. W. "The Adsorption of Alkyl and Alkylaryl Sulfonates on Polar Solids", report to Federal Water Pollution Control Administration, University of California, Berkeley, 1967.

- Fuerstenau, D. W.; Wakamatsu, T.; Faraday Discussions of the Chemical Society, 1975, 59, 157-168.
- Fuoss, R. M. and Kraus, C. A. J. Am. Chem. Soc. 1933, 55, 2387.
- Fuoss, R. M. and Accascina, F. Electrolytic Conductance 1959, Interscience: New York.
- Fuoss, R. M. J. Phys. Chem. 1978, 82, 2427.
- Games, L. M.; Larson, R. J. Environ. Sci. Technol. 1982, 16, 483-488.
- Games, L. M. "Practical Applications and Comparisons of Environmental Exposure Assessment Models" In Aquatic Toxicology and Hazard Assessment: Sixth Symposium, ASTM STP 802; Bishop, W. E., Cardwell, R. D., Heidolph, B. B. Eds.; American Society for Testing and Materials: Philadelphia, 1983, 282-299.
- Gao, Y.; Du, J.; Gu, T. J. Chem. Soc. Faraday Trans 1 1987, 83, 2671-2679.
- Giger, W.; Brunner, P. H.; Schaffner, C. Science 1984, 225, 623-625.
- Goffredi, M. and Shedlovsky, T. J. Phys. Chem. 1967, 71, 2176-2181.
- Goffredi, M. and Shedlovsky, T. J. Phys. Chem. 1967, 71, 2182-2186.
- Greek, B. F.; Layman, P. L. Chem. Eng. News 1990, 68, 37-60.
- Grigo, M. J. of Solution Chem. 1982, 11, 529-537
- Grunwald, E.; Pan, K. C.; and Effio, A. J. Phys. Chem. 1976, 80, 2937.
- Gschwend, P. M.; Wu, S-C. Environ. Sci. Technol. 1985, 19, 90-96.
- Gu, T.; Gao, Y.; He, L. J. Chem. Soc. Faraday Trans 1 1988, 84, 4471-4473.
- Gu, T.; Huang, Z. Colloids and Surfaces 1989, 40, 71-76.
- Hafez, A. M.; Ramadan, M. Sh.; Sadek, H. Electrochimica Acta 1987, 32, 625-628.
- Hand, V. C.; Williams, G. K. Environ. Sci. Technol. 1987, 21, 370-373.
- Hansch, C.; Dunn, W. J. III. J. Pharm. Sci. 1972, 61, 1-7.
- Hassett, J. J.; Means, J. C.; Banwart, W. L.; Wood, S. G. Sorption Properties of Sediments and Energy-Related Pollutants. U.S. Environmental Protection Agency, Report EPA-600/3-80-041, National Technical Information Service, Springfield, VA. 1980.

- Hawes, J. L. and Kay, R. L. J. Phys. Chem. 1965, 69, 2420-2431.
- Hiemenz, P. C. Principles of Colloid and Surface Chemistry 2nd Ed., Marcel Dekker Inc.: New York and Basel, 1986.
- Highsmith, S. J. Phys. Chem. 1975, 79, 1456-1459.
- Holysh, M.; Paterson, S.; Mackay, D.; Bandurraga, M. M. Chemosphere 1986, 15, 3-20.
- Hough, D. B.; Rendall, H. M. "6. Adsorption of Ionic Surfactants" in Adsorption from Solution at Solid/Liquid Interface; Patfitt, G. D.; Rochester, C. H. Eds.; Academic Press: New York, 1983, 247-319.
- Huang, F. and Gilkerson, W. R. J. of Soln. Chem. 1983, 12, 161-170.
- Hunter, R. J. Zeta Potential in Colloid Science. Academic Press: New York, 1986.
- Imboden, D. M.; Schwarzenbach, R. P. in Chemical Processes in Lakes, W. Stumm, Ed., Wiley, New York, 1985.
- Inoue, K.; Kaneko, K.; Yoshita, M. Soil Sci.: Plant Nutr. 1978, 24, 91-102.
- Johnson, C. A. Department of Chemistry, Oregon State University. Experimental Data, 1987.
- Johnson, C. A.; Westall, J. C. Environ. Sci. Technol. 1990, 24, 1869-1875.
- Karickhoff S. W.; Brown, D. S.; Scott, T. A. Water Res. 1979, 13, 241-248.
- Kay, R. L.; Zawoyski, C.; and Evans, D. F. J. Phys. Chem. 1965, 69, 4208-4215.
- Keesom, W. H.; Zelenka, R. L.; Radke C. J. J. Colloid Interface Sci. 1988, 125, 575-585.
- Kissinger, P. T. and Heinemann, W. R. Laboratory Techniques in Electroanalytical Chemistry; Dekker, 1984.
- Klimenko, N.A.; Permilovskaya, A. A.; Koganovskii, A. M. Kolloidn. Zh. 1974, 36, 788-792.
- Koganovskii, A. M.; Klimenko, N. A.; Tryasorukova, A. A. Colloid Journal of USSR (in English); 1974, 36, 790-792.
- Komagata, S. Researches Electrotech. Lab. Tokyo. Comm. No. 348. 1933.

- Kratochvil, B. and Yeager, H. L. "Conductance of Electrolytes in Organic Solvents", Topics in Current Chemistry, 1972, No. 27, 1.
- Krishna Murti, G. S. R.; Volk, V. V.; Jackson, M. L. Soil Sci. Soc. Amer. Proc. 1966, 30, 685-688.
- Larson, R. J. Residue Reviews 1983, 85, 159-171.
- Larson, R. J.; Vashon, R. D. "Chapter 38 Adsorption and Biodegradation of Cationic Surfactants in Laboratory and Environmental System" in Developments in Industrial Microbiology; Vol. 24, Nash III, C. H. and Underkofler, L. A. Eds; 1983.
- Larson, R. J.; Games, L. M. Environ. Sci. Technol. 1981, 15, 1488-1493.
- Law, J. P.; Kunze, G. W. Soil Sci. Soc. Amer. Proc. 1966, 30, 321-327.
- Leo, A.; Hansch, C. J. Org. Chem. 1971, 36, 1539-1544.
- Lewis, M. A.; Suprenant, D. Ecotoxicology and Environmental Safety 1983, 7, 313-322.
- Lewis, M. A.; Wee, V. T. Environ. Tox. Chem. 1983, 2, 105-118.
- Lyman, W. J.; Reehl, W. F.; Rosenblatt, D. H. Handbook of Chemical Property Estimation Methods; McGraw-Hill: New York, 1982.
- Marcus, Y. Ion Solvation; 1985, Wiley-Interscience: London.
- Matesich, M. A.; Nadas, J. A.; and Evans, D. F. J. Phys. Chem. 1970, 74, 4568-4573.
- Mathai, K. G.; Ottewill, R. H. a: Trans. Faraday Soc. 1966, 62, 750-759; b: Trans. Faraday Soc. 1966, 62, 759-769.
- Matthijs, E.; De Henau, H. Tenside Detergents 1985, 22, 299-304.
- McEvoy, J.; Giger, W. Naturwissenschaften. 1985, 72, 429-431.
- Monica, M. D.; Ceglie, A.; and Acostiano, A. Electrochimica Acta 1984, 29, 161.
- Narkis, N.; Bella, B. Water Res. 1985, 19, 815-824.
- Nodvin, S. C.; Driscoll, C. T.; Likens, G. E. Soil Sci. 1986, 142, 69-75.
- Okubo, T. J. of Coll. Interfac. Sci. 1988, 125, 380-385.
- Ono, K.; Konami, H.; and Murakami, K. J. Phys. Chem. 1979, 83, 2665-2669.

- Papadopoulos, G. P. N. and Jannakoudakis, D. Electrochimica Acta 1985, 30, 431-433.
- Pilarczyk, M. and Klinszporn, L. Electrochimica Acta 1986, 31, 185-192.
- Pitzer, K. S. and Mayorga, G. J. Phys. Chem. 1975, 77, 2300-2308.
- Platikanov, D.; Weiss, A.; Lagaly, G. Colloid Polymer Sci. 1977, 255, 907-915.
- Podoll, R. T.; Irwin, K. C.; Brendlinger, S. Environ. Sci. Technol. 1987, 21, 562-568.
- Popovych, O. and Tomkins, R. P. T. Nonaqueous Solution Chemistry; 1981, Wiley-Interscience: New York.
- Reneau, R. B. Jr.; Pettry, D. E. J. Environ. Qual. 1975, 4, 370-375.
- Riddick, J. A.; and Bunger, W. B. Organic Solvents; Wiley-Interscience: New York, 1970.
- Robeck, G. G.; Cohen, J. M.; Sayers, W. T.; Woodward, R. L. Journal WPCF. 1963, 35, 1225-1236.
- Robison, R. A.; Stokes, R. H. Electrolyte Solutions; Butterworths: London, 1968.
- Rosen, M. J. "Surfactants and Interfacial Phenomena"; 1978, John Wiley & Sons.
- Rosky, P. J.; Dudowicz, J. B.; Tembe, B. L.; and Friedman, H. L. J. Chem. Phys. 1980, 73, 3372.
- Sakata, K.; Katayama, A. J. Coll. Interface Sci. 1987, 116, 177-181.
- Sakata, K.; Katayama, A. J. Coll. Interface Sci. 1988, 123, 129-135.
- Sales, D.; Quiroga, J. M.; Gomez-Parra, A. Bull. Environ. Contam. Toxicol. 1987, 39, 385-392.
- Salomon M. and Plichta, E. J. Electrochimica Acta 1985, 30, 113-119.
- Savitsky, A. C.; Wiers, B. H.; Wendt, R. H. Environ. Sci. & Tech. 1981, 15, 1191-1196.
- Scaemhorn, J. F.; Schechter, R. S.; Wade, W. H. J. Coll. Interfac. Sci. 1982, 85, 463-501.

- Schellenberg K.; Leuenberger, C.; Schwarzenbach R. P. Environ. Sci. Technol. 1984, 18, 652-657.
- Scheunert, I.; Vockel, D.; Schmitzer, J. Chemosphere 1987, 16, 1031-1041.
- Schwarzenbach, R. P.; Westall, J. Environ. Sci. Technol. 1981, 15, 1360-1367.
- Schwuger, M. J.; von Rybinsk, W.; Krings, P. "Adsorption from Solution"; Ottewill, R. H.; Rochester, C. H.; Smith, A. L., Eds.; Academic Press: New York, 1983, 185-196.
- Sedlak, R. I.; Booman, K. A. SDA Annual Convention. 1986.
- Shaw, D. J.; Electrophoresis 1969, Academic Press, New York and London.
- Shedlovsky, T. and Kay, R. L. J. Phys. Chem. 1956, 60, 151-155.
- Shoemaker, D. P.; Garland, C. W.; Nibler, J. W. Experiments in Physical Chemistry; fifth Ed.; McGraw-Hill Book Company, 1989.
- Sieglauff, C. L.; Mazur J. J. Colloid Sci. 1960, 15, 437.
- Sieglauff, C. L.; Mazur J. J. Colloid Sci. 1962, 17, 66-85.
- Singh, B. R. Soil Sci. 1984, 138, 346-353.
- Siracusa, P. A.; Somasundaran, P. J. Coll. Interface Sci. 1987, 120, 100-109.
- Sjoblom, J. Finn. Chem. Lett. 1979, 245.
- Sjoblom, J. and Dyhr, H. Acta Chemica Scandinavica A 1981, 35, 219.
- Soehnel, O. and Novatny, P. Densities of Aqueous Solutions of Inorganic Substances; 1985, Elsevier: Amsterdam.
- Somasundaran, P.; Fuerstenau, D. W. J. Phys. Chem. 1966, 70, 90-96.
- Spivey, H. O. and Shedlovsky, T. J. Phys. Chem. 1967, 71, 2165-2171.
- Sposito, G. The Surface Chemistry of Soils. 1986. Oxford University Press: New York.
- Starkey, H. C.; Blackmon, P. C.; Hauff, P. L. "The Routine Mineralogical Analysis of Clay-Bearing Samples", U.S. Geological Survey Bulletin 156, 1981.
- Sukhotin, A. M. and Timofeeva, Z. N. Zhur. Fiz. Khim. 1959, 33, 1602.

- Tanaka, N. and Harada, K. Electrochimica Acta 1976, 21, 615.
- Tartar, H. V.; Lelong, A. L. M. J. Phys. Chem. 1955, 59, 1185.
- Thurman, E. M.; Barber, L. B. Jr.; LeBlanc, D. Journal of Contaminant Hydrology 1986, 1, 143-161.
- Tissier, M. and Douheret, G. J. of Soln. Chem. 1978, 7, 87-98.
- Turner, A. H.; Abram, F. S.; Brown, V. M.; Painter, H. A. Water Res. 1985, 19, 45-51.
- Urano, K.; Saito, M. Chemosphere 1984, 13, 285-292.
- Urano, K.; Saito, M.; Murata, C. Chemosphere 1984, 13, 293-300.
- van den Boomgaard, Th.; Tadros, Th. F.; Lyklema, J. J. Coll. Interface Sci. 1987, 116, 8-16.
- van Os, N. M.; Daane, G. J.; and Bolsman, T. A. B. J. Coll. Interfac. Sci. 1987, 115, 402-409.
- van Senden, K. G.; Koning, J. Fette Seifen Anstrichm. 1968, 70, 36.
- Veith S. D.; Macek, D. J.; Petrocelli, S. R.; Carroll, J. Aquatic Toxicology, Eaton J. G., Passish P. R., Hendricks A. C., Eds; ASTM STP 707, 1980.
- Vilcu, R.; Olteanu, M.; Revue Roumaine de Chimie 1975, 20, 1041-1060.
- Volk, V. V.; Jackson, M. L. Journal WPCF 1968, 40, 205-213.
- Wakamatsu, T.; Fuerstenau, D. W. Adv. Chem. Ser. 1968, 79, 161.
- Wellington, S. L. and Evans, D. F. J. of Soln. Chem. 1983, 12, 815-828.
- Westall, J. Properties of Organic Compounds in Relation to Chemical Binding in Biofilm Processes in Ground Water Research, The Ecological Research Committee of the NFR, Stockholm. pp 65-90. 1984
- Westall, J. C.; Leuenberger, C.; Schwarzenbach, R. P. Environ. Sci. Technol. 1985, 19, 193-198.
- Westall, J. C. FITEQL - A Computer Program for Determination of Chemical Equilibrium Constants from Experimental Data. Version 1.2. Report 86-01, Department of Chemistry, Oregon State University, Corvallis, OR, 1986.
- Westall, J. C. MICROQL-A Chemical Equilibrium Program in BASIC. Version 2 for PC's. Report 86-02, Department of Chemistry, Oregon State University, Corvallis, OR, 1986.

Westall, J. in Geochemical Processes at Mineral Surfaces, Davis, J.; Hayes, K., Eds.; Symposium Series No. 323, American Chemical Society, Washington, D.C. 1986.

Westall, J. in Aquatic Surface Chemistry, W. Stumm, Ed., Wiley: New York, 1987.

Westall, J.; Chen, H.; Zhang, W.; Brownawell, B. Final report to the Soap and Detergent Association, 1989.

Westall, J. C.; Johnson, C. A.; Zhang, W. Environ. Sci. Technol. 1990, 24, 1803-1810.

Wiersema, P. H.; Loeb, A. L.; Overbeek, J. Th. J. Colloid Interface Sci. 1966, 22, 78.

Woodbury, G. W. Jr.; Noll, L. A. Colloids and Surfaces 1988, 33, 301-319.

Yamane, A. N.; Okada, M.; Sudo, R. Water Res. 1984, 18, 1101-1105.

## APPENDICES

## APPENDIX I

A BASIC LANGUAGE PROGRAM

FOR EXPERIMENTAL CONTROL, DATA COLLECTION, AND DATA ANALYSIS

BY PC - LOCK-IN AMPLIFIER SYSTEM

```

1 REM PROGRAM PC-5301L.BAS
2 REM *****
3 REM **          A BASIC LANGUAGE PROGRAM          **
4 REM **    FOR EXPERIMENTAL CONTROL, DATA COLLECTION, AND DATA ANALYSIS    **
5 REM **          BY PC - LOCK-IN AMPLIFIER MEASUREMENT SYSTEM          **
6 REM **                                                                 **
7 REM **          By      Wanjia Zhang          **
8 REM **    Department of Chemistry at Oregon State University          **
9 REM **          July 15, 1987          **
10 REM *****
11 REM 0). With different delay loop (longer loop at low frequency).
12 REM 1). Set,get Freq. X. Y.& Pha at equilibrium from 5Hz to 5KHz by delay loop
13 REM 2). OSC amplitude is set at 0.5 V, no overload, sensitivity = 0.5 V
14 REM 3). Data can be saved on drive B and line print out.
15 REM 4). X & Y TC = 10 s as F < 50 Hz;
16 REM      X & Y TC = 1.0 s as 50 Hz < F < 100 Hz;
17 REM      X & Y TC = 300 ms as 100 Hz < F < 500 Hz;
18 REM      X & Y TC = 100 ms as 500 Hz < F < 5000 Hz
19 REM 5). Give music to indicate the end of measurement
20 REM Controls PAR 5301 via National GPIB 2A
21 DEFDBL A-Z
22 REM Default drive must contain
23 REM      BIB.M
24 REM Boot Disk must contain
25 REM      GPIB.COM
26 REM      DEV=GPIB.COM on CONFIG.SYS
27 REM      GPIB.COM must be version modified with IBCONF.EXE to place DEV2 at 5
28 REM Function
29 REM      Check Status of GPIB, 5301
30 REM      Initialize 5301
31 REM      Enter Command Mode
32 REM      Use CAPS LOCK ***** !!!!!!!! for all command input
33 REM      Handshaking via 5301 Status Byte obtained through Serial Poll
34 REM      Enter QUIT to return PAR 5301 to local and exit command mode
35 REM      Enter INIT to clear PAR 5301 to initial state
36 REM References
37 REM      GPIB Status Word: p. 4-3, GPIB-PC Manual
38 REM      5301 Status Byte: p. VI-4, 5301 Manual
39 REM      5301 Command Set: Plastic card or Section IX of 5301 Manual
40 CLEAR,59000!
41 IBINIT1 = 59000!
42 IBINIT2 = IBINIT1 + 3
43 BLOAD "bib.m",IBINIT1
44 CALL IBINIT1(IBFIND,IBTRG,IBCLR,IBPCT,IBSIC,IBLOC,IBFPC,IBBNA,IBONL,IBRSC,IB
SRE,IBRSV,IBPAD,IBSAD,IBIST,IBDMA,IBEOS,IBTMO,IBEOT,IBRDF,IBWRTF)
45 CALL IBINIT2(IBGTS,IBCAC,IBWAIT,IBPOKE,IBWRT,IBWRTA,IBCMD,IBCMDA,IBRD,IBRDA,
IBSTOP,IBRPP,IBRSP,IBDIAG,IBXTRC,IBRDI,IBWRTI,IBRDIA,IBWRTIA,IBSTAX,IBERRX,IBCNT
X)
46 REM Begin Basic Program Here; Initialize Bus, Instrument *****
47 DIM F(50),NUM(50),FREQ(50),FREN(50),FREV(50),X(50),Y(50),PHA(50),XAMPEA(50),
YAMPEA(50),PHAEA(50),RE(200),IM(200),RP(50),XCP(50),C(50),ZIN(50),A(50),B(50),ZC
ELL(50),FREQUENC(50)
48 NA$="GPIB0" : CALL IBFIND(NA$,BD%)
49 NA$="DEV2" : CALL IBFIND(NA$,PAR%)
50 GOSUB 800 'GPIB STATUS
51 GOSUB 900 '5301 STATUS

```

```

126 IF SPRX<=0 THEN BEEP : STOP : ELSE
127 PRINT "INITIAL STATUS CHECK SUCCESSFUL" : PRINT
140 REM set input EA file, output EA-B file and calculation file *****
142 CLS
144 PRINT "Give three file names for EA, EA-B, and calculation: " : PRINT
145 INPUT INFILE$, OUTFIL$, CALFIL$
146 A$ = "B:" + INFILE$ : B$ = "B:" + OUTFIL$ : C$ = "B:" + CALFIL$
150 OPEN A$ FOR INPUT AS #1
152 OPEN B$ FOR OUTPUT AS #2
154 OPEN C$ FOR OUTPUT AS #3
156 FD$ = "#####          ##.###          ##.###          ###.## ":'set measuri
ng data format
158 FC$=" ##### ##.####^ ^ ^ ^ ##.####^ ^ ^ ^ ##.####^ ^ ^ ^ ##.####^ ^ ^ ^ ##.####^ ^ ^ ^ ##.##
# ##.###"
160 INPUT #1, TIT$, TIT2$
162 IDAT% = 0
164 WHILE NOT EOF(1) : IDAT%=IDAT%+1
166 INPUT #1, I, FREQ(IDAT%), XAMPEA(IDAT%), YAMPEA(IDAT%), PHAEA(IDAT%)
168 WEND
169 CLOSE #1
170 NDAT% = IDAT%
175 MEASNUM = 1
176 GOSUB 4000 : ' Set frequency data (Freq. = 5Hz -- 5KHz)
177 DOA = 110 : ROA = 0
178 GOSUB 4150 : ' Set amplitude of OSC (OA = 110 uV)
179 ' before starting the measurement
180 CLS
182 PRINT "The program started at " TAB(56); DATE$; TAB(71);: PRINT TIME$
184 PRINT
186 PRINT " The measurement will start after 5 mins to approach temperature
188 PRINT " of solution at 25C."
190 ON TIMER (300) GOSUB 270
192 TIMER ON
194 N = 0
196 WHILE N < 1
198 WEND
199 GOTO 280
200 REM set TIMER to repeat measurement every 30 mins to reach equil. *****
210 OPEN B$ FOR OUTPUT AS #2
220 OPEN C$ FOR OUTPUT AS #3
240 MEASNUM = MEASNUM + 1
250 ON TIMER (1800) GOSUB 270
252 TIMER ON
254 N = 0
256 WHILE N < 1
258 WEND
260 GOTO 280
270 N = N + 1
275 RETURN
280 REM ***** start measurment *****
281 CLS
282 PRINT " Now start the measurement." : PRINT
283 GOSUB 1000 : ' Clear PAR 5301
285 GOSUB 4100 : ' Set sensitivity = 500 mV
286 DOA=500 : ROA=3 : GOSUB 4150 : ' Set amplitude of OSC ( OA = 500 mV )
288 NXTC = 8 : GOSUB 4180 : ' Set X, Y TC = 10 s as F ( 50 Hz

```

```

294 FOR IDATX=1 TO NDATA : GOSUB 4200 : 'setting frequency command to 5301
295 NUMVAL = 4
296 IF FLAG(0) = 1 THEN GOTO 500: 'send wanting F,X,Y,PHA command to 5301
297 IF FLAG(7) = 1 THEN GOTO 600: 'get F,X,Y,PHA responses from 5301
300 REM Control via Serial poll *****
310 GOSUB 900 'SERIAL POLL TO GET STATUS BYTE AND FLAGS
410 IF FLAG(1) = 1 THEN PRINT "*** BAD COMMAND (Caps Lock?)" :PRINT:BEEP:ELSE
420 IF FLAG(3) = 1 THEN PRINT "*** UNLOCKED " :PRINT:BEEP:ELSE
430 IF FLAG(4) = 1 THEN PRINT "*** OVERLOADED " :PRINT:BEEP:ELSE
440 IF FLAG(5) = 0 THEN PRINT "*** UNAUTOED " :PRINT:BEEP:ELSE
450 IF FLAG(6) = 1 THEN PRINT "*** SRQ " :PRINT:BEEP:ELSE
460 IF FLAG(0) = 1 THEN 500 'get command to be sent
470 IF FLAG(7) = 1 THEN 600 'read 5301
490 GOTO 300
500 REM Send a command to 5301 for getting response *****
510 IF NUMVAL = 4 THEN GOSUB 3000: 'Send want read F command to 5301
520 IF NUMVAL = 3 THEN A$ = "X" : 'Send want read X command to 5301
530 IF NUMVAL = 2 THEN A$ = "Y" : 'Send want read Y command to 5301
531 IF NUMVAL = 1 THEN A$ = "PHA": 'Send want read PHA to 5301
535 NUMVAL = NUMVAL -1
540 CALL IBWRT (PAR%,A$)
550 PRINT ". ",TAB(40),"Command ";A$; " sent to PAR 5301.": PRINT
595 GOTO 600
600 REM Get a reply from 5301 really *****
610 Z$ = SPACE$(30)
620 CALL IBRD(PAR%,Z$) : ' Get response from 5301
630 IF NUMVAL+1= 4 THEN GOTO 3020 : ' Change F to users unit
640 IF NUMVAL+1= 3 THEN GOTO 3100 : ' Change X to users unit
650 IF NUMVAL+1= 2 THEN GOTO 3200 : ' Change Y to users unit
651 IF NUMVAL+1= 1 THEN GOTO 3300 : ' Change PHA to users unit
655 IF IDATX=8 THEN NXTC=6 : GOSUB 4180: 'set X, Y TC= 1 s as 50 Hz(F<100 Hz
656 IF IDATX=13 THEN NXTC=5 : GOSUB 4180: 'set X, Y TC=0.3s as 100 Hz(F<500 Hz
657 IF IDATX=19 THEN NXTC=4 : GOSUB 4180: 'set X,Y TC=0.1s as 500 Hz(F<5000 Hz
660 IF NUMVAL +1 = 0 THEN NEXT IDATX
690 IF IDATX = NDATA THEN GOTO 295
700 REM one measurement stoped here, set OA = 110 uV *****
710 DOA = 110 : ROA = 0
720 GOSUB 4150 : ' Set amplitude of OSC (OA = 110 uV)
730 ' between the two measurements
750 GOTO 5000 : ' for calculation
800 REM Status word decoding *****
805 PRINT "GPIB STATUS WORD"
810 FOR IX = 0 TO 15 : PRINT USING " \\";HEX$(IX); : NEXT : PRINT
820 FOR IX = 0 TO 14 : PRINT (IBSTAX AND 2^IX)/2^IX; : NEXT
830 IF IBSTAX< 0 THEN IX=1 ELSE IX=0 : PRINT IX
840 PRINT
890 RETURN
900 REM Serial poll *****
905 PRINT "PAR 5301 STATUS BYTE"
910 CALL IBRSP(PAR%,SPR%)
930 FOR IX = 0 TO 7 : PRINT USING " \\";HEX$(IX); : NEXT : PRINT
940 FOR IX = 0 TO 7 : FLAG(IX)=(SPR% AND 2^IX)/2^IX : NEXT
950 FOR IX = 0 TO 7 : PRINT FLAG(IX); : NEXT : PRINT
960 PRINT
990 RETURN
1000 REM Device Clear (set initial parameters) for PAR 5301 *****

```

```

1010 CALL IBCLR(PAR%)
1020 GOSUB 800
1030 GOSUB 900
1050 PRINT "PAR 5301 CLEARED" : PRINT
1090 RETURN
3000 REM change frequency to user's unit *****
3010 A$="OF": N = 1 : GOSUB 900 :RETURN
3020 IF N = 1 THEN FREQ(IDAT%)= VAL(Z%)
3040 N = N - 1
3050 IF N<>0 THEN GOTO 300
3060 FREQ(IDAT%) = FREQ(IDAT%)/1000*(10^NUM(IDAT%))
3065 PRINT TAB(43) "Frequency is: " FREQ(IDAT%) ;: PRINT "Hz"
3070 GOSUB 900
3080 GOTO 296
3100 REM change X to user's unit *****
3115 GOSUB 3500: 'set time control for reading x-output
3120 X(IDAT%) = VAL(Z%)
3130 X(IDAT%) = X(IDAT%)/32*.001
3165 PRINT TAB(43) "X -output is: " ;: PRINT USING "##.###";X(IDAT%) ;:PRINT "
V"
3175 PRINT
3180 GOTO 500
3200 REM change Y to user's unit *****
3220 Y(IDAT%) = VAL(Z%)
3230 Y(IDAT%)=Y(IDAT%)/32*.001
3265 PRINT TAB(43) "Y -output is: " ;: PRINT USING "##.###";Y(IDAT%);:PRINT " V
"
3270 PRINT
3280 GOTO 500
3300 REM change PHA to user's unit *****
3320 PHA(IDAT%) = VAL(Z%)
3330 PHA(IDAT%)=PHA(IDAT%)/10
3365 PRINT TAB(43) "Phase angle is: " ;: PRINT USING "###.##";PHA(IDAT%)
3370 PRINT
3380 GOTO 500
3500 REM delay loop,comparing two x values for equilibrium *****
3505 GOTO 3600 :' read first x value
3510 GOSUB 3700 :' delay loop
3520 GOTO 3600 :' read next x value, compare x with x1
3540 RETURN
3600 REM Subroutine to read x-output *****
3610 CALL IBWRT (PAR%,A%)
3620 Z$ = SPACE$(30) : CALL IBRD (PAR%,Z%)
3630 XAMP=VAL(Z%) : XAMP = XAMP/160
3640 IF ABS(XAMP1-XAMP)=.2 THEN GOTO 3540
3650 XAMP1 = XAMP
3670 GOTO 3510
3700 REM delay loop
3710 PRINT "Delay Loop" : PRINT
3725 FOR CNT = 1 TO NCNT
3730 NEXT
3740 RETURN
4000 REM Set frequency data *****
4030 FOR IDAT% = 1 TO NDATA : READ F(IDAT%) : NEXT
4040 DATA 5000,7000,10000,1500,2000,2500,3000,4000,5000,7000,8000,9000,10000,150
0,2000,2700,4000,5000,6400,8000,10000,1240,1400,1600,1700,1830,2000,3100,4400,50

```

```

00,6100,7000,8000,9200,1000,2000,3100,4400,5000,6100,7000,8000,9200,10000
4045 FOR IDAT% = 1 TO NDAT% : READ NUM(IDAT%) : NEXT
4050 DATA 0,0,0,1,1,1,1,1,1,1,1,1,1,2,2,2,2,2,2,2,3,3,3,3,3,3,3,3,3,3,3,4,
4,4,4,4,4,4,4,4,4
4052 FOR IDAT%=1 TO NDAT% : READ FREQUENC(IDAT%) : NEXT
4054 DATA 5,7,10,15,20,25,30,40,50,70,80,90,100,150,200,270,400,500,640,800,1000
,1240,1400,1600,1700,1830,2000,3100,4400,5000,6100,7000,8000,9200,10000,20000,30
000,44000,50000,61000,70000,80000,92000,100000
4060 RETURN
4100 REM Send setting sensitivity command to 5301 *****
4105 RSEN = 20 : RSEN$ = STR$(RSEN)
4110 A$ = "SEN" + RSEN$ : ' set sensitivity = 500 mV
4120 GOTO 4230
4150 REM Send setting amplitude of OSC command to 5301 *****
4155 DOA$=STR$(DOA) : ROA$=STR$(ROA)
4160 A$ = "OA" + DOA$ + ROA$ : 'set amplitude of OSC equal to 0.5V
4170 GOTO 4230
4180 REM Send setting X,Y time constan command to 5301 *****
4195 NXTC$ = STR$(NXTC)
4196 A$ = "XTC" + NXTC$ : ' set X output time constant command
4197 GOTO 4230
4200 REM Send setting frequency command to 5301 *****
4205 FREQ$ = STR$(F(IDAT%)) : NUM$ = STR$(NUM(IDAT%))
4210 A$ = "OF" + FREQ$ + NUM$
4220 N = 2
4230 CALL IBWRT(PAR%,A%)
4235 PRINT ". ",TAB(40),"Command ";A$; "sent to PAR 5301.": PRINT
4236 IF IDAT% = 1 THEN NCNT=12000 : GOSUB 3700
4237 IF IDAT% = 2 THEN NCNT=12000
4238 IF IDAT% = 8 THEN NCNT= 8000
4239 IF IDAT% = 18 THEN NCNT= 4000
4240 GOSUB 900 'check serial poll to get status byte and flags
4250 IF FLAG(3) = 1 THEN GOTO 4240: PRINT "*** UNLOCKED" :PRINT :BEEP:ELSE
4260 IF FLAG(4) = 1 THEN GOTO 4240: PRINT "*** OVERLOADED" :PRINT :BEEP:ELSE
4270 RETURN
5000 REM calculation of Rp for different Frea. and Rp Ave. from 5-100 Hz *****
5010 CLS
5020 PRINT " Now start the calculation." : PRINT
5100 PI = 3.14159
5110 RM = 50000#
5120 RIN = 100000000# : CIN = .00000000017# :
5130 FOR IDAT% = 1 TO NDAT%
5140 W = 2*PI*FREQUENC(IDAT%)
5150 RE(12)=RM : IM(12)=0
5160 RE(11)=RIN : IM(11)=0
5170 RE(21)=0 : IM(21)=-1/(CIN*W)
5180 RE(41)=XAMPEA(IDAT%) : IM(41)=YAMPEA(IDAT%)
5190 RE(43)=X(IDAT%) : IM(43)=Y(IDAT%)
5200 I=21 : J=11 : K=51 : GOSUB 6600
5210 I=51 : J=12 : K=52 : GOSUB 6600
5230 I=41 : J=43 : K=42 : GOSUB 6200
5240 I=42 : J=52 : K=32 : GOSUB 6400
5250 I=43 : J=32 : K=53 : GOSUB 6400
5260 I=52 : K=62 : GOSUB 6500
5270 I=53 : K=63 : GOSUB 6500
5280 I=62 : K=72 : GOSUB 6700

```

```

5290 I=63 : K=73 : GOSUB 6700
5300 RP(IDATX)=1/RE(63) : XCP(IDATX)=1/IM(63)
5310 C(IDATX)=1/(XCP(IDATX)*W)
5320 ZIN(IDATX)=1/RE(72) : ZCELL(IDATX)=1/RE(73)
5330 A(IDATX)=LOG(FREQUENC(IDATX))/LOG(10) : B(IDATX)=LOG(ABS(ZCELL(IDATX)))/LOG(10)
5335 PRINT USING FC$; FREQUENC(IDATX), RP(IDATX), XCP(IDATX), C(IDATX), ZIN(IDATX), ZCELL(IDATX), A(IDATX), B(IDATX)
5340 NEXT
5400 NX = 13 : RPSUM = 0
5410 FOR IDATX= 1 TO NX
5420 RPSUM = RP(IDATX) + RPSUM
5430 NEXT
5440 RPAVE = RPSUM/13
5442 NCX = 7 : RPSUM1 = 0
5443 FOR IDATX= 1 TO NCX
5444 RPSUM1 = RP(IDATX) + RPSUM1
5446 NEXT
5448 RPAVE1 = RPSUM1/7/.078
5450 RP = RPAVE/.078
5460 ERP = ABS((RP1-RP)/((RP1+RP)/2))
5500 GOSUB 9100
5600 GOTO 8000 : ' for printing out data files
6100 REM add *****
6110 RE(K)=RE(I)+RE(J)
6120 IM(K)=IM(I)+IM(J)
6130 RETURN
6200 REM subtract *****
6210 RE(K)=RE(I)-RE(J)
6220 IM(K)=IM(I)-IM(J)
6230 RETURN
6300 REM multiply *****
6310 RE(K)=RE(I)*RE(J)-IM(I)*IM(J)
6320 IM(K)=RE(I)*IM(J)+IM(I)*RE(J)
6330 RETURN
6400 REM divide *****
6410 RE(K)=(RE(I)*RE(J)+IM(I)*IM(J))/(RE(J)*RE(J)+IM(J)*IM(J))
6420 IM(K)=(-RE(I)*IM(J)+IM(I)*RE(J))/(RE(J)*RE(J)+IM(J)*IM(J))
6430 RETURN
6500 REM inverse *****
6510 RE(K)=RE(I)/(RE(I)*RE(I)+IM(I)*IM(I))
6520 IM(K)=-IM(I)/(RE(I)*RE(I)+IM(I)*IM(I))
6530 RETURN
6600 REM add parallel impedance *****
6610 II=I : JJ=J : KK=K
6620 I=II : K=1 : GOSUB 6500
6630 I=JJ : K=2 : GOSUB 6500
6640 I=1 : J=2 : K=3 : GOSUB 6100
6650 I=3 : K=KK : GOSUB 6500
6660 RETURN
6700 REM polar coordinates *****
6710 RE(K)=SQR(RE(I)*RE(I)+IM(I)*IM(I))
6720 IM(K)=ATN(IM(I)/RE(I))*180/PI
6730 RETURN
8000 REM print out the measurement data *****
8200 CLS

```

```

8210 PRINT "      Now print out the measured and calculated data."
8220 LPRINT "THE NUMBER OF MEASUREMENT: "; MEASNUM; TAB(56); DATE$; TAB(71);:LPR
INT TIME$
8230 LPRINT "DATA FILE: ";OUTFIL$ :LPRINT
8240 LPRINT "Instrument:      CORONA-5301 Lock-in Amplifier"
8250 LPRINT "Program:        PC-5301L.BAS"
8260 LPRINT "Interface:      GPIB Interfacing" : LPRINT
8270 LPRINT "----- INSTRUMENT STATUS -----"
8280 LPRINT "Input Filter:      FLAT "
8290 LPRINT "Reference Mode:      INT F"
8300 LPRINT "OSC Amplitude:      500 mV"
8310 LPRINT "Sensitivity:        500 mV"
8320 LPRINT "AVG. Mode:          EXP "
8330 LPRINT "DYN. RES :          20 dB"
8340 LPRINT "X & Y Time Constant: TC = 10 s as F < 50 Hz; "
8350 LPRINT "                      TC = 1.0 s as 50 Hz < F < 100 Hz;"
8360 LPRINT "                      TC = 300 ms as 100 Hz < F < 500 Hz;"
8370 LPRINT "                      TC = 100 ms as 500 Hz < F < 100 KHz"
8380 LPRINT "X & Y 6/12 dB/OCT:    6 dB/OCT"
8390 LPRINT "X & Y OFFSET:        OFF "
8400 LPRINT "Y EXPAND:            x 1 "
8410 LPRINT "-----": LPRINT
8420 LPRINT TIT$ : LPRINT TAB(8) TIT2$
8430 FOR IDAT% = 1 TO NDATA
8440 LPRINT IDAT%;TAB(10);: LPRINT USING FD$; FREQUENC(IDAT%),X(IDAT%),Y(IDAT%),
PHA(IDAT%)
8450 NEXT IDAT%
8460 LPRINT CHR$(12) : LPRINT
8500 REM print out calculation results *****
8510 LPRINT "THE NUMBER OF MEASUREMENT: "; MEASNUM; TAB(56); DATE$; TAB(71);:LPR
INT TIME$ : LPRINT
8520 LPRINT "ORIGINAL DATA FILES: ";INFILEA$; TAB(33); OUTFIL$ : LPRINT
8530 LPRINT "CALCULATED DATA FILE: "; CALFIL$ : LPRINT : LPRINT
8540 F$="      FREQ      RP      XCP      C      ZIN      ZCELL      LOG(F
) LOG(Zc)"
8550 LPRINT F$ : LPRINT
8565 FOR IDAT% = 1 TO NDATA
8570 LPRINT USING FC$; FREQUENC(IDAT%),RP(IDAT%),XCP(IDAT%),C(IDAT%),ZIN(IDAT%),
ZCELL(IDAT%),A(IDAT%),B(IDAT%)
8580 NEXT
8590 LPRINT : LPRINT : LPRINT : LPRINT
8600 LPRINT " The measuring and calculation program:      PC-5301L.BAS"
8610 LPRINT " The measuring resistor Rm:      50 kilohm "
8620 LPRINT " The capacitance Cin:      170 pF "
8640 LPRINT : LPRINT
8685 LPRINT CHR$(12) :LPRINT
8690 CLS
8700 PRINT "The timer started to work at" TAB(40) DATE$;TAB(55);:PRINT TIME$:PRI
NT
8710 PRINT "This program repeats the measurement every 30 mins until 8 hours pas
s."
8715 PRINT
8720 PRINT "The next measurement will be the ";MEASNUM+1 ;:PRINT "th. measuremen
t. "
8730 REM check number of measurements then save files, stop *****
8740 IF MEASNUM = 1 THEN GOTO 9000 : 'save data files and stop

```

```

8750 RP1 = RP
8800 GOTO 200
9000 REM **** save measured and calculated data in Drive B *****
9005 CLS
9020 PRINT "      Now save the measured and calculated data in Drive B."
9030 PRINT "      The measured data file name is:      "; OUTFIL$
9040 PRINT "      The calculated data file name is:      "; CALFIL$
9050 PRINT
9070 GOTO 9400
9100 REM save measured data *****
9110 PRINT #2,TIT$,TIT2$
9120 FOR IDAT% = 1 TO NDAT%
9130 PRINT #2,IDAT% ;PRINT #2,TAB(10);:PRINT#2,USING FD%; FREQUENC(IDAT%),X(IDAT
%),Y(IDAT%),PHA(IDAT%)
9140 NEXT IDAT%
9200 REM save calculated data *****
9210 PRINT #3,F$,TIT2$
9220 FOR IDAT% = 1 TO NDAT%
9230 PRINT #3,USING FC%; FREQUENC(IDAT%),RP(IDAT%),XCP(IDAT%),C(IDAT%),ZIN(IDAT%
%),ZCELL(IDAT%),A(IDAT%),B(IDAT%)
9240 NEXT IDAT%
9250 CLOSE
9260 RETURN
9400 REM Return PAR 5301 to Local *****
9410 CALL IBLOC(PAR%)
9420 GOSUB 800
9430 GOSUB 900
9440 PRINT "PAR 5301 RETURNED TO LOCAL; IT IS THE END OF THE MEASUREMENT.":PRINT
9500 REM Give music to indicate the end of measurement *****
9510 I = 0
9520 I = I + 1
9530 SOUND 300,5: SOUND 400,5 : SOUND 500,5
9540 IF I = 4 THEN GOTO 9560
9550 GOTO 9520
9560 SOUND 600,50
9999 STOP

```

## APPENDIX II

X-RAY IDENTIFICATION FOR CLAY MINERALS IN ENVIRONMENTAL MATERIALS

### X-ray identification for clay minerals in environmental materials

Qualitative analysis of clay minerals is performed by x-ray diffraction. The principles of the technique are discussed by Shoemaker et al., (1989).

Several methods (described in Chapter 4) have been used to pretreat the clays before x-ray analysis. The purpose of these treatments is to orient the aggregates of the clays and to provide a means of distinguishing one clay from another. Typically, the information from an x-ray spectrum is diffraction spacing, known as D spacing in units of Å, and the Bragg angle, known as  $2\theta$  in units of degrees.

#### Standard D spacings of common clays for x-ray identification.

For some common clays, their standard D spacings and their responses to the treatments are described as follows (Starkey et al. 1981; Carroll, 1970):

(a) Chlorite (or Vermiculite). The typical D spacings (order #) are: 14.2 Å (1); 7.0 - 7.2 Å (2); 3.52 - 3.58 Å (4) for chlorite; 3.50 - 3.55 Å (4) for vermiculite.

For chlorite, the intensity and position of all of these peaks do not change with temperature, however, the 14 Å peak of vermiculite collapses to 10 Å upon heating to 550 °C. Some poorly crystalline chlorite and/or vermiculite samples have been known to become amorphous upon heat treatment. There would be no effect of  $K^+$  or  $Mg^{2+}$  treatment and no effect of  $Mg^{2+}$  ethylene glycolated treatment on the D spacing for both types of clays.

(b) Illite (or Micas). The typical D spacings (order #) are: 10.0 Å (1); 5.0 Å (2); 3.3 Å (3); and 4.45 - 4.60 Å (110 peak).

The heat treatment has no effect on the densities of these peaks. Neither  $K^+$  heat treatment nor  $Mg^{2+}$  ethylene glycolated would affect the D spacing of the peaks. It should be mentioned here that quartz has peaks at 3.34 Å and 4.26 Å, therefore be sure to check the peak at 4.26 Å to distinguish illite peak from quartz peak.

(c) Kaolinite. The typical D spacings (order #) are: 7.2 Å (1); 3.57 - 3.58 Å (2).

The peaks at 7.2 Å as well as 3.57 - 3.58 Å are destroyed at 550 °C. This is a typical phenomenon to distinguish the second order peak of chlorite from the first order peak of kaolinite. There would be no effect of  $Mg^{++}$  glycolated treatment on the D spacings of kaolinite.

(d) Smectite. The typical and specific observations for smectite are that there is a peak at about 14 Å for  $Mg^{2+}$  air dry treatment, and this peak shifts to about 16 - 18 Å by  $Mg^{2+}$  glycolated treatment. Also  $K^+$  air dry peak of smectite at 13 - 14 Å collapses to 10 Å upon heating to 550 °C.

Results of clay mineral analysis for environmental materials. A total of 6 x-ray diffraction spectra scans were run for each sample on the slides of  $K^+$  and  $Mg^{2+}$ , and the ID of the runs were KAD, K110C, K350C, K550C, MGAD, MGGLY regarding to their treatments (see Figure 4.2b). The D spacings and intensities of the peaks for the six samples are listed in Table II. 1 a-f. The tables are arranged in terms of the types of clays and the treatment, therefore, the clay compositions in each sample can be easily recognized. The

information of clay mineral compositions in the samples is summarized in Table II.2. Kaolinite and illite are found to be the major components of the clays in all of the six samples, smectite is found in a large amount in soils EPA-1 and EPA-25.

Table II.1a Results of x-ray identification for clay minerals in soil EPA-1.

<u>D Spacing Å (Intensity cps)</u>						
<u>SLIDE ID:</u>	<u>KAD</u>	<u>K110</u>	<u>K350</u>	<u>K550</u>	<u>MGAD</u>	<u>MGGLY</u>
<u>KAOLINITE</u>						
order#1	7.14(51)	7.14(58)	7.14(47)	7.11(21)	7.14(61)	7.14(45)
order#2	3.59(23)	3.58(25)	3.58(31)		3.56(28)	3.54(25)
<u>ILLITE</u>						
order#1	10.13(37)	10.13(48)	10.03(51)	10.03(60)	10.13(42)	9.93(37)
order#2						
order#3	3.35(40)	3.34(44)	3.33(41)	3.33(57)	3.34(37)	3.33(54)
110 peak						
<u>CHLORITE</u>						
order#1	14.36(20)	14.36(24)			14.36(50)	
order#2	overlap with order #1 peak of kaolinite					
order#3	overlap with order #2 peak of kaolinite					
<u>SMECTITE</u>						
typical						
peak	13 - 14			10	13.32(25)	17.02(49)
<u>QUARTZ</u>						
peak		4.24(23)	4.24(23)			
<u>FELDSPARS</u>						
peak	3.20(32)		3.20(23)	3.20(28)	3.22(21)	3.20(29)

Conclusions: for soil EPA-1, major components of clay are kaolinit, illite, and smectite. Minor components are chlorite, feldspars, and quartz.

Table II.1b Results of x-ray identification for clay minerals in soil EPA-12.

<u>D Spacing Å (Intensity cps)</u>						
<u>SLIDE ID:</u>	<u>KAD</u>	<u>K110</u>	<u>K350</u>	<u>K550</u>	<u>MGAD</u>	<u>MGGLY</u>
<u>KAOLINITE</u>						
order#1	7.14(38)	7.14(30)	7.24(31)		7.14(39)	7.14(44)
order#2	3.58(26)	3.59(26)	3.58(20)		3.58(27)	3.58(25)
<u>ILLITE</u>						
order#1	10.13(56)	10.13(65)	10.18(75)	10.13(67)	10.13(56)	10.03(54)
order#2	4.99(19)	4.99(26)	4.99(25)	4.99(29)	5.01(28)	4.99(29)
order#3	3.33(70)	3.34(75)	3.33(78)	3.33(67)	3.33(71)	3.33(80)
110 peak		4.42(20)				
<u>CHLORITE</u>						
order#1	no evidence for existence of chlorite.					
order#2						
order#3						
<u>SMECTITE</u> no evidence for existence of smectite.						
<u>MONTMORILLONITE + MICA</u>						
peak	28.15(38)				28.39(34)	

Conclusion: For soil EPA-12, major components of clay are kaolinite and illite. The minor components of clay are smectite + mica.

Table II.1c Results of x-ray identification for clay minerals in soil EPA-13.

<u>D Spacing Å (Intensity cps)</u>						
<u>SLIDE ID:</u>	<u>KAD</u>	<u>K110</u>	<u>K350</u>	<u>K550</u>	<u>MGAD</u>	<u>MGGLY</u>
<u>KAOLINITE</u>						
order#1	7.11(170)	7.11(201)	7.11(164)	6.92(14)	7.24(267)	7.24(259)
order#2	3.58(80)	3.58(101)	3.58(85)		3.58(127)	3.58(126)
<u>ILLITE</u>						
order#1	10.13(120)	10.03(158)	10.03(156)	10.03(133)	10.13(169)	10.03(165)
order#2	4.99(39)	5.01(36)	5.01(45)	4.99(46)	4.99(59)	5.01(55)
order#3	3.33(86)	3.33(76)	3.33(76)	3.23(94)	3.33(75)	3.33(111)
110 peak	4.52(21)					
<u>CHLORITE</u>						
order#1	14.36(34)	14.16(27)			14.16(55)	14.16(47)
order#2	overlap with order #1 peak of kaolinite					
order#3	overlap with order #2 peak of kaolinite					
<u>SMECTITE</u>	no evidence for exsistence of smectite.					

---

Conclusion: For soil EPA-13, major components of clay are kaolinite and illite. The minor component is chlorite.

Table II.1d Results of x-ray identification for clay minerals in soil EPA-16.

<u>D Spacing Å (Intensity cps)</u>						
<u>SLIDE ID:</u>	<u>KAD</u>	<u>K110</u>	<u>K350</u>	<u>K550</u>	<u>MGAD</u>	<u>MGGLY</u>
<u>KAOLINITE</u>						
order#1	7.14(74)	7.14(63)	7.24(66)		7.24(104)	7.19(106)
order#2	3.58(31)	3.58(38)	3.58(34)		3.56(53)	3.58(45)
<u>ILLITE</u>						
order#1	10.13(49)	10.18(55)	10.18(55)	10.03(52)	10.13(42)	10.13(51)
order#2	4.99(19)	4.96(20)	5.01(24)	4.99(21)	4.80(28)	4.96(28)
order#3	3.34(58)	3.34(59)	3.34(72)	3.33(76)	3.33(75)	3.34(77)
110 peak	4.75(16)			4.48(19)		
<u>CHLORITE</u>						
order#1	14.67(64)					
order#2	overlap with order #1 peak of kaolinite					
order#3	overlap with order #2 peak of kaolinite					
<u>SMECTITE</u>						
typical peaks					11.06(129)	11.16(102) 15.95(51)
<u>QUARTZ</u>						
peak	4.25(26)			4.29(18)	4.25(25)	4.23(21)
<u>MICAS + VERMICULITE</u>						
peak	30.72(52)					28.15(45)

---

Conclusion: For soil EPA-16, major components of clay are kaolinite vermiculite and illite. Minor components are chlorite, smectite + mica.

Table II.1e Results of x-ray identification for clay minerals in soil EPA-25.

<u>D Spacing Å (Intensity cps)</u>						
<u>SLIDE ID:</u>	<u>KAD</u>	<u>K110</u>	<u>K350</u>	<u>K550</u>	<u>MGAD</u>	<u>MGGLY</u>
<u>KAOLINITE</u>						
order#1	7.14(66)	7.14(72)	7.14(65)		7.14(79)	7.14(88)
order#2	3.58(48)	3.58(43)	3.58(36)		3.56(49)	3.58(39)
<u>ILLITE</u>						
order#1	10.13(51)	10.13(87)	10.14(125)	10.03(95)	10.03(67)	10.13(51)
order#2	5.01(30)	5.01(34)	4.99(34)	5.01(29)	4.92(20)	4.99(27)
order#3	3.35(82)	3.34(63)	3.33(79)	3.33(98)	3.34(84)	3.33(83)
110 peak		4.42(20)				
<u>CHLORITE</u>						
order#1	14.36(51)	13.87(37)			14.36(101)	
order#2	overlap with order #1 peak of kaolinite					
order#3	overlap with order #2 peak of kaolinite					
<u>SMECTITE</u>						
typical	14.36(51)	13.87(37)			14.36(101)	16.05(91)
peaks	10.13(85)	10.13(87)	10.13(125)	10.03(95)	10.03(67)	10.13(51)
<u>QUARTZ</u>						
peak	4.25(26)			4.29(18)	4.25(25)	4.23(21)

Analysis: The peak at about 14 Å shifts to larger spacing (16.05 Å) when it was treated with ethylene glycol. And it shifted to smaller spacing at about 10 Å when it was heated, we can realize this shift from the increase of intensity at 10.03 Å from 110 °C to 350 °C. At 550 °C, the intensity at 10.03 Å decreases because the kaolinite order #1 peak is destroyed. Large amount smectite exist, the smectite may randomly interstratified with chlorite.

Conclusion: For soil EPA-25, major components of clay are kaolinite smectite and illite. Minor component is chlorite.

Table II.1f Results of x-ray identification for clay minerals in Lula Aquifer.

<u>D Spacing Å (Intensity cps)</u>						
<u>SLIDE ID:</u>	<u>KAD</u>	<u>K110</u>	<u>K350</u>	<u>K550</u>	<u>MGAD</u>	<u>MGGLY</u>
<u>KAOLINITE</u>						
order#1	7.11(157)	7.14(158)	7.24(160)		7.14(172)	7.11(171)
order#2	3.58(118)	3.58(128)	3.58(103)		3.58(97)	3.58(108)
<u>ILLITE</u>						
order#1	10.13(132)	10.18(166)	10.13(302)	9.93(272)	10.18(97)	10.13(93)
order#2	5.01(53)	4.99(64)	4.99(75)	4.99(46)	4.96(49)	4.99(44)
order#3	3.33(177)	3.33(158)	3.33(167)	3.33(163)	3.34(126)	3.33(148)
110 peak						
<u>CHLORITE</u>						
order#1	no evidence for exist of chlorite.					
order#2						
order#3						
<u>SMECTITE</u>						
typical peak					12.74(79)	14.67(51)
<u>QUARTZ</u>						
peak	4.22(26)	4.22(23)		4.24(23)		4.18(22)
<u>MONTMORILLONITE + MICA</u>						
peak						28.15(54)

Conclusion: For Lula Aquifer, major components of clay are kaolinite and illite. Minor components are smectite, and smectite + mica.

Table II.2. Clay mineral compositions in the environmental sorbents.

SORBENT	MAJOR COMPONENTS	MINOR COMPONENTS
EPA-1	kaolinite, illite, smectite	chlorite, feldspars, quartz (very little)
EPA-12	kaolinite, illite	smectite + micas
EPA-13	kaolinite, illite	chlorite
EPA-16	kaolinite, illite, vermiculite	micas + smectite
EPA-25	kaolinite, illite, smectite	chlorite
Lula Aquifer	kaolinite, illite	mica + smectite, smectite

## REFERENCES

Department of the Interior U.S. Geological Survey, Bulletin 1563,  
"Flow Sheet of Clay Mineral Identification".

Carroll, D. "Clay Mineral: A Guide to Their X-ray Identification", THE  
GEOLOGICAL SOCIETY OF AMERICA, INC. (1970).

Starkey, H. C.; Blackmon, P. C.; Hauff, P. L. "The Routine  
Mineralogical Analysis of Clay-Bearing Samples", U.S. Geological  
Survey Bulletin 156, 1981.

Shoemaker, D. P.; Garland, C. W.; Nibler, J. W. Experiments in  
Physical Chemistry; fifth Ed.; McGraw-Hill Book Company, 1989.